

**METHYLATED AMINE-UTILISING BACTERIA  
AND MICROBIAL NITROGEN CYCLING  
IN MOVILE CAVE**

---

**DANIELA WISCHER**

**UNIVERSITY  
OF  
EAST ANGLIA**

**PHD 2014**



**METHYLATED AMINE-UTILISING BACTERIA  
AND MICROBIAL NITROGEN CYCLING  
IN MOVILE CAVE**

---

A thesis submitted to the School of Environmental Sciences in fulfilment  
of the requirements for the degree of Doctor of Philosophy

by

**DANIELA WISCHER**

in

**SEPTEMBER 2014**

University of East Anglia,  
Norwich, UK

---

This copy of the thesis has been supplied on condition that anyone who consults it is understood to recognise that its copyright rests with the author and that use of any information derived there from must be in accordance with current UK Copyright Law. In addition, any quotation or extract must include full attribution.



---

## Table of Contents

<b>List of Figures .....</b>	<b>vii</b>
<b>List of Tables.....</b>	<b>xi</b>
<b>Declaration.....</b>	<b>xiii</b>
<b>Acknowledgements .....</b>	<b>xiv</b>
<b>Abbreviations &amp; Definitions .....</b>	<b>xv</b>
<b>Abstract.....</b>	<b>xix</b>
<b>Chapter 1. Introduction .....</b>	<b>1</b>
1.1 Cave ecosystems and Movile Cave .....	2
1.1.1 Hypogenic caves .....	2
1.1.2 Movile Cave – a unique underground ecosystem .....	3
1.1.3 Movile Cave – formation and features.....	4
1.1.4 Conditions in Movile Cave .....	6
1.1.5 Evidence for isolation of Movile Cave .....	7
1.2 Microbiology of Movile Cave .....	8
1.2.1 Primary producers: sulfur, methane and ammonia oxidisers.....	8
1.2.2 Microorganisms of the sulfur cycle .....	9
1.2.3 C <sub>1</sub> metabolism: methanotrophs and methylotrophs .....	10
1.2.4 Nitrogen cycling in Movile Cave.....	11
1.2.5 Other microbial processes in Movile Cave .....	12
1.2.6 Proposed microbial food web of Movile Cave .....	13
1.3 The microbial nitrogen cycle.....	14
1.3.1 Overview of the nitrogen cycle.....	14
1.3.2 Organic nitrogen compounds in the N-cycle .....	16
1.4 Methylotrophy in bacteria .....	18
1.4.1 The concept of methylotrophy .....	18
1.4.2 Methanotrophs .....	19
1.4.3 Methylotrophs .....	22
1.4.4 Formaldehyde oxidation .....	24

---

1.4.5	Formaldehyde assimilation.....	26
1.5	Methylated amines as carbon, energy and nitrogen sources.....	30
1.6	Aims and approach of this PhD project.....	33
1.6.1	Techniques used in this study.....	34
1.6.2	Key questions of the PhD thesis.....	34
<b>Chapter 2.</b>	<b>Materials and Methods.....</b>	<b>38</b>
2.1	Chemicals and reagents .....	39
2.2	Bacterial strains.....	39
2.3	Collection and processing of sample material from Movile Cave.....	39
2.4	DNA stable isotope probing (DNA-SIP) experiments .....	40
2.5	Culture media and growth of control organisms .....	42
2.5.1	Dilute basal salts (DBS) medium .....	43
2.5.2	Mixed carbon solution for DBS-C medium .....	43
2.5.3	Nitrate mineral salts (NMS) medium .....	43
2.5.4	Mineral salts (MS) medium.....	44
2.5.5	Growth of <i>Methylosinus trichosporium</i> OB3b.....	44
2.5.6	<i>Azotobacter</i> medium and growth of <i>Azotobacter vinelandii</i> .....	44
2.5.7	Luria-Bertani (LB) medium .....	45
2.5.8	Super optimal broth with catabolic repressor (SOC) medium .....	45
2.5.9	R2A agar.....	45
2.5.10	Nutrient broth .....	45
2.5.11	Rose-Bengal chloramphenicol agar plates .....	45
2.5.12	Medium for ammonia-oxidising bacteria (Medium 181).....	45
2.5.13	Growth of <i>Nitrosomonas europaea</i> .....	46
2.5.14	Medium for nitrite-oxidising bacteria (Medium 182) .....	46
2.6	Enrichment, isolation and maintenance of methylated amine-utilising bacteria from Movile Cave.....	47
2.6.1	Methylotrophic methylated amine-utilising bacteria .....	47
2.6.2	Non-methylotrophic, methylated amine-utilising bacteria.....	47
2.6.3	Microscopy.....	48

---

2.6.4	Preservation of cultures.....	48
2.6.5	Growth tests of new isolates with methanol and under anoxic conditions.....	48
2.7	DNA extraction, processing and storage.....	49
2.8	Agarose gel electrophoresis.....	49
2.9	Polymerase chain reaction (PCR).....	50
2.10	Purification of PCR products for further applications.....	51
2.11	Design of PCR primers targeting <i>gmaS</i> .....	56
2.11.1	Identification of <i>gmaS</i> sequences and alignment.....	56
2.11.2	Primer sequences and PCR conditions .....	56
2.11.3	Validation of the new primers.....	57
2.12	Denaturing gradient gel electrophoresis (DGGE).....	59
2.13	Cloning of PCR products .....	59
2.14	RFLP analysis of cloned sequences from <sup>13</sup> C-MMA-SIP incubations .....	60
2.15	DNA sequencing and phylogenetic analysis .....	60
2.15.1	Sequencing of PCR products .....	60
2.15.2	Metagenome analysis.....	61
2.15.3	Nucleotide sequence accession numbers .....	62
2.16	N <sub>2</sub> fixation assay (acetylene reduction).....	62
2.17	Colorimetric assays .....	63
2.17.1	Ammonium assay.....	63
2.17.2	Nitrite assay .....	63
2.17.3	Nitrate assay.....	65
2.18	Measuring methylated amine concentrations .....	65
2.19	Isotope pairing experiments for detection of denitrification and anammox .....	65
<b>Chapter 3. Isolation of methylated amine-utilising bacteria from Movile Cave ...67</b>		
3.1	Introduction .....	68
3.2	Isolation of methylotrophic bacteria.....	69
3.3	Isolation of non-methylotrophic bacteria (and yeast).....	75
3.4	Two new methylotrophic strains from Movile Cave: <i>Catellibacterium</i> sp. LW-1 and <i>Mesorhizobium</i> sp. 1M-11.....	79

---

3.4.1	Growth characteristics of <i>Catellibacterium</i> sp. LW-1 and <i>Mesorhizobium</i> sp. 1M-11 .....	80
3.4.2	The genus <i>Catellibacterium</i> .....	82
3.4.3	The genus <i>Mesorhizobium</i> .....	83
<b>Chapter 4. Identification of methylotrophic bacteria in Movile Cave by DNA-SIP with <sup>13</sup>C-MMA .....</b>		<b>84</b>
4.1	Introduction: SIP as a tool in microbial ecology .....	85
4.2	Substrate uptake experiments with MMA, DMA, TMA and <i>in situ</i> concentrations of MMA in Movile Cave .....	86
4.3	DNA-SIP experiments with MMA reveal a shift in the methylotrophic community over time and identify new methylotrophs in Movile Cave .....	87
4.3.1	Analysis of the overall bacterial community in MMA microcosms (unfractionated DNA).....	88
4.3.2	Analysis of <sup>13</sup> C-labelled bacterial communities in MMA microcosms (heavy DNA fractions) .....	89
4.3.3	Analysis of non-labelled bacterial communities in MMA microcosms (light DNA fractions) .....	94
4.3.4	Analysis of labelled and non-labelled bacterial communities in MMA microcosms by cloning and sequencing of 16S rRNA genes .....	95
4.4.	DNA- SIP experiments with DMA corroborate new methylotrophs .....	97
<b>Chapter 5. The indirect methylamine oxidation pathway: Development of new PCR primers and distribution of <i>gmaS</i> in Movile Cave. ....</b>		<b>100</b>
5.1	Introduction: Metabolic pathways of MMA oxidation, key genes and biomarkers .....	101
5.2	Development and validation of <i>gmaS</i> -targeting PCR primers.....	102
5.2.1	Design of PCR primers: Retrieval of <i>gmaS</i> sequences from published genomes.....	102
5.2.2	Design of PCR primers: Multiple alignments of <i>gmaS</i> sequences reveal distinct phylogenetic clusters .....	104
5.2.3	Validation of primers: PCR and sequencing of <i>gmaS</i> genes from control strains.....	108
5.3	Testing <i>gmaS</i> PCR primers on genomic and non-genomic DNA from Movile Cave .....	109
5.3.1	Genomic DNA: few isolates test positive .....	109
5.3.2	Non-genomic DNA: low levels of amplification and double bands .....	110
5.4	Optimisation of <i>gmaS</i> PCR protocols .....	113

5.4.1	Genomic DNA – improved detection of <i>gmaS</i> in isolates.....	113
5.4.2	Non-genomic DNA – Movile Cave samples prove difficult.....	114
5.5	Distribution of <i>gmaS</i> and <i>mauA</i> genes in Movile Cave isolates.....	116
5.5.1	<i>gmaS</i> is present in all MMA-utilising isolates.....	116
5.5.2	<i>mauA</i> is only found in some methylotrophic MMA-utilising isolates...	120
5.6	Preliminary <i>gmaS</i> surveys of Movile Cave floating mat samples.....	121
5.6.1	<i>gmaS</i> genes in MMA enrichments from floating mat correspond with MMA utilisers identified by isolation studies and DNA-SIP.....	121
5.6.2	Metagenome analysis of Movile Cave floating mat reveals additional <i>gmaS</i> sequences.....	122
5.7	Preliminary <i>gmaS</i> surveys of soil and freshwater reveal new <i>gmaS</i> groups ...	123
5.8	Distribution of <i>mauA</i> in Movile Cave.....	126
5.9	Putative <i>gmaS</i> in <i>Cyanobacteria</i> and <i>Actinobacteria</i> .....	126
5.9.1	Putative <i>gmaS</i> genes from soil and freshwater may be <i>cyanobacterial</i> .	126
5.9.2	<i>gmaS</i> surveys uncover putative <i>actinobacterial gmaS</i> sequences.....	127
<b>Chapter 6. The microbial nitrogen cycle in Movile Cave, a first overview.....</b>		<b>129</b>
6.1	Proposed nitrogen cycle in Movile Cave.....	130
6.2	Aims and approach.....	131
6.3	Nitrification in Movile Cave.....	132
6.3.1	Nitrification: a brief introduction.....	134
6.3.2	Potential nitrification rates in Movile Cave.....	137
6.3.3	<i>amoA</i> surveys confirm the presence of AOB and AOA in Movile Cave .....	140
6.3.4	SIP experiments suggest that sulfur oxidisers are the dominant primary producers in Movile Cave and indicate niche separation of AOA and AOB.....	143
6.3.5	Enrichment of ammonia-oxidising bacteria and archaea.....	152
6.3.6	Summary.....	154
6.4	Dinitrogen fixation in Movile Cave.....	154
6.4.1	PCR-based studies suggest a wide phylogenetic diversity of <i>nifH</i> in Movile Cave.....	155
6.4.2	No detection of N <sub>2</sub> -fixing activity in Movile Cave samples.....	156

---

6.5	Anaerobic nitrogen respiration in Movile Cave: Denitrification and anammox ..	157
6.5.1	Introduction to denitrification .....	157
6.5.2	Introduction to anammox .....	158
6.5.3	Denitrification and anammox in Movile Cave .....	159
6.6	Autotrophic microorganisms ( <i>cbbLR</i> / <i>cbbLG</i> / <i>cbbM</i> genes).....	164
<b>Chapter 7. Summary and Outlook .....</b>		<b>167</b>
7.1	Well-known and new methylootrophs are active in Movile Cave.....	168
7.2	Methlyated amines are a nitrogen source for many non-methylootrophs .....	168
7.3	Distribution of the <i>gmaS</i> gene and its use as a biomarker .....	169
7.3.1	<i>gmaS</i> is widespread among methylootrophic and non-methylootrophic bacteria .....	169
7.3.2	New <i>gmaS</i> primers are an effective biomarker .....	169
7.3.3	Preliminary <i>gmaS</i> surveys suggest a wide diversity of <i>gmaS</i> -containing bacteria in the environment .....	170
7.4	Key processes of the nitrogen cycle in Movile Cave.....	170
7.4.1	Nitrifiers are active, but not dominant, primary producers in Movile Cave .....	170
7.4.2	N <sub>2</sub> fixation .....	171
7.4.3	Anaerobic nitrogen respiration .....	171
7.5	Future studies .....	172
7.5.1	Methodological considerations.....	172
7.5.2	H <sub>2</sub> oxidation and anaerobic processes in Movile Cave .....	173
<b>References.....</b>		<b>175</b>
<b>Appendix.....</b>		<b>191</b>
<b>Publications.....</b>		<b>199</b>

---

## List of Figures

<b>Figure 1.1</b>	Location of Movile Cave in Southern Romania, near the town of Mangalia. ....	3
<b>Figure 1.2</b>	Photographs showing some of the invertebrates that inhabit Movile Cave. ....	4
<b>Figure 1.3</b>	Cross-sectional view of Movile Cave .....	5
<b>Figure 1.4</b>	Photograph of an airbell in Movile Cave .....	5
<b>Figure 1.5</b>	Cross-sectional view of an airbell in Movile Cave. ....	8
<b>Figure 1.6</b>	Schematic overview of microbial nutrient cycling in Movile Cave.....	13
<b>Figure 1.7</b>	Key processes in the microbial nitrogen cycle.....	15
<b>Figure 1.8</b>	Nitrogen fractions within the total fixed nitrogen pool.....	17
<b>Figure 1.9</b>	Typical nitrogen components in dissolved and particulate nitrogen fractions.....	17
<b>Figure 1.10</b>	Metabolism of C <sub>1</sub> compounds by aerobic methylotrophs .....	22
<b>Figure 1.11</b>	The ribulose monophosphate (RuMP) cycle.....	27
<b>Figure 1.12</b>	The serine cycle.....	28
<b>Figure 1.13</b>	The reductive Acetyl-CoA pathway.....	29
<b>Figure 1.14</b>	Demethylation of TMA to MMA.....	33
<b>Figure 2.1</b>	DNA markers used for agarose gel electrophoresis .....	50
<b>Figure 2.2</b>	Calibration curves for ammonium assay .....	64
<b>Figure 2.3</b>	Calibration curve for nitrite assay .....	64
<b>Figures 3.1</b>	Micrographs of MA-utilising bacteria isolated from Movile Cave .....	69
<b>Figures 3.2</b>	Phylogenetic relationships of bacterial 16S rRNA gene sequences from Movile Cave.....	73
<b>Figure 3.3</b>	Micrographs of <i>Caulobacter</i> sp. isolated from Movile Cave.....	74

---

<b>Figure 3.4</b> Micrograph of a liquid enrichment culture containing <i>Oleomonas</i> , <i>Bacillus</i> and <i>Paenibacillus</i> . .....	76
<b>Figure 3.5</b> Micrographs of <i>Oleomonas</i> isolates from Movile Cave.....	76
<b>Figure 3.6</b> Swarming growth of <i>Oleomonas</i> sp. O1 and <i>Oleomonas</i> sp. O3.....	77
<b>Figure 3.7</b> Dividing cells of the methylotrophic yeast <i>Rhodotorula rubra</i> , isolated from Movile Cave .....	78
<b>Figure 3.8</b> MAR image showing filamentous fungi in a sample of Movile Cave mat .....	78
<b>Figure 3.9</b> Micrographs of <i>Azospirillum</i> and <i>Paenibacillus</i> isolates from Movile Cave.....	79
<b>Figure 3.10</b> Micrographs of <i>Catellibacterium</i> sp. LW-1 and <i>Mesorhizobium</i> sp. 1M-11, methylotrophic isolates from Movile Cave. ....	80
<b>Figure 4.1</b> Decrease of MMA concentration over time in enrichment cultures from floating mat samples.....	87
<b>Figure 4.2</b> DGGE analysis of bacterial 16S rRNA gene fragments from unfractionated DNA from <sup>13</sup> C-MMA-SIP incubations. ....	89
<b>Figure 4.3</b> Agarose gel images of bacterial 16S rRNA genes fragments amplified from fractionated DNA of <sup>13</sup> C-MMA-SIP incubations.....	90
<b>Figure 4.4</b> DGGE analysis of bacterial 16S rRNA gene fragments from light and heavy DNA fractions from <sup>13</sup> C-MMA incubations of Movile Cave water .....	93
<b>Figure 4.5</b> RFLP profiles of cloned 16S rRNA gene sequences from fractions F8 and F10 of DNA from <sup>13</sup> C-MMA-SIP experiments .....	96
<b>Figure 4.6</b> Agarose gel electrophoresis of bacterial 16S rRNA genes amplified from <sup>13</sup> C-DMA-SIP DNA following fractionation.....	97
<b>Figure 4.7</b> DGGE analysis and identities of bacterial 16S rRNA gene fragments in heavy DNA fractions from <sup>13</sup> C-DMA incubations .....	99
<b>Figure 5.1</b> Schematic views of the direct and indirect MMA oxidation pathways.....	102
<b>Figure 5.2</b> Gene neighbourhoods of <i>gmaS</i> genes from representative organisms, indicating location of <i>mgd</i> and <i>mgs</i> .....	103

<b>Figure 5.3</b> Amino-acid based, phylogenetic tree of <i>gmaS</i> sequences from MMA-utilising isolates and published bacterial genomes .....	105
<b>Figures 5.4</b> Nucleotide sequence alignments for design of <i>gmaS</i> PCR primers <i>gmaS</i> _557f, <i>gmaS</i> _970r and $\beta$ _ $\gamma$ _gmaS_1332r .....	106 f.
<b>Figure 5.5</b> Agarose gel images of 16S rRNA gene PCR products and <i>gmaS</i> PCR products of MMA-utilising control strains using the new <i>gmaS</i> primer sets .....	109
<b>Figure 5.6</b> Agarose gel image of PCR products obtained from non-genomic DNA using new <i>gmaS</i> primers.....	110
<b>Figure 5.7</b> Agarose gel image of PCR products obtained with primers 557f / 970r (targeting $\alpha$ -proteobacterial <i>gmaS</i> ) .....	111
<b>Figure 5.8</b> Agarose gel image of <i>gmaS</i> PCR products obtained for DNA from floating mat samples.....	112
<b>Figure 5.9</b> Agarose gel image of PCR products obtained with primers 557f / 1332r (targeting $\beta$ - and $\gamma$ -proteobacterial <i>gmaS</i> ) after two rounds of PCR.....	113
<b>Figure 5.10</b> Agarose gel image of PCR products obtained with primers 557f / 1332r (targeting $\beta$ - and $\gamma$ -proteobacterial <i>gmaS</i> ).....	115
<b>Figure 5.11</b> Agarose gel electrophoresis image following reamplification (using primers M13f / M13r) of <i>gmaS</i> clones .....	116
<b>Figure 5.12</b> Amino acid-based, phylogenetic tree of <i>gmaS</i> sequences derived from published bacterial genomes, methylotrophic and non-methylotrophic bacterial isolates and clone library sequences from Movile Cave .....	118
<b>Figure 5.13</b> Agarose gel image of <i>gmaS</i> PCR products obtained from non-genomic DNA samples with primer sets 557f / 970r, targeting $\alpha$ -proteobacterial <i>gmaS</i> , and 557f / 1332r, targeting $\beta$ -proteobacterial and $\gamma$ -proteobacterial <i>gmaS</i> , using optimised PCR .....	123
<b>Figure 5.14</b> <i>gmaS</i> phylogenetic tree incorporating <i>gmaS</i> sequences cloned from soil and lake sediment.....	125
<b>Figure 6.1</b> Schematic overview of the proposed nitrogen cycle in Movile Cave.....	131

---

<b>Figure 6.2</b> Ammonium depletion and nitrite production in microcosms set up from Movile Cave water and floating mat for the selective enrichment of nitrifiers .....	138
<b>Figure 6.3</b> Nitrite production (and depletion) in ammonium enrichment cultures from Movile Cave.....	138
<b>Figure 6.4</b> Nitrite production, plotted alongside ammonium depletion in Movile Cave enrichment cultures with added $\text{NH}_4^+$ .....	139
<b>Figure 6.5</b> DGGE profiles of the bacterial community in $^{13}\text{CO}_2 / \text{NH}_4^+$ SIP enrichments set up with Movile Cave water .....	144
<b>Figures 6.6</b> DGGE profiles of the bacterial communities in $^{13}\text{CO}_2 / \text{NH}_4^+$ SIP enrichments set up with (a) Movile Cave water and (b) floating mat.....	146 f.
<b>Figure 6.7</b> DGGE profiles of the bacterial community in $^{13}\text{CO}_2 / \text{NH}_4^+$ SIP enrichments set up with Movile Cave floating mat.....	148
<b>Figure 6.8</b> Agarose gel electrophoresis of bacterial 16S rRNA gene fragments amplified from fractionated DNA of $^{13}\text{CO}_2 / \text{NH}_4^+$ SIP enrichments.....	149
<b>Figure 6.9</b> DGGE analysis of bacterial 16S rRNA PCR products from fractionated DNA of $^{13}\text{CO}_2 / \text{NH}_4^+$ SIP enrichments.....	150
<b>Figure 6.9</b> Agarose gels of bacterial and archaeal <i>amoA</i> genes amplified from $^{13}\text{CO}_2 / \text{NH}_4^+$ SIP enrichments.....	152
<b>Figure 6.10</b> Phase contrast microscopy of nitrifying enrichments set up with Movile Cave water.....	153
<b>Supplementary Figures S1</b> DGGE profiles of bacterial 16S rRNA gene fragments from control incubations of Movile Cave water with no added substrate.....	193 f.
<b>Supplementary Figures S2</b> Phylogenetic affiliations of putative <i>gmaS</i> sequences from <i>Cyanobacteria</i> and <i>Actinobacteria</i> with proteobacterial <i>gmaS</i> sequences.....	196 ff.

## List of Tables

<b>Table 1.1</b> Overall reactions for methane oxidation with different electron acceptors.....	21
<b>Table 1.2</b> Overall reactions for aerobic and anaerobic oxidation of methylated substrates ....	24
<b>Table 2.1</b> Substrates used for SIP incubations as part of the Movile Cave food web project .....	40
<b>Table 2.2</b> Details of PCR primers used in this study.....	52 ff.
<b>Table 2.3</b> Names and accession numbers of all <i>gmaS</i> and <i>glnA</i> sequences used for primer design.....	58
<b>Table 3.1</b> Growth of bacterial isolates from Movile Cave on MAs with and without added carbon.....	71
<b>Table 3.2</b> Characteristics of two new methylotrophic strains from Movile Cave .....	81
<b>Table 5.1</b> Optimised PCR conditions for <i>gmaS</i> PCR .....	114
<b>Table 5.2</b> Movile Cave isolates – MA metabolism and functional gene markers .....	121
<b>Table 6.1</b> Group-specific PCR primers used in this study.....	133
<b>Table 6.2</b> Group-specific genes detected in different parts of Movile Cave by PCR amplification .....	141
<b>Table 6.3</b> Phylogenetic affiliations of bacterial <i>amoA</i> sequences from Movile Cave.....	142
<b>Table 6.4</b> Phylogenetic affiliations of archaeal <i>amoA</i> sequences from Movile Cave .....	143
<b>Table 6.5</b> Phylogenetic affiliations of <i>nifH</i> sequences from Movile Cave .....	156
<b>Table 6.6</b> Phylogenetic affiliations of <i>nirK</i> sequences from Movile Cave.....	161
<b>Table 6.7</b> Phylogenetic affiliations of <i>nirS</i> sequences from Movile Cave .....	162
<b>Table 6.8</b> Phylogenetic affiliations of 16S rRNA gene sequences obtained from Movile Cave with anammox-specific PCR primers.....	163
<b>Table 6.9</b> Phylogenetic affiliations of <i>cbbLR</i> sequences from Movile Cave .....	165

<b>Table 6.10</b> Phylogenetic affiliations of <i>cbbLG</i> sequences from Movile Cave.....	165
<b>Supplementary Table S1</b> Gibbs free energies of formation ( $\Delta G_f$ ).....	192
<b>Supplementary Table S2</b> Phylogenetic affiliations of 16S rRNA genes from no-substrate control incubations.....	194 f.

## Declaration

I declare that the work presented in this thesis was conducted by me under the direct supervision of Professor J. Colin Murrell, with the exception of those instances where the contribution of others has been specifically acknowledged. None of the work presented has been previously submitted for any other degree. Some of the data presented in Chapters 3 - 5 have been published in Wischer D, Kumaresan D, Johnston A, El Khawand M, Stephenson J, Hillebrand-Voiculescu AM, Chen Y, Murrell JC. (2015). Bacterial metabolism of methylated amines and identification of novel methylotrophs in Movile Cave. *ISME J* 9: 195-206 [doi:10.1038/ismej.2014.102]. The introductory material on cave ecosystems in general and Movile Cave in particular presented in Chapter 1, written by me for this PhD thesis, was used for the following review articles: Kumaresan D, Wischer D, Stephenson J, Hillebrand-Voiculescu A, Murrell JC. (2014). Microbiology of Movile Cave - A Chemolithoautotrophic Ecosystem. *Geomicrobiol J* 31: 186-19 [doi:10.1080/01490451.2013.839764], and Kumaresan D, Hillebrand-Voiculescu A, Stephenson J, Wischer D, Chen Y, Murrell JC. (2015) Microbial life in unusual cave ecosystems sustained by chemosynthetic primary production. In: Engels A (ed). *Microbial life in cave ecosystems* (in press).

Daniela Wischer

## Acknowledgements

First and foremost I want to thank my supervisor Prof Colin Murrell for the opportunity to do my PhD in his lab, as well as the expert guidance and support throughout the project. I also want to thank Dr Yin Chen for his expert input into the project. I furthermore want to thank everybody from the Murrell lab, past and present, at Warwick and UEA - it has been a great privilege and pleasure to be part of the group and to work with you all. I would furthermore like to thank my colleague Jason Stephenson for the good team work throughout the Movable Cave project.

I also want to thank everybody who has been involved in the Movable Cave project along the way (Rich, Deepak, Alex, Vlad), the good friends I made during my time in Leamington Spa, as well as the many people during my PhD who have given me support and advice, both work and home-related.

A special thank you to Prof Andy Johnston and everybody in his group at UEA for making us feel welcome and offering advice and support.

I would also like to acknowledge the scholarships I was issued by the University of Warwick and the University of East Anglia.

I would also like to express my sincere thanks to lab managers at Warwick and UEA, Paul from IT, everybody in the prep rooms, stores and elsewhere in the department who have kept things running!

A big thank you goes to Andrew Crombie for being an eternal source of wisdom and support throughout my PhD and for always being happy to help, even at the busiest of times!

I also want to thank Ollie - for driving me to the airport at the last minute and for generally always being eager to help - and my fellow PhD students for the dynamic discussions and fun-filled lunch breaks. A special mention to Antonia Johnston for her hands-on help and post-lab advice!

I would also like to thank Simon Williams for his kind help with 454 sequence data, as well as Inés Bellini for her hands-on help with process measurements in the final stage of my PhD, even if neither data made it into the final results.

I am indebted to Jean P. Euzéby and the good people who maintain the LPSN for bringing light into the jungle of phylogenetic misannotation.

I finally want to thank my family, both in Germany and Wales, for all the love and support you have given me over the last years, as well as my husband Dave for funding me during the final stage of my PhD and for giving me a beautiful son.

## Abbreviations & Definitions

<b>ADP</b>	adenosine diphosphate
<b>AMO</b>	ammonia monooxygenase
<b><i>amoA</i></b>	gene encoding alpha subunit of ammonia monooxygenase
<b>AMP</b>	adenosine monophosphate
<b>Anammox</b>	anaerobic ammonium oxidation
<b>ANME</b>	anaerobic methane-oxidising archaea
<b>AOA</b>	ammonia-oxidising archaea
<b>AOB</b>	ammonia-oxidising bacteria
<b>AOM</b>	anaerobic oxidation of methane
<b>ATP</b>	adenosine triphosphate
<b>ATU</b>	allylthiourea
<b>BLAST</b>	basic local alignment search tool
<b>blastn</b>	BLAST search: nucleotide to nucleotide
<b>blastx</b>	BLAST search: translated nucleotide to protein
<b>bp</b>	base pairs
<b>BSA</b>	bovine serum albumin
<b>CAMERA</b>	Community Cyberinfrastructure for Advanced Microbial Ecology Research and Analysis
<b>CBB</b>	Calvin-Benson-Bassham cycle
<b><i>cbbLR</i></b>	(RuBisCO) large-subunit gene, form I, green type
<b><i>cbbLG</i></b>	(RuBisCO) large-subunit gene, form I, red type
<b><i>cbbM</i></b>	(RuBisCO) large-subunit gene, form II
<b>CFU</b>	colony forming units
<b>DBS</b>	dilute basal salts
<b>DBS-C</b>	dilute basal salts with added carbon
<b>DGGE</b>	denaturing gradient gel electrophoresis
<b>DH</b>	dehydrogenase
<b>DMA</b>	dimethylamine
<b>DMF</b>	dimethylformamide
<b>DMSO</b>	dimethylsulfoxide
<b>DNA</b>	deoxyribonucleic acid
<b>DNMS</b>	dilute nitrate mineral salts
<b>dNTP</b>	deoxynucleotide triphosphate
<b>DRNA</b>	dissimilatory reduction of nitrate to ammonium
<b>EDTA</b>	ethylenediaminetetraacetic acid
<b>g</b>	gram
<b>g</b>	acceleration due to gravity
<b>G3P</b>	glyceraldehyde 3-phosphate
<b>GDH</b>	glutamate dehydrogenase
<b><i>glnA</i></b>	gene for glutamine synthetase
<b>GMA</b>	gamma-glutamylmethylamide synthetase

<b><i>gmaS</i></b>	gene for gamma-glutamylmethanamide synthetase
<b>G</b>	Gibbs free energy (measurement of a system's usable energy content)
<b><math>\Delta G</math></b>	$\Delta G$ of a reaction = the change in Gibbs free energy
<b><math>\Delta G^0</math></b>	$\Delta G$ under "standard conditions" (defined as concentration of reactants and products at 1.0 M; temperature at 25°C; pressure at 1.0 ATM) and pH0
<b><math>\Delta G^{0'}</math></b>	$\Delta G$ under "standard conditions" (see above) and pH7
<b><math>\Delta G^{0'} &lt; 0</math></b>	exergonic (energy-releasing) reaction (reaction is spontaneous)
<b><math>\Delta G^{0'} &gt; 0</math></b>	endergonic (energy-requiring) reaction (reaction is not spontaneous)
<b><math>\Delta G_f^0</math></b>	Gibbs free energy of formation of a compound (= the change in Gibbs free energy that accompanies the formation of 1 mole of a substance in its standard state from its constituent elements in their standard states)
<b><math>\Delta G_f^{0'}</math></b>	Gibbs free energy of formation of a compound at pH7 $\Delta G^{0'}$ of a reaction can be calculated from $\Delta G_f^{0'}$ of its compounds as follows: $\Delta G^{0'} = \sum \Delta G_f^{0'}_{[products]} - \sum \Delta G_f^{0'}_{[reactants]}$
<b>GOGAT</b>	glutamine oxoglutarate aminotransferase (glutamate synthase)
<b>GS</b>	glutamine synthetase
<b>H<sub>4</sub>Folate</b>	tetrahydrofolate
<b>H<sub>4</sub>MPT</b>	tetrahydromethanopterin
<b>HEPES</b>	4-(2-hydroxyethyl)-1-piperazineethanesulfonic acid
<b><i>hzo</i></b>	hydrazine oxidoreductase gene
<b>IC</b>	ion chromatography
<b>Identity</b>	the extent to which two (nucleotide or amino acid) sequences have the exact same residues at the same positions in an alignment, often expressed as a percentage
<b>IMG</b>	Integrated Microbial Genomes
<b>JGI</b>	Joint Genome Institute
<b>L</b>	litre
<b>LB</b>	Luria Bertani
<b>LPSN</b>	List of prokaryotic names with standing in nomenclature
<b>M</b>	molar
<b>MADH</b>	methylamine dehydrogenase
<b>MAR</b>	microautoradioactivity
<b><i>mauA</i></b>	gene for methylamine dehydrogenase
<b>mg</b>	milligram
<b><i>mgd</i></b>	gene for NMG dehydrogenase
<b><i>mgS</i></b>	gene for NMG synthase
<b>min</b>	minute
<b>ml</b>	millilitre
<b>mM</b>	millimolar
<b>MMA</b>	Monomethylamine
<b>mol</b>	mole
<b>MPN</b>	most probable number
<b>MRC</b>	Marine <i>Roseobacter</i> Clade
<b>MS</b>	mineral salts

---

<b>µg</b>	microgram
<b>µl</b>	microlitre
<b>NAD<sup>+</sup></b>	nicotinamide adenine dinucleotide (oxidised form)
<b>NADH</b>	nicotinamide adenine dinucleotide (reduced form)
<b>NADP<sup>+</sup></b>	nicotinamide adenine dinucleotide phosphate (oxidised form)
<b>NADPH</b>	nicotinamide adenine dinucleotide phosphate (reduced form)
<b>NCBI</b>	National Centre for Biotechnology Information (USA)
<b>NCIMB</b>	The National Collection of Industrial, Marine and Food Bacteria (UK)
<b>n-damo</b>	nitrite-dependent anaerobic methane oxidation
<b>ng</b>	nanogram
<b><i>nifH</i></b>	dinitrogenase reductase gene
<b><i>nirK</i></b>	gene for dissimilatory nitrite reductase (copper-containing form)
<b><i>nirS</i></b>	gene for dissimilatory nitrite reductase (heme-containing form)
<b>NMG</b>	<i>N</i> -methylglutamate
<b>NMS</b>	nitrate mineral salts
<b>NOB</b>	nitrite-oxidising bacteria
<b><i>nxrB</i></b>	gene for nitrite oxidoreductase
<b>OD<sub>540</sub></b>	optical density at 540 nm
<b>ORF</b>	open reading frame
<b>PBS</b>	phosphate buffered saline
<b>PCR</b>	polymerase chain reaction
<b>PEP</b>	phosphoenolpyruvate
<b>PIPES</b>	1,4-piperazinediethanesulfonic acid
<b>psi</b>	pound force per square inch
<b>RFLP</b>	restriction fragment length polymorphism
<b>RNA</b>	ribonucleic acid
<b>rpm</b>	revolutions per minute
<b>rRNA</b>	ribosomal ribonucleic acid
<b>RuBisCO</b>	ribulose 1,5-bisphosphate carboxylase-oxygenase
<b>RuMP</b>	ribulose monophosphate
<b>s</b>	seconds
<b>SDS</b>	sodium dodecyl sulfate
<b>SI</b>	sequence identity
<b>Similarity</b>	the extent to which two amino acid sequences have the exact same and / or chemically similar amino acids (positive substitutions) at the same positions in an alignment, often expressed as a percentage
<b>SOB</b>	super optimal broth / sulfur-oxidising bacteria
<b>SOC</b>	super optimal broth with catabolic repressor
<b>SRB</b>	sulfate-reducing bacteria
<b>TAE</b>	tris acetate EDTA
<b>TBE</b>	tris borate EDTA
<b>TCA</b>	trichloroacetic acid / tricarboxylic acid
<b>TCE</b>	trichloroethylene
<b>TEMED</b>	<i>N,N,N',N'</i> -tetramethyl-ethane-1,2-diamine
<b>TMA</b>	trimethylamine

<b>TMAO</b>	trimethylamine <i>N</i> -oxide
<b>Tris</b>	tris(hydroxymethyl)aminomethane
<b>UEA</b>	University of East Anglia
<b>v/v</b>	volume to volume
<b>w/v</b>	weight to volume
<b>X-gal</b>	5-bromo-4-chloro-3-indoyl- $\beta$ -D-galactoside

## Abstract

Movile Cave is an unusual, isolated ecosystem which harbours a complex population of microorganisms, fungi and endemic invertebrates. In the absence of light and with no fixed carbon entering the cave, life is sustained by non-phototrophic microorganisms such as sulfur and methane oxidisers. Also present are methylotrophs that use one-carbon compounds such as methanol and methylated amines as their sole source of carbon and energy. Produced during putrefaction, methylated amines are likely to be major degradation products in Movile Cave. Further to being methylotrophic substrates, they are also a nitrogen source for many non-methylotrophic bacteria.

The role of methylated amines as carbon and nitrogen sources for Movile Cave bacteria was investigated using a combination of DNA stable isotope probing and cultivation studies. Both, well-characterised and novel methylotrophs were identified: *Methylotenera mobilis* dominated  $^{13}\text{C}$ -monomethylamine SIP enrichments, while members of *Catellibacterium*, *Cupriavidus* and *Altererythrobacter* were also active. Cultivation studies consolidated SIP results in obtaining the first methylotrophic isolates from the genera *Catellibacterium* and *Mesorhizobium*. Pathways for monomethylamine (MMA) metabolism were investigated using new PCR primers designed to target *gmaS*, the gene for gamma-glutamylmethylamide synthetase, a key enzyme of the recently characterised indirect MMA oxidation pathway. This pathway is also present in bacteria that use MMA only as a nitrogen source, while the well-characterised, direct MMA oxidation pathway involving methylamine dehydrogenase (*mauA*) is found only in methylotrophs. *gmaS* was present in all MMA-utilising isolates, while *mauA* was found only in some methylotrophs, suggesting the indirect pathway is the major mode of MMA oxidation both in methylotrophs and non-methylotrophs from Movile Cave. Preliminary *gmaS* surveys revealed a high diversity of *gmaS*-containing bacteria. The roles of  $\text{N}_2$  fixers and nitrifiers were also investigated. Both bacterial and archaeal ammonia oxidisers were found to be active; however, sulfur oxidisers appeared to be the dominant autotrophs in Movile Cave.



## **Chapter 1. Introduction**

## 1.1 Cave ecosystems and Movile Cave

### 1.1.1 Hypogenic caves

On the continental earth, 97% of all unfrozen freshwater lies beneath the surface, while lakes and rivers make up only 2% (Gilbert & Deharveng, 2002). Caves are characterised by complete darkness, nearly constant air and water temperatures and relative humidity near saturation. They are generally challenging environments to colonise due to nutrient and energy limitations as well as possible oxygen deprivation (Engel 2007). The formation of cave systems usually results from seepage of meteoric surface waters into karst formations. As such, the energy required for the formation of these caves is entirely supplied by water, air, gravity and fauna from the surface (Forti *et al.*, 2002). Similarly, the biological communities within these caves are dependent on the flow of nutrients and energy from the surface (Forti *et al.*, 2002; Engel 2007). However, a small percentage of the world's caves are of hypogenic origin, formed by fluids rising up from below. In these cases, the energy needed to dissolve the rock and support the biological communities inhabiting the caves is supplied by ascending water and gases (Forti *et al.*, 2002).

The geochemistry of hypogenic caves differs depending on the origin of the rising waters, the type of host rock and the temperature and composition of the released gases. For biological studies, the most interesting hypogenic caves are those with still active emissions of gases such as hydrogen sulfide (H<sub>2</sub>S) and / or methane (CH<sub>4</sub>) resulting in an ongoing supply of energy sources which can support extremely rich and specialised ecosystems (Forti *et al.*, 2002). In these cases, the food web is sustained through non-phototrophic carbon fixation by chemolithoautotrophic primary producers.

Only few hypogenic caves have been studied so far, the two best known being Movile Cave in Romania and Frasassi Cave in Italy. Both caves are high in hydrogen sulfide and harbour rich and specialised ecosystems. Unlike Frasassi however, Movile Cave also contains substantial amounts of methane (Engel, 2007). Another important difference is that while Frasassi receives some input of meteoric water from above, Movile Cave is the only known cave ecosystem that is completely sealed off from the surface (Sârbu *et al.*, 1996; Forti *et al.*, 2002).

### 1.1.2 Movile Cave – a unique underground ecosystem

Movile Cave is an unusual underground ecosystem located near Mangalia in south-eastern Romania, a few kilometres from the Black Sea (Figure 1.1). The cave was discovered by geologist C. Lascu in 1986, when an artificial shaft dug for geological investigations created access to the narrow cave passages. What makes Movile Cave unique is the fact that, unlike other caves, it does not receive any input of water from the surface, due to layers of impermeable clays and loess that cover the limestone in which the cave is developed (Forti *et al.*, 2002).

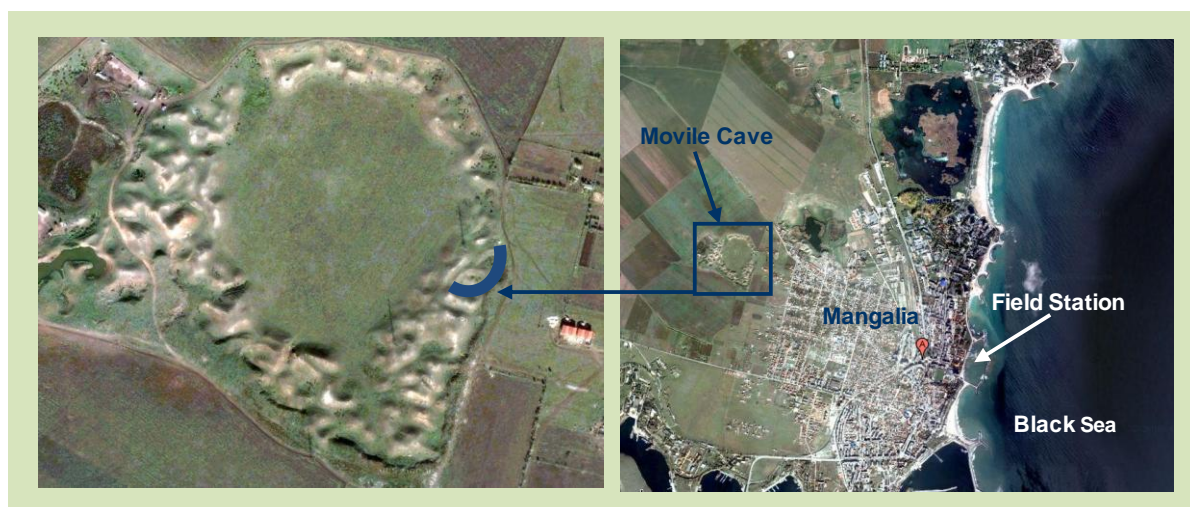


**Figure 1.1** Location of Movile Cave in Southern Romania, near the town of Mangalia.

(Images taken from Google Maps, <https://maps.google.co.uk/>)

Since no photosynthesis occurs within Movile Cave and no fixed carbon enters from above, life in the cave is maintained entirely by chemosynthesis (i.e. microorganisms using energy sources other than light). Despite the lack of photosynthetically fixed carbon, the cave hosts a remarkable diversity of invertebrates, such as worms, insects, spiders and crustaceans (Figure 1.2). There is paleogeographical evidence to suggest that some of these animal species invaded Movile Cave as early as 5.5 million years ago (Sârbu & Kane, 1995). Over time, these organisms have become troglomorphic, meaning they have adapted to life in the dark, and many of the species found are endemic to Movile Cave (33 out of 48 invertebrate species, Sârbu *et al.*, 1996).



**Figure 1.2** Photographs showing some of the invertebrates that inhabit Movile Cave.

Photos courtesy of Science Photo Library Limited (<http://www.sciencephoto.com>).

Sulfidic, chemosynthesis-based cave systems like Movile Cave bear resemblance to deep-sea hydrothermal vents, which when discovered in the 1970s (e.g. reviews by Lutz & Kennish, 1993; Van Dover *et al.*, 2002; Campbell 2006) demonstrated that ecosystems exist where life is independent from photosynthetically fixed carbon. By comparison, Movile Cave allows much easier access than deep-sea vents, therefore providing a valuable model-system for the study of a microbially driven, light-independent food web.

### 1.1.3 Movile Cave – formation and features

Although located only 20 m below ground, Movile Cave is completely isolated from the surface by thick layers of impermeable clay and loess which cover the limestone in which the cave is developed, preventing any infiltration of meteoric waters and reducing gas exchange between the cave and the surface (Sârbu & Kane, 1995). While the upper passages of the cave (~200 m long) are completely dry (as a consequence of the lack of water infiltration from the surface), the lower level (~40 m long) is partly flooded by hydrothermal waters which contain high amounts of hydrogen sulfide ( $\text{H}_2\text{S}$ ), methane ( $\text{CH}_4$ ) and ammonium ( $\text{NH}_4^+$ ) (Figure 1.3) (Sârbu & Lascu, 1997). This creates an active redox interface where bacteria oxidise the reduced compounds from the water using  $\text{O}_2$  from the atmosphere. Consequently, cave communities live only in proximity to the redox interface, while the upper dry non-sulfidic cave passages are devoid of fauna (Forti *et al.*, 2002). Several air bells are present in the lower cave level (Figures 1.3 and 1.4).

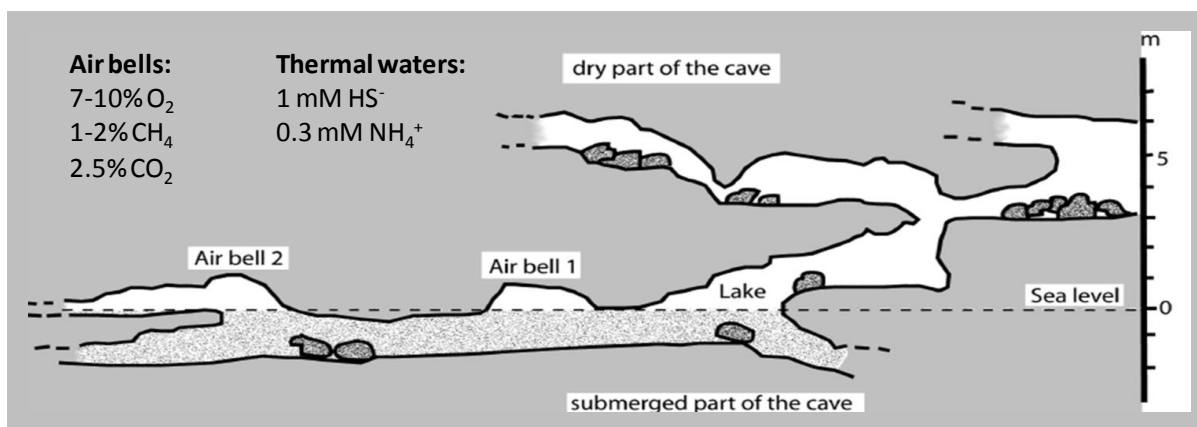


**Figure 1.3** Cross-sectional view of Movile Cave

(Image taken from Muschiol & Traunspurger (2007), *Nematology* 9: 271-284)

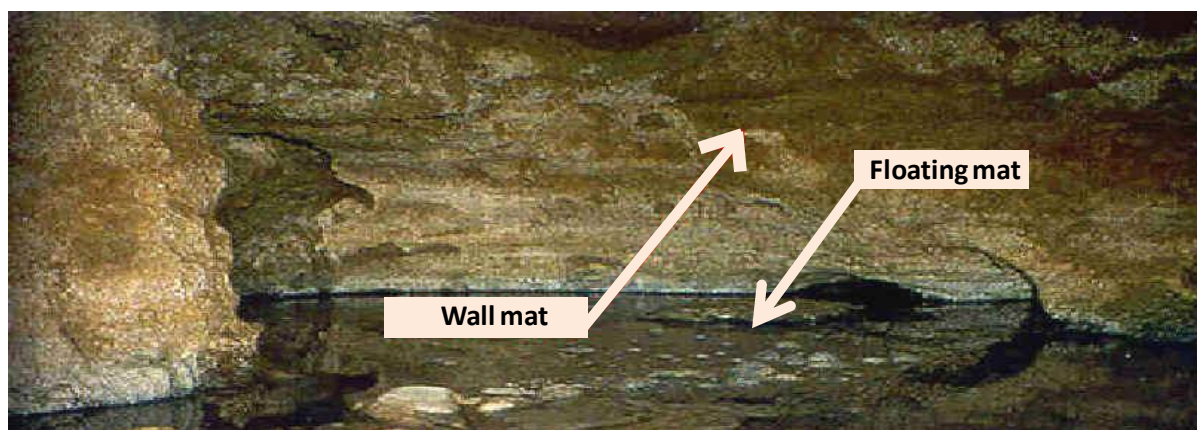
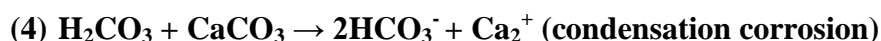
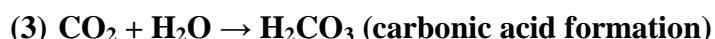
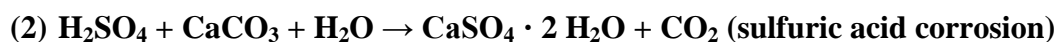


**Figure 1.4** Photograph of an airbell in Movile Cave

(Image modified from URL: <http://www.geo.utexas.edu/ChemHydro/images/microh1.jpg>)

Movile Cave is formed from two major corrosion processes: condensation corrosion by  $\text{CO}_2$  and acid corrosion by sulfuric acid (Sârbu & Lascu, 1997; Sârbu, 2000). Sulfuric acid ( $\text{H}_2\text{SO}_4$ ) corrosion which is active in the lower partially submerged cave passages is a result of the oxidation of  $\text{H}_2\text{S}$  to  $\text{H}_2\text{SO}_4$  in the presence of oxygen from the cave atmosphere (1). Sulfuric acid then reacts with the limestone walls of the cave, causing accelerated erosion and leading to formation of gypsum (calcium sulfate) deposits on the cave walls along with release of  $\text{CO}_2$  (2). This type of corrosion is highly efficient and also furthers condensation corrosion due to the release of large quantities of  $\text{CO}_2$  (Forti *et al.*, 2002). Condensation corrosion, which is a much slower process, affects the walls in the upper dry passages of the cave and occurs when warm water vapour from the thermal waters ascends and condenses on the colder walls and ceilings in the upper cave passages.  $\text{CO}_2$  from the cave atmosphere dissolves in the condensate to form carbonic acid (3) which dissolves the carbonate bedrock

forming bicarbonate (4) (Sârbu & Lascu, 1997). CO<sub>2</sub> is released from (i) limestone dissolution, (ii) the biological oxidation of methane and (iii) heterotrophic respiration processes (Sârbu *et al.*, 1996). Due to the absence of H<sub>2</sub>S in the upper cave levels, no effects of sulfuric acid corrosion are encountered here (Sârbu, 2000).



#### 1.1.4 Conditions in Movile Cave

##### (i) Water

The water flooding the lower level of the cave is of hydrothermal origin and high in H<sub>2</sub>S (0.2-0.3 mM), CH<sub>4</sub> (0.02 mM) and NH<sub>4</sub><sup>+</sup> (0.2-0.3 mM), while oxidised compounds are nearly absent. The flow rate of the water is extremely low and its physiochemical properties are not affected by seasonal climatic changes (Sârbu, 2000). The pH of the water is kept at 7.4 due to the buffering capacity of the carbonate bedrock. Dissolved oxygen ranges between 9-16 μM at the water surface and decreases to less than 1 μM after the first few cm, with the deeper water being essentially anoxic (Sârbu, 2000).

##### (ii) Cave atmosphere

The air temperature in the cave ranges between 19 and 21°C, with the upper dry level being slightly cooler than the air in the proximity to the thermal water, thereby favouring condensation corrosion (Sârbu, 2000). The mean temperature remains constant throughout the year and is considerably higher than the average for the region (8°C; Sârbu & Kane, 1995). The relative humidity ranges between 98 and 100%. The atmosphere in the cave is depleted in oxygen and rich in CO<sub>2</sub> and CH<sub>4</sub>. The upper dry level of the cave contains 20-21% O<sub>2</sub> and 1-1.2% CO<sub>2</sub>, while the airbells in the lower level contain only 7-10% O<sub>2</sub> and up to 2.5% CO<sub>2</sub>, as well as 1-2% of methane. H<sub>2</sub>S is found in proximity to the air-water interface but not in the upper level (Sârbu, 2000). Chemoautotrophic microorganisms thrive along the redox interface created between the oxygen in the atmosphere and the reduced compounds in the water, thereby rapidly depleting the oxygen. Extensive microbial mats composed of bacteria, fungi

and protozoa float on the water surface (kept afloat by rising CH<sub>4</sub> bubbles) and grow on the limestone walls of the cave (Sârbu *et al.*, 1994).

### 1.1.5 Evidence for isolation of Movile Cave

Since the discovery of Movile Cave, numerous studies have provided evidence that the karst system is well isolated from the surface and based entirely on autochthonous carbon fixed chemolithoautotrophically. For instance, the radioactive artificial nuclides <sup>90</sup>Sr and <sup>137</sup>Cs which were released as a result of the 1986 Chernobyl nuclear accident were found in high concentrations in soil and in lakes surrounding Movile Cave, as well as in the Black Sea and in sediments of other caves, but have not been detected in Movile Cave (Sârbu & Kane, 1995). Further proof that the cave is isolated comes from the absence of faecal streptococci or pesticides (the area surrounding the cave is heavily farmed) which would indicate contamination from above (Sârbu *et al.*, 1994).

#### (i) Incorporation of [<sup>14</sup>C] and RuBisCO activity

Incubation of microbial mat samples from the cave with [<sup>14</sup>C]-labelled bicarbonate resulted in incorporation of radioactive carbon into microbial lipids, giving evidence for chemoautotrophic carbon fixation at the redox interface (Sârbu *et al.*, 1991). Furthermore, activity of ribulose-1,5-bisphosphate carboxylase / oxygenase (RuBisCO), an enzyme of the Calvin cycle, was shown in mat homogenates as well as in bacterial cell lysates cultured from cave water, supporting the hypothesis that food is being produced *in situ* (Sârbu & Popa, 1992, cited after Sârbu *et al.*, 1994).

#### (ii) Isotopic signatures

Conclusive evidence that the cave is a self-sustained ecosystem came from stable isotope ratio analyses of carbon (<sup>13</sup>C / <sup>12</sup>C) and nitrogen (<sup>15</sup>N / <sup>14</sup>N), a useful technique for studying food webs because organisms fractionate isotopes in predictable ways (Sârbu *et al.*, 1996). The studies showed that organisms in the cave are isotopically lighter for both carbon and nitrogen than those from the surface (which depend on food produced photoautotrophically by green plants), suggesting their dependence on chemoautotrophically fixed carbon (Sârbu & Kane, 1995; Sârbu *et al.*, 1996). In addition, all forms of inorganic carbon in the cave are isotopically lighter than those from the surface (Figure 1.5). The lighter CO<sub>2</sub> in the cave atmosphere appears to be a mixture of some heavier CO<sub>2</sub> from the dissolution of limestone by

sulfuric acid and light CO<sub>2</sub> released during the oxidation of methane by methanotrophic bacteria and respiration processes of heterotrophic organisms (Sârbu *et al.*, 1996, Sârbu, 2000).

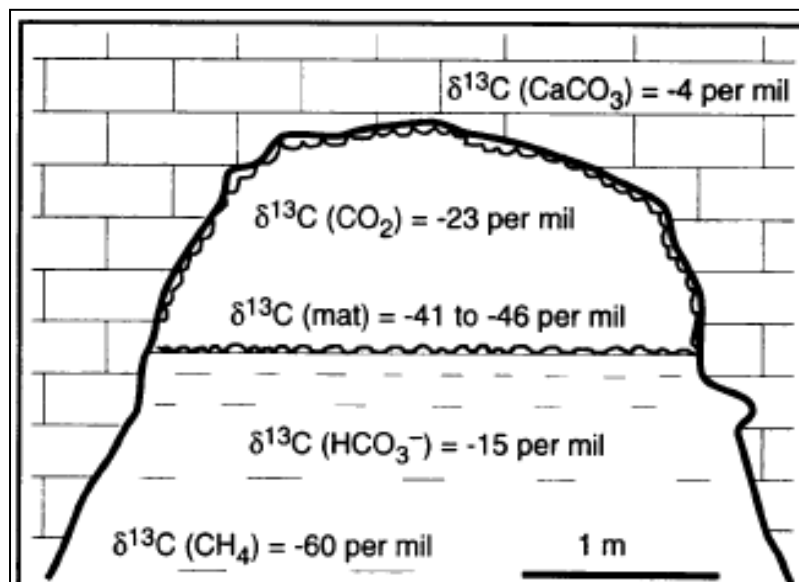


**Figure 1.5** Cross-sectional view of an airbell in Movile Cave, indicating isotopic carbon signatures (Sârbu *et al.* (1996) *Science*. 272: 1953-1955).

## 1.2 Microbiology of Movile Cave

### 1.2.1 Primary producers: sulfur, methane and ammonia oxidisers

Among the major primary producers in Movile Cave are microorganisms which derive energy from the oxidation of methane and reduced sulfur compounds, respectively. Nitrifying bacteria are also active in the cave (Chen *et al.*, 2009) although their relative contribution to primary production is still unknown. CO<sub>2</sub> fixation by ammonia- and nitrite-oxidising bacteria related to *Nitrosomonas*, *Nitrospira* and *Candidatus Nitrotoga* was shown in DNA-SIP experiments with <sup>13</sup>C-labelled bicarbonate by Chen *et al.* (2009), suggesting that ammonia and nitrite oxidation may be further important primary production processes in this isolated ecosystem.

### 1.2.2 Microorganisms of the sulfur cycle

#### (i) Sulfur-oxidising bacteria

Earlier studies on the microbiology of Movile Cave have focussed in particular on the sulfur cycle (Sârbu *et al.*, 1994; Vlăsceanu *et al.*, 1997; Rohwerder *et al.*, 2003). Sulfur-oxidising bacteria (SOB) are major primary producers in Movile and include species of *Thiobacillus* and *Beggiatoa* as shown by isolation-based work and microscopy of samples from floating mats (Sârbu *et al.*, 1994; Vlăsceanu *et al.* 1997). Most probable number (MPN) studies by Rohwerder *et al.* (2003) found that in addition to aerobic SOB, facultatively anaerobic SOB using nitrate ( $\text{NO}_3^-$ ) as an alternative electron acceptor are also active, and present in comparably high numbers as aerobic SOB ( $10^7$  CFU per gram dry weight of mat), suggesting that both groups contribute substantially to the biomass produced. The coupling of sulfur oxidation to denitrification could be a possible explanation for the lack of detectable  $\text{NO}_3^-$  in the water of Movile Cave.

Rohwerder *et al.* (2003) also found extremely acidophilic SOB, which is interesting considering the pH of the water in Movile Cave is kept neutral due to the buffering capacity of the limestone. However, Sârbu (2000) reported pH values of 3.8 – 4.5 on the surface of the microbial mats covering the limestone walls in the remote airbells, suggesting that not all of the sulfuric acid produced by SOB is immediately buffered. DNA-SIP experiments using  $^{13}\text{C}$ -labelled bicarbonate by Chen *et al.* (2009) showed that SOB from the *Beta*- and *Gammaproteobacteria* (*Thiobacillus*, *Thiovirga*, *Thiothrix*, *Thioploca*) were particularly active in assimilating  $\text{CO}_2$ . In addition to these aerobic SOB, 16S rRNA gene-based clone libraries of crude DNA constructed in the same study also revealed sequences related to *Sulfuricurvum*, an anaerobic SOB within the *Epsilonproteobacteria* (Chen *et al.*, 2009), supporting the earlier findings by Rohwerder *et al.* (2003). A similar 16S rRNA gene-based analysis of the microbial community in Movile Cave mats by Porter *et al.* (2009) identified above mentioned SOB as well as sequences related to *Halothiobacillus* and *Thiomonas* in the *beta*- and *gammaproteobacterial* group, and *Sulfurospirillum* in the *epsilonproteobacterial* group. It is worth noting that no *Archaea* capable of oxidising reduced sulfur compounds have been reported from Movile Cave or in fact any other sulfidic caves to date, probably due to the fact that most of these grow at elevated temperatures (Engel, 2007; Chen *et al.*, 2009).

(ii) *Sulfate-reducing bacteria*

Although less abundant than SOB (Rohwerder *et al.*, 2003), sulfate-reducing bacteria (SRB) have been found to be present in Movile Cave. They appear to belong to a higher trophic level, using the organic carbon released by SOB and other primary producers as the electron donor (Rohwerder *et al.*, 2003). While dissimilatory sulfate reduction is phylogenetically widespread, sulfate reducers in sulfidic caves appear to fall mainly within the *Deltaproteobacteria*, as the other groups of SRB tend to grow at temperatures above 70°C (Engel, 2007). Sequences related to members of the family *Desulfobulbaceae* were found by two independent 16S rRNA gene based clone library analyses (Chen *et al.*, 2009; Porter *et al.*, 2009).

### 1.2.3 *C*<sub>1</sub> metabolism: methanotrophs and methylotrophs

(i) *Methanotrophs*

In addition to H<sub>2</sub>S, CH<sub>4</sub> is present in high concentrations in the water and the atmosphere of the airbells and is an important energy source for microbial primary producers in Movile Cave. First indications for biological methane oxidation in Movile Cave came from isotopic signatures (Sârbu *et al.*, 1996). DNA-SIP experiments using <sup>13</sup>CH<sub>4</sub> (Hutchens *et al.*, 2004) revealed members of *Methylomonas*, *Methylococcus* and *Methylocystis* / *Methylosinus* as active methanotrophs in Movile Cave, supplying the wider food web with fixed organic carbon while also releasing CO<sub>2</sub> which in turn is used by autotrophic microorganisms (such as SOB). 16S rRNA gene based surveys by Porter *et al.* (2009) also detected *Methylomonas*-related sequences in crude DNA.

(ii) *Methylotrophs*

In addition to methane-oxidisers, methylotrophic bacteria which oxidise one-carbon (C<sub>1</sub>) compounds such as methanol (CH<sub>3</sub>OH) and methylated amines have been found to be both abundant and active in the cave (Hutchens *et al.*, 2004; Chen *et al.*, 2009). Culture-based studies by Rohwerder *et al.* (2003) showed numbers of culturable methylotrophs in the floating mats of around 10<sup>6</sup> CFU per gram dry weight of mat. 16S rRNA gene-based studies by Chen *et al.* (2009) suggested that the obligate methylated amine-utilising methylotroph *Methylotenera mobilis* was present in high numbers, while *Methylophilus* and *Methylovorus* were also detected. Similar studies by Porter *et al.* (2009) also detected 16S rRNA sequences

related to *Methylothera* and *Methylophilus*. Activity of the methanol-utilising genera *Methylophilus* and *Hyphomicrobium* was demonstrated by Hutchens *et al.* (2004): These organisms were co-enriched in  $^{13}\text{CH}_4$  incubation experiments as a result of cross-feeding, suggesting that they had assimilated  $^{13}\text{CH}_3\text{OH}$  excreted by methanotrophs. These studies suggested that cycling of  $\text{C}_1$  compounds is an important process in Movile Cave. Methylated amines are likely to be produced in large amounts in Movile Cave as a result of the degradation of the extensive, organic-rich microbial mats on the water surface, and used as growth substrates by specialised microorganisms.

#### 1.2.4 Nitrogen cycling in Movile Cave

##### (i) Nitrification

Previous studies on the microbiology of Movile Cave have focused largely on sulfur and carbon cycling, leaving the nitrogen cycle largely unexplored. However, recent DNA-SIP based studies by Chen *et al.* (2009) implied that ammonia- and nitrite-oxidising bacteria may be important primary producers in Movile Cave alongside sulfur- and methane-oxidising bacteria. Further indication for nitrification comes from isotopic signatures; while ammonia / ammonium ( $\text{NH}_3 / \text{NH}_4^+$ ) in the cave water is isotopically heavy; nitrogen in the microbial mat is isotopically lighter by approximately 10 per mil in comparison. A better understanding of the nitrogen cycle in Movile Cave is needed to determine whether these differences in isotopic signatures are due to ammonia assimilation, or chemolithoautotrophic ammonia oxidation (Sârbu *et al.* 1996).

##### (ii) Denitrification

While  $\text{NH}_4^+$  concentrations in the cave waters are relatively high (0.2-0.3 mM), nitrate ( $\text{NO}_3^-$ ) has not been detected (Sârbu *et al.* 2000). This indicates rapid turnover of  $\text{NO}_3^-$  by either assimilatory  $\text{NO}_3^-$  reduction or denitrification. Many facultatively anaerobic sulfur oxidisers such as *Thiobacillus denitrificans* are known to also be able to use  $\text{NO}_3^-$  as an alternative electron acceptor for respiration when oxygen is depleted. Sulfur oxidation-linked to denitrification may therefore be an important process in Movile Cave. Aforementioned findings by Rohwerder *et al.* (2003) support this hypothesis; they detected high numbers of SOB in anoxic MPN enrichments with thiosulfate ( $\text{S}_2\text{O}_3^{2-}$ ) and  $\text{NO}_3^-$ . 16S rRNA gene-based clone libraries of crude DNA by Chen *et al.* (2009) furthermore revealed sequences related to the denitrifying *Denitratisoma*.

(iii) *N<sub>2</sub>-fixation*

Microbial dinitrogen (N<sub>2</sub>) fixation may be a further significant process of the nitrogen cycle in Movile Cave. Many bacteria in Movile Cave are known to be capable of N<sub>2</sub>-fixation (e.g. *Thiobacillus denitrificans*, *Beggiatoa* and *Methylocystis*; Sârbu *et al.*, 1994; Vlăsceanu *et al.* 1997; Hutchens *et al.*, 2004). However, reduction of N<sub>2</sub> to NH<sub>3</sub> / NH<sub>4</sub><sup>+</sup> is highly energy-consuming and generally carried out during limitation of other nitrogen sources. Despite the relatively high reported standing concentrations of NH<sub>4</sub><sup>+</sup> in Movile Cave (0.2 – 0.3 mM in the water, Sârbu *et al.*, 2000) there may well be nitrogen-depleted areas within the microbial mats where N<sub>2</sub> fixation could play a role.

### 1.2.5 *Other microbial processes in Movile Cave*

The microbial population in the anoxic zones of the water and sediment in Movile Cave are largely unexplored. Considering the high amounts of organic matter from floating mats, and oxygen being largely unavailable as an electron acceptor, fermentation and anaerobic respiration, (using alternative electron acceptors such as NO<sub>3</sub><sup>-</sup>, NO<sub>2</sub><sup>-</sup>, SO<sub>4</sub><sup>2-</sup>, CO<sub>2</sub> and carboxylic acids) are likely to be of significance in these parts. In a recent study, the first methanogenic archaeon was isolated from a floating mat in Movile Cave (Ganzert *et al.*, 2014). In addition to growing autotrophically with H<sub>2</sub> / CO<sub>2</sub>, the organism was also able to utilise C<sub>1</sub> compounds including MMA, DMA and TMA, thereby highlighting a further role for methylated amines as carbon and energy source for anaerobic, methylotrophic microorganisms. The study also suggests that part of the CH<sub>4</sub> in Movile Cave may be derived from methanogenesis.

Hydrogen (H<sub>2</sub>), produced during fermentation processes, may be an additional major energy source for microorganisms in Movile Cave: H<sub>2</sub> is produced in large amounts during anaerobic degradation of organic matter, and a physiologically wide range of bacteria and archaea, both aerobic and anaerobic, can use H<sub>2</sub> chemolithotrophically (Fuchs & Schlegel, 2007). Anaerobic H<sub>2</sub>-oxidisers include denitrifiers, sulfate reducers, methanogens and acetogens. Hydrogenotrophs are often facultative chemolithoautotrophs (i.e. also able to use organic compounds for growth), and include species of *Paracoccus*, *Ralstonia* and *Hydrogenphaga* (Fuchs & Schlegel, 2007), representatives of which were also identified in this PhD project (see Chapters 3 and 4).

### 1.2.6 Proposed microbial food web of Movile Cave

Figure 1.6 gives a schematic overview of the proposed microbial food web in Movile Cave (modified from Kumaresan *et al.*, 2014), with those compounds and functional genes involved in nitrogen cycling highlighted in red:

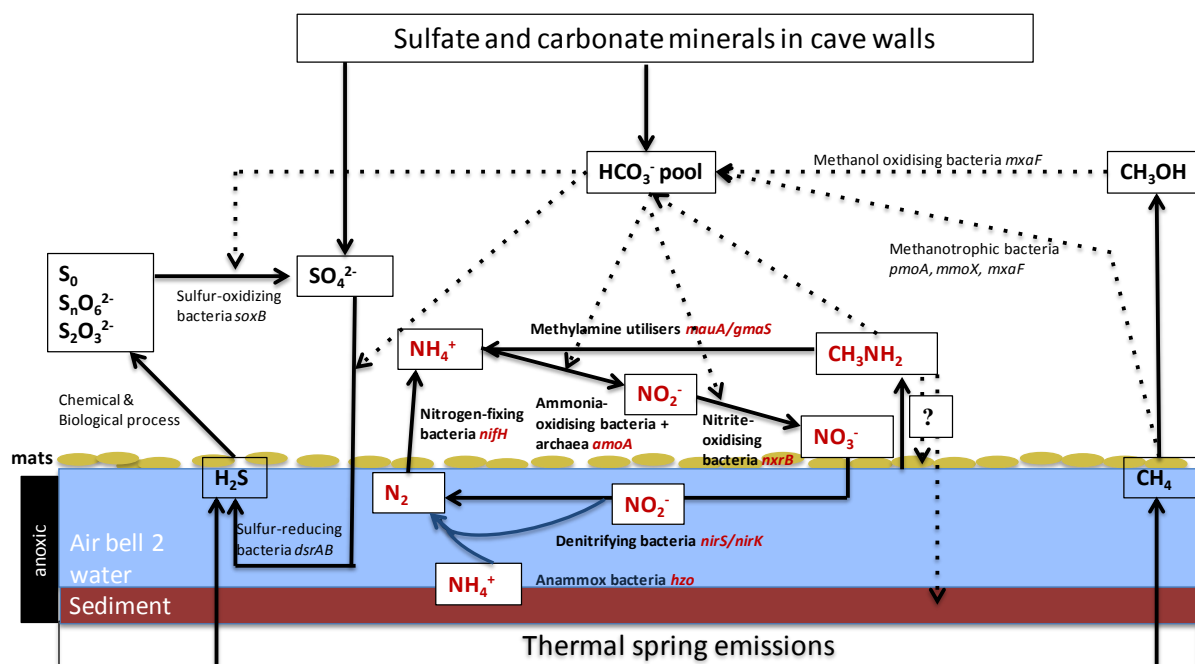


**Figure 1.6** Schematic overview of microbial nutrient cycling in Movile Cave

(Image modified from Kumaresan *et al.*, 2014)

Two of the major energy sources in Movile Cave, methane ( $\text{CH}_4$ ) and hydrogen sulfide ( $\text{H}_2\text{S}$ ), enter the cave with hydrothermal waters from below (Sârbu & Kane, 1995; Sârbu & Lascu, 1997). Methane-oxidising bacteria convert the  $\text{CH}_4$  to methanol ( $\text{CH}_3\text{OH}$ ), providing a carbon and energy source for non-methanotrophic methylotrophs in the cave, while also releasing  $\text{CO}_2$  (Hutchens *et al.*, 2004, Chen *et al.*, 2009). Additional sources of  $\text{CO}_2$  (or bicarbonate) are respiration processes by heterotrophic bacteria, and the dissolution of the limestone in the cave walls (Sârbu *et al.*, 1996, Sârbu, 2000). This bicarbonate pool serves as a carbon source for autotrophic sulfur oxidisers, which (along with the methane oxidisers) are the major primary producers in this self-sustained ecosystem (see section 1.2.2 (i)) They produce sulfate ( $\text{SO}_4^{2-}$ ) from the oxidation of reduced sulfur compounds, which (together with sulfate minerals released from the cave walls) serves as an electron acceptor for sulfate-reducing bacteria (SRB) who thrive in the anoxic regions of the water and sediment (see section 1.2.2 (ii)).  $\text{CO}_2$  is also fixed by nitrifying bacteria and archaea: these organisms convert ammonia / ammonium ( $\text{NH}_3 / \text{NH}_4^+$ ) to nitrite ( $\text{NO}_2^-$ ) and nitrate ( $\text{NO}_3^-$ ), both of

which are electron acceptors for denitrifying microorganisms, anaerobes who convert oxidised nitrogen compounds back to dinitrogen ( $N_2$ ) (see sections 1.2.4 (i) and (ii)). A further possible process in anoxic parts of the water and sediment of the cave could be the anaerobic oxidation of  $NH_4^+$  coupled to reduction of  $NO_2^-$  by anammox bacteria. In addition to being an energy source for nitrifiers (and possibly anammox bacteria),  $NH_4^+$  is also likely to be the main nitrogen source for the microorganisms of Movile Cave. Finally, dinitrogen ( $N_2$ )-fixing microorganisms may grow in ammonium-depleted areas of the floating mats, reducing  $N_2$  from the atmosphere, along with  $N_2$  released by denitrifiers and from thermal emissions, back to  $NH_4^+$ . In addition to the  $NH_4^+$  released during mineralisation (ammonification) of organic nitrogen from dying cells,  $NH_4^+$  may also enter the cave with hydrothermal emissions. Additionally, excess  $NH_4^+$  may be released by methylotrophic bacteria growing on methylated amines. Methylated amines are released during putrefaction, i.e. degradation of proteins from the organic-rich mats. They are a carbon and energy source for aerobic, methylotrophic bacteria and anaerobic, methylotrophic archaea, as well as a nitrogen source for many non-methylotrophic bacteria (see sections 1.2.3 (ii) and 1.5).

### **1.3 The microbial nitrogen cycle**

This section only gives a brief overview of the microbial nitrogen cycle. More detailed introductory material on individual processes of the nitrogen cycle (nitrification,  $N_2$  fixation, denitrification and anammox) can be found in the relevant sections in Chapter 6.

#### *1.3.1 Overview of the nitrogen cycle*

Nitrogen is one of the key elements required by all living organisms as it is an essential building block of nucleic acids and proteins. Nitrogen exists in many oxidation states in the environment ( $NH_3$  /  $NH_4^+$  being the most reduced and  $NO_3^-$  being the most oxidised). Reductive and oxidative conversions of these nitrogen compounds make up the biogeochemical nitrogen cycle. Many of the processes of the nitrogen cycle are mediated exclusively by microorganisms. The nitrogen recycled on Earth is mostly in fixed form, such as  $NH_4^+$  and  $NO_3^-$ . However, the short supply of such compounds means that nitrogen is often the growth-limiting nutrient in the environment (Madigan *et al.*, 2009). The vast majority of nitrogen in nature exists as gaseous dinitrogen ( $N_2$ ) which is highly inert and therefore not biologically available for most organisms; only a relatively small number of microorganisms are able to use  $N_2$  as a cellular nitrogen source by nitrogen fixation (Madigan *et al.*, 2009).

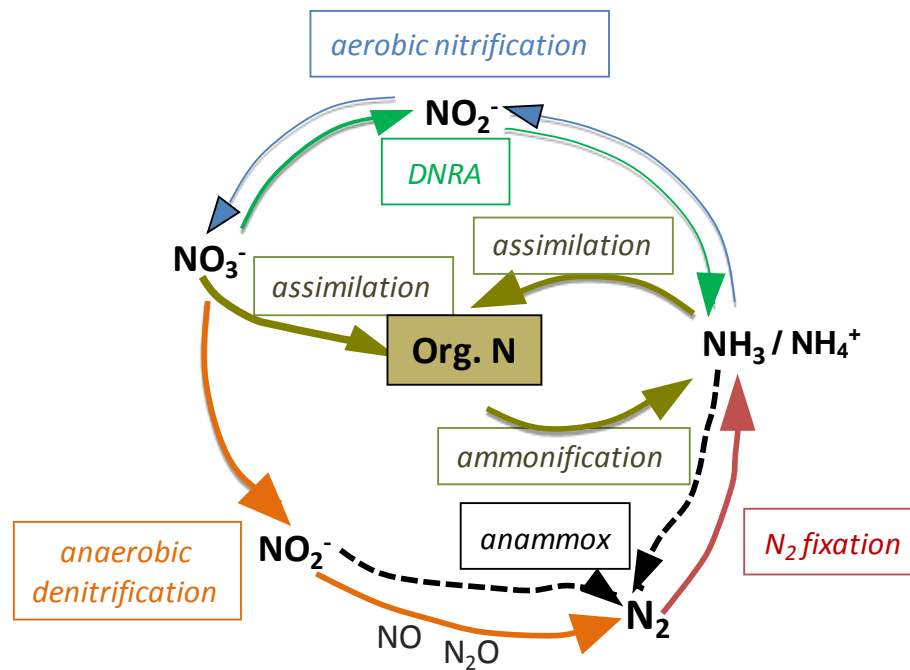


**Figure 1.7** Key processes in the microbial nitrogen cycle

**Microbial  $\text{N}_2$  fixation**, the reduction of gaseous  $\text{N}_2$  to ammonia / ammonium ( $\text{NH}_3 / \text{NH}_4^+$ ) by specialised microorganisms is therefore a crucial step in the nitrogen cycle, making nitrogen biologically available for other microorganisms (see Chapter 6, section 6.4). Microorganisms subsequently assimilate  $\text{NH}_4^+$  into cell material in the form of organic nitrogen (nucleotides and amino groups of protein) during **ammonia assimilation**. When organic matter is mineralised by bacteria and fungi, **ammonification (de-amination)** degrades the organic nitrogen back into  $\text{NH}_4^+$ . Unlike microorganisms, plants generally rely on nitrate ( $\text{NO}_3^-$ ) as a nitrogen source (Madigan *et al.*, 2009). Like plants, many microorganisms are also able to assimilate  $\text{NO}_3^-$  into cell nitrogen (**nitrate assimilation**).  $\text{NO}_3^-$  is generated by **nitrification**, the oxidation of  $\text{NH}_4^+$  to  $\text{NO}_3^-$ , a process carried out by two separate groups of aerobic, chemolithoautotrophic bacteria and archaea: the ammonia oxidisers and the nitrite oxidisers, which are able to gain energy from these reactions (see Chapter 6, section 6.3.1). Nitrification is therefore a key process in controlling the availability of nitrogen for plants. The nitrogen cycle is completed by the reduction of  $\text{NO}_3^-$  via  $\text{NO}_2^-$  to  $\text{N}_2$  in the process of **denitrification**, carried out by a wide range of (facultatively) anaerobic bacteria in the absence of oxygen as an electron acceptor (see Chapter 6, section 6.5.1). Denitrification is the main means by which gaseous  $\text{N}_2$  is formed biologically (Madigan *et al.*, 2009). An alternative form of  $\text{NO}_3^-$  respiration is the **dissimilatory reduction of nitrate to ammonium (DRNA)** via  $\text{NO}_2^-$ . The key organisms carrying out DNRA in the environment are still unknown. The ecological niche of DNRA in comparison to denitrification and the

conditions that favour the one or the other  $\text{NO}_3^-$  respiration pathway have yet to be determined (Kraft *et al.*, 2011). A second route of  $\text{N}_2$  generation (in addition to denitrification) is the recently discovered process of **anaerobic ammonia oxidation (anammox)** (Jetten *et al.*, 2009), a process carried out by specialised anaerobic bacteria able to survive by coupling the oxidation of  $\text{NH}_4^+$  to the reduction of  $\text{NO}_2^-$ , resulting in the generation of  $\text{N}_2$  and thereby bypassing the classic coupling of aerobic nitrification to denitrification (Trimmer *et al.*, 2003; see Chapter 6, section 6.5.2).

### 1.3.2 Organic nitrogen compounds in the N-cycle

Methylated amines, the central subject of this PhD study, are part of the dissolved organic nitrogen fraction (DON). Studies of the biogeochemical nitrogen cycle typically focus on the dissolved *inorganic* nitrogen (DIN) fraction which, in aquatic environments, is the sum of  $\text{NO}_3^-$ ,  $\text{NO}_2^-$  and  $\text{NH}_4^+$  (Worsfold *et al.*, 2008). However, recent studies have highlighted that the DON pool, derived from the growth and decay of living organisms, is the dominant form of dissolved nitrogen in aquatic ecosystems (as much as 60 – 68%) (Figure 1.8), and a large fraction of DON is now known to be bioavailable for microorganisms (reviews by Bronk, 2002; Berman & Bronk, 2003; Worsfold *et al.*, 2008). In certain oligotrophic systems DON is believed to provide the majority of nitrogen requirements (Worsfold *et al.*, 2008). The DON fraction is therefore becoming increasingly recognised as an important source of N-nutrition for microorganisms as well as phytoplankton. Several studies have furthermore pointed out that organic nitrogen far exceeds inorganic nitrogen in environments where human impact has not altered the nitrogen cycle (van Bremen, 2002; Neff, 2003). Up to 80% of the DON pool is comprised of low molecular mass (< 1 kDa) DON, including monomeric and small polymeric compounds such as urea, amino acids, nucleotides, purines, pyrimidines and (methylated) amines. However, the large majority of the low molecular mass DON fraction ( $\geq 86\%$ ) is not identifiable at the molecular level (Worsfold *et al.*, 2008). Proteins and polypeptides are the major components of the high molecular mass (HMM) polymeric DON pool (> 1 kDa) (Figure 1.9; Worsfold *et al.*, 2008).

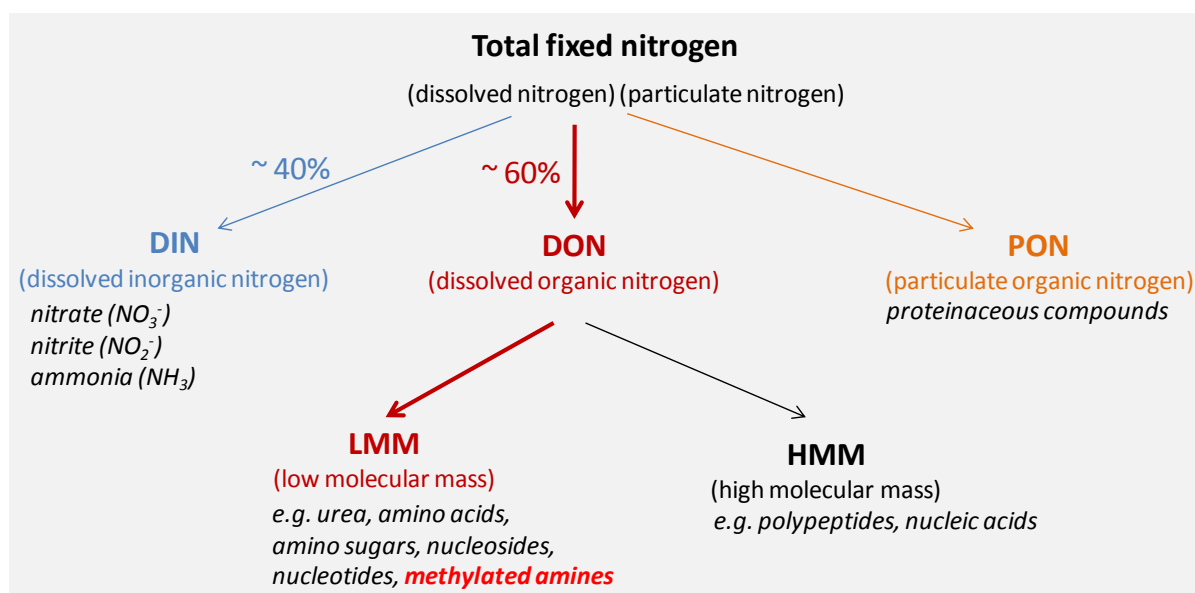


**Figure 1.8** Nitrogen fractions within the total fixed nitrogen pool.

(Based on review by Worsfold *et al.*, 2008)

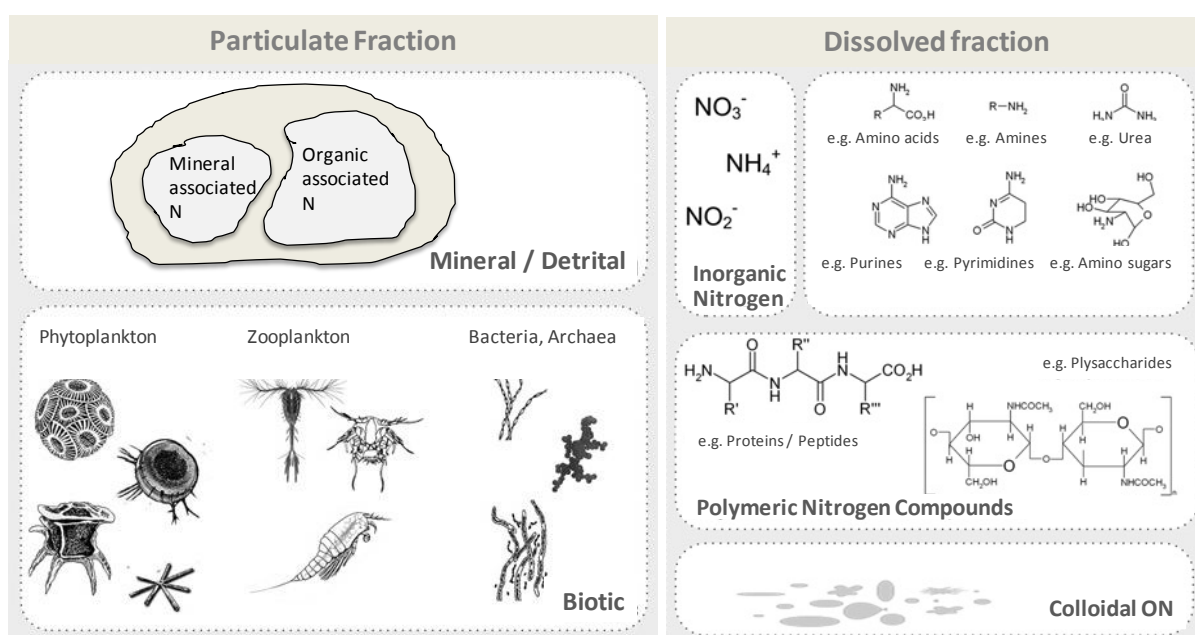


**Figure 1.9** Typical nitrogen components in dissolved and particulate nitrogen fractions

(Image modified from Worsfold *et al.*, 2008)

Laboratory studies as far back as the 1970s and 1980s have shown that both bacteria and phytoplankton are able to use organic nitrogen compounds such as amino acids, urea and amines as their sole source of nitrogen (North & Stephens, 1971; McCarthy, 1972; Wheeler 1977, Wheeler & Kirchman, 1986; North, 1975). However, the study of the DON pool has lagged behind that of DIN largely due to the analytical challenges involved in measuring this

chemically complex mixture (a comprehensive review of analytical methods for DON determination was published by Worsford *et al.*, 2008). More recent studies evaluating the productivity of coastal marine bacteria and phytoplankton (Seitzinger & Sanders, 1999) demonstrated the rapid utilisation of DON from rainwater by microorganisms, coupled to a response in biomass comparable to that of equivalent amounts of  $\text{NH}_4^+$ , and a marked change in community composition. Similarly, Zubkov *et al.* (2003) showed the dominance of certain *Cyanobacteria* in oligotrophic waters as a result of their high rate of DON uptake, illustrating the selective advantage over those microorganisms restricted to  $\text{NH}_4^+$ ,  $\text{NO}_3^-$  and  $\text{NO}_2^-$ . A number of studies on nitrogen uptake in soils (recently reviewed by Geisseler *et al.*, 2010) have furthermore illustrated that direct uptake of low molecular weight DON into microbial cells is a major route of nitrogen assimilation in the terrestrial environment.

## 1.4 Methylo-trophy in bacteria

### 1.4.1 The concept of methylo-trophy

Methylo-trophs are organisms capable of using reduced substrates with no carbon-carbon bonds, i.e. one-carbon ( $\text{C}_1$ ) compounds, as their sole source of carbon and energy (Anthony, 1982; Lidstrom, 2006; Chistoserdova *et al.*, 2009). Bacterial methylo-trophs are generally divided into two groups; (i) those that can use  $\text{CH}_4$  (= **methanotrophs**) and (ii) those that cannot use  $\text{CH}_4$  but are able to use  $\text{C}_1$  compounds such as methanol, formate, methylated sulfur compounds or methylated amines (= non-methanotrophic methylo-trophs, usually referred to simply as **methylo-trophs**). Microorganisms that use carbon monoxide ( $\text{CO}$ ) as their sole carbon and energy source are referred to as carboxidotrophs and are not generally included in the definition of methylo-trophy (for reviews on carboxidotrophs see King & Weber, 2007 and Oelgeschläger & Rother, 2008).

Methylo-trophs have evolved unique biochemical pathways for both energy and carbon metabolism (Lidstrom, 2006). A distinct feature of methylo-trophic metabolism is the central role of formaldehyde ( $\text{HCHO}$  or  $\text{CH}_2\text{O}$ ), a key intermediate representing the branching point from which carbon is either further oxidised to  $\text{CO}_2$  for energy generation, or assimilated into cell biomass. Depending on the pathway used, formaldehyde can be in free form or bound to tetrahydrofolate ( $\text{H}_4\text{Folate}$ ) as 5,10-methylenetetrahydrofolate ( $\text{CH}_2= \text{H}_4\text{Folate}$ ) (Fuchs & Schlegel, 2007). Part of the formaldehyde generated from  $\text{C}_1$  compounds is oxidised to  $\text{CO}_2$  for energy generation, while the other part is assimilated into biomass by one of several

distinct pathways (see below) (Lidstrom, 2006). Some methylotrophs (so-called “autotrophic methylotrophs”, Anthony 1982) oxidise all the formaldehyde to  $\text{CO}_2$ , and then assimilate  $\text{CO}_2$  into biomass via the classic Calvin-Benson cycle.

### 1.4.2 Methanotrophs

#### (i) *Aerobic methanotrophs*

Methane ( $\text{CH}_4$ ) is the most abundant hydrocarbon in nature, and, due to its solubility in water, a readily available substrate for microorganisms. However, because  $\text{CH}_4$  is very stable, only a few specialised bacteria are able to attack the  $\text{CH}_4$  molecule (Fuchs & Schlegel, 2007). Methanotrophs are widespread in aquatic and terrestrial environments wherever there are stable sources of methane (Madigan *et al.*, 2009). Classically, methanotrophs belong to either the *Alpha-* or *Gammaproteobacteria*. Recently however, acidophilic methanotrophs belonging to the largely uncultivated phylum *Verrucomicrobia* have been identified by several independent studies (Op den Camp *et al.*, 2009). Most methanotrophic bacteria are highly specialised for growth on  $\text{CH}_4$  and unable to use other alkanes or organic compounds (Fuchs & Schlegel, 2007). Many methanotrophs can however use methanol, and there are a few exceptions who can also use multi-carbon compounds (Boden, 2008), such as the facultative methanotroph *Methylocella silvestris* (Crombie & Murrell, 2014).

Methanotrophs oxidise  $\text{CH}_4$  to  $\text{CO}_2$  and water via the intermediates methanol ( $\text{CH}_3\text{OH}$ ), formaldehyde ( $\text{HCHO}$ ), and formate ( $\text{HCOO}^-$ ) (Trotsenko and Murrell, 2008). The first step in the oxidation of  $\text{CH}_4$  is catalysed by methane monooxygenase (MMO), a complex, copper-containing enzyme. MMO hydroxylates  $\text{CH}_4$  by incorporating one oxygen atom from  $\text{O}_2$  into the molecule, producing methanol. The oxidation of  $\text{CH}_4$  to methanol uses NADH and  $\text{O}_2$  and does not contribute to energy generation (Fuchs & Schlegel, 2007). Methanol is further oxidised to formaldehyde by methanol dehydrogenase. Part of the formaldehyde produced is assimilated into cell carbon, part is further oxidised to  $\text{CO}_2$  for energy generation (Fuchs & Schlegel, 2007). The requirement of  $\text{O}_2$  as a reactant in the initial oxidation step of methane explains why methanotrophic bacteria are generally obligate aerobes (Madigan *et al.*, 2009). There are however some bacteria and archaea able to oxidise methane under anoxic conditions, by coupling methane oxidation either to sulfate reduction (Knittel & Boetius, 2009), denitrification (Ettwig *et al.*, 2010; Haroon *et al.*, 2013) or reduction of iron or manganese oxides (Beal *et al.*, 2009).

(ii) *Methane oxidation under anoxic conditions*

In recent years, a number of studies have revealed that there are microorganisms able to oxidise methane under anoxic conditions (Knittel & Boetius, 2009; Ettwig *et al.*, 2010; Haroon *et al.*, 2013). In some cases, the anaerobic oxidation of methane (AOM) is afforded by symbiotic relationships between microorganisms, in other cases a single microorganism is able to carry out the process. In some cases, the responsible microorganisms have not yet been identified.

Anaerobic methane oxidation (AOM) driven by  $\text{SO}_4^{2-}$  is mediated by a syntrophic consortium of archaea and sulfate-reducing bacteria (Knittel & Boetius, 2009). The archaeal partner is the “anaerobic methanotroph” (ANME). ANME archaea are very closely related to methanogenic archaea and it has been suggested that AOM is an enzymatic reversal of methanogenesis (Scheller *et al.*, 2010). Because the responsible organisms have not been isolated, it is still unclear how the syntrophic partners interact and which intermediates are exchanged between the archaeal and bacterial cell. Similarly, AOM coupled to the reduction of manganese (birnessite) and iron (ferrihydrite), respectively, has been demonstrated in enrichment cultures containing both bacteria and archaea from marine methane seeps (Beal *et al.*, 2009).

Nitrite-dependent anaerobic methane oxidation (n-damo) is a recently discovered process mediated by the uncultivated bacterium *Candidatus Methylophilus oxyfera* (member of the NC10 phylum). Based on isotopic labelling experiments, it is hypothesised that *M. oxyfera* has an unusual intra-aerobic pathway for the production of oxygen via the dismutation of nitric oxide (NO) into  $\text{N}_2$  and  $\text{O}_2$  (Ettwig *et al.*, 2010). While *Candidatus M. oxyfera* oxidises  $\text{CH}_4$  in the absence of oxygen, the organism still employs the classic oxygen-requiring MMO (Chistoserdova, 2011). ANME-archaea had previously been co-enriched with *Candidatus M. oxyfera* in bioreactors fed with  $\text{CH}_4$  and  $\text{NO}_3^-$ , raising the possibility that this ANME group may be involved in AOM coupled to  $\text{NO}_3^-$  reduction (Hu *et al.*, 2011; cited after Haroon *et al.*, 2013).

Following on from the discovery of nitrite-driven AMO by *Candidatus M. oxyfera*, a recent study confirmed that the co-enriched ANME archaea, members of a novel archaeal lineage, are able to perform AMO coupled to nitrate reduction (Haroon *et al.*, 2013). The organism, *Methanoperedens nitroreducens*, is able to perform methane oxidation without a partner organism via reverse methanogenesis with  $\text{NO}_3^-$  as the terminal electron acceptor. Interestingly, the  $\text{NO}_2^-$  produced by *M. nitroreducens* is reduced to  $\text{N}_2$  through a syntrophic

relationship with an anammox bacterium. It has been suggested that the genes for  $\text{NO}_3^-$  reduction have been laterally transferred from a bacterial donor (Haroon *et al.*, 2013).

**Table 1.1** Overall reactions for methane oxidation with different electron acceptors.

<b>Methane oxidation process:</b>	<b>Overall reaction</b>
Aerobic:	$\text{CH}_4 + \text{O}_2 \rightarrow \text{CO}_2 + 2 \text{H}_2$
Coupled to sulfate reduction:	$\text{CH}_4 + \text{SO}_4^{2-} \rightarrow \text{HCO}_3^- + \text{HS}^- + \text{H}_2\text{O}$
Coupled to nitrite reduction:	$3 \text{CH}_4 + 8 \text{NO}_2^- + 8 \text{H}^+ \rightarrow 3 \text{CO}_2 + 4 \text{N}_2 + 10 \text{H}_2\text{O}$
Coupled to nitrate reduction:	$\text{CH}_4 + 4 \text{NO}_3^- \rightarrow \text{CO}_2 + 4 \text{NO}_2^- + 2 \text{H}_2\text{O}$
Coupled to manganese reduction:	$\text{CH}_4 + 4 \text{MnO}_2 + 7 \text{H}^+ \rightarrow \text{HCO}_3^- + 4 \text{Mn}^{2+} + 5 \text{H}_2\text{O}$
Coupled to iron reduction:	$\text{CH}_4 + 8 \text{Fe}(\text{OH})_3 + 15 \text{H}^+ \rightarrow \text{HCO}_3^- + 8 \text{Fe}^{2+} + 21 \text{H}_2\text{O}$

(iii) *Formaldehyde metabolism in methanotrophs*

In aerobic methanotrophic bacteria, there are two possible pathways for the assimilation of formaldehyde into cell material: the **ribulose monophosphate (RuMP) cycle** in *gammaproteobacterial* (type I) methanotrophs, or the **serine pathway** in *alphaproteobacterial* (type II) methanotrophs. Some methanotrophs also possess the Calvin-Benson cycle in addition to one of the above pathways, however, only *verrucomicrobial* methanotrophs appear to rely on this route for carbon fixation (Chistoserdova, 2011). Both the RuMP and the serine pathway are also used by non-methanotrophic methylotrophs (details of the pathways are given below in section 1.4.5). The remaining formaldehyde (used for energy generation) is oxidised first to formate and then further to  $\text{CO}_2$  via either one of two unrelated pathways: The first pathway employs enzymes that use the coenzyme **tetrahydrofolate (H<sub>4</sub>Folate)**; the second pathway employs the coenzyme **tetrahydromethanopterin (H<sub>4</sub>MPT)**. At the end of either pathway, electrons from the oxidation of formaldehyde enter the electron transport chain generating a proton motive force from which ATP is synthesised (Madigan *et al.*, 2009). Both pathways are also used by methylotrophs (see below).

### 1.4.3 Methylootrophs

Methylootrophs who use  $C_1$  compounds other than  $CH_4$  are widespread in nature and very diverse, including not only aerobic bacteria, but also yeasts as well as some methanogenic archaea. However, this PhD thesis focuses on aerobic methylootrophic bacteria. Aerobic methylootrophic bacteria include obligate methylootrophs, specialised for use of a few  $C_1$  compounds (e.g. *Methylotenera*, Kalyuzhnaya *et al.*, 2006a), as well as many generalists (facultative methylootrophs) who can use organic acids and sugars, and use  $C_1$  compounds when other substrates are limiting (Fuchs & Schlegel, 2007). Representatives of aerobic methylootrophic bacteria are found within proteobacterial phyla as well as in gram-positive bacteria (Lidstrom, 2006, Boden, 2008).  $C_1$  substrates used by methylootrophs include methanol, methylated amines, halogenated methanes and methylated sulfur species (Anthony, 1982; Lidstrom, 2006). Figure 1.10 gives an overview of the metabolism of  $C_1$  compounds by aerobic methylootrophic bacteria (Lidstrom, 2006).

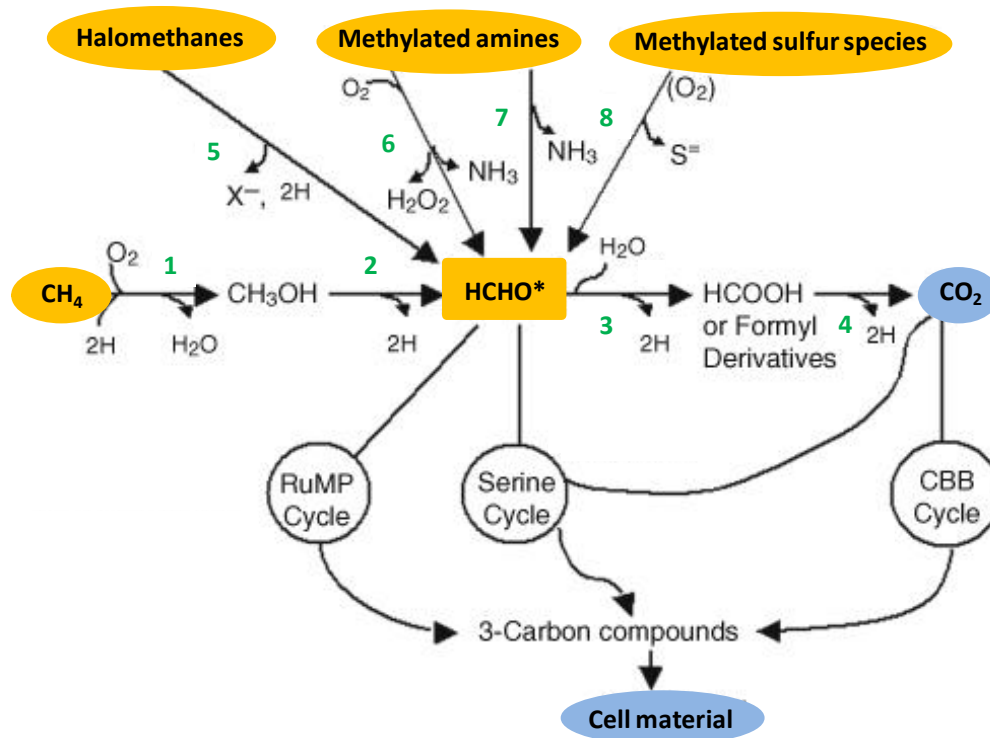


**Figure 1.10** Metabolism of  $C_1$  compounds by aerobic methylootrophs (Lidstrom, 2006)

1, methane monooxygenases; 2, methanol dehydrogenase; 3 formaldehyde oxidation system; 4 formate dehydrogenase, 5, halomethane oxidation system; 6, methylated amine oxidases; 7, methylamine dehydrogenase (or indirect pathway described in Figure 5.1b); 8, methylated sulfur dehydrogenase or oxidase. Abbreviations: RuMP = ribulose monophosphate, CBB = Calvin-Benson-Bassham. \*Note that formaldehyde ( $HCHO$ ) can be bound to  $H_4$ Folate as  $CH_2=H_4$ Folate in some pathways. Image adapted from Lidstrom, 2006

### Anaerobic methylotrophs

While most well-studied methylotrophs are obligate aerobes, denitrifying methylotrophs - such as *Paracoccus denitrificans* and many *Hyphomicrobium* species - are known (Chistoserdova, 2009). However, methylotrophy coupled to use of electron acceptors other than O<sub>2</sub> has so far only been shown for methanotrophs (see above). It has been suggested however that there may be a link between methanol utilisation and denitrification (Chistoserdova, 2009; Kalyuhznaya *et al.*, 2009): Methanol is commonly used as a denitrification-enhancing compound in waste water treatment and several known methylotrophs (belonging to *Methylophilaceae*, *Rhodocyclaceae*, *Paracoccus* and *Hyphomicrobium*, respectively) have been detected in the sludge communities (Chistoserdova, 2009). While it remains unclear whether the same organisms that perform denitrification consume methanol (Chistoserdova, 2009), some methylotrophs from the genus *Methylotenera* have been reported to require NO<sub>3</sub><sup>-</sup> for growth on methanol under aerobic conditions, even when NH<sub>4</sub><sup>+</sup> is present, suggesting use of NO<sub>3</sub><sup>-</sup> as an electron acceptor rather than just a source of nitrogen (Kalyuhznaya *et al.*, 2009). However, none of the above organisms have shown growth under anoxic conditions when tested (Kalyuhznaya *et al.*, 2009), making further studies necessary to determine whether methanol is oxidised anaerobically.

There are some methanogenic archaea (from the order *Methanosarcinales*) that are able to use C<sub>1</sub> compounds such as methanol or methylated amines as their sole source of carbon and energy in the absence of H<sub>2</sub> as an electron donor. In this case, the C<sub>1</sub> substrate functions both as electron donor and electron acceptor (=disproportionation): Some of the methyl groups are oxidised to CO<sub>2</sub> (which is then assimilated into cell carbon via the reductive acetyl-CoA pathway), and some methyl groups are reduced to CH<sub>4</sub>, using the electrons released from the oxidation part of the pathway (Fuchs & Schlegel, 2007).

For example: **4 CH<sub>3</sub>OH → 3 CH<sub>4</sub> + CO<sub>2</sub> + 2 H<sub>2</sub>O**

In this example, one molecule of methanol is oxidised to CO<sub>2</sub>, providing enough electrons for the reduction of three molecules of methanol to CH<sub>4</sub>. Or, in other words, three molecules of methanol have to be reduced to methane for the oxidation of one molecule of methanol to CO<sub>2</sub>. A methanogenic archaeon capable of methylotrophic growth on methylated amines was recently isolated from Movile Cave (Ganzert *et al.*, 2014), indicating that methylated amines may be an important growth substrate not only for aerobic methylotrophs, but also for methanogenic archaea thriving in the anoxic regions of Movile Cave.

A further group of strict anaerobes able to grow methylotrophically are the homoacetogenic bacteria, organisms that catalyse the formation of acetate from CO<sub>2</sub> or C<sub>1</sub> units (Diekert & Wohlfahrt, 1994). Like methanogens, these organisms mainly use H<sub>2</sub> plus CO<sub>2</sub> as growth substrates. Instead of H<sub>2</sub>, homoacetogens can also use multi-carbon compounds and C<sub>1</sub> compounds (e.g. CO, formate or methyl compounds) as electron donors (Madigan *et al.*, 2009). The most important methyl substrates used by homoacetogens are methanol, methyl chloride and methoxylated aromatic compounds (only the methoxyl group is used in the latter case) (Diekert & Wohlfahrt, 1994).

**Table 1.2** Overall reactions for aerobic and anaerobic oxidation of methylated substrates

Methylotrophic substrate	Aerobic Oxidation (Aerobic bacteria)	Anaerobic disproportionation ( <i>Methanosarcinales</i> )	Anaerobic oxidation (Homoacetogenic bacteria)
Methanol	2 CH <sub>3</sub> OH + 3 O <sub>2</sub> → 2 CO <sub>2</sub> + 4 H <sub>2</sub> O (ΔG <sup>0r</sup> = -1379 kJ mol <sup>-1</sup> )	4 CH <sub>3</sub> OH → 3 CH <sub>4</sub> + CO <sub>2</sub> + 2 H <sub>2</sub> O (ΔG <sup>0r</sup> = -265 kJ mol <sup>-1</sup> )	4 CH <sub>3</sub> OH + 2 CO <sub>2</sub> + 2 H <sub>2</sub> O → 3 C <sub>2</sub> H <sub>3</sub> O <sub>2</sub> <sup>-</sup> + 7 H <sup>+</sup> + 4 OH <sup>-</sup> (ΔG <sup>0r</sup> = -672 kJ mol <sup>-1</sup> )
MMA	2 CH <sub>3</sub> NH <sub>2</sub> + 3 O <sub>2</sub> + 2 H <sup>+</sup> → 2 NH <sub>4</sub> <sup>+</sup> + 2 CO <sub>2</sub> + 2 H <sub>2</sub> O (ΔG <sup>0r</sup> = -1339 kJ mol <sup>-1</sup> )	4 CH <sub>3</sub> NH <sub>2</sub> + 2 H <sub>2</sub> O + 4 H <sup>+</sup> → 3 CH <sub>4</sub> + CO <sub>2</sub> + 4 NH <sub>4</sub> <sup>+</sup> (ΔG <sup>0r</sup> = -94 kJ mol <sup>-1</sup> )	4 CH <sub>3</sub> NH <sub>2</sub> + 2 CO <sub>2</sub> + 6 H <sub>2</sub> O → 3 C <sub>2</sub> H <sub>4</sub> O <sub>2</sub> + 4 NH <sub>4</sub> <sup>+</sup> + 4 OH <sup>-</sup> ? (ΔG <sup>0r</sup> = -333 kJ mol <sup>-1</sup> )
DMA	(CH <sub>3</sub> ) <sub>2</sub> NH + 3 O <sub>2</sub> + H <sup>+</sup> → NH <sub>4</sub> <sup>+</sup> + 2 CO <sub>2</sub> + 2 H <sub>2</sub> O (ΔG <sup>0r</sup> = -1359 kJ mol <sup>-1</sup> )	2(CH <sub>3</sub> ) <sub>2</sub> NH + 2 H <sub>2</sub> O + 2H <sup>+</sup> → 3 CH <sub>4</sub> + CO <sub>2</sub> + 2 NH <sub>4</sub> <sup>+</sup> (ΔG <sup>0r</sup> = -131 kJ mol <sup>-1</sup> )	2 (CH <sub>3</sub> ) <sub>2</sub> NH + 2 CO <sub>2</sub> + 7 H <sub>2</sub> O → 3 C <sub>2</sub> H <sub>4</sub> O <sub>2</sub> + 2 NH <sub>4</sub> <sup>+</sup> + 5 OH <sup>-</sup> + 3H <sup>+</sup> ? (ΔG <sup>0r</sup> = -451 kJ mol <sup>-1</sup> )
TMA	2 (CH <sub>3</sub> ) <sub>3</sub> N + 9 O <sub>2</sub> + 2 H <sup>+</sup> → 2 NH <sub>4</sub> <sup>+</sup> + 6 CO <sub>2</sub> + 6 H <sub>2</sub> O (ΔG <sup>0r</sup> = -4084 kJ mol <sup>-1</sup> )	4 (CH <sub>3</sub> ) <sub>3</sub> N + 6 H <sub>2</sub> O + 4 H <sup>+</sup> → 9 CH <sub>4</sub> + 3 CO <sub>2</sub> + 4 NH <sub>4</sub> <sup>+</sup> (ΔG <sup>0r</sup> = -414 kJ mol <sup>-1</sup> )	4 (CH <sub>3</sub> ) <sub>3</sub> N + 6 CO <sub>2</sub> + 6 H <sub>2</sub> O + 4H <sup>+</sup> → 9 C <sub>2</sub> H <sub>4</sub> O <sub>2</sub> + 4 NH <sub>4</sub> <sup>+</sup> ? (ΔG <sup>0r</sup> = -160 kJ mol <sup>-1</sup> )

ΔG<sup>0r</sup> calculations are based on ΔG<sub>f</sub><sup>0r</sup> values for aqueous compounds at pH7 as listed in Supplementary Table S1, Appendix. Note: Growth of homoacetogens with methylated amines has not yet been reported to the author's knowledge.

#### 1.4.4 Formaldehyde oxidation

Oxidation of formaldehyde is an important step in methylotrophic metabolism, not only in terms of energy generation but also to keep intracellular levels of formaldehyde at non-toxic levels. Many methylotrophs possess more than one formaldehyde oxidation pathway (Chistoserdova, 2011).

(i) *Linear pathways*

There are four linear pathways for formaldehyde oxidation: The simplest formaldehyde oxidation system is by one of several **formaldehyde dehydrogenases** which convert formaldehyde to formate. Formaldehyde dehydrogenases can be NAD<sup>-</sup>, mycothiol- or glutathione-linked (Lidstrom, 2006). However, it has been suggested that formaldehyde dehydrogenases function mainly in formaldehyde detoxification rather than playing a major dissimilatory role (Lidstrom *et al.*, 2006). An alternative formaldehyde oxidation pathway in methylotrophs involves tetrahydrofolate (H<sub>4</sub>Folate), a coenzyme widely involved in C<sub>1</sub> transformations (Fuchs & Schlegel, 2007). In this pathway, formaldehyde is bound to H<sub>4</sub>Folate as **5,10-methylene tetrahydrofolate (CH<sub>2</sub>=H<sub>4</sub>Folate)**, which is then oxidised to formate and H<sub>4</sub>Folate. A third, analogous, formaldehyde dissimilation pathway, involves tetrahydromethanopterin (H<sub>4</sub>MPT), a cofactor which also functions as a C<sub>1</sub> carrier during the reduction of CO<sub>2</sub> to CH<sub>4</sub> by methanogenic *Archaea* (Fuchs & Schlegel, 2007). In this pathway formaldehyde is bound to H<sub>4</sub>MPT as **methylene tetrahydromethanopterin (CH<sub>2</sub>=H<sub>4</sub>MPT)**, which is then oxidised to methenyl H<sub>4</sub>MPT (CH-H<sub>4</sub>MPT). The details of the final oxidation step in this pathway are still not known. This elaborate, multi-enzyme pathway appears to be the most widespread formaldehyde oxidation system in methylotrophs (although serving an auxiliary function in those organisms that possess the cyclic formaldehyde oxidation pathway) (Chistoserdova, 2011). In all three of these pathways, the resulting formate is oxidised to CO<sub>2</sub> by formate dehydrogenase (Lidstrom, 2006). Finally, anaerobic methylotrophs use the **reductive acetyl-CoA pathway** (see below); this pathway serves both the oxidation of C<sub>1</sub> compounds to CO<sub>2</sub> and the assimilation of C<sub>1</sub> compounds into cell material via acetyl-CoA.

(ii) *Cyclic pathway*

In addition to these linear formaldehyde oxidation pathways, a **cyclic formaldehyde oxidation pathway** exists which employs the reactions and enzymes of the ribulose monophosphate (RuMP) pathway used for formaldehyde assimilation (see below), with addition of the enzyme 6-phosphogluconate dehydrogenase (Lidstrom 2006; Chistoserdova, 2011). In methylotrophs possessing this pathway along with one of the linear pathways, the cyclic pathway seems to be the major mode of formaldehyde detoxification and oxidation (Chistoserdova, 2011).

### 1.4.5 Formaldehyde assimilation

The assimilation of formaldehyde into one of the precursor molecules that enter central metabolism for assimilation into biomass can proceed via a number of pathways: In the **RuMP cycle** all carbon is assimilated at the level of formaldehyde, while in the **serine cycle**, some carbon is assimilated at the level of CO<sub>2</sub>. Those methylootrophs that use the **Calvin-Benson cycle** assimilate all C<sub>1</sub> units at the level of CO<sub>2</sub> (Fuchs & Schlegel, 2007, Chistoserdova, 2011). In principle, the aerobic formaldehyde assimilation pathways could also function in anaerobes (Fuchs, 2009). However, anaerobic methylootrophs use the **reductive acetyl CoA pathway** (the same pathway that is also used for CO<sub>2</sub> fixation by strictly anaerobic autotrophs).

#### 1) Ribulose monophosphate cycle (RuMP cycle)

The ribulose monophosphate cycle (RuMP cycle, also hexulose phosphate cycle; Figure 1.11) is used by type I methanotrophs and some facultative methylootrophs. This cyclic pathway involves the condensation of formaldehyde with a five-carbon acceptor molecule, followed by oxidation of the resulting six-carbon compound (Lidstrom, 2006). The carbohydrate products of the RuMP cycle are three-carbon sugar phosphate molecules, or **triose phosphates**, (also glyceraldehyde 3-phosphate, G3P). The net reaction after three rounds of the cycle is (Fuchs & Schlegel, 2007):



Three formaldehyde molecules thus generate one triose phosphate which enters the central metabolism for assimilation into cell carbon. The RuMP cycle therefore bears similarity to the Calvin-Benson cycle (Fuchs & Schlegel, 2007). The substrate for the initial reaction in this pathway, ribulose-5-phosphate (RuMP), is very similar to the C<sub>1</sub> acceptor in the Calvin-Benson cycle, ribulose 1,5 bisphosphate (Madigan *et al.*, 2009).

A schematic overview of the RuMP cycle is given in **Figure 1.11**: In the first step of assimilation, free formaldehyde is added to the metabolite ribulose-5-phosphate **(1)**. The product of this condensation reaction, hexulose-6-phosphate, is then isomerised to fructose-6-phosphate **(2)**. Out of three molecules fructose-6-phosphate, two are assimilated into four molecules triose phosphate (via the intermediate fructose-1,6-bisphosphate), a step that requires two molecules of ATP **(3)**. One molecule of triose phosphate leaves the cycle for cell synthesis **(4)**; the remaining three are rearranged together with the third molecule of fructose-

6-phosphate to re-generate the formaldehyde acceptor ribulose-5-phosphate (5) (Fuchs & Schlegel, 2007; Madigan *et al.*, 2009). Only two enzymes, hexulose phosphate synthase (HPS) and hexulose 6-P isomerase (HPI), are specific to the RuMP cycle (Chistoserdova 2011) (the remaining enzymes of this pathway are common in sugar transformations in many organisms), and high activities of these enzymes are typically signatures of methylotrophy via the RuMP cycle (Anthony, 1982, Lidstrom, 2006). It should be noted however that the RuMP cycle is also used for formaldehyde detoxification by non-methylotrophic bacteria (Chistoserdova, 2011).

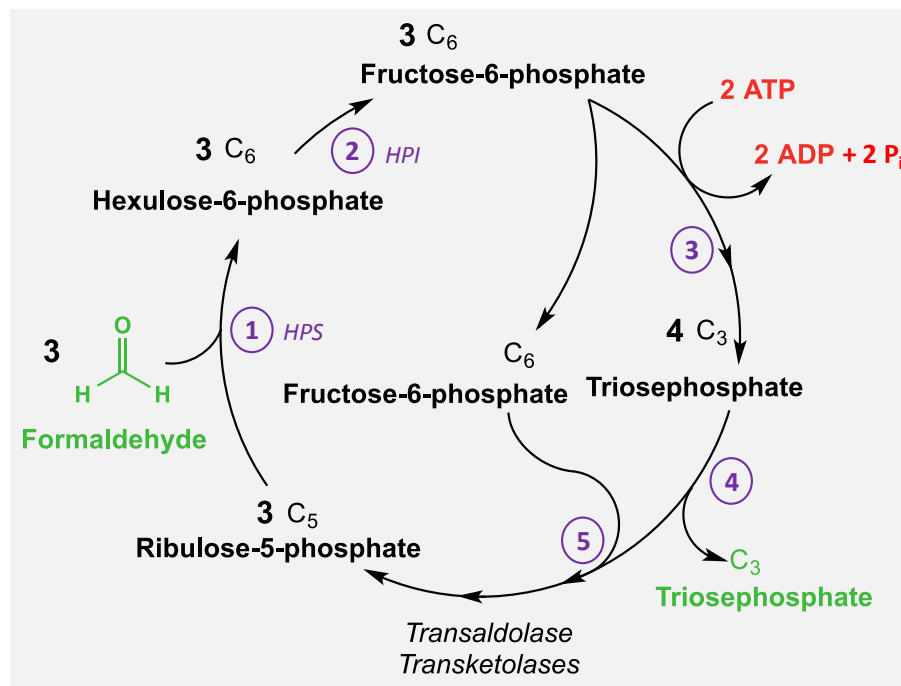


**Figure 1.11** The ribulose monophosphate (RuMP) cycle

Abbreviations: HPS, hexulose phosphate synthase; HPI, hexulose 6-P isomerase

The RuMP cycle is more efficient than the serine cycle because all of the carbon for cell material is derived from formaldehyde, and because formaldehyde is at the same oxidation level as cell material, no reducing power is needed (Madigan *et al.*, 2009).

## 2) Serine cycle

In this pathway, a two-carbon unit, acetyl-CoA, is synthesised from one molecule of 5,10-methylenetetrahydrofolate ( $\text{CH}_2=\text{H}_4\text{Folate}$ ) and one molecule of  $\text{CO}_2$  through a series of reactions involving amino acids and organic acids (**Figure 1.12**):  $\text{CH}_2=\text{H}_4\text{Folate}$  (abbreviated as  $\text{CH}_2=\text{THF}$  in Figure) and glycine are condensed to form serine, releasing  $\text{H}_4\text{Folate}$  (THF in

Figure) (1). Serine is further converted to PEP in a stepwise reaction (2-5) via hydroxypyruvate, glycerate (using one NADH) and 3-phosphoglycerate (using 1 ATP). Under addition of a molecule of CO<sub>2</sub>, PEP is converted to oxaloacetate (6), which in turn is reduced to malate (using one NADH) (7). Malate is activated to malyl-coA (using 1 ATP) (8) which is cleaved into two C<sub>2</sub>-compounds, acetyl-CoA and glyoxylate (9). The amino group from serine is transferred onto glyoxylate (10), thus regenerating the formaldehyde acceptor glycine, completing the cycle. In total, the serine pathway requires two NADH for reducing power and two ATP for energy for every acetyl-CoA synthesised. Acetyl-CoA is assimilated into biomass via the glyoxylate cycle (Fuchs & Schlegel, 2007). The serine pathway is specific to methylotrophs (Chistoserdova, 2011) but it uses a number of enzymes also involved in other common metabolic pathways (such as the citric acid cycle) and one enzyme, serine transhydroxymethylase (STHM), unique to this pathway (Madigan *et al.*, 2009). The other two key enzymes of the serine cycle are hydroxypyruvate reductase (HPR) and serine glyoxylate aminotransferase (SGA) (Chistoserdova, 2011). The overall reaction of the serine cycle can be summarised as:

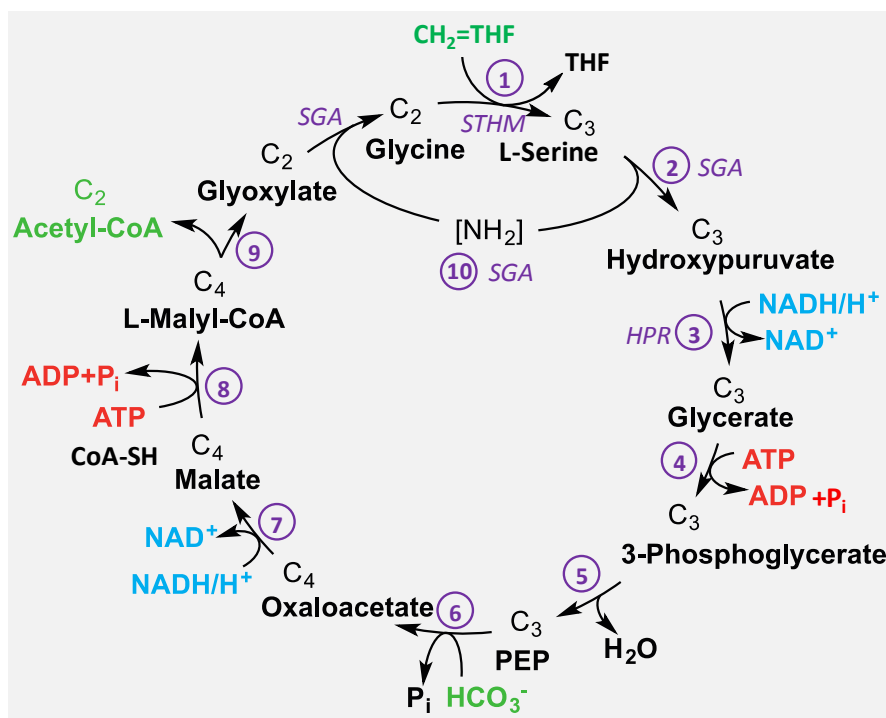
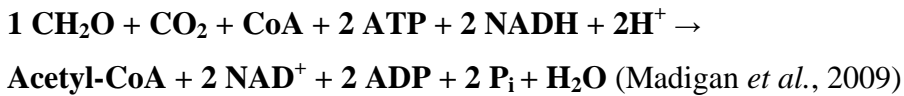


**Figure 1.12** The serine cycle

Abbreviations: THF, tetrahydrofolate; STHM, serine transhydroxymethylase; CoA-SH, Coenzyme A  
SGA, serine glyoxylate aminotransferase; HPR, hydroxypyruvate reductase

### 3) Reductive Acetyl-CoA pathway (anaerobic pathway)

The reductive acetyl-CoA pathway (also Wood-Ljungdahl pathway) is used by strict anaerobes as a means of carbon fixation as well as energy conservation from  $\text{CO}_2$  or  $\text{C}_1$  compounds (Fuchs & Schlegel, 2007). In addition to anaerobic autotrophs (homoacetogens, methanogens, some sulfate reducing bacteria and archaea) this unusual pathway is also used by anaerobic methylotrophs (i.e. certain methanogens and homoacetogens, see above). The reductive acetyl-CoA pathway catalyses the parallel reduction of two  $\text{C}_1$  units (from  $\text{CO}_2$  or  $\text{C}_1$  compounds) to acetyl-CoA, catalysed by the bifunctional key enzyme CO dehydrogenase / acetyl-CoA synthase (**Figure 1.13**): one  $\text{C}_1$  molecule is reduced to the methyl group of acetyl-CoA (by a series of reactions involving either the coenzyme  $\text{H}_4\text{Folate}$  or the coenzyme  $\text{H}_4\text{MPT}$ ), while the other  $\text{C}_1$  unit ends up in the carbonyl position. The two units are then assembled to form acetyl-CoA. ATP is synthesised when a sodium motive force is established during the formation of acetyl CoA (in homoacetogens, there are additional energy-conserving steps during the conversion of acetyl-CoA to acetate.) Acetyl-CoA, the end product of the pathway, is subsequently converted to triose phosphate which enters central metabolism for assimilation of carbon into cell material (Madigan *et al.*, 2009; Fuchs & Schlegel, 2007).

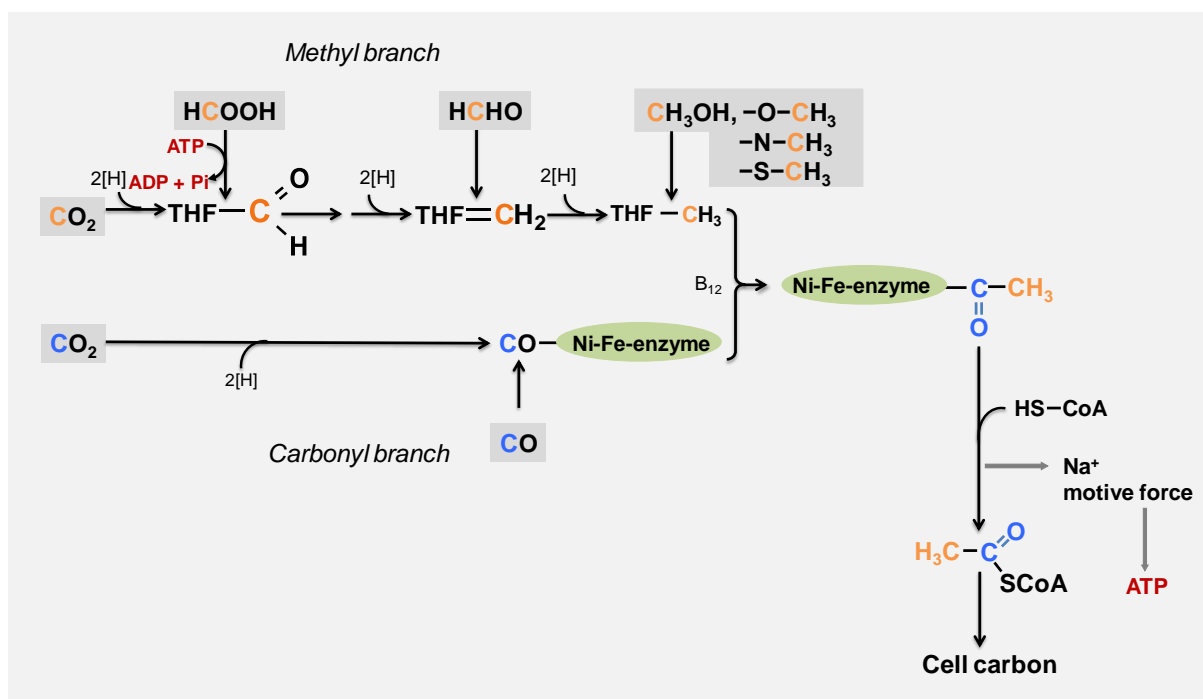


**Figure 1.13** The reductive Acetyl-CoA pathway (image adapted from Fuchs & Schlegel, 2007)

Abbreviations: THF, tetrahydrofolate; HS-CoA, Coenzyme A

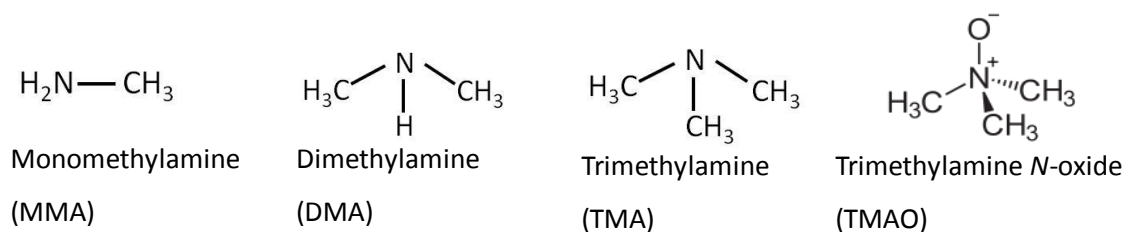
#### 4) Assimilation of C<sub>1</sub> units via the Calvin-Benson cycle

In addition to the above pathways which assimilate carbon at the level of formaldehyde, some methylotrophs assimilate carbon at the level of CO<sub>2</sub> (resulting from the oxidation of formaldehyde), using the classic Calvin-Benson cycle. These methylotrophs are sometimes referred to as “autotrophic methylotrophs” (Anthony, 1982). Some methylotrophs use the Calvin-Benson cycle as their only means of C<sub>1</sub> assimilation, others in addition to other C<sub>1</sub> assimilatory cycles (assimilation of C<sub>1</sub> compounds at the oxidation state of formaldehyde affords major energy savings compared to carbon assimilation from CO<sub>2</sub>, Madigan *et al.*, 2009). Methylotrophs that use the Calvin-Benson cycle include *alphaproteobacterial* methylotrophs (e.g. species of *Paracoccus* and *Xanthobacter*), methanotrophic *Verrucomicrobia* (*M. infernorum*) and methanotrophs of the NC10 phylum (*Candidatus M. oxyfera*) (Chistoserdova, 2011).

### 1.5 Methylated amines as carbon, energy and nitrogen sources

The role of methylated amines as carbon, energy and nitrogen sources for bacteria in Movile Cave is the main subject explored in this PhD thesis. Methylated amines are dissolved organic nitrogen compounds produced during the decomposition of protein (Lee, 1988; Neff *et al.*, 2003). Typically, methylated amines are associated with saline ecosystems (Lee, 1988; Wang & Lee, 1990; Abdul-Rashid *et al.*, 1991, Gibb *et al.*, 1995; Fitzsimons *et al.*, 1997, 2001, 2006), where they are largely produced during degradation of trimethylamine *N*-oxide (TMAO) and glycine betaine, compounds commonly used as protein-stabilising osmolytes by marine organisms (Barrett, 1985; King, 1988; Lin & Timasheff, 1994). Major anthropogenic sources of methylated amines are animal husbandry, biomass-burning and pesticides (Latypova *et al.*, 2010). There are fewer studies on the distribution of methylated amines in terrestrial and freshwater environments (e.g. Yu *et al.*, 2002). Usually, methylated amines are present at low concentrations in natural environments, likely due to rapid microbial degradation (Oremland *et al.*, 1982; King *et al.*, 1983, cited after Latypova *et al.*, 2010).

Formally, methylated amines are derivatives of ammonia, where one or more hydrogen atoms have been replaced with a methyl group, resulting in primary, secondary or tertiary amines:



Methylotrophs utilising methylated amines as a carbon and energy source are phylogenetically diverse, ubiquitous in the environment and often metabolically versatile (e.g. Bellion & Hersh, 1972; Colby & Zatman, 1973; Levering *et al.*, 1981; Anthony, 1982; Bellion & Bolbot, 1983; Brooke & Attwood, 1984; Kalyuzhnaya *et al.*, 2006b; Boden *et al.*, 2008). New methylotrophs are still being identified from a wide range of environments, including genera not previously associated with methylotrophy, and novel metabolic pathways (see recent reviews by Chistoserdova *et al.*, 2009; Chistoserdova 2011). Generally, methylotrophs who use methylated amines for carbon and energy purposes also use the resulting  $\text{NH}_4^+$  as a nitrogen source. However, there may be exceptions where additional  $\text{NH}_4^+$  is required for growth on methylated amines (Chistoserdova, 2009).

In addition to being methylotrophic substrates, methylated amines can also be used as a nitrogen (but not carbon) source by a wide range of non-methylotrophic bacteria (Bicknell & Owens, 1980). As discussed above, dissolved organic nitrogen (DON) compounds are increasingly being recognised as a major source of nitrogen for microorganisms and phytoplankton (Bronk, 2002; Berman & Bronk, 2003; Worsfold *et al.*, 2008). While utilisation of monomethylamine (MMA) as a bacterial nitrogen source was reported over 40 years ago (Budd & Spencer, 1968, Bicknell & Owens, 1980; Murrell & Lidstrom, 1983; Glenn & Dillworth, 1984), details of the metabolic pathways involved have only recently been identified (Latypova *et al.*, 2010; Chen *et al.*, 2010a, 2010b). The details of these pathways are covered in the introduction to Chapter 5. Sequestering nitrogen without assimilating the carbon from methylated amines means that the  $\text{C}_1$  units from MAs need to be further oxidised. In *Roseobacter* Clade bacteria it has been shown that  $\text{H}_4\text{F}$  is the  $\text{C}_1$  carrier for this (Chen, 2012), but other  $\text{C}_1$  oxidation pathways (see above) might be used by other non-methylotrophs.

For completeness, it should be pointed out that recent studies on methylated amine metabolism in the ocean have revealed that some heterotrophic bacteria appear to oxidise  $\text{C}_1$  compounds (including TMA and TMAO) purely for energy generation, without assimilating the carbon (Boden *et al.*, 2011; Sun *et al.*, 2011; Lidbury *et al.*, 2014). These studies suggest

that methylated amines, in addition to being methylotrophic substrates and nitrogen sources, may also be important energy sources for heterotrophic bacteria.

### **Metabolism of methylated amines**

Metabolism of higher methylated amines (DMA, TMA, TMAO) involves the stepwise demethylation of the substrate to MMA, removing one methyl group a time (Anthony, 1982). This means metabolism of methylated amines always involves the utilisation of MMA. In general, the methyl groups of methylotrophic substrates are oxidised to the level of formaldehyde by oxidases and / or dehydrogenases (the dehydrogenases are generally coupled to energy metabolism while the oxidases are usually non-energy conserving, Lidstrom, 2006).

TMA can be oxidised to DMA via two different pathways in Proteobacteria (Anthony, 1982; Lidstrom, 2006; Chen, 2012): In the first pathway, TMA is oxidised to DMA and formaldehyde by TMA dehydrogenase. In the second pathway, a TMA monooxygenase oxidises TMA to TMAO, which is subsequently demethylated to DMA and formaldehyde by TMAO demethylase. This pathway is also used by non-methyltrophs to sequester N from TMA (Chen, 2012). DMA is oxidised to MMA and formaldehyde by DMA monooxygenase. The detailed MMA oxidation pathways are covered in the introduction to Chapter 5 in connection with key marker genes for the identification of methylated amine-utilising bacteria. Briefly, MMA utilisation occurs either by oxidation of MMA into formaldehyde (by MMA dehydrogenase or MMA oxidase), only found in methylotrophic bacteria so far (Gruffaz *et al.*, 2014), or by an indirect pathway involving the stepwise oxidation to methylene- $H_4F$  via one or more methylated amino acids. In both cases, the resulting intermediate formaldehyde is metabolised via the normal methylotrophic assimilatory and dissimilatory pathways (see above).

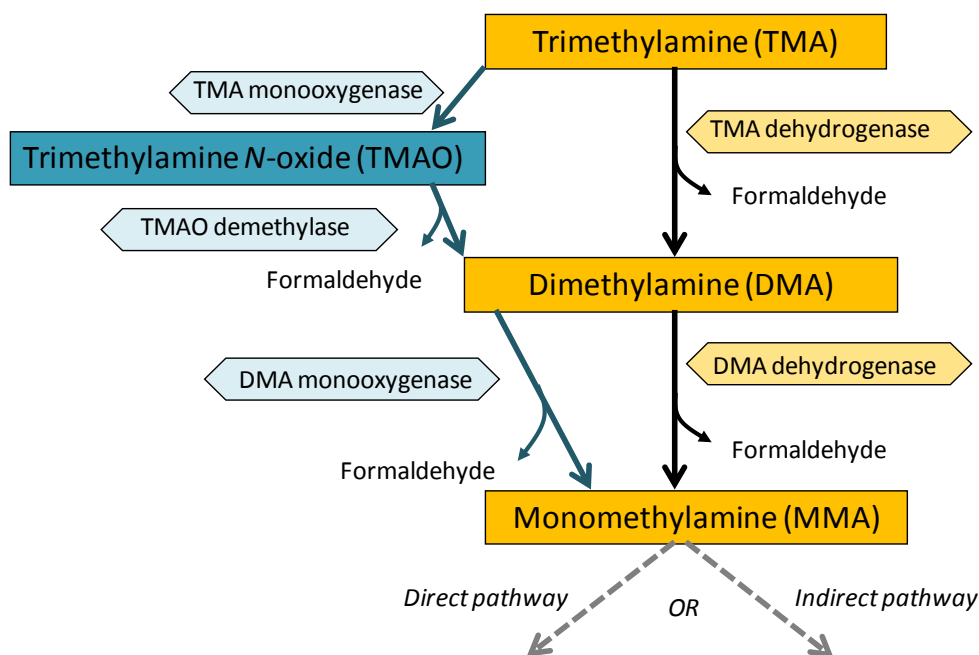


**Figure 1.14** Demethylation of trimethylamine (TMA) to monomethylamine (MMA) (Image modified from Chen, 2012). For monomethylamine oxidation pathways see Figure 5.1

The  $\text{NH}_4^+$  produced during the degradation of methylated amines is used as a nitrogen source through assimilation into glutamine and glutamate, the precursors for the synthesis of cellular nitrogen compounds, via one of the bona fide  $\text{NH}_4^+$  assimilation pathways: Glutamate can be synthesised either via an NADP-linked glutamate dehydrogenase (GDH), or via the combined action of glutamine synthetase (GS) and glutamate synthase (glutamine oxoglutarate aminotransferase, GOGAT) in the GS-GOGAT pathway. The latter pathway is generally used under low  $\text{NH}_4^+$  concentrations, due to the higher affinity of GS to  $\text{NH}_4^+$  compared with GDH (Baev *et al.*, 1997; Chen, 2012).

## 1.6 Aims and approach of this PhD project

As outlined above, existing studies of the microbial food web in Movile Cave have not yet investigated the nitrogen cycle in this unusual ecosystem. Therefore, the overall aim of this PhD project was to gain insight into selected processes of the microbial nitrogen cycle in Movile Cave and identify key organisms actively involved in these processes. With the emphasis being on the utilisation of methylated amines as both carbon and nitrogen sources, the project also touched upon the carbon cycle in Movile Cave. (Previous studies on methylotrophy in Movile Cave have focused on methane and methanol utilisation; Hutchens *et al.*, 2004). In addition to methylated amine utilisation, the roles of nitrification and

N<sub>2</sub>-fixation were investigated. Other aspects of the nitrogen cycle were only touched upon using PCR-based studies. In the course of the PhD project the focus shifted increasingly towards methylated amine utilisation as this aspect generated the most results. Studies conducted on nitrification, N<sub>2</sub> fixation and other aspects of the nitrogen cycle, while producing some interesting results, are of a preliminary nature and require further investigation.

### *1.6.1 Techniques used in this study*

To determine the microbial key players involved in selected processes relating to nitrogen and carbon cycling in Movile Cave, an integrated approach combining cultivation-based studies and molecular methods was used. As a key method, DNA-stable isotope probing (SIP, Radajewski *et al.*, 2000; Murrell & Whiteley, 2010) was applied as it allows linking the microbial processes of interest to the phylogenetic identity of the active organisms. Isolation studies, process-based measurements and PCR based surveys of key genes were also applied.

### *1.6.2 Key questions of the PhD thesis*

The specific research questions of this PhD thesis were:

- 1. What is the role of methylated amines as a carbon and nitrogen source for bacteria in Movile Cave?***

The role of methylated amines as carbon and nitrogen sources for microorganisms in Movile Cave was addressed by a combination of DNA-SIP and isolation-based studies. Methylotrophic bacteria (organisms utilising C<sub>1</sub> compounds as their sole source of carbon and energy) are known to be present and active in Movile Cave from previous studies (Hutchens *et al.*, 2004; Chen *et al.* 2009). Furthermore, the high organic matter content in the floating mats warrants it likely that methylated amines are major degradation products. Methylated amine-utilising bacteria were therefore expected to play a significant role in the cycling of carbon and nitrogen in the cave.

DNA-SIP with <sup>13</sup>C-labelled MMA and DMA was applied to identify active methylotrophic bacteria in Movile Cave. The SIP incubations were analysed over a time course in order to monitor any changes in the active community and detect possible cross-feeding effects. To consolidate results from SIP experiments, bacterial isolates

retrieved from selective enrichments with methylated amines were tested with respect to their metabolic capabilities. In addition, PCR primers targeting *gmaS*, a key gene in the recently characterised indirect MMA oxidation pathway were developed as part of this PhD project. The new primers were used to determine the distribution of *gmaS* among bacterial isolates from Movile Cave. The presence of *gmaS* in Movile Cave enrichment cultures and floating mat samples was also assessed using the new primers.

***Hypothesis:***

Methylated amines are a major degradation product in Movile Cave (derived from the decomposition of extensive organic mats) and are an important source of carbon, energy and nitrogen for Movile Cave bacteria.

***Aims:***

- *Identification of major methylated amine-utilising methylotrophs in Movile Cave*
  - *Identification of bacteria using methylated amines as a nitrogen source*
  - *Characterisation of methylated amine-utilising isolates from Movile Cave*
  - *Development of new PCR primers for the detection of methylated-amine utilising bacteria*
2. ***What is the contribution of nitrifying microorganisms to primary production in Movile Cave?***

The second key question of this PhD was to determine the role of nitrifying bacteria (and possibly archaea) to primary production in Movile Cave. SIP-based studies by Chen *et al.* (2009), have suggested that the oxidation of ammonia and nitrite may be important autotrophic processes in Movile Cave, supplying fixed carbon into the food web. So far however, sulfur oxidisers are believed to be the main CO<sub>2</sub>-fixing microorganisms in Movile Cave. DNA-SIP studies with <sup>13</sup>C-labelled bicarbonate (with and without added energy sources in form of ammonia or reduced sulfur compounds) were set up with water and microbial mat to determine the most active autotrophs. In addition to 16S rRNA gene-based primers, bacterial and archaeal *amoA* gene-specific primers and *nrxB*-specific primers were used as biomarkers to determine the presence of nitrifiers in the SIP-

incubations. Potential nitrification rates were determined by monitoring ammonium consumption and nitrite production over time.

***Hypothesis:***

Nitrifying microorganisms play a major role in CO<sub>2</sub> fixation in the Movile Cave food web.

***Aims:***

- *To assess whether nitrifiers have an active role in CO<sub>2</sub> fixation in Movile Cave in addition to sulfur oxidisers*
- *To identify key autotrophs in Movile Cave*
- *To determine whether archaea may have a role in ammonia oxidation in addition to bacterial nitrifiers in Movile Cave*

3. ***Is there a potential role for N<sub>2</sub>-fixers in Movile Cave?***

To determine whether there is a possible contribution of microbial N<sub>2</sub> fixation to the nitrogen cycle in Movile Cave, acetylene reduction assays were carried out with water and floating mat samples to detect any N<sub>2</sub>-fixing activity. Many bacteria in the cave (e.g. *Beggiatoa*) are known to be capable of diazotrophic growth and, while standing concentrations of NH<sub>4</sub><sup>+</sup> in the cave waters are relatively high, there may be NH<sub>4</sub><sup>+</sup>-depleted zones in which N<sub>2</sub>-fixation becomes important. In addition to process-based measurements, PCR-based surveys of *nifH* genes in Movile Cave were carried out in order to assess the presence of microorganisms with the genetic potential to fix N<sub>2</sub>, and to assess their diversity. Potential DNA-SIP experiments with <sup>15</sup>N-labelled N<sub>2</sub> were intended based on whether or not N<sub>2</sub> fixers were found to be active in Movile Cave.

***Hypothesis:***

N<sub>2</sub>-fixing microorganisms thrive in the floating mats and provide an important nitrogen source for the wider food web in Movile Cave.

***Aims:***

- *To determine whether there is N<sub>2</sub>-fixing activity in microbial mats in Movile Cave*

- *To assess the diversity of N<sub>2</sub> fixers in Movile Cave using nifH-targeting PCR primers*
- *To identify active N<sub>2</sub>-fixing microorganisms using DNA-SIP with <sup>15</sup>N-labelled N<sub>2</sub>*

4. ***Do denitrification and / or anaerobic ammonium oxidation take place in Movile Cave?***

The microbial community in anoxic regions of Movile Cave is still largely unexplored, even though sulfate-reducing bacteria and denitrifying bacteria have been detected (Rohwerder *et al.*, 2003; Chen *et al.*, 2009). PCR-based surveys of key genes for denitrification and anammox (*nirS*, *nirK* and *hzs*) were conducted on water and sediment samples in addition to process-based studies (isotope pairing experiments).

## **Chapter 2. Materials and Methods**

## 2.1 Chemicals and reagents

All analytical-grade chemicals used in this thesis were obtained from Fisher Scientific (Loughborough, UK), Melford Laboratories Ltd (Ipswich, UK) or Sigma-Aldrich Corporation (St Louis, USA). Reagents of special grade for molecular biology were purchased from Bioline Reagents Ltd. (London, UK), Fermentas Molecular Biology Tools (Leon-Rot, Germany), Promega UK (Southampton, UK) and Roche Diagnostics Ltd. (Burgess Hill, UK). Gases (acetylene, CO<sub>2</sub>, oxygen and nitrogen) were obtained either from BOC (Manchester, UK) or Sigma-Aldrich. Dehydrated culture media and agar were purchased from Oxoid Ltd (Cambridge, UK). General purpose buffers and solutions were prepared according to Sambrook and Russell (2001).

## 2.2 Bacterial strains

*Agrobacterium tumefaciens* C58, *Mesorhizobium loti* MAFF303099, *Pseudomonas fluorescens* SBW25, *Pseudomonas sp.* IMKW, *Sinorhizobium meliloti* 1021 and *Rhizobium leguminosarum* bv. *viciae* 3841 were kindly provided by Yin Chen.

*Azotobacter vinelandii* DJ: Kindly provided by Ray Dixon.

*Methylosinus trichosporium* OB3B: Kindly provided by Julie Scanlan.

*Methylocella silvestris* BL2: Kindly provided by Andrew Crombie.

*Nitrosomonas europaea* NCIMB 11850: Obtained from culture collection of NCIMB Ltd, Aberdeen, UK.

## 2.3 Collection and processing of sample material from Movile Cave

All sample material for this work was collected from Movile Cave, near the town of Mangalia in Romania (for a map of the cave, refer to Figure 1.3). Water and floating mat samples for enrichment and isolation experiments were collected from the lake room and the two air bells in October 2009, refrigerated in the nearby field station and processed within 48 hours. Biofilm covering the limestone walls of both air bells was scraped off into sterile Bijoux tubes. Similar samples for further isolation experiments, stable isotope probing (SIP) enrichments and nucleic acid extractions were obtained from Movile Cave in April 2010 and April 2011. Floating mat samples for metagenome analysis were collected in April 2011. Material for DNA work was centrifuged at 5,000 ×g within one hour of sampling and frozen

at -20°C for storage until processing. DNA-SIP incubations were set up within one hour of sampling, and incubated in the dark at 21°C (see below). Water and sediment material for analytical measurements and isotope pairing experiments was transferred into *Nalgene* bottles which had been acid-washed with HCl and autoclaved beforehand. Bottles were filled to the top to preserve anoxic conditions, refrigerated and processed within 48 hours. Water and sediment for measurement of standing methylamine concentrations were also collected in acid washed *Nalgene* bottles and frozen within 1 hour of sampling.

## 2.4 DNA stable isotope probing (DNA-SIP) experiments

To identify key organisms playing an active role in the cycling of C<sub>1</sub> compounds in Movile Cave, SIP incubations were set up with a range of <sup>13</sup>C-labelled C<sub>1</sub> compounds. Additionally, to identify active chemolithoautotrophs in Movile Cave, <sup>13</sup>C-bicarbonate SIP incubations were set up with and without the addition of 1 mM of different inorganic energy sources. Incubations without addition of energy sources were set up to identify the most active CO<sub>2</sub> fixers under natural conditions. Incubations with added energy sources were set up to stimulate growth of specific chemolithoautotrophs, i.e. nitrifiers or sulfur oxidisers, respectively. Table 2.1 lists all SIP incubations that were set up as part of the Movile Cave food web project; those SIP experiments analysed as part of this PhD project are highlighted.

**Table 2.1** Substrates used for SIP incubations as part of the Movile Cave food web project

	Labelled substrates	Additional unlabelled compounds
01	<sup>13</sup> CH <sub>4</sub> – methane	–
02	<sup>13</sup> CH <sub>3</sub> OH – methanol	–
03	<sup>13</sup> CHOOH <sup>-</sup> – formate	–
04	<sup>13</sup> C <sub>6</sub> H <sub>12</sub> O <sub>6</sub> – glucose	–
05	<sup>13</sup> CH <sub>3</sub> NH <sub>2</sub> – monomethylamine	–
06	( <sup>13</sup> CH <sub>3</sub> ) <sub>2</sub> NH – dimethylamine	–
07	H <sup>13</sup> CO <sub>3</sub> – bicarbonate	NH <sub>4</sub> <sup>+</sup> – ammonium
08	H <sup>13</sup> CO <sub>3</sub> – bicarbonate	S <sub>2</sub> O <sub>3</sub> <sup>2-</sup> – thiosulfate
09	H <sup>13</sup> CO <sub>3</sub> – bicarbonate	S <sub>4</sub> O <sub>6</sub> <sup>2-</sup> – tetrathionate
10	H <sup>13</sup> CO <sub>3</sub> – bicarbonate	–
11	H <sup>13</sup> CO <sub>3</sub> – bicarbonate	<sup>12</sup> CH <sub>4</sub> – methane
12	<sup>13</sup> CH <sub>4</sub> – methane	H <sup>12</sup> CO <sub>3</sub> – bicarbonate

**SIP incubations with  $^{13}\text{C}$ -MMA**

SIP experiments with monomethylamine (MMA) were set up in April 2010 using water from Airbell 2. The SIP incubations were set up at the field station near the cave within one hour of sampling. For each incubation, a 20 ml aliquot of cave water was added to a pre-sterilised 120 ml serum vial containing 50  $\mu\text{mol}$  of  $^{13}\text{C}$ -labelled or unlabelled ( $^{12}\text{C}$ ) MMA (dissolved in 0.2 ml sterilised distilled water), to give a final concentration of 2.5 mM added substrate. Control incubations with no added MMA (referred to as “no-substrate controls” from here on) were also set up. No floating mat material was used and no replicates could be set up due to limitations in the amount of sample material available (the sample material was used for additional SIP experiments with methane and sulfur compounds as well as isolation experiments and MAR-FISH). All serum vials were immediately re-sealed with a butyl rubber cap and an aluminium crimping lid and incubated at 21°C in the dark. Samples for  $t_0$  ( $t = 0$  days) were prepared by spinning down 20 ml of cave water (5,000  $\times g$ ), discarding the supernatant and freezing the pellet. SIP incubations and no-substrate controls were harvested at time intervals of 48 hours ( $t=1$ ), 96 hours ( $t=2$ ) and four weeks ( $t=3$ ) (separate microcosms were set up for each time point, and the samples were harvested by spinning down the entire contents of the microcosm).

**SIP incubations with  $^{13}\text{C}$ -DMA**

SIP experiments with dimethylamine (DMA) were set up as described above for MMA, adding 50  $\mu\text{mol}$  of  $^{13}\text{C}$ -labelled or unlabelled ( $^{12}\text{C}$ ) DMA to 20 ml cave water (final concentration of 2.5 mM). The same batch of cave water was used and enrichments were harvested at the same time points as for MMA-SIP enrichments.

**SIP incubations with  $^{13}\text{C}$ -bicarbonate and ammonium sulfate**

SIP experiments with  $^{13}\text{C}$ -labelled bicarbonate (for simplicity referred to as  $^{13}\text{CO}_2$  throughout the text) were set up in April 2010, using water from Airbell 2, and in April 2011, using water and floating mat material from Airbell 2. To enhance growth of nitrifying microorganisms, ammonium sulfate was added as an energy source. The first set of incubations (2010) was set up as described above; 50  $\mu\text{mol}$  of labelled or unlabelled bicarbonate was added to 20 ml of cave water along with 1 mM  $(\text{NH}_4)_2\text{SO}_4$ . Incubation conditions and harvesting time points were the same as described above for MMA and DMA.

In April 2011, SIP experiments with  $^{13}\text{C}$ -labelled bicarbonate and ammonium sulfate were repeated using (i) water and (ii) floating mat material from Airbell 2 (separate experiments).

This time, incubations were set up on site in duplicates. For cave water, the sample volume was increased to 50 ml in a 120 ml serum vial. Since the floating mats contain a lot more biomass than water, 20 ml of total sample volume were used as before.  $^{13}\text{C}$ -bicarbonate (or  $^{12}\text{C}$ -bicarbonate for controls with unlabelled substrate) was added to the samples to a final concentration of 2.5 mM,  $(\text{NH}_4)_2\text{SO}_4$  concentrations were 1 mM. Samples were incubated in the dark at 21°C and terminated at the following three time points: 48 h (t1), 1 week (t2), 2 weeks (t3). Incubations with cave water were sacrificed by centrifuging (20 min at 14 000  $\times g$ ) the entire 50 ml sample volume from each time point at, and freezing of the pellets for DNA extraction. For floating mat enrichments, the same flask was used for all three time points, removing 5 ml of sample at each time point, centrifuging it (20 min at 2 800  $\times g$ ) and freezing the pellet at -20°C for DNA extraction. No-substrate controls were set up for both water and mat and incubated and harvested in the same way as the other samples. Samples for  $t_0$  ( $t = 0$  days) were prepared within 1 hour of sampling by (i) centrifuging 20 ml of cave water, discarding the supernatant and freezing the pellet at -20°C (ii) freezing 30 ml of floating mat material at -20°C.

### **Ultracentrifugation and fractionation of DNA**

From each sample, up to 1  $\mu\text{g}$  of total extracted DNA was added to caesium chloride (CsCl) solutions for isopycnic ultracentrifugation and gradient fractionation following the protocol described by Neufeld *et al.* (2007b) to separate  $^{13}\text{C}$ -labelled DNA from unlabelled ( $^{12}\text{C}$ ) DNA. Density of the fractions was measured using a digital refractometer (Reichert AR200 Digital Refractometer).

## **2.5 Culture media and growth of control organisms**

All culture media were prepared using distilled water and sterilised by autoclaving at 15 psi and 121°C for 15 minutes. Phosphate buffers were prepared and autoclaved separately and added to the media once cooled down, in order to avoid precipitation. Solutions sensitive to autoclaving such as methylated amines, trace element and vitamin solutions were sterilised by filtration through 0.2  $\mu\text{m}$  pore-size sterile syringe filters (Sartorius Minisart, Göttingen, Germany). For solid media, 1.5% bacteriological agar No. 1 (LP0011, Oxoid) was added to media prior to autoclaving.

### 2.5.1 Dilute basal salts (DBS) medium

Movile Cave isolates were grown in dilute basal salts (DBS) medium, modified after Kelly & Wood (1998) by Rich Boden (to resemble ionic composition of Movile Cave water) and containing no nitrogen source. The modified medium contained (per litre): 0.1 g  $\text{MgSO}_4 \cdot 7\text{H}_2\text{O}$ , 0.05 g  $\text{CaCl}_2 \cdot 2\text{H}_2\text{O}$ , 0.11 g  $\text{K}_2\text{HPO}_4$ , 0.085 g  $\text{KH}_2\text{PO}_4$ , at pH 6.8 - 7.3. The medium was supplemented with 0.25 ml / L of a vitamin solution (Kanagawa *et al.*, 1982), and 1ml / L of a trace element solution adapted from Kelly & Wood (1998) containing (per 1 L): 50 g ethylenediaminetetraacetic acid (EDTA), 11 g NaOH, 5 g  $\text{ZnSO}_4 \cdot 7\text{H}_2\text{O}$ , 7.34 g  $\text{CaCl}_2 \cdot 2\text{H}_2\text{O}$ , 2.5 g  $\text{MnCl}_2 \cdot 6\text{H}_2\text{O}$ , 0.5 g  $\text{CoCl}_2 \cdot 6\text{H}_2\text{O}$ , 0.5 g  $(\text{NH}_4)_6\text{Mo}_7\text{O}_{24} \cdot 4\text{H}_2\text{O}$ , 5 g  $\text{FeSO}_4 \cdot 7\text{H}_2\text{O}$ , 0.2 g  $\text{CuSO}_4 \cdot 5\text{H}_2\text{O}$ , adjusted to pH 6.0. For an additional nitrogen source (for control enrichments and ammonia oxidisers) 0.5 g  $(\text{NH}_4)_2\text{SO}_4$  per litre was added to the medium (final concentration of 7.5 mM  $\text{NH}_3$  in the medium).

### 2.5.2 Mixed carbon solution for DBS-C medium

For growth of non-methylotrophic methylated amine utilising bacteria, a solution containing a mixture of six different carbon compounds (comprising glucose, fructose, succinate, glycerol, pyruvate, acetate) was added to DBS medium at a final concentration of 5 mM total carbon. The solution was prepared as a 10 × stock, aliquoted into 100 ml batches, autoclaved and added to DBS medium prior to adjustment of pH and autoclaving.

### 2.5.3 Nitrate mineral salts (NMS) medium

$\text{NO}_3^-$  mineral salts (NMS) medium (Whittenbury *et al.*, 1970) was used for growth of *Methylosinus trichosporium* OB3B which was used as a control organism for the nitrogen fixation (acetylene reduction) assay. The medium was prepared from five separate stock solutions as follows: A 10 × salts solution (solution 1) contained per litre: 10 g  $\text{MgSO}_4 \cdot 7\text{H}_2\text{O}$ , 2 g  $\text{CaCl}_2 \cdot 2\text{H}_2\text{O}$  and 10 g  $\text{KNO}_3$ . A 10,000 × iron - EDTA solution (solution 2) contained per 100 ml: 3.8 g  $\text{Fe}^{3+}$  - EDTA. A 1,000 × sodium molybdate solution (solution 3) contained per litre: 0.26 g  $\text{NaMoO}_4$ . A 1,000 × trace elements solution (solution 4) contained per 5 L: 2.5 g  $\text{FeSO}_4 \cdot 7\text{H}_2\text{O}$ , 2g  $\text{ZnSO}_4 \cdot 7\text{H}_2\text{O}$ , 0.075g  $\text{H}_3\text{BO}_3$ , 0.25 g  $\text{CoCl}_2 \cdot 6\text{H}_2\text{O}$ , 1.25 g EDTA disodium salt, 0.1  $\text{MnCl}_2 \cdot 4\text{H}_2\text{O}$ , 0.05  $\text{NiCl}_2 \cdot 6\text{H}_2\text{O}$ . A separately autoclaved phosphate buffer (solution 5) contained per litre: 71.6 g  $\text{Na}_2\text{HPO}_4 \cdot 12\text{H}_2\text{O}$  and 26 g  $\text{KH}_2\text{PO}_4$ , adjusted to pH 6.8. For 1 L of 1 × MS medium, 100 ml of solution 1, 0.1 ml of solution 2 and 1 ml of both solution 3 and solution 4 were diluted to 1 L.

After autoclaving, 10 ml of the 100 × phosphate buffer solution was added to the cooled medium.

#### 2.5.4 Mineral salts (MS) medium

Mineral salts (MS) medium was a modification of NO<sub>3</sub><sup>-</sup> Mineral Salts (NMS) medium (Whittenbury *et al.*, 1970) by omitting the KNO<sub>3</sub>. Mineral salts (MS) medium was used for diazotrophic growth of *Methylosinus trichosporium* OB3B.

#### 2.5.5 Growth of *Methylosinus trichosporium* OB3b

*M. trichosporium* OB3b was initially grown in a 250 ml quickfit flask containing 50 ml NMS medium (containing NO<sub>3</sub><sup>-</sup>) supplemented with 20% (v/v) methane. The culture was incubated at 30°C with shaking. Once turbid (after 3 days), the culture was used to inoculate a 250 ml flask containing 50 ml MS medium (with no added nitrogen source). The flask was flushed with N<sub>2</sub> to remove O<sub>2</sub>. O<sub>2</sub> and CH<sub>4</sub> were subsequently added to final concentrations of 10% (v/v) and 20% (v/v), respectively. The culture was grown at 30°C with shaking to an OD<sub>540</sub> of ~0.25, at which point the culture was used to inoculate a 1L flask containing 250 ml MS medium. The flask was treated in the same way as the previous one for growth with N<sub>2</sub> and incubated at 30°C with shaking.

#### 2.5.6 *Azotobacter* medium and growth of *Azotobacter vinelandii*

*Azotobacter vinelandii* DJ was used as a positive control for the nitrogen fixation (acetylene reduction) assay. The organism is able to fix N<sub>2</sub> at atmospheric oxygen conditions. When re-growing the organism from a plate or frozen stock, fixed nitrogen was initially added to the liquid medium to promote growth. Once turbid, *A. vinelandii* was transferred into nitrogen-free medium. The medium was prepared according to Strandberg & Wilson (1967) and consisted of the following solutions: Solution 1 which contained (per litre): 440 g sucrose, 4.4 g MgCl<sub>2</sub> · 6H<sub>2</sub>O and 1.98 g CaCl<sub>2</sub>. Solution 2 which contained (per litre): 17.6 g K<sub>2</sub>HPO<sub>4</sub>, 4.4 g KH<sub>2</sub>PO<sub>4</sub> and 0.31 g Na<sub>2</sub>SO<sub>4</sub>. For 200 ml of 1 x medium, 8 ml of solutions 1 and 2 (both autoclaved separately) were added to 180 ml sterile water once cool. The medium was further supplemented with 5 ml of a 1M NH<sub>4</sub>-acetate solution (left out when growing diazotrophically), 200 µl of a 60 mM FeSO<sub>4</sub> solution, 200 µl of a 1 mM NaMoO<sub>4</sub> solution, all of which had been separately autoclaved. For solid medium, 1.5% agar were added to the water and autoclaved prior to adding the remaining ingredients.

### 2.5.7 *Luria-Bertani (LB) medium*

LB medium (Sambrook and Russell, 2001) was used for growth of transformed *Escherichia coli* JM109 cells. It contained (per litre): 10 g tryptone, 5 g yeast extract and 10 g NaCl.

### 2.5.8 *Super optimal broth with catabolic repressor (SOC) medium*

SOC medium for transformations was prepared by adding 20 mM of glucose (filter-sterilised) to autoclaved SOB medium. SOB medium contained (per litre): 5 g yeast extract, 20 g tryptone, 0.5 g NaCl, 2.5 mM KCl (10 ml of a 250 mM solution), all adjusted to pH 7 prior to autoclaving, and 10 mM MgCl<sub>2</sub> (5 ml of a 2 M solution, filter-sterilised, added after autoclaving).

### 2.5.9 *R2A agar*

R2A agar (CM0906) was purchased in the form of dehydrated culture medium from Oxoid and prepared according to the manufacturer's instructions.

### 2.5.10 *Nutrient broth*

Nutrient broth (CM0001) was purchased in the form of dehydrated culture medium from Oxoid and prepared according to the manufacturer's instructions.

### 2.5.11 *Rose-Bengal chloramphenicol agar plates*

Rose-Bengal chloramphenicol agar (90 mm plates) for elimination of bacterial contaminants from methylotrophic yeast isolates was purchased from Oxoid.

### 2.5.12 *Medium for ammonia-oxidising bacteria (Medium 181)*

The medium recipe for ammonia-oxidising bacteria was obtained from the list of culture media on the NCIMB website (NCIMB Ltd, Aberdeen, UK). It was used for growth of *Nitrosomonas europaea* NCIMB 11850 and enrichment of ammonia-oxidising bacteria and archaea from cave water. Two separate stock solutions were prepared for the medium. Solution I contained (per litre): 235 mg (NH<sub>4</sub>)<sub>2</sub>SO<sub>4</sub>, 200 mg KH<sub>2</sub>PO<sub>4</sub>, 40 mg CaCl<sub>2</sub> · 2H<sub>2</sub>O and 40 mg MgSO<sub>4</sub> · 7H<sub>2</sub>O. Solution II contained (per 100 ml): 50 mg FeSO<sub>4</sub> · 7H<sub>2</sub>O and 50 mg NaEDTA. 1 ml of each stock solution was added to 1 L distilled water. The final concentration of NH<sub>3</sub> in the medium was 3.4 mM. The medium was additionally

supplemented with 300 µl of a 1% phenol red solution of pH indication. After autoclaving, a sterile 5% Na<sub>2</sub>CO<sub>3</sub> solution was added to the medium until the colour turned to pale pink (indicating neutral pH). Further Na<sub>2</sub>CO<sub>3</sub> was added during incubation to restore pink colouration.

### 2.5.13 *Growth of Nitrosomonas europaea*

Lyophilised cells of *Nitrosomonas europaea* were revived by adding 0.5 ml of 181 medium to the glass vial and leaving to incubate for 1 h at 20°C, occasionally mixing by carefully flicking the tube. 200 µl of the culture was then transferred into 10 ml of 181 medium in a sterile glass universal for incubation at 20°C in the dark with gentle shaking (100 rpm). After 1 week of incubation, the 10 ml culture was transferred into 40 ml fresh medium in a 250 ml conical flask. Incubation was continued at 20°C in the dark, shaking at 100 rpm. After 3 days of incubation, a decrease of the pH had caused the indicator in the medium to change colour from light pink to colourless. Neutral (to slightly alkaline) pH was restored by adding sterile 5% Na<sub>2</sub>CO<sub>3</sub> solution (200 µl) and incubation was continued. Further 5% Na<sub>2</sub>CO<sub>3</sub> (80 µl) was added the following day to re-adjust the pH. After incubating the culture for a further 3 days, the colour of the medium had remained pink, indicating that cells had reached the stationary phase and no further growth was occurring. 10 ml aliquots of the culture were used to inoculate each of 5 new 250 ml flasks containing 40 ml fresh medium. Flasks were incubated as before. The pH was re-adjusted to neutral when the colour changed to clear (after 4 days of incubation). Once growth stagnated (colour remained pink), each of the 50 ml cultures was transferred into a 2 L conical flask containing 450 ml medium. Incubation was performed as before, adjusting the pH with 5% Na<sub>2</sub>CO<sub>3</sub> as necessary, until growth stagnated. Cultures were then pooled and used for DNA extraction as described in 2.7.

### 2.5.14 *Medium for nitrite-oxidising bacteria (Medium 182)*

The medium recipe for nitrite-oxidising bacteria was obtained from the list of culture media on the NCIMB website and prepared in the same way as Medium 181 except that NaNO<sub>2</sub> (0.247 g/l) replaced (NH<sub>4</sub>)<sub>2</sub>SO<sub>4</sub>.

## 2.6 Enrichment, isolation and maintenance of methylated amine-utilising bacteria from Movile Cave

### 2.6.1 *Methylotrophic methylated amine-utilising bacteria*

For selective enrichment of bacteria that use methylated amines as a carbon and energy source (i.e. methylotrophs) as well as nitrogen source, 1 mM of either monomethylamine (MMA), dimethylamine (DMA) or trimethylamine (TMA) was added to a 20 ml sample of cave water in sterile 120 ml serum vials. For mat and biofilm, 2 g of sample material was placed into 27 ml serum vials and made up to a final volume of 4 ml with DBS medium. After flushing the headspace of each vial with N<sub>2</sub>, 7% (v/v) O<sub>2</sub> and 3.5% (v/v) CO<sub>2</sub> were added in an attempt to simulate the cave atmosphere. Samples were incubated at 21°C in the dark for four weeks, during which time substrate uptake was monitored. After four weeks, 10 ml (for water samples) or 4 ml (for mat samples) of fresh DBS medium were added and cultures were spiked with 20 mM MMA, 10 mM DMA, or 10 mM TMA, respectively. After re-adjusting the headspace as previously described, enrichment cultures were re-incubated at 21°C in the dark. On turbidity (two weeks), dilutions were spread onto agar plates (DBS medium, 1.5% agar) containing 5 mM MMA, DMA, or TMA as sole carbon and nitrogen source. Plates were incubated at 21°C in the dark. Visible, single colonies were transferred onto fresh plates containing the same substrate as before. Colonies were examined by microscopy and a selection of morphotypes was re-plated to isolate a variety of methylotrophs. Once purity was confirmed by microscopy, individual isolates were transferred into liquid DBS media (containing 5 mM MMA, DMA, or TMA) to distinguish true methylotrophs from organisms possibly growing on agar. Once grown in liquid, isolates were transferred back onto methylated amine plates, as well as R2a plates, to confirm purity.

### 2.6.2 *Non-methylotrophic, methylated amine-utilising bacteria*

In a separate enrichment approach, heterotrophic bacteria capable of using methylated amines as a nitrogen but not carbon source (i.e. non-methylotrophs) were isolated. These enrichments were set up analogous to methylotroph enrichments, using the same sample material as described above. In addition to 1 mM of either MMA, DMA or TMA, a mixture of alternative carbon compounds (comprising glucose, fructose, succinate, glycerol, pyruvate and acetate) was added to a final concentration of 5 mM. Flasks were incubated at 30°C with shaking. Upon growth (2 weeks), enrichments were transferred into fresh medium (1 ml culture in

25 ml medium) and incubated as before. Once turbid (2-5 days), dilutions of the enrichment cultures were spread onto agar plates ( $10^{-3}$ ;  $10^{-5}$ ;  $10^{-7}$  dilution) containing DBS medium with 5 mM of the carbon mixture (from hereon referred to as DBS-C) and 1 mM of either MMA, DMA, or TMA as the only added nitrogen source. The spread plates were incubated at 30°C for 2 – 5 days and a selection of colonies (ca 10 per substrate) were then transferred onto fresh plates for isolation.

After a series of transfers on plates, isolates were transferred into liquid DBS medium containing 1mM of the respective methylated amine and 5 mM carbon mixture. Isolates obtained in this way were additionally tested for growth in liquid medium containing no alternative carbon source to detect any co-enriched methylophs, as well as in liquid medium containing carbon sources but no methylated amines to eliminate the possibility that they might be fixing  $N_2$  rather than using methylated amines as nitrogen source. Purity was confirmed as described above by using microscopy and growth on R2A plates.

### 2.6.3 *Microscopy*

Cells were routinely observed at 1,000 × magnification in phase-contrast under a Zeiss Axioskop 50 microscope, 130 VA Typ B, and documented using the AxioCam camera system and Axiovision Rel 4.8 software (all supplied by Carl Zeiss Ltd, Cambridge UK).

### 2.6.4 *Preservation of cultures*

For maintenance, bacterial (and yeast) isolates were routinely kept on either DBS or DBS-C agar plates supplemented with MMA, DMA or TMA. Isolates were furthermore preserved as freezer stocks in 2 ml cryovials with 20% sterile glycerol added to 2 ml of liquid culture. If the OD was low, the concentration of cells was increased by centrifuging a larger volume (20 min at 2,000 g), and re-suspending the cell pellet in 2 ml of the supernatant. In addition to glycerol stocks, cell “slurries” were prepared by centrifuging 50 ml of a culture, discarding the supernatant and re-suspending the cell pellet in the remaining liquid for transfer into a 2 ml cryogenic vial which was submerged in liquid  $N_2$  for rapid freezing of cells. Frozen cell stocks were kept at -80°C.

### 2.6.5 *Growth tests of new isolates with methanol and under anoxic conditions*

To test growth of the new isolates *Catellibacterium* sp. LW-1 and *Mesorhizobium* sp. 1M-11 with methanol, 20 ml DBS medium were added into 150 ml Quickfit flasks and supplemented

with 0.2% methanol as the sole carbon and energy source and 1 mM NH<sub>3</sub> as nitrogen source. After inoculation flasks were incubated at 30°C for 1 week. Control incubations were set up with DBS-C medium (i.e. containing sugars and carboxylic acids, see 2.5.2) plus methanol and NH<sub>3</sub>.

To test for growth in the absence of oxygen, the isolates were incubated in 20 ml medium (either DBS-C medium or DBS medium with 5 mM MMA) supplemented with 1 mM NH<sub>4</sub><sup>+</sup> and 3 mM of either NO<sub>3</sub><sup>-</sup> or NO<sub>2</sub><sup>-</sup> as an alternative electron acceptor in 120 ml serum vials flushed with O<sub>2</sub>-free N<sub>2</sub> for 20 minutes. Analogous incubations were set up without any added NO<sub>3</sub><sup>-</sup> or NO<sub>2</sub><sup>-</sup> to test for potential growth without any electron acceptor (i.e. fermentation).

## 2.7 DNA extraction, processing and storage

DNA from Movile Cave samples, SIP enrichments and bacterial isolates obtained in this study was prepared using enzymatic lysis of cells followed by phenol-chloroform extraction as described by Neufeld *et al.* (2007a). DNA from soil and lake sediment samples retrieved from the University of East Anglia campus (used for *gmaS* primer validation, see later) was extracted using the FastDNA® SPIN Kit for soil by MP Biomedicals LLC. DNA quality and concentration was assessed using an ND-1000 spectrophotometer (NanoDrop Technologies Inc., USA). DNA was routinely stored in nuclease-free water at -20°C.

## 2.8 Agarose gel electrophoresis

DNA samples and gene fragments amplified by PCR (see below) were analysed by agarose gel electrophoresis using a 1% (w/v) agarose gel in 1 x TBE buffer. Ethidium bromide (0.5 µg ml<sup>-1</sup>) was added directly to gels before casting. For sizing of DNA fragments, GeneRuler™ 1kb DNA (Fermentas) ladder was used as a marker unless otherwise stated. For RFLP analysis and DNA fragments of less than 250 bp size, the GeneRuler™ 100 bp Plus DNA ladder was used instead. Gels were viewed under the Gel Doc XR gel documentation system by Bio-Rad (Hercules, CA, USA) using Amber Filter 5206 (Bio-Rad).

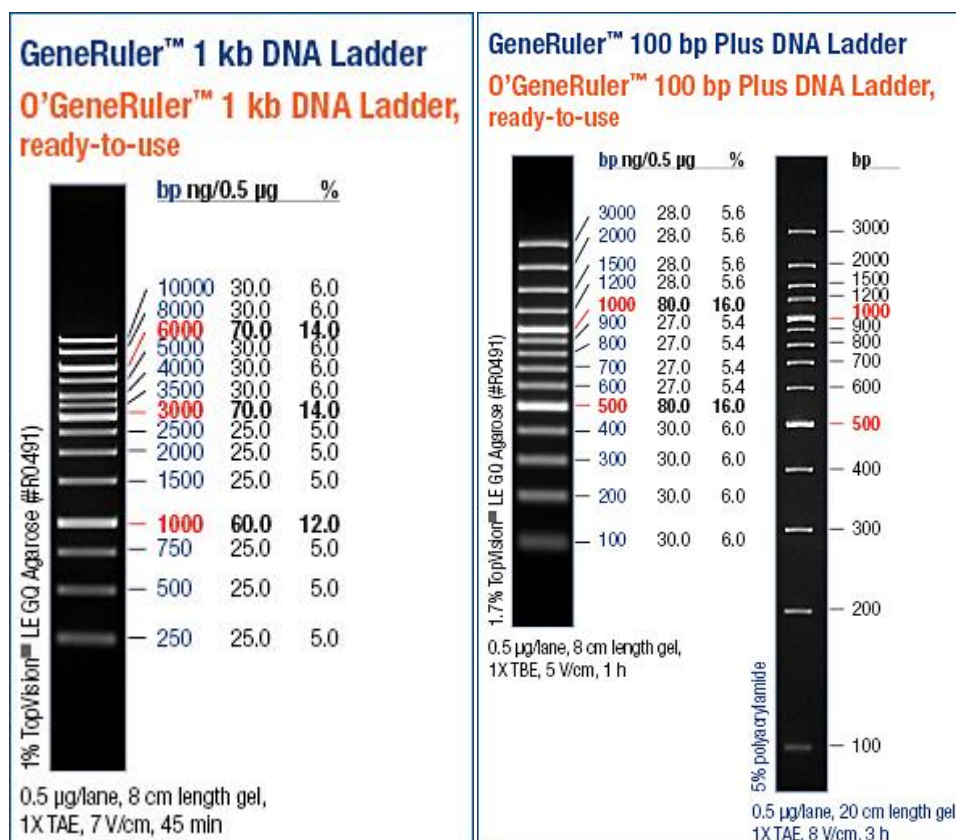


Figure 2.1 DNA markers used for agarose gel electrophoresis

## 2.9 Polymerase chain reaction (PCR)

Polymerase chain reaction (PCR) amplification of DNA fragments was carried out using a Tetrad thermal cycler (Bio-Rad). Reactions were prepared on ice and typically contained (in 50 µl reaction volumes): 1x reaction buffer containing 1.5 mM MgCl<sub>2</sub> (Fermentas), 0.2 mM of each dNTP (Fermentas), 2.5 units recombinant Taq DNA polymerase (Fermentas), 1-2 µl each of 10 µM forward and reverse primer solutions (synthesized by Invitrogen, Life Technologies Ltd, Paisley, UK) and 1 µl of a 3.5% (w/v) BSA solution. For improved performance when amplifying *gmaS* genes, PCR reagents by Bioline (MyTaq™ DNA polymerase, supplied with reaction buffer containing dNTPs) were used instead of Fermentas reagents, resulting in a higher level of amplification. For direct PCR of bacterial colonies, 2.5 µl of DMSO (concentrated solution) were added to the reaction. Typically, 1 µl template DNA (concentration between 30 – 50 ng / µl) was used. Negative controls without template were included in all cases. The PCR mixture was brought to a final volume of 50 µl with sterile deionised water. The typical PCR amplification profile consisted of (i) an initial denaturation step at 94°C for 5 min (extended to 10 min for colony PCR), followed (ii) by 30 – 35 cycles of denaturation at 94°C, 30s; annealing (temperature dependent on primers), 30s;

elongation at 72°C (time dependent on amplicon length, 1 min / kb) and (iii) a final elongation step of 8 min at 72°C. PCR products were then maintained at 4°C (-20°C for long term storage). Generally, PCR protocols were adapted from publications; if necessary, annealing temperatures and cycle numbers were adjusted for optimisation. In some cases, touchdown PCR protocols were used in order to increase efficiency without losing specificity of amplification. Gene fragments to be analysed by DGGE were amplified using the same PCR conditions as otherwise but with a GC-clamp (Muyzer *et al.*, 1993) attached to the 5' end of one of the primers. Table 2.2 gives details of the primers used in this study.

## 2.10 Purification of PCR products for further applications

Following agarose gel electrophoresis, PCR products producing well-defined bands were purified using either the QIA Quick Gel Purification Kit by Qiagen (Crawley, UK) or the Nucleospin Gel Extraction Kit by Machery-Nagel (Düren, Germany) according to manufacturers' instructions (without gel-excision, using the centrifugation protocols). Gel excision was used only if alternative amplification products could not be eliminated by optimising PCR conditions (*gmaS* PCR products of Movile Cave methylamine enrichments obtained using primer set 557f / 1332r).

As an alternative to using kits, larger numbers of PCR products were purified using PEG purification (Sambrook *et al.*, 2001). Briefly, a solution containing 20% PEG-8000 and 2.5 M NaCl (sterilised by autoclaving) was added to PCR products at 0.6 times the volume of the PCR product in a 0.5 ml Eppendorf tube. After 30 min incubation in a 37°C water bath, the mixture was centrifuged in a tabletop centrifuge at maximum speed for 30 min at 20°C. After removal of the supernatant, the non-visible pellet was washed with 100 µl of 70% ethanol (mixing by vortexing), before centrifugation at maximum speed for 20 min at 4°C and removal of the supernatant. The washing step was repeated and the pellet air-dried next to a Bunsen burner or under a flow hood. Finally, the purified product was resuspended in 10-12 µl of sterile, nuclease-free water.

**Table 2.2** Details of PCR primers used in [this study](#)

References	Primer sequences (5'-3')	Target gene	Amplicon length (bp)	Annealing temperature (°C)	Cycles
27f	AGAGTTTGATCMTGGCTCAG	Bacterial 16S rRNA gene	~1460	55	30-35
1492r	TACGGYACCTTGTTAGGACTT				
A109f	ACKGCTCAGTAACACGT	Archaeal 16S rRNA gene (1 <sup>st</sup> step of nested PCR)	~850	45	35
958r	YCCGGCGTTGAMTCCAATT				
Saf(i)-GCF*	<u>CGCCCCCGCCGGCGGGGGGGGGGG</u> <u>GCACGGGGGGCTAYGGGGCGCAGCAGG</u>	Archaeal 16S rRNA gene (2 <sup>nd</sup> step of nested PCR)	~190	53.5	35
Saf(ii)-GCF*	<u>CGCCCCCGCCGGCGGGGGGGGGGG</u> <u>GCACGGGGGGCTACGGGGCGCAGAGGG</u>				
PARCH519r	TTACCGCGGCKGCTG				
A109f	ACKGCTCAGTAACACGT	Archaeal 16S rRNA gene (1 <sup>st</sup> step of nested PCR)	~1380	55	30
1492r modified	GYAYACCTTGTTACGACTT				
771f	ACGGTGAGGGATGAAAGCT	<i>Thaumarchaeal</i> 16S rRNA gene	~190	55	25
957-GCr	<u>CGCCCCCGCCGGCGGGGGGGGGGG</u> <u>GCACGGGGGGCGGGGTTGACTCCAATTG</u>	gene (2 <sup>nd</sup> step of nested PCR)			
amo111f	TTYTAYACHGAYTGGGCHTGGACATC	Archaeal <i>amoA</i> (ammonia monooxygenase)	~557	55	30-35

Table 2.2 (continued)

amo643r	Treusch (2005)	TCCCACCTTGWACCARGCGGCCATCCA			
340f	Gantner <i>et al.</i> (2011)	CCCTAYGGGGYGCASCAG	Archaeal 16S rRNA gene	~660	57
1000r	Gantner <i>et al.</i> (2011)	GGCCAIGCACACYWCYTCTC			30
amoA-1f	Rotthauwe <i>et al.</i> (1997)	GGGGTTTCTACTGGTGGT	$\beta$ -proteobacterial <i>amoA</i>	~490	60
amoA-1f-GC	Nicolaisen <i>et al.</i> (2002)	<u>CGCCGCGGGCGGGGGGGGGGGGCGG- GGGGTTTCTACTGGTGGT</u>	(ammonia monooxygenase)		35
amoA-2r	Rotthauwe <i>et al.</i> (1997)	CCCCTCKGSAAAGCCTTCITC			
nxB169f	Maixner (2010)	TACATGTGGTGGAAACA	<i>Nitrospira</i> / <i>Nitrospina nxr</i>	~460	56
nxB638r	Maixner (2010)	CGGTTCTGGTCRATCA	(nitrite oxidoreductase)		30-35
189f	Holmes <i>et al.</i> (1995)	GGNGACTGGGACTTCTGG	$\gamma$ -proteobacterial (ammonia monooxygenase) / <i>pmoA</i>	~490	56
682r	Holmes <i>et al.</i> (1995)	GAASGCNGAGAAAGAASGC	(methane monooxygenase)		30
Arch-amoAf	Francis <i>et al.</i> (2005)	STAATGGTCTGGCTTAGACG	Archaeal <i>amoA</i>	~630	53
Arch-amoAr	Francis <i>et al.</i> (2005)	GCGGCCATCCATCTGTATGT	(ammonia monooxygenase)		35
cbbLR1f	Selesi <i>et al.</i> (2005)	AAGGAYGACGAGAAACATC	<i>cbbL</i>	~820	57
cbbLR1r	Selesi <i>et al.</i> (2005)	TCGGTCCGGSGTGTAGTTGAA	(Form I RuBisCO, red form)		32

Table 2.2 (continued)

cbbLG1f	Selesi <i>et al.</i> (2005)	GGCAACGTGTTCGGSTTCAA	<i>cbbL</i> (Form I RuBisCO, green form)	~1030	62	32
cbbLG1r	Selesi <i>et al.</i> (2005)	TTGATCTCTTTTCCACGTTTCC				
cbbMf	Giri <i>et al.</i> (2004)	ATCATCAARCCSAARCTSGGCCTGCCGTCCC	<i>cbbM</i> Form II RuBisCO	~400	52	25-30
cbbMr	Giri <i>et al.</i> (2004)	MGAGGTGACSGRCRCCGTGRCCRCGCMCGRTG				
mauAf1	Neufeld <i>et al.</i> (2007a)	ARKCYTYGYGABTAYTGGCG	<i>mauA</i> (Methylamine dehydrogenase)	~310	54	35
mauAr1	Neufeld <i>et al.</i> (2007a)	GARAYVGTGCARTGRTARGTC				
mauAI-252f	Hung (2012)	GCACTGTTCCATCGACGGCA	<i>mauA</i> ( $\alpha$ - <i>proteobact.</i> ) (Methylamine dehydrogenase)	~230	51	30
mauAI-490r	Hung (2012)	GCGCCGAAGCACCAGATGAT				
mauAII-232f	Hung (2012)	AAGTCTTGGGATTACTGGCG	<i>mauA</i> ( $\beta$ / $\gamma$ - <i>proteobact.</i> ) (Methylamine dehydrogenase)	~330	48	30
mauAII-562r	Hung (2012)	GACCGTGCAATGGTAGGTCA				
Amx368f	Schmid <i>et al.</i> (2003)	CCTTTCGGGCATTGCGAA	Bacterial 16S rRNA gene of <i>Brocadia</i> & <i>Kuenenia</i>	~450	62	30
Amx820r	Schmid <i>et al.</i> (2000)	AAAACCCCTCTACTTAGTGCCC				
hzocl1f1	Schmid <i>et al.</i> (2008)	TGYAAGACYTGYCAYTGG	Hydroxylamine / hydrazine oxidoreductase gene	~470	50	30
hzocl1r2	Schmid <i>et al.</i> (2008)	ACTCCAGATRTGCTGACC				
nifHf	Mehta <i>et al.</i> (2003)	GGHAARGGGHGGHATHGGNAART	<i>nifH</i>	~400	55	35
nifHr	Mehta <i>et al.</i> (2003)	GGCATNGCRAANCCVCCRCANAC	Dinitrogenase (iron protein)			

Table 2.2 (continued)

nirS1f	Braker <i>et al.</i> (1998)	CCTAYTGGCCGCCRCART	<i>nirS</i>	~890	45 / 56 → 40 / 51	10
nirS6r	Braker <i>et al.</i> (1998)	CGTTGAACTTRCCGGT	(Dissimilatory nitrite reductase; Cu-Nir)		0.5°C decrease cycle <sup>-1</sup>	
					43 / 54	25
nirK1f	Braker <i>et al.</i> (1998)	GGMATGGTKCCSTGGCA	<i>nirK</i>	~510	45 / 56 → 40 / 51	10
nirK5r	Braker <i>et al.</i> (1998)	GCCTCGATCAGRTRTRGG	(Dissimilatory nitrite reductase; CDI-Nir)		0.5°C decrease cycle <sup>-1</sup>	
					43 / 54	25
Euk82f	López-García <i>et al.</i> (2003)	GAAACTGCGAATGGCTC	Eukaryotic 18S rRNA gene	~430	55	30
Euk516-GCr	Diez <i>et al.</i> (2001)	<u>CGCCCCGGGGCGCCCCCGGGGGGGGGGGGG</u> ACGGGGGACCAGACTTGCCC				
M13f	Invitrogen	GTAAAACGACGGCCAG	Insert-flanking regions	Insert size +	55	30
M13r	Invitrogen	CAGGAACAGCTATGAC	of pGEM®-T Easy Vector	~200 bp		

Forward primers Saf1 and Saf2 were used at a molar ratio of 2:1

Underlined sequence sections represent GC-clamps (Muyzer *et al.*, 1993) and are not homologous to DNA sequences.

## 2.11 Design of PCR primers targeting *gmaS*

There is currently one *gmaS* primer set available, published recently (Chen, 2012) and targeting specifically the marine Roseobacter Clade (MRC). This primer set therefore does not cover *gmaS* from non-marine bacteria, which is why new *gmaS* PCR primers were designed in this study.

### 2.11.1 Identification of *gmaS* sequences and alignment

Three new PCR primers were designed based on multiple alignment of 34 *gmaS* sequences derived from (i) methylotrophic isolates confirmed to use the NMG / GMA mediated pathway and (ii) bacterial genomes published on the Integrated Microbial Genomes (IMG; Markowitz *et al.*, 2010) platform of the Joint Genome Institute (JGI). Genomes were screened for *gmaS*-related sequences using *gmaS* from *Methylocella silvestris* as a query sequence. Corresponding full length sequences included both *gmaS* and glutamine synthetase type III (*glnA*) sequences, due to the high level of sequence similarity between the two genes. A complete list of all *gmaS* and *glnA* sequences used for primer design is given in Table 2.3. In order to identify genuine *gmaS* sequences, the gene neighbourhood of all obtained sequences was manually inspected for predicted neighbouring open reading frames (ORFs) typically found adjacent to *gmaS* (genes for NMG dehydrogenase and NMG synthase subunits). Confirmed *gmaS* sequences included many sequences mis-annotated as *glnA*. For primer design, multiple sequence alignments of chosen sequences were established with the Clustal X program (Thompson *et al.*, 1997) and viewed using the GeneDoc software (Nicholas *et al.*, 1997). Because of their sequence similarity to *gmaS*, a number of *glnA* sequences were included in the alignment in order to identify suitable primer-binding regions specific only to *gmaS*.

### 2.11.2 Primer sequences and PCR conditions

The resulting forward primer *gmaS*\_557f (GARGAYGCSAACGGYCAGTT) was used in all cases, with the reverse primers  $\alpha$ \_gmaS\_970r (TGGGTSCGRTRTTGCCSG) and  $\beta$ \_gmaS\_1332r (GTAMTCSAYCCAYTCCATG) being used to target the *gmaS* gene of non-marine *Alphaproteobacteria* and that of *Beta*- and *Gammaproteobacteria*, respectively. PCR products were 410 bp and 775 bp respectively. After testing a range of conditions, touchdown PCR protocols for *gmaS* amplification were used as follows: For *gmaS*\_557f /  $\alpha$ \_gmaS\_970r, an initial step at 94°C for 5 min was followed by 10 cycles of denaturation at 94°C for 45 seconds,

annealing at variable temperatures for 45 seconds, and extension at 72°C for 1 min. In the first cycle, the annealing temperature was set to 60°C, and for each of the 9 subsequent cycles the annealing temperature was decreased by 1°C. This was followed by 30 cycles of 45 sec at 94°C, 45 sec at 56°C and 1 min at 72°C, and a final extension time of 8 min at 72°C. For *gmaS*\_557f /  $\beta$ \_ $\gamma$ \_gmaS\_1332r, an initial step at 94°C for 5 min was followed by 10 cycles of denaturation at 94°C for 45 seconds, annealing at variable temperatures for 45 seconds (starting at 55°C in the first cycle and decreasing by 1 degree for each of the 9 subsequent cycles), and extension at 72°C for 1 min. This was followed by 35 cycles of 45 sec at 94°C, 45 sec at 52°C and 1 min at 72°C, and a final extension time of 8 min at 72°C.

### 2.11.3 Validation of the new primers

The primer sets were tested for their specificity by (i) amplification and sequencing of *gmaS* genes from genomic DNA of the following bacterial strains known to use the indirect MMA oxidation pathway (kindly provided by Dr Yin Chen): *Sinorhizobium meliloti* 1021, *Mesorhizobium loti* MAFF303099, *Rhizobium leguminosarum* bv. *viciae* 3841, *Agrobacterium tumefaciens* C58 and *Pseudomonas fluorescens* SBW. For further validation of the primers, *gmaS* genes were amplified from DNA extracted from (ii) MMA enrichments from Movable Cave (iii) samples from a floating mat in Movable Cave (iv) soil and freshwater sediment from a small lake (the “Broad”) located on the University of East Anglia campus. *GmaS*-based clone libraries were constructed for (ii) – (iv) and a total of 30 clones were randomly selected for sequencing.

**Table 2.3** Names and accession numbers of all *gmaS* and *glnA* sequences used for primer design

<i>glnA</i>	Strain	Accession Number	Author
	<i>Methylococcus capsulatus</i> str. Bath	<a href="#">NC_002977.6</a>	Ward <i>et al.</i> , 2004
	<i>Synechocystis</i> sp. PCC 6803	<a href="#">NC_000911.1</a>	Thelwell <i>et al.</i> , 1998
	<i>Acidithiobacillus ferrooxidans</i> ATCC 53993	<a href="#">NC_011206.1</a>	Lucas <i>et al.</i> , 2008
	<i>Escherichia coli</i> O157:H7 str. Sakai	<a href="#">NC_002695.1</a>	Bergholz <i>et al.</i> , 2007
	<i>Clostridium saccharobutylicum</i>	<a href="#">P10656</a>	Janssen <i>et al.</i> , 1988
	<i>Lactobacillus johnsonii</i> NCC 533	<a href="#">NC_005362.1</a>	van der Kaaij <i>et al.</i> , 2004
<i>gmaS</i>			
	<i>Methyloversus mays</i>	<a href="#">AB333782.1</a>	Yamamoto <i>et al.</i> , 2008
	<i>Thiomicrospira crunogena</i> XCL-2	<a href="#">NC_007520.2</a>	Scott <i>et al.</i> , 2006
	<i>Methyloversus glucosetrophus</i> SIP3-4	<a href="#">NC_012969.1</a>	Lucas <i>et al.</i> , 2009
	<i>Rubrobacter xylanophilus</i> DSM 9941	<a href="#">NC_008148.1</a>	Copeland <i>et al.</i> , 2006
	<i>Thioalkalivibrio sulfidophilus</i> HL-EbGr7	<a href="#">NC_011901.1</a>	Lucas <i>et al.</i> , 2008
	<i>Pseudomonas fluorescens</i> SBW25	<a href="#">NC_012660.1</a>	Silby <i>et al.</i> , 2009
	<i>Pseudomonas mendocina</i> ymp	<a href="#">NC_009439.1</a>	Copeland <i>et al.</i> , 2007
	<i>Xanthobacter autotrophicus</i> Py2	<a href="#">NC_009720.1</a>	Copeland <i>et al.</i> , 2007
	<i>Burkholderia phymatum</i> STM815	<a href="#">NC_010625.1</a>	Copeland <i>et al.</i> , 2008
	<i>Methylobacterium populi</i> BJ001	<a href="#">NC_010725.1</a>	Copeland <i>et al.</i> , 2008
	<i>Azorhizobium caulinodans</i> ORS 571	<a href="#">NC_009937.1</a>	Tsukada <i>et al.</i> , 2009
	<i>Methylobacterium extorquens</i> PA1	<a href="#">NC_010172.1</a>	Copeland <i>et al.</i> , 2007
	<i>Azospirillum</i> sp. B510	<a href="#">NC_013855.1</a>	Taneko <i>et al.</i> , 2008
	<i>Rhodobacterales</i> bacterium HTCC2150	<a href="#">NZ_AAXZ01000014.1</a>	Kang <i>et al.</i> , 2010
	<i>Rhodopseudomonas palustris</i> HaA2	<a href="#">NC_007778.1</a>	Oda <i>et al.</i> , 2008
	<i>Roseobacter</i> sp. AzwK-3b	<a href="#">NZ_ABCR01000005.1</a>	Francis <i>et al.</i> , 2007
	<i>Roseovarius</i> sp. 217	<a href="#">NZ_AAMV01000001.1</a>	Murrell <i>et al.</i> , 2006
	<i>Ruegeria pomeroyi</i> DSS-3	<a href="#">NC_003911.11</a>	Moran <i>et al.</i> , 2007
	<i>Bradyrhizobium</i> sp. ORS 278	<a href="#">NC_009445.1</a>	Giraud <i>et al.</i> , 2007
	<i>Roseobacter litoralis</i> Och 149	<a href="#">NC_015730.1</a>	Brinkhoff <i>et al.</i> , 2007
	<i>Methylocella silvestris</i> BL2	<a href="#">NC_011666.1</a>	Lucas <i>et al.</i> , 2008
	<i>Roseobacter</i> sp. SK209-2-6	<a href="#">NZ_AAYC01000011.1</a>	Ward <i>et al.</i> , 2006
	<i>Roseobacter</i> sp. MED193	<a href="#">NZ_AANB01000005.1</a>	Pinhassi <i>et al.</i> , 2006
	<i>Agrobacterium tumefaciens</i> str. C58	<a href="#">NC_003063.2</a>	Goodner <i>et al.</i> , 2001
	<i>Sinorhizobium fredii</i> NGR234	<a href="#">NC_012587.1</a>	Schmeisser <i>et al.</i> , 2009
	<i>Mesorhizobium loti</i> MAFF303099	<a href="#">NC_002678.2</a>	Kaneko <i>et al.</i> , 2000
	<i>Fulvamarina pelagi</i> HTCC2506	<a href="#">NZ_AATP01000002.1</a>	Kang <i>et al.</i> , 2010
	<i>Sinorhizobium meliloti</i> 1021	<a href="#">NC_003047.1</a>	Capela <i>et al.</i> , 2001
	<i>Agrobacterium radiobacter</i> K84	<a href="#">NC_011983.1</a>	Slater <i>et al.</i> , 2009
	<i>Sinorhizobium medicae</i> WSM419	<a href="#">NC_009636.1</a>	Copeland <i>et al.</i> , 2007
	<i>Hoeflea phototrophica</i> DFL-43	<a href="#">NZ_ABIA02000018.1</a>	Wagner-Dobler <i>et al.</i> , 2007
	<i>Agrobacterium vitis</i> S4	<a href="#">NC_011988.1</a>	Setubal <i>et al.</i> , 2009
	<i>Rhizobium leguminosarum</i> bv. viciae 3841	<a href="#">NC_008384.1</a>	Young <i>et al.</i> , 2006
	<i>Rhizobium etli</i> CIAT 652	<a href="#">NC_010998.1</a>	Gonzalez <i>et al.</i> , 2008

## 2.12 Denaturing gradient gel electrophoresis (DGGE)

DGGE of bacterial 16S rRNA gene fragments was carried out using the DCode™ Universal Mutation Detection System (Bio-Rad) according to the manufacturer's directions. PCR products were loaded on a 1 mm thick vertical gel containing 8% (w/v) polyacrylamide (acrylamide-bisacrylamide, 37.5:1) in 1x Tris-acetate-EDTA (TAE) buffer. A linear gradient of 30 - 70% denaturant (with 100% denaturant corresponding to 7 M urea and 40% (v/v) de-ionised formamide) was used for the separation of 16S rRNA gene fragments. A molecular marker generating nine distinct bands on the DGGE gel was used as reference to allow comparison between gels. Electrophoresis was conducted for 16 h at 80 V. Gels were stained using 3 µl SYBR® Gold Nucleic Acid Gel Stain (Invitrogen) in 50 ml TAE buffer for 45 min in the dark. Gels were rinsed with TAE buffer and bands were viewed under the Bio-Rad Gel Doc XR gel documentation system using Amber Filter 5206 (Bio-Rad). For gene sequence analysis, well-defined DNA bands were physically excised from the gel with sterile, disposable gel excision tips and placed in 1.5 ml centrifuge tubes containing 20 µl sterilised water. The DNA was allowed to passively diffuse into the water at 4°C overnight. 1 µl of the eluate was used as a template for re-amplification using the same PCR conditions and primers described above. Re-amplified gene products were analysed by DGGE once more to confirm they were single sequences. If multiple bands appeared, the band of the correct position was again excised and re-amplified. Positive re-amplification products were sequenced.

## 2.13 Cloning of PCR products

Cloning of PCR products from 16S rRNA genes and functional genes (bacterial *amoA*, archaeal *amoA*, *cbbl*, *cbbm*, *gmaS*, *mauA*, *nifH*, *nirS*, *nirK*) was carried out using the Promega pGEM®-T Easy Vector system as described by the manufacturer: PCR products were inserted into the pGEM®-T Easy Vector and transformed into chemically competent *Escherichia coli* JM109 cells. Transformants were streaked on LB-ampicillin plates supplemented with IPTG (50 µl of a 0.2 M solution) and X-Gal (25 µl of a 40 mg/ml solution) for white / blue selection. White colonies were selected randomly and re-amplified using primer set M13f / M13r. PCR products were analysed on a 1% (w/v) agarose gel and amplification products of the correct length were submitted to sequencing analysis using either the M13f or M13r primer (or both).

## 2.14 RFLP analysis of cloned sequences from <sup>13</sup>C-MMA-SIP incubations

In order to complement results from DGGE analysis, 16S rRNA genes from <sup>13</sup>C-MMA-SIP key fractions (heavy and light DNA) of t<sub>3</sub> (5 weeks incubation) were amplified with bacterial 16S rRNA gene-specific primer set *27f* / *1492r* for establishment of clone libraries. Restriction fragment length polymorphism (RFLP) analysis was carried out to ensure sequencing of a diversity of clones. Twenty out of ninety white colonies randomly picked from each library were re-amplified using *27f* / *1492r* for establishing a RFLP profile. Restriction enzymes were chosen using the online tool NEBCUTTER (Vincze *et al.*, 2003) and imposing them on aligned Movicave 16S rRNA gene sequences from methylamine isolates and DGGE bands. This was done in order to ensure selection of restriction enzymes generating distinct profiles for the different sequences expected. Enzymes *BseGI* and *Eco88I* were chosen, and 16S rRNA gene PCR products of 30 clones (18 for F8 and 12 for F11) were digested and analysed on a 2% (w/v) agarose gel. Clones with distinct profiles were selected for sequencing and amplified using M13f / M13r (to obtain the full 16S rRNA gene sequence).

## 2.15 DNA sequencing and phylogenetic analysis

### 2.15.1 Sequencing of PCR products

DNA sequencing of PCR products employed the Sanger method on a 3730A automated sequencing system (PE Applied Biosystems). To determine approximate phylogenetic affiliations, partial 16S rRNA gene sequences were analysed with the Basic Local Alignment Search Tool (BLAST) on the NCBI GenBank database (Altschul *et al.*, 1990). Species annotations were verified using the List of Prokaryotic Names with Standing in Nomenclature (LPSN) available online at <http://www.bacterio.net/>. The LPSN was also used for retrieving sequences of type species and type strains. Amino acid and nucleotide-based phylogenetic trees were established using the MEGA5 program (Tamura *et al.*, 2011). The evolutionary history was inferred by neighbour-joining (Saitou & Nei, 1987). For nucleotide-based trees, the evolutionary distances were computed using the maximum composite likelihood method (Tamura *et al.*, 2004). For amino-acid based trees, the evolutionary distances were computed using the Poisson correction method (Zuckerandl & Pauling, 1965). All positions containing gaps and missing data were eliminated. Bootstrap analysis (1000 replicates) was performed to provide confidence

estimates for phylogenetic tree topologies (Felsenstein *et al.* 1985). Phylogenetic analysis of *gmaS* genes was carried out on amino acid level; the number of positions in the final data set was 135 amino acids (for *alphaproteobacterial gmaS*) and 250 amino acids (for *gamma-* and *betaproteobacterial gmaS* genes), respectively.

### 2.15.2 Metagenome analysis

Metagenomic DNA extracted from samples of a floating mat from Movile Cave was sent to UCL Genomics, University College London, UK for 454 sequencing analysis using the Genome Sequencer FLX System from Roche (Margulies *et al.*, 2005). The obtained metagenome data were submitted to the MG-RAST v.3.0 online server (Meyer *et al.*, 2008) for quality control and automatic analysis. The data were screened for *gmaS* and *mauA* sequences by running a blastx comparison on the MG-RAST v.3.0 online server, selecting the GenBank and JGI databases for annotation.

For a more in-depth screening for *mauA* and *gmaS* sequences (not relying on annotation), a nucleotide-based, local BLAST database was established from the metagenome data using the BLAST+ software package available at <ftp://ftp.ncbi.nlm.nih.gov/blast/executables/blast+/LATEST/> (Camacho *et al.*, 2009). To remove low quality reads and redundant sequences, the raw metagenome data were first submitted to workflows within the Community Cyberinfrastructure for Advanced Microbial Ecology Research and Analysis (CAMERA) portal (Sun *et al.*, 2011). The processed, non-redundant data set was then used to establish a local BLAST database. The *gmaS* sequences from *Methylocella silvestris* and *Pseudomonas fluorescens* were used as query sequences to identify *gmaS* sequences in the metagenome. Similarly, *mauA* sequences from *Methylobacterium extorquens* LW-1 and *Methylothermobacter mobilis* were used as queries to detect *mauA* genes. Sequence comparison was carried out on amino acid level. Sequence hits with a minimum stringency *e*-value cut-off of  $10^{-5}$ , a minimum sequence identity of 65% and a minimum length of 65 amino acids were then analysed using blastx. In order to confirm that sequences were genuine *gmaS*, the gene neighbourhood of the nearest related sequence hits originating from published bacterial genomes available on the IMG platform were manually inspected for predicted neighbouring ORFs associated with *gmaS* (as done previously for primer design).

### 2.15.3 Nucleotide sequence accession numbers

Nucleotide gene sequences of 16S rRNA genes and *gmaS* genes analysed during this PhD project were deposited in the GenBank nucleotide sequence database under the accession numbers KM083620–KM083705.

## 2.16 N<sub>2</sub> fixation assay (acetylene reduction)

N<sub>2</sub>-fixing (i.e. nitrogenase) activity in mat samples from Movile Cave was assayed using the method described by Dilworth (1966), which assays the reduction of acetylene (C<sub>2</sub>H<sub>2</sub>) to ethylene (C<sub>2</sub>H<sub>4</sub>) using gas chromatography. A Pye Unicam 104 gas chromatograph fitted with a Porapak N column using N<sub>2</sub> as a carrier gas was employed in conjunction with a flame ionization detector (FID) at the following settings:

Injector temperature: 120°C

Column temperature: 100°C (isothermal)

Detector temperature: 150°C

The sample injection volume was 100 µl. A standard mixture of acetylene and ethylene was prepared by injecting 100 µl of each gas into a serum flask of 1,079 ml total volume. The standard mixture produced two clearly distinguishable peaks; at the above settings, retention times were: ethylene 0.89 min; acetylene 1.29 min. The assay was carried out within 48 hours of sampling using floating mat samples that had been refrigerated immediately after sampling. Mat samples of ~2 g were made up to a final volume of ~4 ml with sterile water in 27 ml serum vials, sealed with rubber seals and flushed for at least 15 min with argon. O<sub>2</sub> was injected into the headspace to a final concentration of 5%. After gentle shaking of the vials at 20°C for 5 min, C<sub>2</sub>H<sub>2</sub> was injected to a final concentration of 1%. Nitrogenase-mediated production of headspace C<sub>2</sub>H<sub>4</sub> was monitored every 15 min for at least 3 hours, starting 5 minutes following the addition of substrate. Two organisms capable of fixing N<sub>2</sub> were tested as positive controls for the assay; (i) the fast-growing methanotroph *Methylosinus trichosporium* OB3b, (ii) the heterotroph *Azotobacter vinelandii*. As better results were obtained with *A. vinelandii*, this organism was chosen as a positive control. Ethylene production was quantified by comparison with known concentrations of standards.

## 2.17 Colorimetric assays

Colorimetric assays were used to assay  $\text{NH}_3$  consumption coupled to nitrite and  $\text{NO}_3^-$  production in SIP enrichments. Cell culture aliquots of 1.5 ml were centrifuged to pellet cells ( $16\,000 \times g$  for 5 min) and 1 ml supernatant was removed to fresh tubes for assaying. Standard solutions and dilutions were prepared with MQ water.

### 2.17.1 Ammonium assay

Ammonium was assayed following the method described by Solórzano (1969), scaled down for a sample of 1 ml and measurement in 1 ml cuvette. Briefly, 40  $\mu\text{l}$  of a 10% phenol-ethanol solution and 40  $\mu\text{l}$  of a 0.5% sodium nitroprusside solution were added to 1 ml sample (or standard solution). 200  $\mu\text{l}$  of hypochlorite solution (Fisher Scientific) were added to 1 ml alkaline solution (100 g trisodium citrate and 5g NaOH in 500 ml water) and mixed, 100  $\mu\text{l}$  of this solution was then added to the sample. After 1 h incubation at 20°C, absorbance was measured at 640 nm. Standards were prepared (i) between 0 and 50  $\mu\text{M}$  and (ii) between 0.1 and 10 mM, as (SIP) incubations from Movile Cave samples were in the mM range. A stock solution of 100 mM ammonium sulfate was used (rather than ammonium chloride used in the original protocol) as cave waters are high in sulfur compounds. Because of the two ammonium atoms in the  $(\text{NH}_4)_2\text{SO}_4$  molecule, standards were diluted with MQ water 1:2 for the assay (0.5 ml MQ + 0.5 ml standard solution). Samples and standards above 50  $\mu\text{M}$  were diluted 1:100 with water in 10 ml glass universals prior to the assay. 1 ml of the dilution was then transferred to a 1.5 ml centrifuge tube where the assay was carried out.

### 2.17.2 Nitrite assay

Nitrite was assayed using Griess' reagent (Sigma-Aldrich). 0.5 ml of Griess' reagent was added to 0.5 ml of sample (or standard solution) and incubated for 30 min at room temperature. Standards were prepared between 25  $\mu\text{M}$  and 2.5 mM using  $\text{KNO}_2$ . Absorbance was read at 520 nm, samples above 0.5 mM were diluted 1:10 when measured.

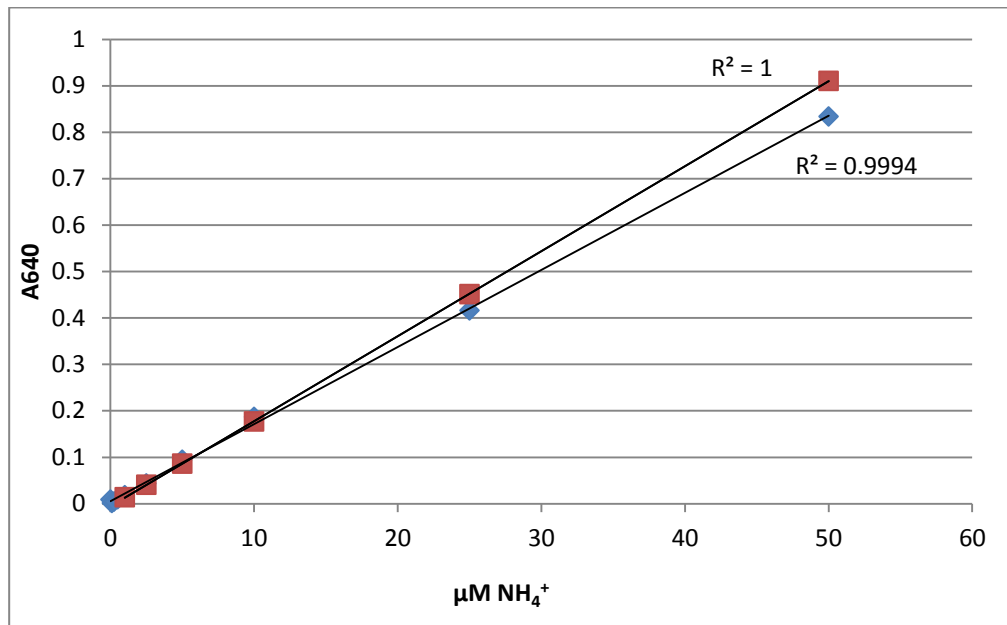


Figure 2.2 Calibration curves for ammonium assay

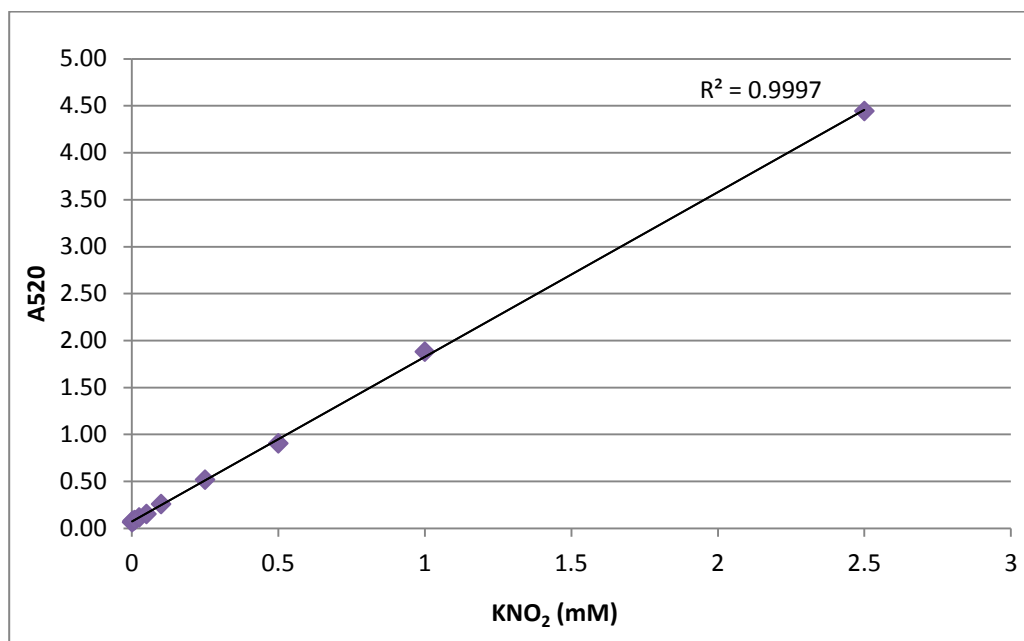


Figure 2.3 Calibration curve for nitrite assay

### 2.17.3 Nitrate assay

Nitrate was first reduced to nitrite using zinc dust and then assayed in the same way as nitrite. Standards were prepared using  $\text{KNO}_3$ . 50 mg zinc was added to 1 ml sample (or standard solution) in Eppendorf tubes and incubated (rotating) for 1 hour at room temperature. Following incubation, tubes were centrifuged (5 min at  $16\,000 \times g$ ) and 0.5 ml supernatant was removed to fresh tubes and mixed with Griess' reagent as before.

## 2.18 Measuring methylated amine concentrations

At the time of the SIP experiments, no robust analytical method for monitoring concentrations of methylated amines was available. Colorimetric assays were initially employed but produced unsatisfactory results. Towards the end of the project, an ion-chromatographic method for measuring methylated amines was developed by Yin Chen allowing quantification of MMA, DMA and TMA down to concentrations of  $1 \mu\text{M}$  (Lidbury *et al.*, 2014).

## 2.19 Isotope pairing experiments for detection of denitrification and anammox

During the 2011 sampling campaign, anoxic water and sediment samples from Movile Cave were incubated with different isotopes of  $\text{NH}_4^+$ ,  $\text{NO}_2^-$  and  $\text{NO}_3^-$ , as described by Trimmer *et al.* (2003), in order to investigate whether denitrification and / or anaerobic ammonia oxidation (anammox) take place in the cave. Anoxic water from Airbell 2 in Movile Cave collected in a 1 L acid-washed, autoclaved *Nalgene* bottle (see 2.3) was filled into 50 pre-evacuated 12 ml Exetainer<sup>®</sup> screw capped glass vials (Labco Limited, Ceredigion, UK) within 48 h of sampling (using a glass pipette, filled to the top), sealed, and left to pre-incubate at room temperature in the dark for 1 week. Similarly, sediment that had been collected from Airbell 2 in acid-washed, sterile 50 ml Falcon tubes was transferred into Exetainer<sup>®</sup> vials within 48 h of sampling. Into each vial, ~2 ml sediment were transferred and topped up with anoxic Airbell 2 water, sealed and pre-incubated for 1 week. Following pre-incubation,  $^{15}\text{N}$ -labelled and unlabelled ( $^{14}\text{N}$ ) substrates were added to a final concentration of  $50 \mu\text{M}$  for each substrate by injection through the septum using sterile syringes (yellow tip) as follows:

- 1)  $^{15}\text{NH}_4^+ + ^{14}\text{NO}_2^-$
- 2)  $^{15}\text{NH}_4^+ + ^{14}\text{NO}_3^-$
- 3)  $^{14}\text{NH}_4^+ + ^{15}\text{NO}_2^-$
- 4)  $^{14}\text{NH}_4^+ + ^{15}\text{NO}_3^-$
- 5)  $^{15}\text{NH}_4^+$  only (anammox control)
- 6) no substrate (control)

The incubations were set up in replicates of five. Incubations were stopped after 5 days by injecting  $\text{ZnCl}_2$  into the vials to inhibit microbial activity as described by Trimmer *et al.* (2003). Samples were analysed by mass spectrometry in Mark Trimmer's laboratory at QMU London as described by Trimmer *et al.* (2003).

---

### **Chapter 3. Isolation of methylated amine-utilising bacteria from Movile Cave**

### 3.1 Introduction

Methylated amines, produced during degradation of organic matter (Anthony, 1982; Barret & Kwan, 1985; Burg & Ferraris, 2008), are hypothesised to be an important intermediate in the microbial food web of Movile Cave, resulting from decomposition of the extensive microbial mats floating on the cave water. Like methane and methanol, methylated amines are one-carbon (C<sub>1</sub>) compounds that serve as a carbon and energy source for certain methylotrophic bacteria. *Methylothera mobilis*, an obligate, monomethylamine (MMA)-utilising methylotroph (Kalyuzhnaya *et al.*, 2006a), was found to be highly abundant in Movile Cave (Chen *et al.*, 2009). However, no dedicated studies have so far been carried out on the role of methylated amines as a microbial food source in Movile Cave. In addition to being methylotrophic substrates, methylated amines are also a source of nitrogen (but not carbon) for a range of non-methylotrophic bacteria. The purpose of the isolation work described in this chapter was to identify bacteria from Movile Cave capable of using methylated amines as a source of carbon, nitrogen or both, and to carry out studies with regard to their MMA-oxidation pathways. All isolates were preserved for future work, providing a collection of organisms for further physiological and molecular studies on methylated amine-utilising bacteria.

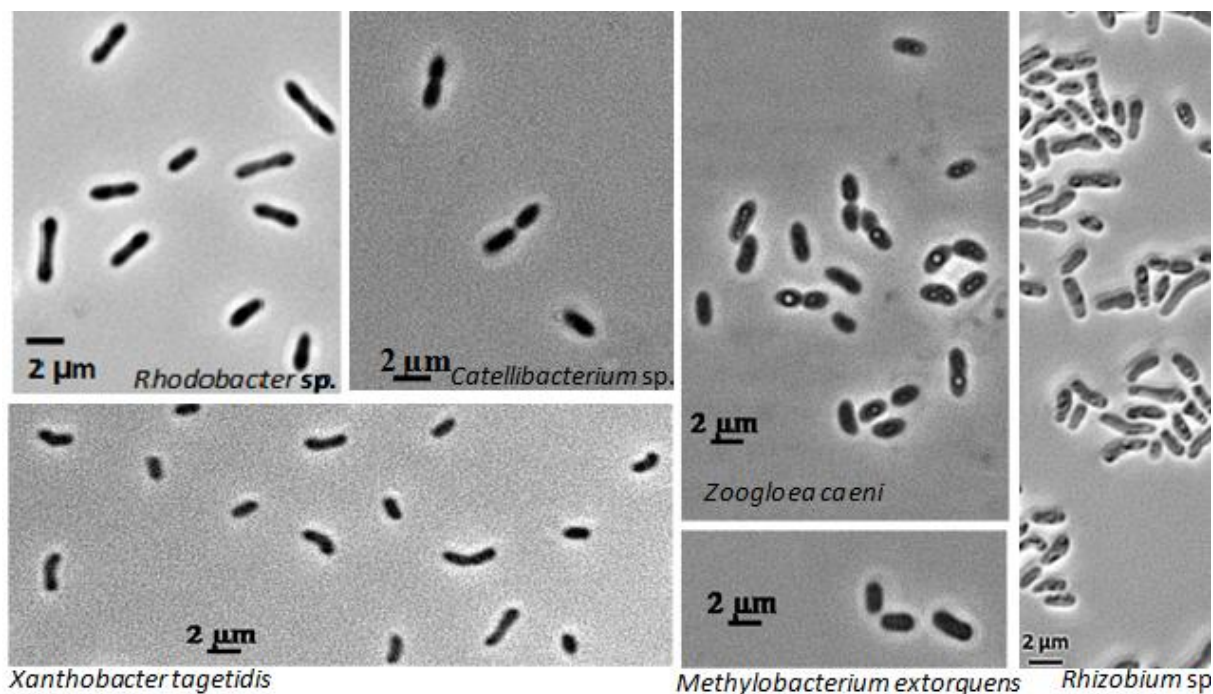
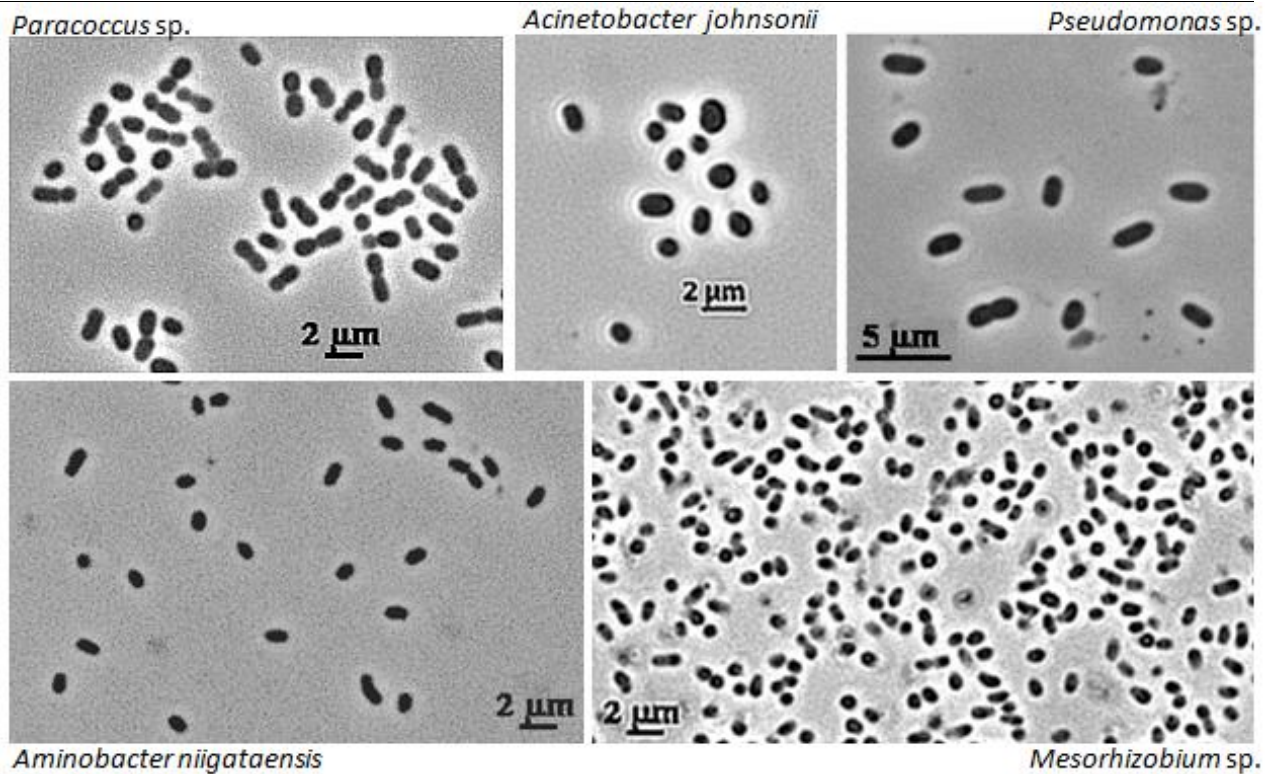


Figure 3.1 a

Clockwise from top left: *Rhodobacter* sp. 1W-5; *Catellibacterium* sp. LW-1; *Zoogloea caeni* A2-14M; *Rhizobium* sp. A2-25M-y3a; *Methylobacterium extorquens* 2W-7; *Xanthobacter tagetidis* LW-13.



**Figure 3.1 b**

Clockwise from top left: *Paracoccus* sp. 2W-61; *Acinetobacter johnsonii* 1W-58; *Pseudomonas* sp. 1W-57Y; *Aminobacter niigataensis* 2W-12; *Mesorhizobium* sp. 1M-11.

**Figures 3.1a & b** Micrographs of methylated amine-utilising bacteria isolated from Movile Cave. Images were taken of cultures grown on DBS-MMA (methylotrophs) and DBS-C MMA (non-methylotrophs).

### 3.2 Isolation of methylotrophic bacteria

Bacteria from Movile Cave capable of using methylated amines as a carbon, energy and nitrogen source were selectively enriched and isolated using three different methylated amines: monomethylamine (MMA), dimethylamine (DMA) and trimethylamine (TMA). Liquid enrichments were set up in small microcosms (120 ml serum vials) with sample material from (i) cave water, (ii) floating mat material and (iii) wall biofilm material, derived from the lake room and air bells (for a map of Movile Cave see Figure 1.3 in Chapter 1) and supplemented with 1 mM of MMA, DMA or TMA as the sole added source of carbon and nitrogen (for details refer to Chapter 2, section 2.6). After 2 weeks of incubation at 21°C in the dark, the enrichments showed turbidity and subcultures were transferred onto agar plates containing 5 mM of MMA, DMA or TMA as sole carbon and nitrogen source (the same substrate was used as before in the

liquid enrichment). A range of isolates differing in colony appearance and cell morphology (Figures 3.1a and b) were obtained and purified by a series of transfers on plates (over 60 organisms were originally isolated, however, not all were kept as many were identified as members of the same species while others turned out not to use methylated amines, see below). The purified isolates were then transferred into liquid media once again to confirm utilisation of methylated amines and rule out possible growth on trace organic compounds in the agar.

Seven methylotrophic strains were isolated (Table 3.1, Figures 3.2a and b), as identified by 16S rRNA gene sequencing analysis of over 60 isolates purified from the enrichments. Of the three substrates, methylotrophic organisms obtained on MMA showed the highest level of diversity, while DMA and TMA enrichments were dominated by *Xanthobacter tagetidis* (which was not isolated on MMA). There were also differences in the diversity of the methylotrophic communities obtained from different sample materials: While methylotrophs isolated from water were very diverse, enrichments obtained from floating mat and wall biofilm samples were heavily dominated by *Xanthobacter tagetidis*. Additionally, *Methylobacterium extorquens* was only isolated from Airbell 2 (the most remote part of the cave).

In addition to well-characterised methylotrophic bacteria such as *Methylobacterium*, *Aminobacter* and *Xanthobacter*, two novel methylotrophs were isolated: A member of the relatively newly described genus *Catellibacterium* (Tanaka *et al.*, 2004; Liu *et al.*, 2010, Zheng *et al.*, 2011; Zhang *et al.*, 2012), named *Catellibacterium* sp. LW-1, was isolated from a Movable Cave lake water enrichment with MMA as sole carbon and nitrogen source. 16S rRNA gene sequences relating to this organism were also detected in heavy DNA fractions from <sup>13</sup>C-MMA enrichments (see Chapter 4, section 4.3.2, text and Figure 4.4), as well as DMA-enrichments (see Chapter 4, section 4.4., text and Figure 4.7) indicating that *Catellibacterium* may play a significant role in the cycling of methylated amines in Movable Cave. Another new methylotroph, *Mesorhizobium* sp. 1M-11, was isolated from an MMA enrichment set up with floating mat samples from Airbell 1. While a strain of the closely related *Mesorhizobium loti* (99% based on 16S rRNA gene comparison) has been shown to use MMA as a nitrogen source (Chen *et al.*, 2010b), at the time of writing, the Movable Cave isolate presents the first methylotrophic member of the genus *Mesorhizobium*.

**Table 3.1** Growth of bacterial isolates from Movile Cave on methylated amines with and without added carbon

Isolates	Phylogeny <sup>(1)</sup>	Identity <sup>(2)</sup> (%)	Isolation source	Growth on methylated amines				Growth on R2A	
				MMA + C	DMA + C	TMA + C	MMA		DMA
<i>Alphaproteobacteria</i>									
2W-7	<i>Methylobacterium extorquens</i>	100	Airbell 2, water	+	+	+	+	+	+
LW-13	<i>Xanthobacter tagetidis</i>	100	Lake, water	+	+	+	+	+	+
A2-1D	<i>Paracoccus yeei</i>	100	Airbell 2, water + mat	+	+	+	+	+	+
2W-61	<i>Paracoccus yeei</i>	98	Airbell 2, water	+	+	+	+	+	+
2W-12	<i>Aminobacter niigataensis</i>	100	Airbell 2, water	+	+	+	+	+	+
LW-1	<i>Catellibacterium caeni</i>	99	Lake, water	+	-	+	+	-	+
1M-11	<i>Mesorhizobium loti</i>	99	Airbell 1, floating mat	+	+	+	+	+	+
A2-41x	<i>Shinella yambaruensis</i>	98	Airbell 2, water + mat	+	-	-	-	na	na
1W-5	<i>Rhodobacter blasticus</i>	96	Airbell 1, water	+	+	+	-	-	+
O1	<i>Oleomonas sagaranensis</i>	98	Airbell 2, water + mat	+	+	-	-	-	+
O3	<i>Oleomonas sagaranensis</i>	99	Airbell 2, water + mat	+	-	-	-	-	+
A2-25M-y3a	<i>Rhizobium rosetiformans</i>	97	Airbell 2, water + mat	+	*	*	-	*	-
<i>Gammaproteobacteria</i>									
1W-58	<i>Acinetobacter johnsonii</i>	100	Airbell 1, water	+	+	+	-	-	+
2W-62	<i>Acinetobacter lwoffii</i>	100	Airbell 2, water + mat	+	+	-	-	-	+
1W-57Y	<i>Pseudomonas oryzihabitans</i>	99	Airbell 1, water	+	-	-	-	-	+
A2-25M-y3b	<i>Pseudomonas kuykendallii</i>	99	Airbell 2, water + mat	+	*	*	-	*	+
<i>Betaproteobacteria</i>									
A2-14M	<i>Zoogloea caeni</i>	100	Airbell 2, water + mat	+	+	+	-	-	+

Abbreviations: MMA, monomethylamine; DMA, dimethylamine; TMA, trimethylamine; C, carbon mixture (glucose, fructose, sucrose, acetate, pyruvate, succinate, glycerol); na, not analysed. Carbon sources were supplied at 5 mM, nitrogen sources at 1 mM. Growth was at 21 °C in dilute basal salts medium.

<sup>(1)</sup> All organisms in the column refer to the type strains of the respective species (as listed on LSPN).

<sup>(2)</sup> Identity refers to 16S rRNA gene sequence identity over 750 bp. \*These isolates have not yet been tested on DMA and TMA due to time limitations.

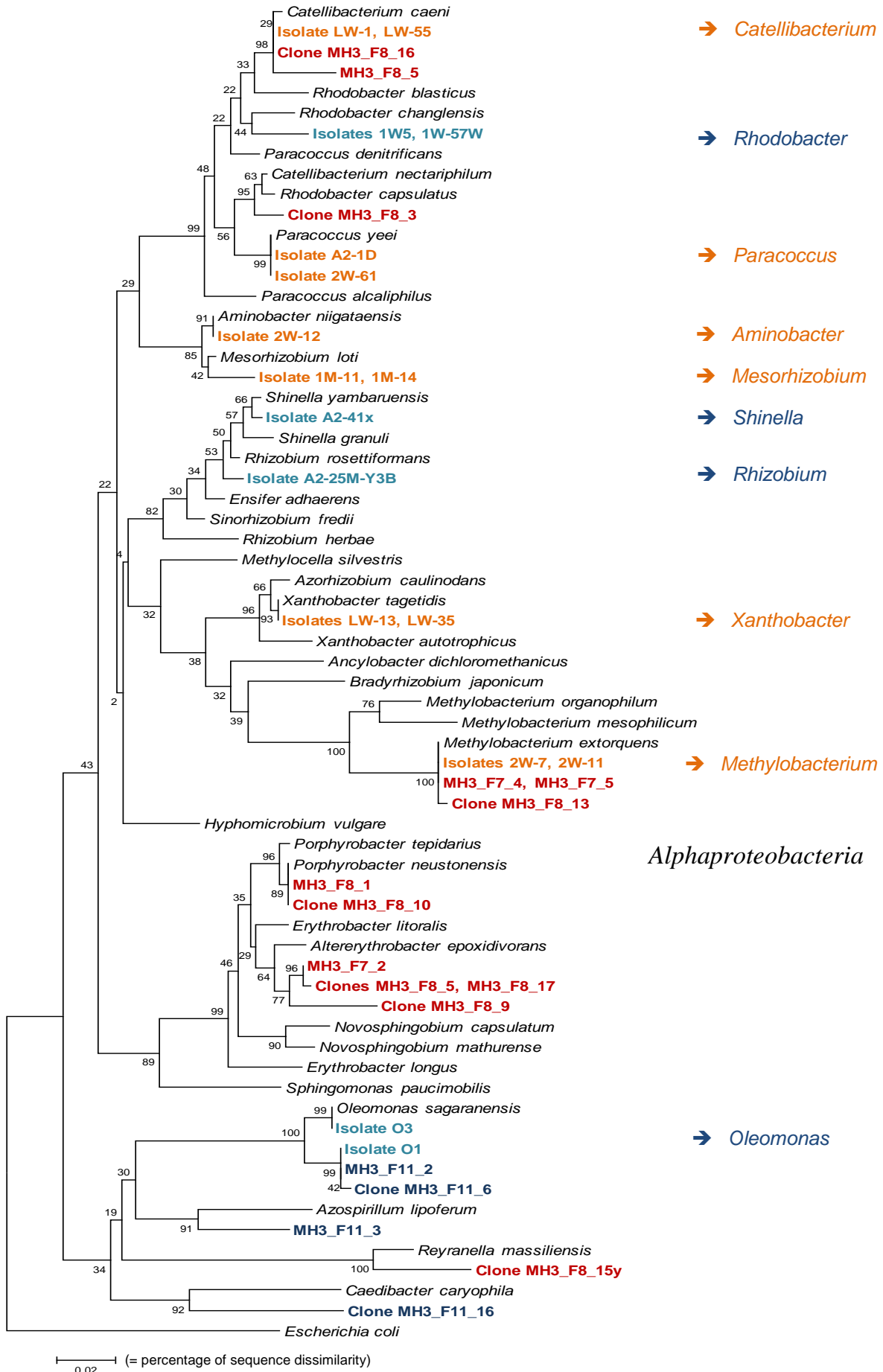


Figure 3.2a

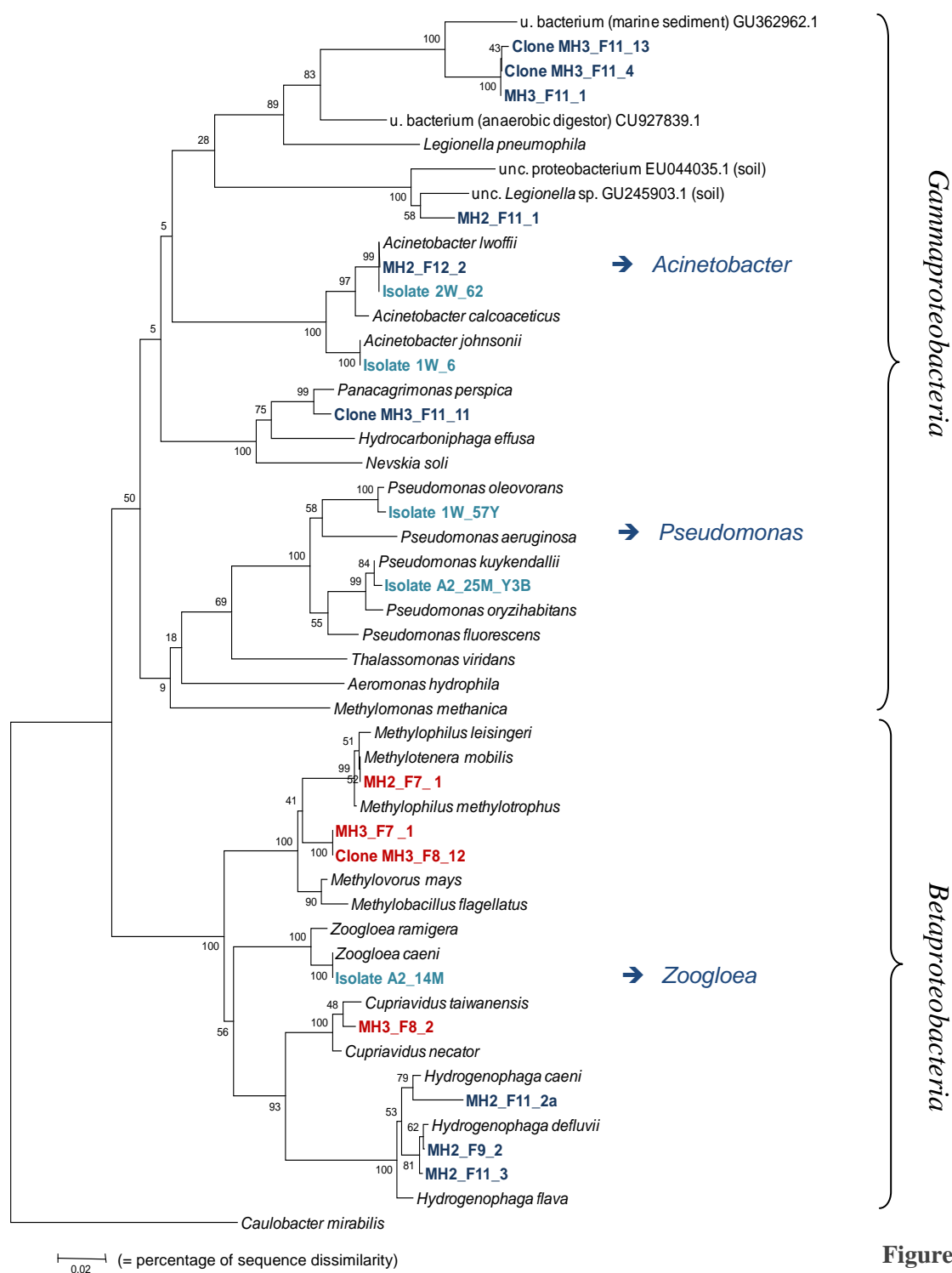
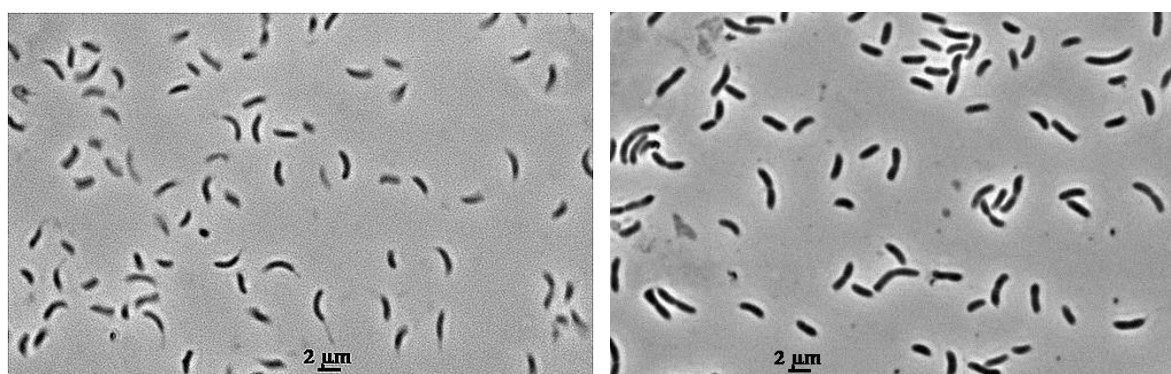


Figure 3.2b

**Figures 3.2a & b** Phylogenetic relationships of bacterial 16S rRNA gene sequences (~700 bp) retrieved from Movile Cave isolates grown on methylated amines, DGGE bands and clone libraries from SIP enrichments with MMA; (a) *Alphaproteobacteria*, (b) *Gamma*- and *Betaproteobacteria*. Methylophilic isolates are coloured orange; non-methylophilic isolates are blue. Red-coloured sequences are derived from heavy DNA fractions (i.e. methylophilic), dark-blue-coloured ones from light fractions (non-methylophilic). Trees were established using the neighbour-joining method (1,000 bootstrap replicates) and the maximum composite likelihood method for computing evolutionary distances. Numbers at nodes indicate bootstrap values. All bacterial sequences refer to type strains (as listed on LPSN), unless strain names are indicated. Abbreviations: u., uncultured; unc., uncultured.

A number of isolates obtained on methylated amines initially appeared to grow methylotrophically but ceased to grow after several subcultures. Some of these organisms were subsequently found to use methylated amines as a nitrogen source only (*Rhodobacter*, *Pseudomonas*). Meanwhile, a number of isolates did not show growth in liquid medium even after alternative carbon sources (glucose, fructose, succinate, glycerol, pyruvate and acetate) were added, and were therefore discarded. For instance, strains of *Sinorhizobium* / *Ensifer* (99% identity to *Sinorhizobium morelense* / *Ensifer adhaerens*) were highly abundant in enrichments with DMA as the sole carbon and nitrogen source (based on microscopic observations and 16S rRNA gene sequencing of colonies). They initially grew well on plates with DMA as the sole carbon and nitrogen source, but growth ceased after several generations. Unlike the aforementioned organisms, *Sinorhizobium* / *Ensifer* also failed to grow with methylated amines as a nitrogen source once additional carbon was provided. Similarly, several isolates of *Caulobacter* (99% identity to *Caulobacter segnis*) were obtained from MMA, DMA and TMA enrichments set up with samples from floating mat and wall biofilm. While producing some growth on DBS-C MMA plates (Figure 3.3), they were unable to grow in liquid DBS-C MMA medium.



**Figure 3.3** Micrographs showing growth of a *Caulobacter* sp. isolated from Movile Cave on DBS-C MMA plates (left) and on R2A plates, (right). While producing some growth on plates with MMA as sole nitrogen source, the organism did not grow in liquid medium unless  $\text{NH}_4^+$  was added.

All of the methylotrophic isolates obtained in the course of this PhD were found to be facultative, i.e. also able to use sugars or carboxylic acids for growth. Furthermore, all methylotrophs could use all three methylated amines as sole growth substrates *in situ*, with the exception of *Catellibacterium* sp. LW-1, which was unable to utilise DMA (Table 3.1). Generally, fastest growth occurred with MMA, with the exception of all *Xanthobacter tagetidis* isolates, which grew rapidly on TMA but showed rather weak growth on MMA and DMA.

### 3.3 Isolation of non-methylotrophic bacteria (and yeast)

In a separate experiment, heterotrophic bacteria capable of using methylated amines as a nitrogen (but not carbon) source were enriched and isolated using the same sample material as used for isolation of methylotrophs. MMA, DMA or TMA, respectively, were the only added nitrogen sources in these enrichments, with a mixture of sugars and carboxylic acids (comprising glucose, fructose, succinate, glycerol, pyruvate and acetate) added as alternative carbon and energy sources. Growth was visible in liquid enrichments as flakes of biomass material after two weeks of incubation at 21°C in the dark. Subcultures of these enrichments showed turbidity after several days of incubation. Dilutions of the subcultures were then transferred onto agar plates (the solid media contained the same substrate as used in the respective liquid enrichment), and a range of colony types became visible within a few days of incubation. Following purification on plates, the individual isolates were grown in liquid medium, generating a total of ten non-methylotrophic bacterial isolates capable of using methylated amines as nitrogen sources (identified by 16S rRNA gene sequencing), including *Alpha*-, *Beta*-, and *Gammaproteobacteria* (Table 3.1, Figures 3.2a and b). Purification of non-methylotrophs was noticeably more difficult than for methylotrophs since contaminants were harder to eliminate with the added carbon in the medium. Co-enriched heterotrophic organisms (Figure 3.4) probably used  $\text{NH}_4^+$ , released by MA utilisers, as a nitrogen source. Several isolates transferred into liquid from what was believed to be single colonies on plates turned out to be contaminated, e.g. *Oleomonas* (Figure 3.5). Dilution to extinction approaches were not successful in obtaining pure cultures either. The swarming growth and lack of single colonies of *Oleomonas* on plates (Figure 3.6) presented an additional challenge for purification of this organism. In some cases, R2A plates proved useful for purification purposes, however some MA-utilisers (namely *Rhizobium* sp. A2-25M-y3a and *Shinella* sp. A2-41x) were unable to grow on R2A.

The facultative methylotrophs *Xanthobacter tagetidis* and *Paracoccus yeei*, isolated previously under methylotrophic conditions (see section 3.2.), were also isolated from microcosms with methylated amines and added multi-carbon compounds. Other methylotrophs, such as *Methylobacterium*, were not detected, indicating they may be outgrown by heterotrophs under these conditions.

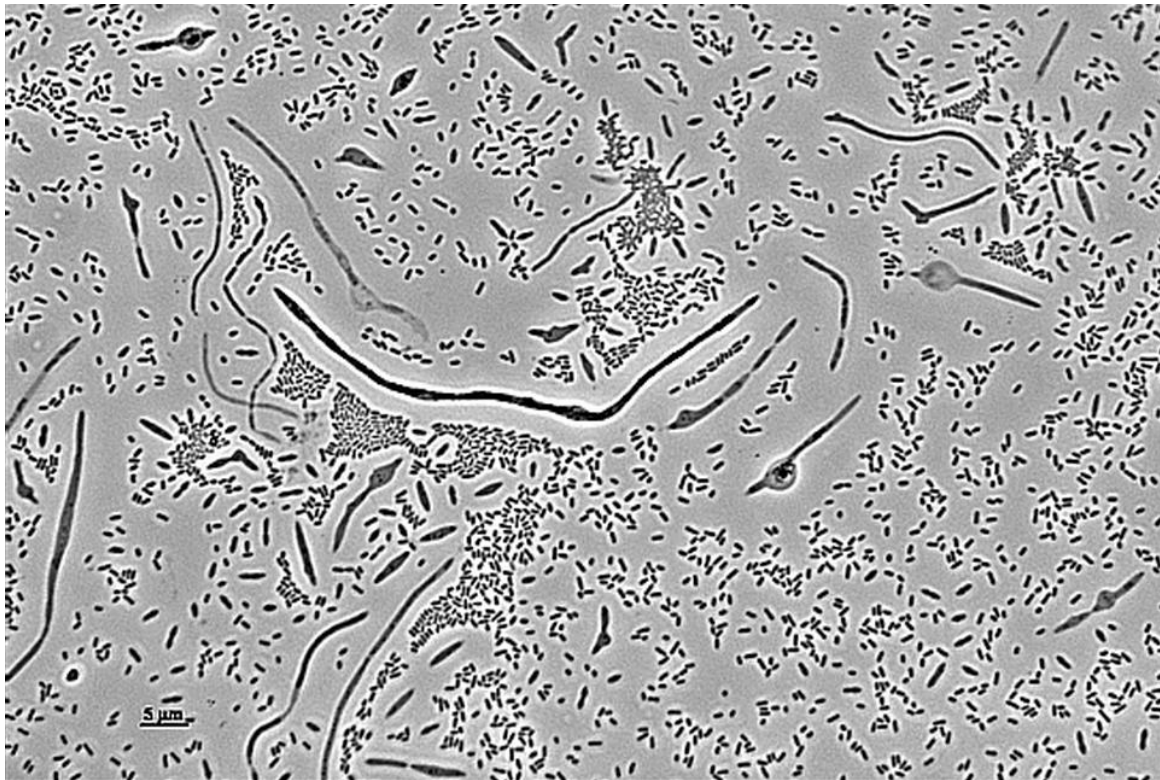


**Figure 3.4** Micrograph of a liquid enrichment culture (DBS-C MMA, 30°C, pH 5.5) that resulted in isolation of species of *Oleomonas* (short rods), *Bacillus* and *Paenibacillus* (filamentous bacteria). Only *Oleomonas* was subsequently found to use MMA as a nitrogen source.

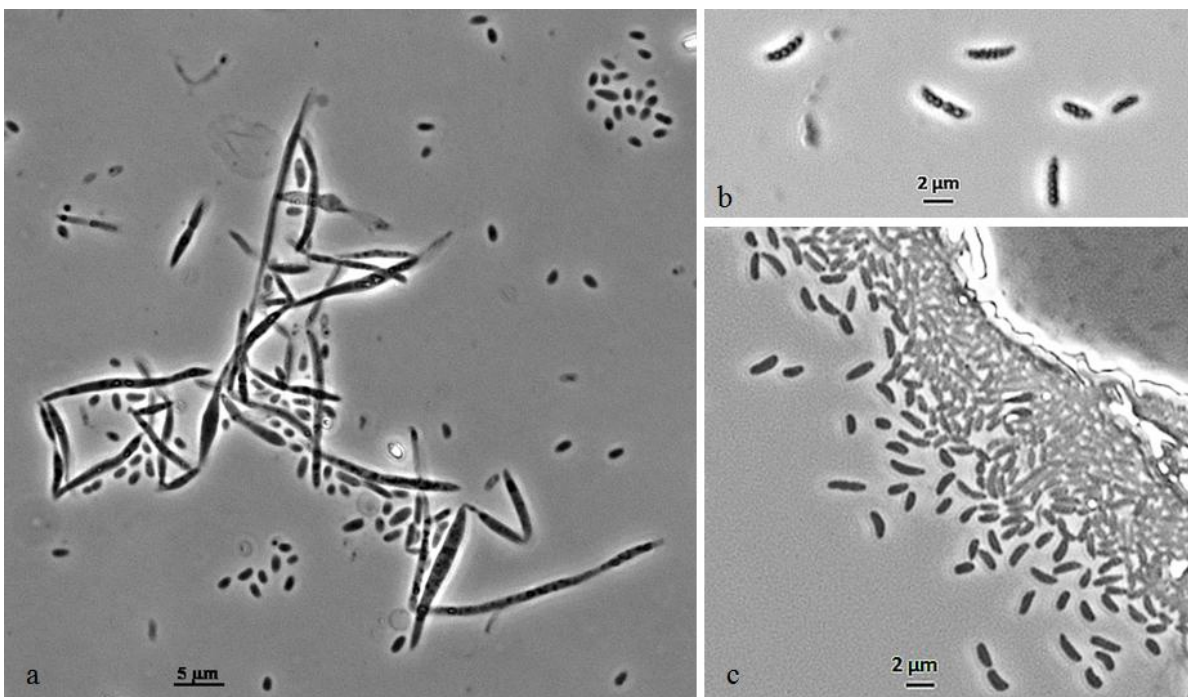


**Figure 3.5** Micrographs of *Oleomonas* isolates from Movile Cave.

Left: Liquid culture of *Oleomonas* sp. O3 with co-enriched filamentous bacterium.

Right: Purified cultures of *Oleomonas* sp. O1 (top) and *Oleomonas* sp. O3 (bottom).



**Figure 3.6** Swarming growth of *Oleomonas* sp. O1 (left) and *Oleomonas* sp. O3 (centre and right) on plates made purification of these isolates difficult.

All of the non-methylotrophic isolates used MMA as a nitrogen source, while only some could use DMA and TMA (Table 3.1), suggesting that many lack the enzymes for demethylation of secondary and tertiary methylated amines to MMA. Of the two closely related *Oleomonas* strains (both isolated from Airbell 2 mat / water enrichments with MMA as a nitrogen source), *Oleomonas* sp. O1 was able to use both MMA and DMA, while *Oleomonas* sp. O3 could only use MMA. Of the two *Acinetobacter* isolates, *Acinetobacter johnsonii* (isolated from Airbell 1 water with MMA as a nitrogen source) was able to use MMA, DMA and TMA as nitrogen sources, while *Acinetobacter lwoffii* (isolated from Airbell 2 water with MMA as a nitrogen source) could use only MMA and DMA. *Acinetobacter lwoffii* was also detected in  $^{12}\text{C}$ -DNA fractions from MMA-SIP (see Chapter 4, sections 4.3.3 and 4.4; Figures 4.4 and 4.7), suggesting that this organism, and other non-methylotrophs, may play an active role in the cycling of methylated amines in Movile Cave.

In addition to bacterial isolates, a methylotrophic, pink yeast was isolated from a number of enrichments (Figure 3.7). The isolate shared 100% 16S rRNA gene sequence identity to *Rhodotorula rubra*, a euryhaline yeast of marine origin (Robertson & Button, 1979). While the isolate was able to use MMA, DMA and TMA as nitrogen sources, it could grow methylotrophically only with methanol as a carbon source. These results agree with studies of other methylotrophic yeast species, all of which seem to be able to use methanol, but not methylated amines as a carbon source (van Dijken & Bos, 1981; Negruță *et al.*, 2010; Yurimoto *et al.*, 2011). The identification of a methanol- and methylated amine-utilising yeast is of interest as fungi comprise a large part of the floating mats in Movile Cave (based on microscopic observations, Figure 3.8, and results published by Sârbu *et al.*, 1994) and may therefore play a significant role in the cycling of one-carbon compounds in Movile Cave.

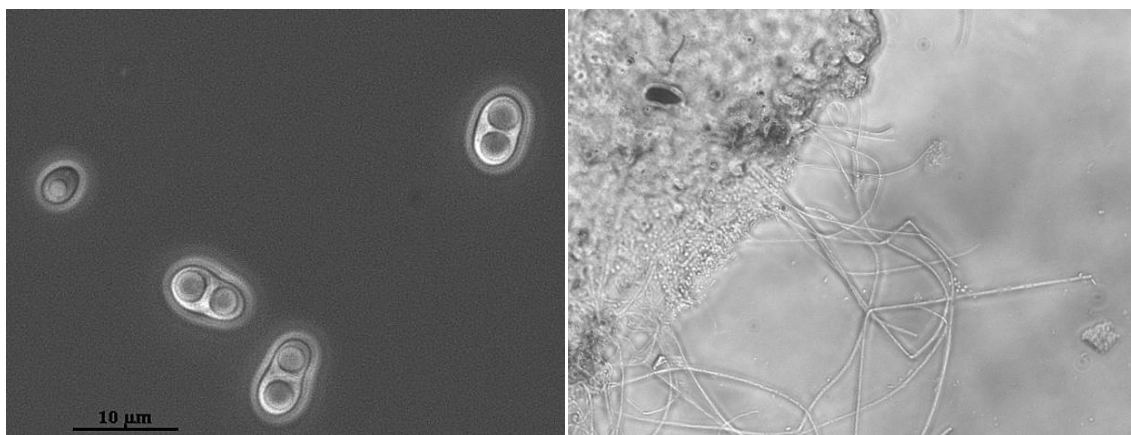


**Figure 3.7 (left)** Dividing cells of the methylotrophic yeast *Rhodotorula rubra*, isolated from Movile Cave

**Figure 3.8 (right)** MAR image showing filamentous fungi in a sample of Movile Cave mat. (copyright Rich Boden)

In addition to *alpha*-, *beta*-, and *gamma*proteobacterial isolates, several gram-positive bacteria from the classes *Actinobacteria* (*Arthrobacter*, *Brevibacterium*, *Micrococcus*) and *Firmicutes* (*Bacillus*, *Paenibacillus*) were isolated from enrichments with methylated amines and added carbon. However, while growing well on plates with MMA as the sole nitrogen source, none of these organisms produced any growth in liquid media unless ammonium was added (suggesting they may have been scavenging trace amounts of nitrogen present in the agar). This was somewhat surprising as *Arthrobacter*, *Bacillus*, *Brevibacterium* and *Micrococcus* are all known to contain methylotrophic species, some of which also grow on MMA (e.g. Levering *et al.*, 1981; Dijkhuizen *et al.*, 1988; Nešvera *et al.*, 1991; Boden *et al.*, 2008; Hung *et al.*, 2011). Consulting the literature on these organisms did not indicate any special growth requirements that had not been met, and control incubations with added ammonium produced rapid growth. Both *Bacillus* sp. and *Paenibacillus* sp. (Figure 3.9b) initially seemed to grow well in liquid medium with MMA as the only nitrogen source, and were preserved as glycerol stocks. Unfortunately, upon restreaking the glycerol stocks on R2A, it became clear that both *Bacillus* and *Paenibacillus* were contaminated with *Oleomonas*. After purification, both isolates maintained good growth on plates with MMA as the sole nitrogen source, but showed no growth whatsoever in liquid DBS-C MMA medium once the *Oleomonas* was removed. These results confirm that the gram-positive bacterial strains isolated from Movile Cave do not use MMA as a nitrogen source in liquid medium.

As with the gram-positive isolates, a *Sphingopyxis* sp. isolate grew well on solid but not liquid DBS-C MMA medium. Similarly, isolates of *Azospirillum* sp. (Figure 3.9a) and

*Aeromonas hydrophila* did initially produce good growth in liquid medium with MMA as the sole nitrogen source. Curiously however, these strains lost this ability over a number of generations. Published genome data of the *Azospirillum* strain B510 NC\_013855 show that this organism carries the *gmaS* gene on a plasmid. This may also be true for the above Movile Cave isolates, suggesting they may have lost the genetic potential to utilise MMA over time.

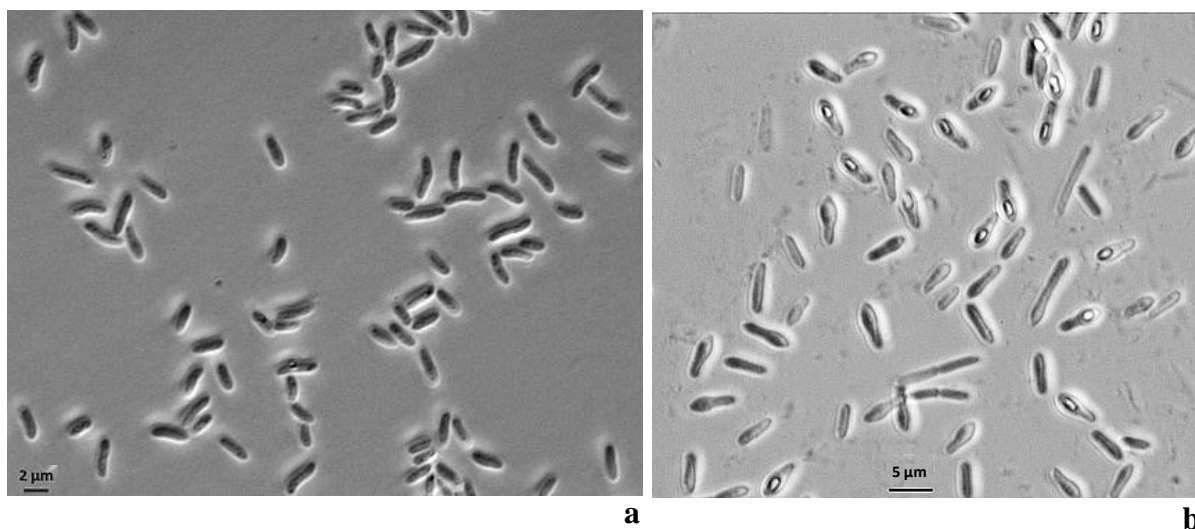


**Figure 3.9** *Azospirillum* (left) and *Paenibacillus* (right) isolates from Movile Cave. *Azospirillum* lost the ability to grow with MMA as a nitrogen source. Putative pure cultures of *Paenibacillus* appearing to grow with MMA as a nitrogen source turned out to contain *Oleomonas*. Images shown were of cultures growing on R2A medium.

### 3.4 Two new methylotrophic strains from Movile Cave:

#### *Catellibacterium* sp. LW-1 and *Mesorhizobium* sp. 1M-11

Two of the six methylotrophic strains isolated from Movile Cave in the course of this PhD belong to bacterial genera which have not previously been shown to grow methylotrophically: *Catellibacterium* sp. LW-1, isolated from lake water, and *Mesorhizobium* sp. 1M-11, isolated from a floating mat. Both strains were isolated with MMA as the sole carbon and nitrogen source and are facultative in their use of methylated amines, as they are also able to utilise multi-carbon compounds for growth (a mixture of glucose, fructose, succinate, glycerol, pyruvate and acetate was used). Cells of *Catellibacterium* sp. LW-1 were non-motile, short rods (1 - 1.5 μm; Figures 3.1 and 3.10a), while cells of *Mesorhizobium* sp. 1M-11 were motile rods with varying length: (~1 μm on MMA medium; Figure 3.1, and ~2.5 μm on DMA medium; Figure 3.10b). Details of growth characteristics and 16S rRNA gene phylogeny of the two isolates are summarised in Table 3.2.

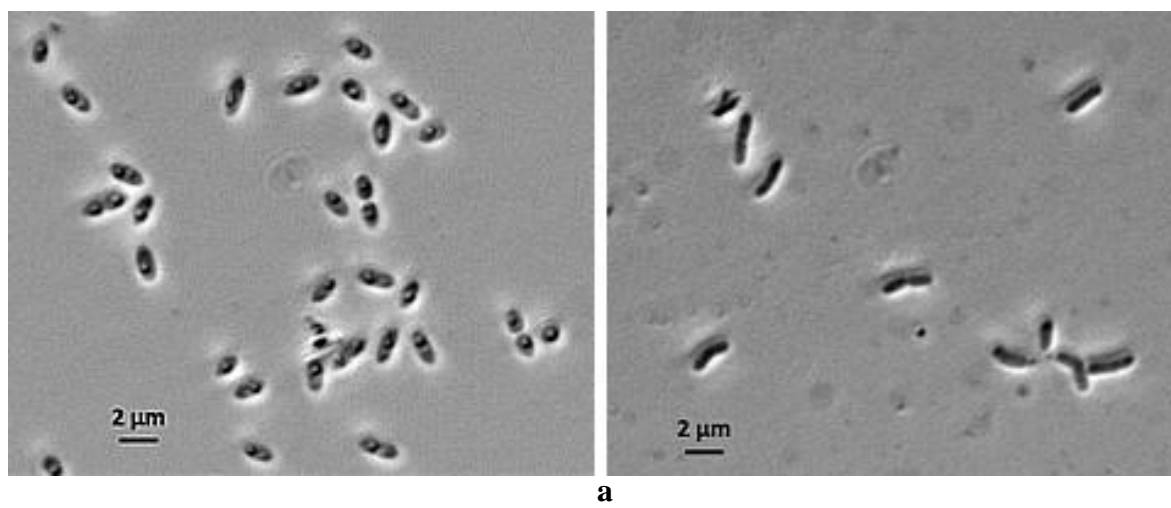


**Figure 3.10** Micrographs of *Catellibacterium* sp. LW-1 (a) and *Mesorhizobium* sp. 1M-11 (b), methylotrophic isolates from Movile Cave.

### 3.4.1 Growth characteristics of *Catellibacterium* sp. LW-1 and *Mesorhizobium* sp. 1M-11

While *Mesorhizobium* sp. 1M-11 grew on all three methylated amines tested, *Catellibacterium* sp. LW-1 was unable to grow on DMA, but grew equally well with MMA or TMA. Generation times for *Mesorhizobium* sp. 1M-11 on methylated amines were in the range of 11.6 – 17.3 h, and significantly shorter when multi-carbon compounds were supplied (< 4 h). Meanwhile, *Catellibacterium* sp. LW-1 grew with similar generation times on MMA (4.6 h) or TMA (3.6 h) as with multi-carbon compounds (< 4 h) when substrate concentrations were not limiting.

When growing on methylated amines, *Mesorhizobium* sp. 1M-11 furthermore exhibited a much longer lag phase (25-30 h) than on multicarbon compounds ( $\leq 5$  h). *Catellibacterium* sp. LW-1 exhibited a similar lag phase ( $\leq 5$  h) on multicarbon compounds. However, when growing on methylated amines, the lag phase of *Catellibacterium* sp. LW-1 was significantly shortened by the use of fresh inoculum into pre-warmed fresh medium, reducing the lag phase from 20 h to  $\leq 5$  h. In contrast, the activity of the inoculum had no noticeable effect on the growth of *Mesorhizobium* sp. 1M-11.

PCR primers targeting the gene for gamma-glutamylmethylamide synthetase (*gmaS*), a key enzyme of the recently discovered indirect MMA-oxidation pathway, developed in this PhD (see Chapter 5), detected *gmaS* in both *Mesorhizobium* sp. 1M-11 and *Catellibacterium* sp. LW-1 (Chapter 5, section 5.5., Table 5.2). Additionally, genome sequencing of the two isolates (carried out by Deepak Kumaresan) revealed the presence of

the gene for methylamine dehydrogenase (*mauA*), indicative of the conventional, direct MMA oxidation pathway in *Catellibacterium* sp. LW-1, but not in *Mesorhizobium* sp. 1M-11. These findings pose the question whether the observed differences in doubling time between the two isolates (< 4 h compared to > 11 h) when growing methylotrophically on MMA might be due to the higher energy requirements of the indirect MMA pathway (1 ATP per reaction is used, see Figure 5.1b in Chapter 5) compared to the *mauA*-mediated pathway. Detailed chemostat experiments will be required to establish whether this is the case. It will also be interesting to understand the regulation of the two MMA-oxidising pathways in *Catellibacterium* sp. LW-1 under different growth conditions. Quantitative PCR and expression studies could also give valuable clues as to the expression and regulation of these two enzyme systems.

**Table 3.2** Characteristics of two new methylotrophic strains from Movile Cave

	<i>Catellibacterium</i> sp. LW-1	<i>Mesorhizobium</i> sp. 1M-11
<b>Isolation source / substrate</b>	Lake water / MMA	Airbell 1 floating mat / MMA
<b>16S rRNA gene phylogeny</b>	99% <i>Catellibacterium caeni</i> ( <i>Rhodobacteraceae</i> , <i>Rhodobacterales</i> , <i>Alphaproteobacteria</i> )	99% <i>Mesorhizobium loti</i> ( <i>Phyllobacteriaceae</i> , <i>Rhodobacterales</i> , <i>Alphaproteobacteria</i> )
<b>Morphology</b>	Short rods	Rods, varying length
<b>Motility</b>	Immotile	Motile
<b>Carbon sources:</b>		
MMA / DMA / TMA	+ / - / +	+ / + / +
Methanol	-	-
Multi-carbon compounds	+	+
<b>Doubling times (d):</b>		
MMA	d = 4.6 h	d = 13.8 h
DMA	No growth	d = 11.6 h
TMA	d = 3.6 h	d = 17.3 h
Multi-carbon compounds	d = 3.6 h	d = 3.6 h
<b>MMA oxidation key genes</b>	<i>gmaS</i> + <i>mauA</i> *	<i>gmaS</i>

Abbreviations: MMA, monomethylamine; DMA, dimethylamine; TMA, trimethylamine. Results marked \* are based on genome analysis, as initial PCR-based screening did not detect the *mauA* gene in either isolate.

There was no difference in the growth behaviour of either organism when MMA was replaced with ammonium as the nitrogen source, and neither of the strains was able to grow without the addition of a fixed nitrogen source. No growth occurred under anoxic conditions with nitrite, nitrate, or without added electron acceptors under the conditions used (for details see Chapter 2, section 2.6.5). Neither *Catellibacterium* nor *Mesorhizobium* were able to use methanol as a carbon source, while controls with methanol and added MMA produced good growth, ruling out a toxic effect from the methanol. Interestingly, the *Catellibacterium* species most closely related to the Movile isolate, *C. caeni*, has been reported to utilise methanol as a carbon source (Zheng *et al.*, 2011).

### 3.4.2 *The genus Catellibacterium*

The genus *Catellibacterium*, belonging to the family *Rhodobacteraceae*, is relatively new, comprising, at the time of writing, five validated species: *Catellibacterium nectariphilum* (Tanaka *et al.*, 2004), *Catellibacterium aquatile* (Liu *et al.*, 2010), *Catellibacterium caeni* (Zheng *et al.*, 2011), *Catellibacterium changlense* (Anil Kumar *et al.*, 2007; Zheng *et al.*, 2011) and *Catellibacterium nanjingense* (Zhang *et al.*, 2012). *Catellibacterium* is closely related to several other genera of the *Rhodobacter* Clade, namely *Paracoccus*, *Rhizobium* and *Gemmobacter*. The exact classification of species assigned to these genera is in places not entirely clear and has been interpreted differently by different authors (in a recent publication, the suggestion was made to re-assign all species of *Catellibacterium* to *Gemmobacter*; Chen *et al.*, 2013). However, the genus *Catellibacterium* is of interest as several of its species have been isolated in connection with their ability to degrade various pesticides, namely propargite, methomyl, propanil and butachlor (Shen *et al.*, 2007; Xu *et al.*, 2009; Zhang *et al.*, 2012; Zheng *et al.*, 2012). Growth on C<sub>1</sub> compounds has not been reported for this genus so far, with the exception of *C. caeni* which grows on methanol (Zheng *et al.*, 2011). At the time of writing, the only available *Catellibacterium* genome is that of *C. nectariphilum*. No genes associated with MMA oxidation (*gmaS* or *mauA*) have been detected in this genome, suggesting that this organism does not have the genetic capability to utilise methylated amines.

### 3.4.3 The genus *Mesorhizobium*

Rhizobia, a collective term used for bacteria of the genera *Mesorhizobium*, *Rhizobium*, *Sinorhizobium* and *Bradyrhizobium*, are soil and rhizosphere bacteria which are able to establish intracellular N<sub>2</sub>-fixing symbioses with leguminous plants (e.g. reviews by Bottomley, 1992; Martinez-Romero, 2006; Hayat *et al.*, 2010; Lindström *et al.*, 2010; Laranjo *et al.*, 2014). In a legume nodule, the host provides C<sub>4</sub> dicarboxylates to symbiotic Rhizobia as the carbon source; Rhizobia fix atmospheric nitrogen (N<sub>2</sub>) and provide ammonia to the host as a nitrogen source in return (Prell & Poole, 2006). Rhizobia have received much attention in the last few decades since they account for at least half of all biologically fixed nitrogen in agriculture, and are the most important route for sustainable nitrogen input into the agro-ecosystems (Lindström *et al.* 2010). The genus *Mesorhizobium* is therefore mainly known for its legume-nodulating, N<sub>2</sub>-fixing strains. *Mesorhizobium loti* which, based on 16S rRNA gene analysis, is 99% identical to the Movable Cave isolate *Mesorhizobium* sp. 1M-11, is a model organism for legume-rhizobia symbioses (e.g. Kaneko *et al.*, 2000; Uchiumi *et al.*, 2004; Tatsukami *et al.*, 2013). An important feature of the *M. loti* genome (Kaneko *et al.*, 2000) is the arrangement of the symbiotic N<sub>2</sub> fixation genes in a cluster on a 500 kb segment of DNA, called the “symbiosis island”, which is horizontally transferred to non-symbiotic *Mesorhizobium* species, conferring the ability to fix nitrogen symbiotically (Sullivan & Ronson, 1998; Uchiumi *et al.*, 2004). Non-symbiotic *Mesorhizobium* strains are found in nature that lack a symbiotic island (Sullivan *et al.*, 1996). In addition to the symbiotic lifestyle, rhizobia also have a free-living condition and can survive in soils through many environment stresses, such as nutrient starvation (Uchiumi *et al.*, 2004). Even though genome and transcriptome analyses of rhizobia have been carried out, their lifestyle in the environment remains largely unknown (Tatsukami *et al.*, 2013).

At the time of writing, the Movable Cave isolate *Mesorhizobium* sp. 1M-11 represents the first member of the genus *Mesorhizobium* shown to grow methylotrophically. However, while unable to use methylated amines as a carbon source, utilisation of methylated amines as a nitrogen source has recently been demonstrated for a closely related *Mesorhizobium loti* strain (Chen *et al.*, 2010b). Furthermore, *Mesorhizobium loti* has been shown to contain *gmaS*, encoding a key enzyme for the indirect MMA oxidation pathway. Interestingly, despite being 99% related based on 16S rRNA gene comparison, the *gmaS* gene sequences of *Mesorhizobium* sp. 1M-11 and *Mesorhizobium loti* affiliate with different clusters in the *gmaS* tree (see Figure 5.12).

**Chapter 4. Identification of methylotrophic bacteria in Movile Cave by  
DNA-stable isotopic probing (SIP) with  $^{13}\text{C}$ -monomethylamine**

## 4.1 Introduction: SIP as a tool in microbial ecology

To identify major MMA-utilising bacteria in Movile Cave and follow the flow of C<sub>1</sub>-carbon down the food chain, SIP experiments with <sup>13</sup>C-labelled monomethylamine (MMA) and dimethylamine (DMA) were set up as a key experiment of this PhD thesis. A time-course approach was chosen in order to assess changes in the methylotrophic community and reveal potential cross-feeding over time following incubation with <sup>13</sup>C-labelled substrates.

The microbial food web in Movile Cave is highly complex and to a large extent still unexplored. While traditional, culture-based approaches (including isolation and most probable number (MPN) counts) have generated valuable information on physiological groups present in the cave, (Sârbu *et al.*, 1994; Vlăsceanu *et al.*, 1997; Rohwerder *et al.*, 2003), microorganisms that are difficult to cultivate under laboratory conditions may remain undetected by these methods. Molecular-based studies have also been used to assess the microbial diversity in Movile Cave based on 16S rRNA genes (Chen *et al.*, 2009; Porter *et al.*, 2009). While these methods have the advantage of detecting uncultivated members of the microbial community, phylogenetic information alone does not generally provide insight into the physiological roles of these organisms. Many species are metabolically versatile and even closely related organisms may carry out different processes. Furthermore, many of the generated DNA sequences may relate to so far uncharacterised organisms which can therefore not be identified.

Stable isotope probing (SIP) techniques (Radajewski *et al.*, 2000; Murrell & Whiteley, 2010) can overcome some of the above-mentioned limitations and have therefore become invaluable tools in microbial ecology. SIP is achieved by incubation of an environmental sample with a labelled substrate, such as [<sup>13</sup>C]-enriched carbon compounds, or [<sup>15</sup>N]-enriched nitrogen compounds. When organisms consume the substrate, the heavy isotopes are incorporated into all of their cellular constituents, e.g. DNA, RNA, protein. Subsequent analysis of labelled biomarker molecules allows the identification of those organisms growing on the specific substrates. The SIP technique thereby allows linking microbial processes to the microorganisms actively involved, including those that may be difficult to isolate.

Both DNA-SIP and RNA-SIP have been successfully applied in the study of methylotrophic communities from a broad range of environments (e.g. Radajewski, 2002; Lueders *et al.*, 2004; Nercessian *et al.*, 2005; Neufeld *et al.*, 2007a, 2008; Moussard *et al.*, 2009; Antony *et al.*, 2010). While DNA-SIP is less sensitive than RNA-SIP (growth of the active organism is required in order for the DNA to replicate and become sufficiently labelled

with  $^{13}\text{C}$ ), it is easier, owing to the less fragile nature of DNA, and has the advantage of allowing access to the full genome of the labelled organism. DNA-SIP has been successfully used for the identification of active methanotrophs (Hutchens *et al.*, 2004) and autotrophs (Chen *et al.*, 2009) in Movile Cave. However, no SIP studies dedicated to methylated amine utilisers in Movile Cave have been carried out. In this thesis, DNA-SIP time-course experiments with  $^{13}\text{C}$ -labelled MMA and DMA were carried out in order to expand on previous studies of methylotrophic bacteria in Movile Cave.

## **4.2 Substrate uptake experiments with MMA, DMA, TMA and *in situ* concentrations of MMA in Movile Cave**

Prior to incubating cave water samples with  $^{13}\text{C}$ -labelled substrate, substrate uptake experiments with unlabelled MMA, DMA and TMA (2.5 mM substrate added to 20 ml sample in 120 ml vials, for details see Chapter 2, section 2.4) were carried out in order to get an indication of the rates of consumption of the different methylated amines in Movile Cave microcosms. The obtained data would then be used to determine the harvesting time points used in the SIP experiments. Results of substrate uptake experiments revealed that all three substrates tested were consumed in the microcosms. However, methylated amine concentrations are difficult to measure; at the time of the SIP experiments, there was no reliable and convenient method of measuring the concentrations. Colorimetric assays following the depletion of methylated amines did not result in robust results and had to be abandoned. As a result, the time points for the SIP experiments were chosen randomly (at 48 hours, 96 hours, 5 weeks; see sections 4.3 and 4.4 below).

Since then, a sensitive ion chromatography (IC) -based method with a detection limit of 1  $\mu\text{M}$  MMA has been developed (Lidbury *et al.*, 2014). Retrospective measurements of MMA concentrations in SIP enrichments, carried out on frozen supernatant that had been preserved, showed the depletion of MMA over time (Figure 4.1.): In enrichments set up with floating mat material, the MMA concentration had decreased to 0.03 mM at t=3 (5 weeks of incubation), i.e. only about 0.5% of the added 2.5 mM substrate were left (not taking into account any intrinsic MMA in the mat). At the same time point, in enrichments set up with cave water, about 5% of substrate (0.12 mM of 2.5 mM MMA) was left, suggesting more rapid MMA turnover in the floating mats.

The IC-based method was also used to measure standing concentrations of MMA in cave water samples (filtered and frozen immediately after sampling). The concentrations were

below the detection limit of the ion chromatograph (i.e. below 1  $\mu\text{M}$ ), suggesting that MMA is rapidly turned over by microorganisms in Movile Cave. MMA concentrations in floating mat samples were not measured due to time limitations but are estimated around 5 mM based on concentrations measured in SIP enrichments (after 48 h of incubation a concentration of 7.5 mM MMA was measured, although only 2.5 mM had been added to the incubation).

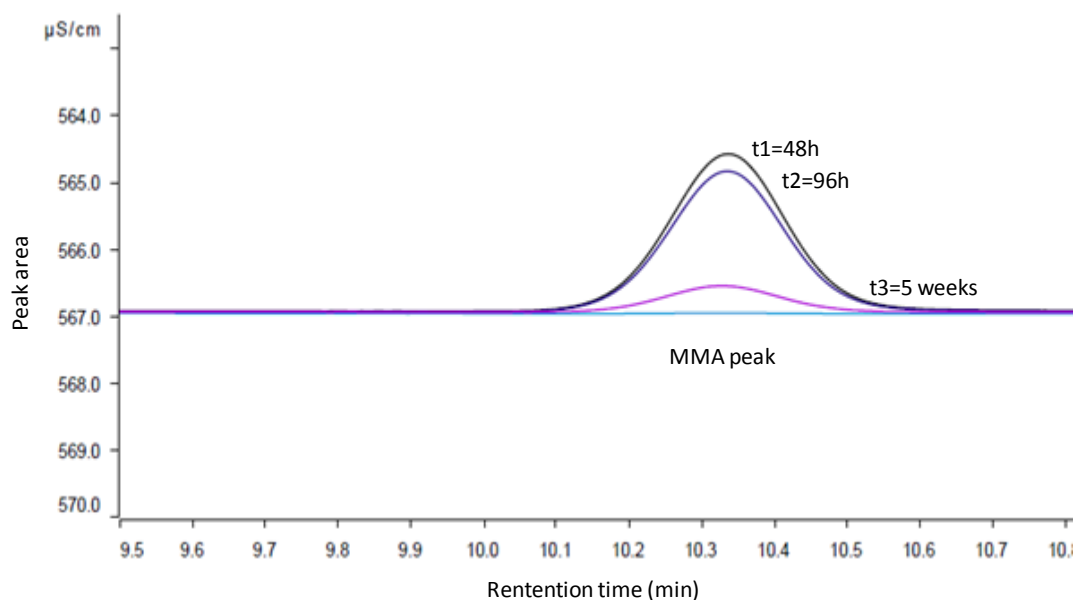


**Figure 4.1** Decrease of MMA concentration over time in enrichment cultures from floating mat samples, measured by ion chromatography of frozen supernatant.

### **4.3 DNA-SIP experiments with MMA reveal a shift in the methylotrophic community over time and identify new methylotrophs in Movile Cave**

For the identification of active methylated amine-utilising bacteria in Movile Cave, cave water samples were incubated in separate SIP experiments with either  $^{13}\text{C}$ -labelled MMA or  $^{13}\text{C}$ -labelled DMA ( $^{13}\text{C}$ -labelled TMA was not readily available) in small microcosms (120 ml serum vials, see below). The SIP-incubations were set up by adding 50  $\mu\text{mol}$  labelled substrate to 20 ml cave water in 120 ml serum vials and incubating at 21°C in the dark over a 5-week time course (a detailed description of the SIP set up is given in Chapter 2, section 2.4). Microcosms with cave water and 50  $\mu\text{mol}$  of *unlabelled* ( $^{12}\text{C}$ ) MMA or DMA were set up alongside and treated in the same way; these incubations served as controls to confirm the  $^{13}\text{C}$ -label did not affect the enrichment. Additionally, control incubations with no added substrate (referred to as “no-substrate controls” from here on) were set up as a second set of controls (to determine whether the community changes observed in SIP enrichments were a result of methylated amine addition). No floating mat material was used in the SIP

experiments and no replicates could be set up due to limitations in the amount of sample material available (the sample material was used for additional SIP experiments with methane and sulfur compounds as well as isolation experiments and MAR-FISH). However,  $^{12}\text{C}$ -MMA and  $^{13}\text{C}$ -MMA enrichments practically functioned as replicates for the overall change in the bacterial community (see below). SIP incubation samples were harvested at 3 time points: t=1 (48 h); t=2 (96 h); t=3 (5 weeks). A separate microcosm was set up for each time point and samples were harvested by centrifuging ( $5,000 \times g$ ) the entire content of the respective microcosm and discarding the supernatant. Samples for t=0 were prepared by spinning down 20 ml of cave water immediately after sampling). The samples were then processed by (i) extracting DNA, (ii) performing ultracentrifugation and fractionation for the separation of heavy (labelled) from light (unlabelled) DNA, (iii) performing DGGE of fractionated and unfractionated (native) DNA, and (iv) sequence analysis of significant DGGE bands.

#### *4.3.1 Analysis of the overall bacterial community in MMA microcosms (unfractionated DNA)*

Prior to ultracentrifugation of DNA, the overall change in the microbial communities in cave water microcosms following incubation with MMA was assessed. This was done by denaturing gradient gel electrophoresis (DGGE) of bacterial 16S rRNA gene amplicons from unfractionated DNA of each of the time points (for both  $^{13}\text{C}$ -MMA and  $^{12}\text{C}$ -MMA). The purpose of this was to firstly determine whether incubation with MMA had resulted in any microbial enrichment, and to secondly assess whether replicate microcosms ( $^{13}\text{C}$ -MMA and  $^{12}\text{C}$ -MMA enrichments) produced similar community profiles. Comparison of DGGE profiles from different time points showed no significant differences between the t=0 and t=1 (48 hours) samples. However, at t=2 (96 hours) and t=3 (5 weeks), the bacterial communities had significantly changed (Figure 4.2). The DGGE profiles obtained for enrichments with  $^{13}\text{C}$ -MMA were highly similar to those obtained with  $^{12}\text{C}$ -MMA (Figure 4.2), except for the final time point (t=3), most likely due to more pronounced bottle effect after 5 weeks incubation.

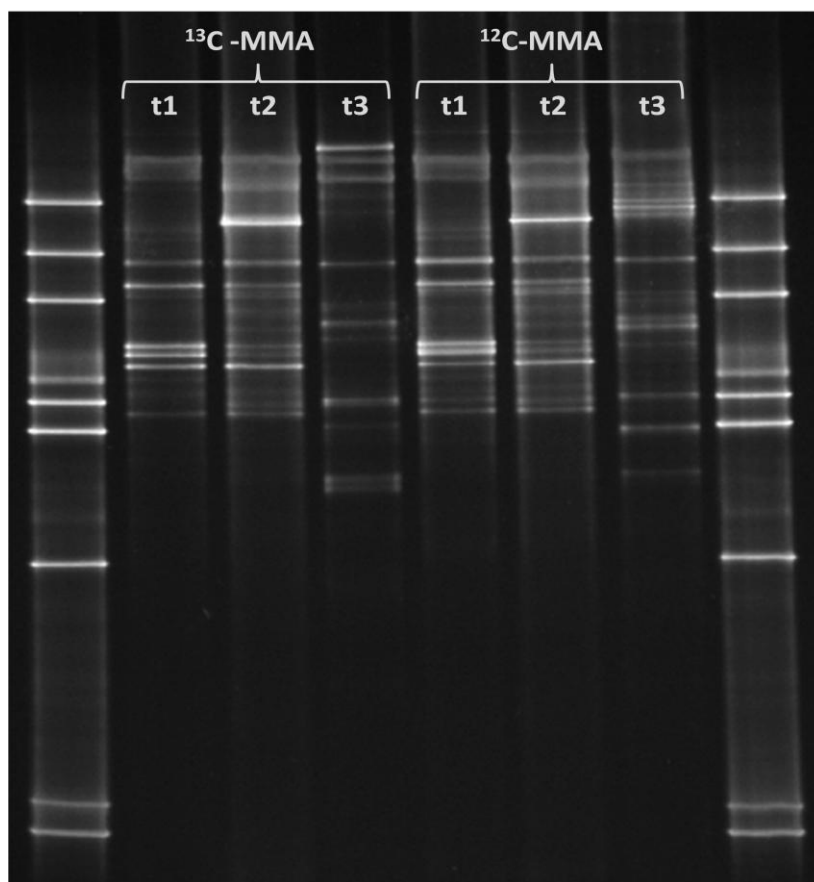


**Figure 4.2** DGGE analysis of bacterial 16S rRNA gene fragments (341f-GC / 907r) amplified from native (unfractionated) DNA from incubations of Movile Cave water with  $^{13}\text{C}$ -MMA (left) and unlabelled MMA (right), after 48 hours (t=1), 96 hours (t=2) and 5 weeks (t=3).

#### 4.3.2 Analysis of $^{13}\text{C}$ -labelled bacterial communities in MMA microcosms (heavy DNA fractions)

For identification of active methylotrophs, DNA extracted from all time points was subjected to CsCl density gradient centrifugation and fractionation, allowing separation of  $^{13}\text{C}$ -labelled DNA (contained in heavy fractions) from non-labelled,  $^{12}\text{C}$ -DNA (contained in light fractions). Bacterial 16S rRNA gene fragments were amplified from all DNA fractions and analysed by DGGE and Sanger sequencing. Due to the low amount of biomass in the cave water (and the limitations with regard to sample volume), the total yield of DNA extracted from the microcosms was rather low at  $\leq 1000$  ng per microcosm. Therefore, all available DNA was used for ultracentrifugation, and all analyses following fractionation were carried out on PCR-amplified DNA only. After CsCl density gradient centrifugation, a total of 11 – 12 DNA fractions were obtained for each sample. Measuring the density of each fraction using a digital refractometer confirmed that a gradient had formed correctly across the fractions (Figure 4.3).

(i) *Agarose gel analysis of fractionated DNA*

Agarose gel electrophoresis of bacterial 16S rRNA gene amplicons obtained from the respective CsCl gradient fractions indicated a clear concentration of DNA at the expected densities (according to Neufeld *et al.*, 2007) although separation of DNA was somewhat smeared across neighbouring fractions (Figure 4.3). Sample t=1 (48 h) of the  $^{13}\text{C}$ -MMA incubation yielded visible bands in the light fractions where non-labelled DNA was expected (fractions 10-12, density range of 1.712 - 1.701  $\text{g ml}^{-1}$ ), but did not contain detectable amounts of labelled (heavy) DNA. This suggests that no significant incorporation of MMA, i.e. enrichment of methylotrophs, had occurred in the first 48 hours of incubation. This time point was therefore not further analysed. In contrast, samples t=2 (96 h) and t=3 (5 weeks) of the  $^{13}\text{C}$ -MMA incubation yielded PCR products in light fractions of the CsCl gradient, as well in the density range of 1.719 – 1.726 (fractions F7-F8), where heavy,  $^{13}\text{C}$ -labelled DNA was expected. As expected, no DNA was observed in heavy fractions of any of the control incubations with unlabelled,  $^{12}\text{C}$ -MMA.

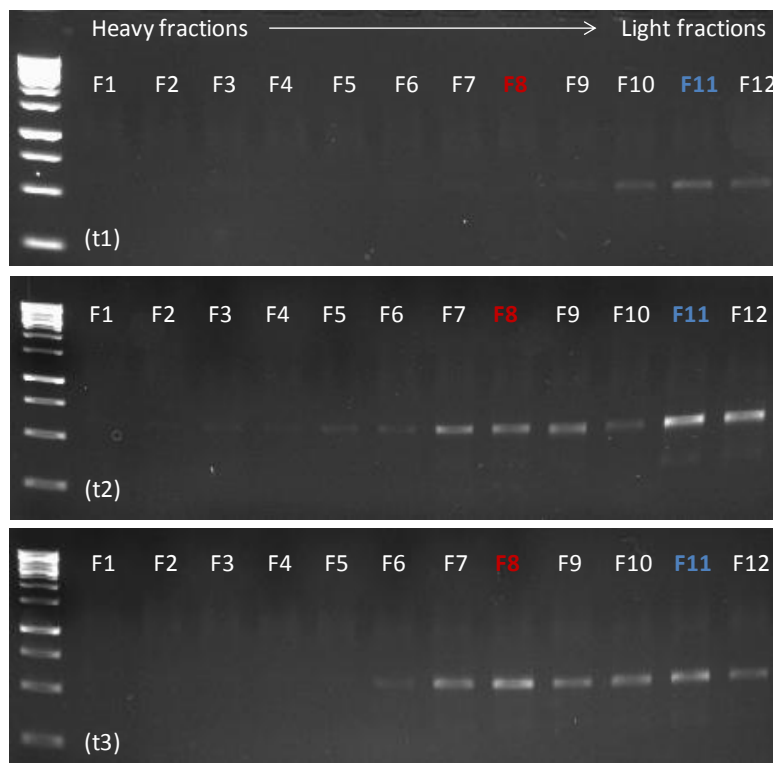


**Figure 4.3** Agarose gel images of bacterial 16S rRNA genes fragments (341f-GC / 907r) amplified from fractionated DNA of  $^{13}\text{C}$ -MMA-SIP incubations at different time points (t1 = 48 h; t2 = 96 h; t3 = 5 weeks), indicating a shift from light towards heavy DNA over time.  $^{13}\text{C}$ -labelled DNA is expected at a density of  $\sim 1.725 \text{ g ml}^{-1}$  (fractions F7-F8). Non-labelled DNA is expected in the upper fractions, in the density range of 1.70-1.72 (fractions F10-F12). Abbreviations: F1- F12 = Fractions 1 - 12.

(ii) *DGGE analysis and 16S rRNA gene sequencing of <sup>13</sup>C-labelled DNA*

Following agarose gel electrophoresis, bacterial 16S rRNA genes amplified from relevant fractions of <sup>13</sup>C-MMA incubations (fractions F7-F12; Figure 4.3) were analysed by DGGE in order to compare <sup>13</sup>C-labelled and non-labelled bacterial communities at time points t2 (96 h) and t3 (5 weeks). DGGE profiles of 16S rRNA genes amplified from heavy and light DNA from t2 and t3 revealed major differences in the bacterial community composition at the two time points (Figure 4.4). A single 16S rRNA band appeared in the heavy fractions of the t2 sample (F7-1 of Figure 4.4a). Sequence analysis of the excised band identified this as the 16SrRNA gene sequence from *Methylothera mobilis* (99% identity, sequence MH2\_F7\_1 in Figure 3.2b), an obligate methylophilic bacterium (Kalyuzhnaya *et al.*, 2006a) known to be abundant in Movile Cave (Chen *et al.*, 2009). This result indicates that only *M. mobilis* had incorporated significant amounts of <sup>13</sup>C-carbon at 96 hours, suggesting it was the most active methylophilic bacterium in the earlier stages of MMA incubation. The same 16S rRNA gene band was also prominent in the DGGE profile of the unfractionated t=2 sample (Figure 4.2; Figure 4.4b left), suggesting that *M. mobilis* also dominated the overall bacterial community as a result of selective enrichment with MMA.

DGGE profiles of the bacterial communities present in heavy CsCl fractions after 5 weeks of incubation (t=3) were noticeably different from those at 96 h (t=2) of incubation based on DGGE profiles (Figure 4.4): The DGGE band affiliated with *Methylothera mobilis* band was no longer present. Instead, 16S rRNA gene profiling revealed a number of different phylotypes in heavy CsCl fractions, suggesting a more diverse bacterial community had incorporated the <sup>13</sup>C-label from MMA after 5 weeks of incubation. Sequence analysis of these DGGE bands identified 16S rRNA gene sequences affiliating with *Methylovorus* (97% identity to *Methylovorus menthalis*; sequence MH3\_F8\_2 in Figure 3.2b) and *Methylobacterium extorquens* (100% sequence identity; sequences MH3\_F7\_4 and MH3\_F7\_5 in Figure 3.2a), both of which are well-characterised facultative methylophilic bacteria known for growth on methylated amines as carbon sources. *M. extorquens* was also isolated from Movile Cave water and floating mat samples in this PhD project (see Chapter 3, section 3.2). Other 16S rRNA gene bands from DGGE profiles affiliated with sequences from bacterial genera not generally associated with methylophilicity or methylated amine utilisation: *Catellibacterium* (98% identity to *Catellibacterium caeni*, sequence MH3\_F8\_5 in Figure 3.2a), *Porphyrobacter* (99% identity to *Porphyrobacter neustonensis*; sequence MH3\_F8\_1 in Figure 3.2a), *Altererythrobacter* (99% identity to *Altererythrobacter epoxidivorans*;

sequence MH3\_F7\_2 in Figure 3.2a) and *Cupriavidus* (99% identity to *Cupriavidus necator*, formerly known as *Ralstonia eutropha*, sequence MH3\_F8\_2 ).

The *Catellibacterium* 16S rRNA gene sequence identified from DGGE gels shared 98% sequence identity with the 16S rRNA gene sequence from *Catellibacterium* sp. LW-1, a novel facultative methylotroph isolated from Movile Cave during this PhD with MMA as the only source of carbon, energy and nitrogen (see Chapter 3, section 3.2). Cloned 16S rRNA gene sequences from <sup>13</sup>C-labelled DNA from t=3 (see 4.3.4.) also included sequences that shared 100% identity with the 16S rRNA gene from the methylotrophic *Catellibacterium* isolate (clone sequence MH3\_F8\_16 in Figure 3.2a). *Catellibacterium*-related sequences were furthermore identified in heavy DNA fractions from <sup>13</sup>C-DMA enrichments (see 4.4). Taking these results together, *Catellibacterium* is likely to be among the most active MMA-utilising methylotrophs in Movile Cave.

Since no representatives of *Cupriavidus*, *Porphyrobacter* or *Altererythrobacter* have been isolated from Movile Cave, these organisms have not been tested for growth with methylated amines. However, the published genome of *Cupriavidus necator* (*Ralstonia eutropha*), an organism capable of growing on aromatic and chloroaromatic compounds (Perez-Pantoja *et al.*, 2008) was found to contain *gmaS*: When aligned with *glnA* and *gmaS* sequences, the gene annotated as *glnA* clearly fell within the *betaproteobacterial gmaS* cluster (see Figure 5.12), indicating at least the genetic potential for MMA utilisation. *gmaS* genes associated with *Cupriavidus* were also identified from metagenome data of Movile Cave mat (Jason Stephenson, personal communication), suggesting that this organism may indeed play a role in MMA utilisation in the cave. Furthermore, strains of *Cupriavidus necator* have recently been reported to grow methylotrophically on formaldehyde and methanol (Habibi & Vahabzadeh, 2013). Methylotrophic growth on methanol and methylated amines has also been reported for strains of a different *Ralstonia* species, *Ralstonia pickettii* (Hung *et al.*, 2011). *Porphyrobacter* are *alphaproteobacterial*, bacteriochlorophyll-producing chemoheterotrophs. The genus *Porphyrobacter* is of interest because of the ability of several species to degrade polycyclic aromatic hydrocarbons (Hiraishi *et al.*, 2002; Wang *et al.*, 2012). To date, methylotrophy has been reported only for one strain of *Porphyrobacter neustonensis*, which was able to utilise MMA as sole carbon and energy source (Fuerst *et al.*, 1993). Like *Porphyrobacter*, *Altererythrobacter* belong to the family of the *Erythrobacteraceae* and contain several species known to degrade polycyclic aromatic hydrocarbons (Kwon *et al.*, 2007; Teramoto *et al.*, 2010). Methylotrophic growth has not been reported for this genus.

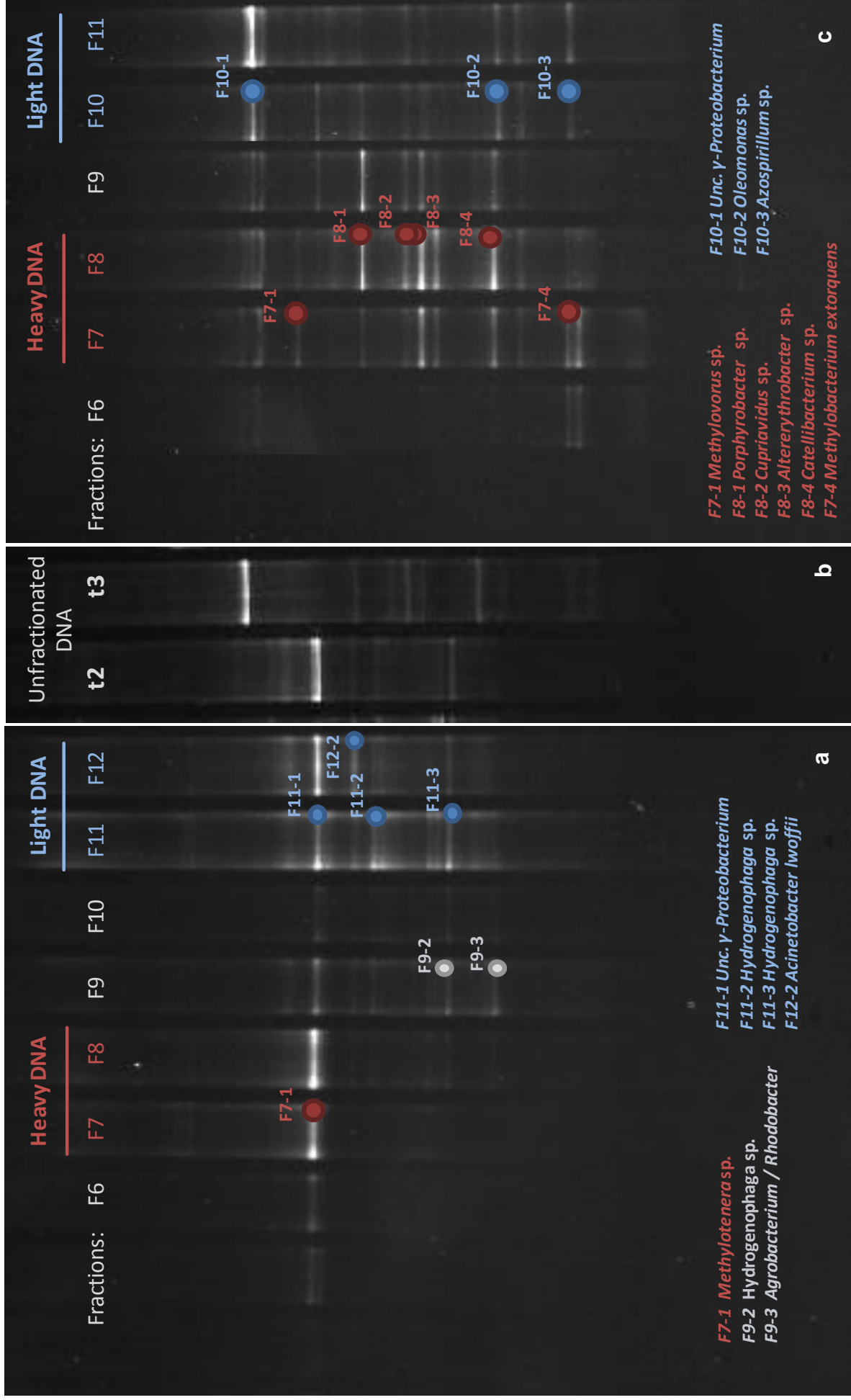


**Figure 4.4** DGGE analysis of bacterial 16S rRNA gene fragments (341f-GC / 907r) amplified from light and heavy DNA fractions from <sup>13</sup>C-MMA incubations of Mobile Cave water after 96 hours (a) and 5 weeks (b). DGGE profiles of unfractionated DNA of both time points were run alongside the fractions for reference (b).

While it cannot be ruled out that cross-feeding of carbon through the microbial food chain led to  $^{13}\text{C}$ -labelling of some non-methylotrophic organisms in the microcosms, all 16S rRNA gene sequences obtained from DGGE profiles of heavy DNA (i.e.  $^{13}\text{C}$ -labelled organisms) were exclusive to enrichments with added MMA, and were not detected in “no-substrate controls” (Supplementary Figure S1; Supplementary Table S2). This suggests that those organisms were enriched as a result of incubation with MMA, even if the labelling was secondary (i.e. due to cross-feeding of  $^{13}\text{C}$ -carbon). While DGGE-based analysis does not provide quantitative data, it is worth noting that 16S rRNA gene bands related to *Porphyrobacter* and *Altererythrobacter* were of very high intensity (similar to that of the *Catellibacterium* 16S rRNA gene band, and much more intense than those of *Methylobacterium* or *Methylovorus*; Figure 4.4). Additionally, 16S rRNA gene sequences related to *Porphyrobacter* and *Cupriavidus* were also identified in heavy DNA fractions of SIP enrichments with  $^{13}\text{C}$ -labelled DMA (see section 4.4. and Figure 4.7). These results, taken together with several reports of methylotrophic growth in *Cupriavidus* and *Porphyrobacter neustonensis*, suggest that unrecognised methylotrophs may be key players in methylated amine metabolism in Movile Cave.

#### 4.3.3 Analysis of non-labelled bacterial communities in MMA microcosms (light DNA fractions)

##### (iii) DGGE analysis and 16S rRNA gene sequencing of non-labelled DNA

The non-methylotrophic bacterial community co-enriched in  $^{13}\text{C}$ -MMA incubations was investigated by sequence analysis of 16S rRNA gene bands excised from DGGE profiles of non-labelled DNA (light CsCl gradient fractions; Figure 4.3). 16S rRNA gene sequences from non-labelled DNA at both time points contained a diversity of mostly heterotrophic bacteria, amongst which was the non-methylotrophic MMA utiliser *Acinetobacter lwoffii* (100% sequence identity; sequence MH2\_F12\_2 in Figure 3.2b), an organism which was isolated from Movile Cave water with MMA as sole nitrogen source in this thesis (see Chapter 3, section 3.3). Additionally, several sequences affiliated with 16S rRNA genes of members of the *Hydrogenophaga* (sequences MH2\_F9\_2; MH2\_F11\_3 and MH2\_F11\_2a in Figure 3.2b), a genus often associated with hydrogen and sulfur metabolism, containing species with heterotrophic as well as chemolithoautotrophic lifestyles. Other 16S rRNA gene sequences related to the genera *Azospirillum*, *Rhodobacter* and *Oleomonas* (species of which were also isolated with MMA as nitrogen source, see Chapter 3, section 3.3), respectively. Finally,

some 16S rRNA gene sequences from light fractions were not closely related to sequences from any cultivated representatives (as little as 84-87% identity).

While sequences related to *Hydrogenophaga*, *Azospirillum*, *Rhodobacter* and *Oleomonas* were also identified in “no substrate control” incubations (indicating that these may be abundant organisms in Movile Cave), *Acinetobacter*-related sequences were not detected in incubations without added MMA (Supplementary Figure S1; Supplementary Table S2), suggesting that *Acinetobacter lwoffii* was enriched in light fractions of  $^{13}\text{C}$ -MMA incubations due to its ability to use MMA as a nitrogen source (as shown by isolation studies, Chapter 3, section 3.3).

#### 4.3.4 Analysis of labelled and non-labelled bacterial communities in MMA microcosms by cloning and sequencing of 16S rRNA genes

To complement results obtained from DGGE profiling, bacterial 16S rRNA gene-based clone libraries were constructed from  $^{13}\text{C}$ -MMA-SIP key fractions (F8 and F10 in Figure 4.4c) of the final time point (t=3; 5 weeks incubation). Of the clones containing the correct insert size, 30 were randomly selected for restriction fragment length polymorphism (RFLP) analysis. RFLP analysis of the cloned 16S rRNA genes was carried out using a double digest approach with restriction enzymes *BseGI* and *Eco88I*. These restriction enzymes were chosen for their high level of discrimination between bacterial 16S rRNA gene sequences from Movile Cave as determined by alignment of 16S rRNA gene sequences obtained from DGGE bands of MMA-SIP microcosms (sections 4.3.2. and 4.3.3.) and Movile Cave isolates (Chapter 3) and visualisation of restriction sites.

The resulting RFLP profiles of cloned 16S rRNA genes indicated a high level of phylogenetic diversity within both  $^{13}\text{C}$ -labelled and non-labelled bacterial communities (Figures 4.5a and b). 14 clones with different RFLP profiles were selected for sequencing. The 16S rRNA gene sequences obtained from these clones correlated with those previously obtained from DGGE profiling of MMA-SIP microcosms. 16S rRNA gene-based phylogenetic trees in Figures 3.2a and b (Chapter 3) provide an overview of the ( $^{13}\text{C}$ -labelled and un-labelled) sequences identified from MMA-SIP enrichments and from methylated amine-utilising bacteria isolated from Movile Cave (see Chapter 3).

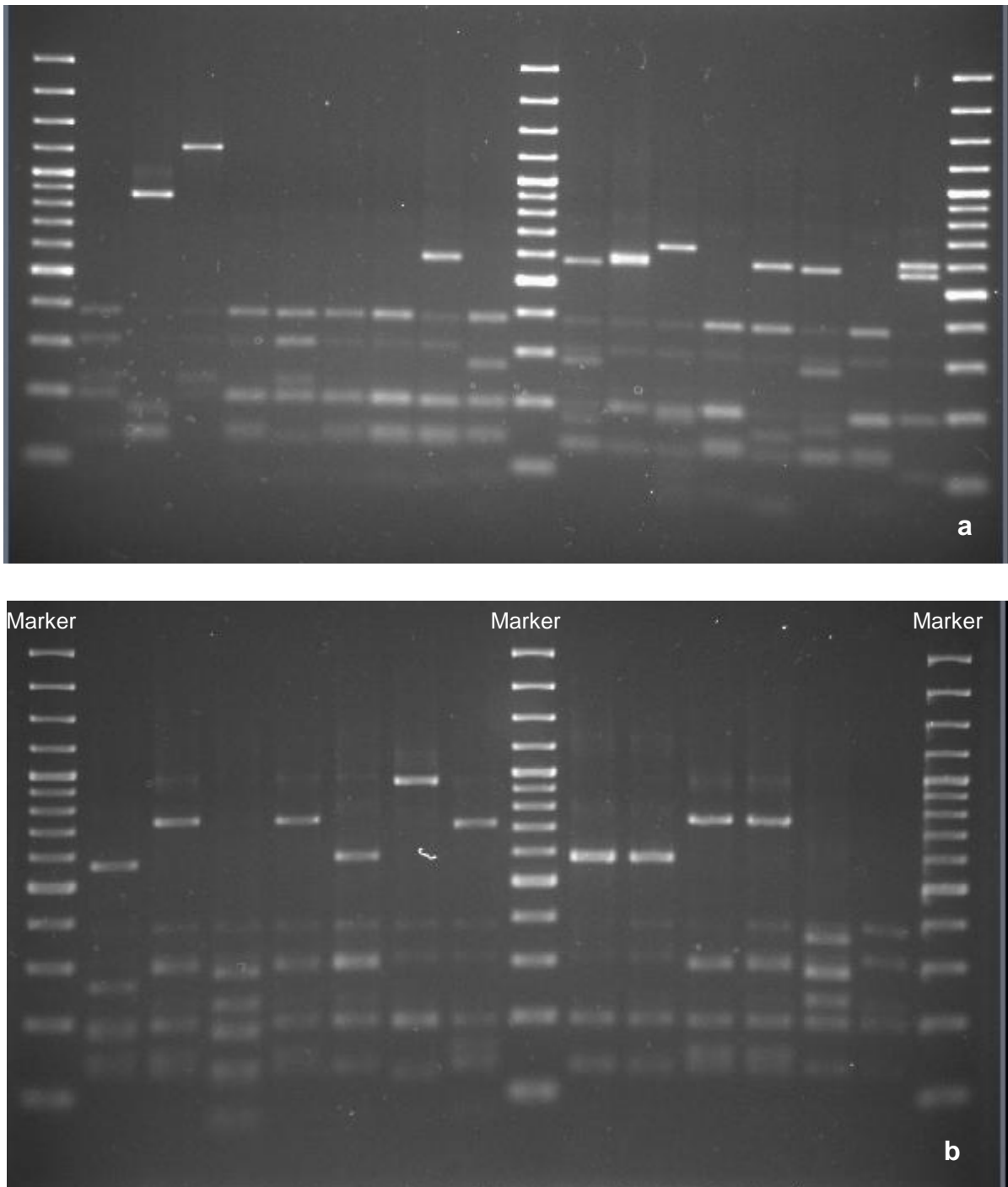


**Figure 4.5 a & b** RFLP profiles of cloned 16S rRNA gene sequences (27f /1492r) from fractions F8 (top) and F10 (bottom) of CsCl gradients generated with DNA obtained from  $^{13}\text{C}$ -MMA-SIP experiments after 5 weeks ( $t=3$ ), following enzymatic digest with *Bse*GI and *Eco*88I.

#### 4.4. DNA- SIP experiments with DMA corroborate new methylotrophs

SIP enrichments were also set up from Movile Cave water with  $^{13}\text{C}$ -labelled DMA. The yield of DNA obtained from these enrichments (at all time points) was even less than for MMA, with 400 - 500 ng DNA per microcosm, which is at the lower end of what is required for successful fractionation and retrieval of  $^{13}\text{C}$ -labelled DNA. Due to the low DNA concentrations, precipitated DNA from fractions was not run directly on agarose gels, but was immediately amplified with 16S rRNA gene PCR primers 341f-GC / 907r. The amplification products were then analysed by agarose gel electrophoresis. Only time point t=3 (5 weeks of incubation) showed incorporation of  $^{13}\text{C}$ -label into DNA. Therefore, all results here refer to t=3 only. Agarose gel electrophoresis of bacterial 16S rRNA genes amplified from fractionated DNA indicated a concentration of DNA at expected densities (Figure 4.6).

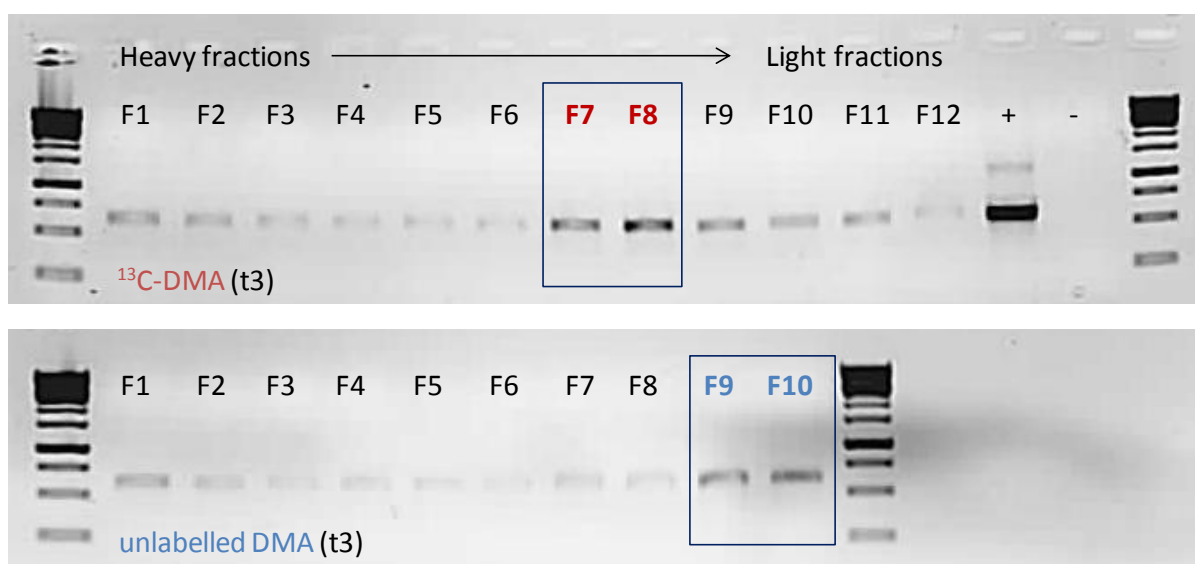


**Figure 4.6** Agarose gel electrophoresis of bacterial 16S rRNA genes amplified from DMA-SIP DNA following fractionation. Samples retrieved from incubations with  $^{13}\text{C}$ -labelled DMA show concentration of DNA in heavy fractions (top), while DNA is concentrated in light fractions in the case of control incubations with unlabelled ( $^{12}\text{C}$ ) DMA (bottom).

However, for both the  $^{13}\text{C}$ -DMA and the  $^{12}\text{C}$ -DMA enrichment, a faint band was visible across all fractions. This was initially thought to be due to contamination of the glycogen used for precipitation of fractionated DNA. However, the glycogen batch used was found to be clean. The additional bands are most likely a result of residual DNA from the sample which had not migrated to the expected fractions, combined with the low stringency of the PCR conditions (required to generate sufficient PCR product from the low DNA concentrations in the sample).

DGGE analysis of bacterial 16S rRNA genes from all fractions supported this: Community profiles of light and heavy key fractions differed visibly, with distinct bands clearly assignable to  $^{13}\text{C}$ -labelled or non-labelled DNA (Figure 4.7). DGGE bands visible in non-specific fractions appeared at the same positions as those in key fractions, but were significantly fainter, suggesting these products were indeed a result of amplification of residual DNA from the sample that had not completely migrated through the CsCl gradient during ultracentrifugation, rather than a contamination following fractionation. Comparison of DGGE profiles and 16S rRNA gene sequence identities from the  $^{13}\text{C}$ -DMA enrichment and the unlabelled ( $^{12}\text{C}$ ) DMA control enrichment showed some differences in the community composition of the two microcosms. This is likely due to a “bottle effect”, which will be more pronounced after 5 weeks of incubation (as was also the case to some extent with  $t=3$  of the MMA-SIP enrichments, see Figure 4.2). These differences in community composition further reduce the probability of contamination, since both samples were processed at the same time, using the same reagents.

Bacterial 16S rRNA gene sequences (500 bp fragments) were obtained for a number of prominent DGGE bands. While no known methylotrophs were identified, it is interesting to note that 16S rRNA gene sequences from heavy fractions corresponded to those obtained from  $^{13}\text{C}$  MMA enrichments (see 4.3.2.), namely *Catellibacterium* (99% identity to *C. caeni*), *Cupriavidus* (99% identity to *C. necator*) and *Porphyrobacter* (98% identity to *Porphyrobacter tepidarius*). The *Catellibacterium* 16S rRNA gene sequence shared 99% sequence identity with the methylotrophic *Catellibacterium* isolate *Catellibacterium* sp. LW-1 (see Chapter 3, section 3.2), and 98% sequence identity with the *Catellibacterium* sequence from  $^{13}\text{C}$ -MMA enrichments (over 500 bp). No 16S rRNA gene sequence data could be generated from DGGE bands excised from light fractions of the  $^{13}\text{C}$ -DMA enrichment. However, some 16S rRNA gene sequences were obtained from the unlabelled DMA enrichment. These included the non-methylotrophic MMA utiliser *Acinetobacter lwoffii* (100% identity), also previously detected in light fractions of  $^{13}\text{C}$ -MMA enrichments and isolated with MMA as a nitrogen source from Movile Cave water (see Chapter 3). A further prominent 16S rRNA gene sequence was most closely related to the 16S rRNA gene of *Catellibacterium nectariphilum* (Tanaka *et al.*, 2004; 97% sequence identity), an organism not closely related to *C. caeni* based on 16S rRNA gene sequences (94% sequence identity).

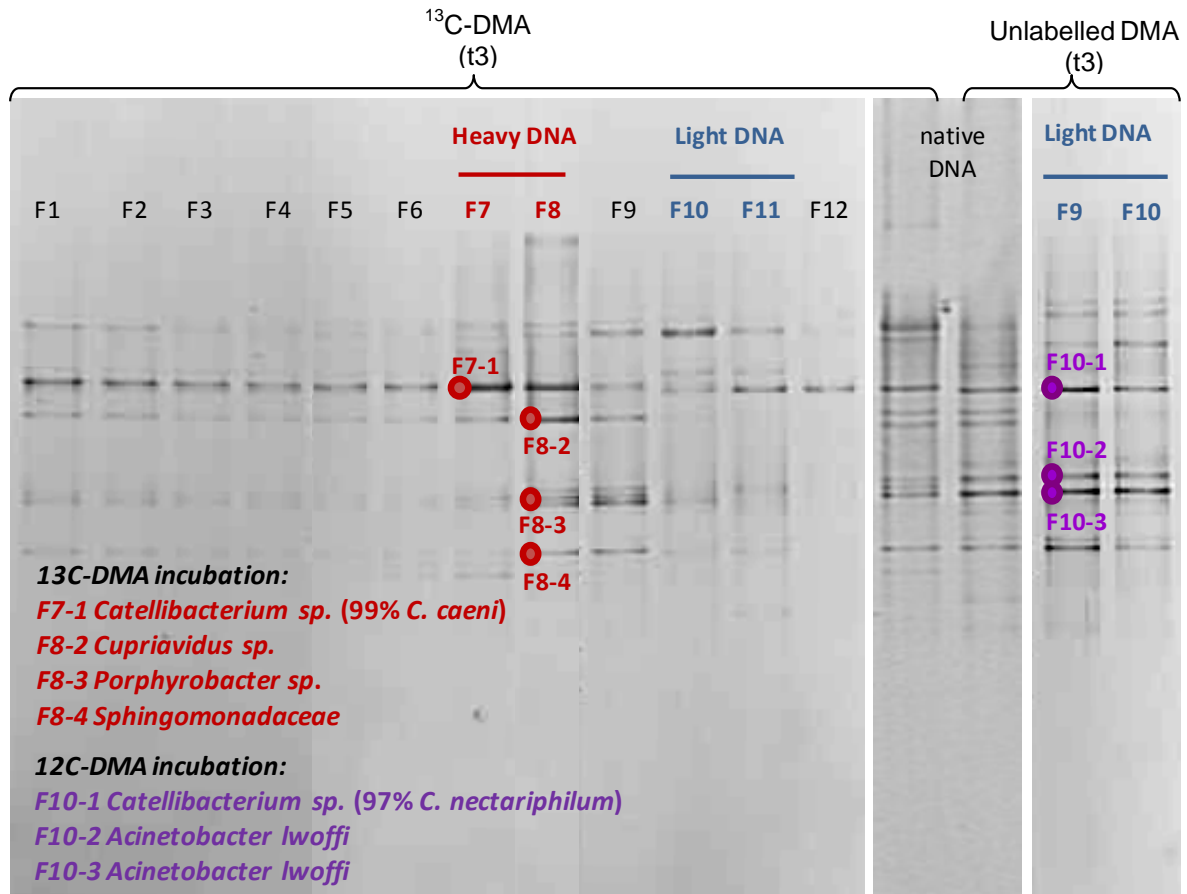


**Figure 4.7** DGGE analysis and identities of bacterial 16S rRNA gene fragments in heavy DNA fractions from  $^{13}\text{C-DMA}$  incubations (left) and from incubations with unlabelled ( $^{12}\text{C}$ ) DMA (right) of Mobile Cave water after 5 weeks of incubation. DGGE profiles of unfractionated DNA of both enrichments are shown for reference (centre).

**Chapter 5. The indirect methylamine oxidation pathway: Development of new PCR primers and distribution of *gmaS* in Movile Cave.**

## 5.1 Introduction: Metabolic pathways of MMA oxidation, key genes and biomarkers

All bacteria that use methylated amines as growth substrates (both methylotrophically and non-methylotrophically) convert monomethylamine (MMA) into the central intermediate formaldehyde. Formaldehyde (HCHO or CH<sub>2</sub>O) can be in free form or bound to tetrahydrofolate (H<sub>4</sub>Folate) as 5,10-methylenetetrahydrofolate (CH<sub>2</sub>=H<sub>4</sub>Folate). HCHO or CH<sub>2</sub>=H<sub>4</sub>Folate present the branching points at which carbon is either oxidised further to CO<sub>2</sub>, or assimilated into cell carbon via the pathways described in Chapter 1 (section 1.4.5). The enzymes (and associated genes) involved in the oxidation of MMA are therefore valuable biomarkers for the identification of bacteria utilising methylated amines. There are two possible pathways for the oxidation of MMA by bacteria (Figures 5.1a and b): In the well-characterised, direct MMA oxidation pathway, a single enzyme oxidises MMA to formaldehyde, releasing NH<sub>4</sub><sup>+</sup> (Figure 5.1a). In methylotrophic gram-positive bacteria the enzyme responsible is MMA oxidase, while in gram-negative methylotrophs it is MMA dehydrogenase (MADH) (Anthony, 1982). The MADH-based pathway has long been characterised, and PCR primers are available for *mauA*, the gene coding for the small subunit of MADH (Neufeld *et al.*, 2007a). Naturally, these primers do not detect all MMA-utilising bacteria.

A second, indirect pathway involves the stepwise conversion of MMA to H<sub>4</sub>Folate-bound formaldehyde (i.e. CH<sub>2</sub>=H<sub>4</sub>Folate) via two methylated amino acids, gamma-glutamylmethylamide (GMA) and *N*-methylglutamate (NMG) (Latypova *et al.*, 2010; Chistoserdova, 2011) (Figure 5.1b). Although this pathway has been known since the 1960s (Kung & Wagner, 1969), the enzymes and genes involved have only recently been characterised (Latypova *et al.*, 2010; Chen *et al.*, 2010a): In the first step, the methyl group of MMA is transferred onto glutamate, yielding GMA. This reaction is catalysed by the enzyme GMA synthetase (*gmaS*). GMA is then converted to NMG by a putative NMG synthase (*mgsABC*), and finally to CH<sub>2</sub>=H<sub>4</sub>Folate by NMG dehydrogenase (*mgdABCD*). A variation of this pathway is found in *Methyloversatilis universalis* FAM5, where *gmaS* is not essential for oxidation of MMA to CH<sub>2</sub>=H<sub>4</sub>Folate via NMG (Latypova *et al.*, 2010). The substrate specificity of NMG synthase is not well established and it is proposed that both MMA and GMA can be used as a substrate for this enzyme (Chen, 2010a). Importantly, the indirect, GMA / NMG mediated pathway has recently been found to be used also by non-methylotrophic bacteria, i.e. bacteria which use methylated amines as nitrogen sources only

(Chen *et al.*, 2010b; Chen 2012). This pathway may therefore be of particular significance in Movile Cave. Meanwhile, the direct, MADH-based pathway appears to be restricted to organisms capable of using methylated amines as carbon sources.

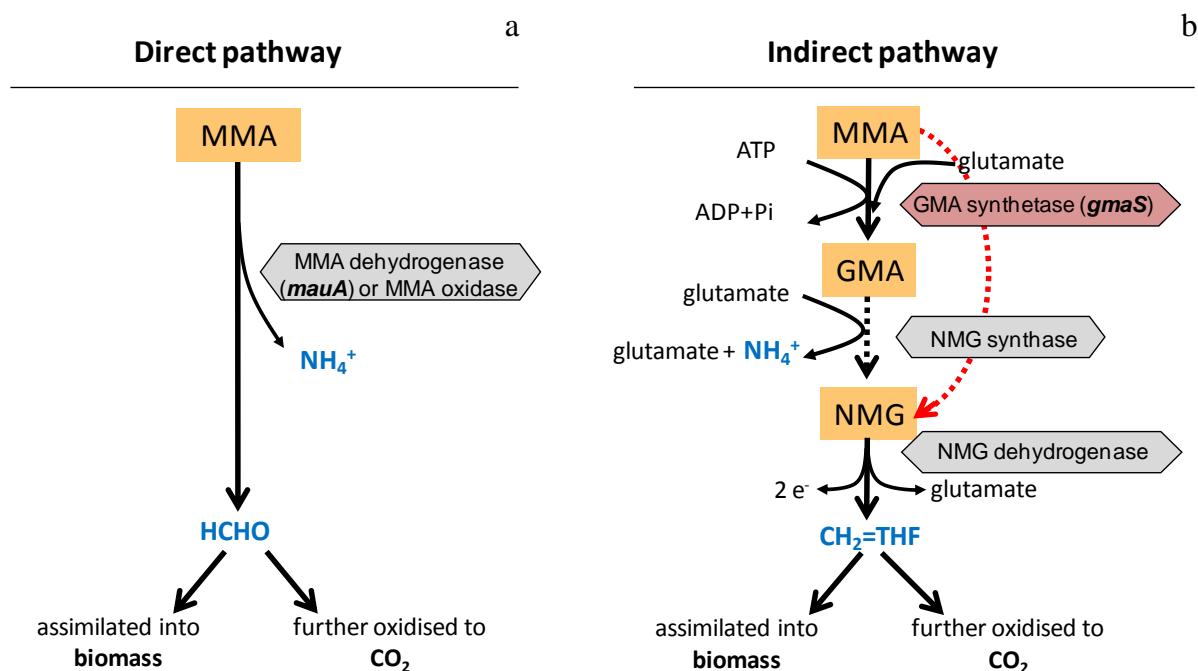


**Figure 5.1** Schematic views of the direct (a) and indirect (b) MMA oxidation pathways. Abbreviations: MMA, monomethylamine; GMA, gamma-glutamylmethylamide; NMG, *N*-methylglutamate; THF, tetrahydrofolate. The indirect MMA oxidation pathway can proceed without GMA as an intermediate (red broken arrow) in *Methyloversatilis universalis* FAM5. (Illustrations modified from Chen *et al.*, 2010b).

Recently, the first *gmaS*-targeting PCR primer set has become available (Chen, 2012). However, this primer set was designed specifically for the Marine *Roseobacter* Clade (MRC), and therefore may not detect *gmaS* from non-marine bacteria. In order to provide a biomarker for MMA-utilisers undetected by current PCR primers, three new *gmaS* PCR primers were designed in this PhD project, based on alignments of non-marine *gmaS* sequences derived from bacterial isolates and published bacterial genomes.

## 5.2 Development and validation of *gmaS*-targeting PCR primers

### 5.2.1 Design of PCR primers: Retrieval of *gmaS* sequences from published genomes

Three new *gmaS* PCR primers were designed in this study, based on a multiple alignment of 34 *gmaS* sequences derived from (i) five MMA-utilising control strains confirmed to use the

NMG / GMA mediated pathway (kindly provided by Dr Yin Chen, for details see Chapter 2, section 2.10) and (ii) bacterial genomes published on the Integrated Microbial Genomes (IMG) platform of the Joint Genome Institute (JGI). Published genomes were screened for *gmaS*-related sequences using *gmaS* from *Methylocella silvestris* as a query sequence (Chen *et al.*, 2010a). Corresponding full length sequences retrieved from the database consisted of *gmaS*, but also glutamine synthetase type III (*glnA*) sequences (a functionally unrelated enzyme involved in  $\text{NH}_4^+$  assimilation), due to the high level of sequence similarity between these two genes (for a detailed analysis refer to Chen *et al.*, 2010b). In order to identify genuine *gmaS* sequences, the gene neighbourhood of all obtained sequences was manually inspected for predicted neighbouring open reading frames (ORFs) typically found adjacent to *gmaS* (namely, genes encoding NMG dehydrogenase and NMG synthase, Figure 5.2). This way, many sequences annotated as *glnA* on IMG were identified to be in fact *gmaS* sequences. The identities of NMG dehydrogenase (*mgd*) and NMG synthase (*mgs*) were predicted based on illustrations of gene organisation of *gmaS*, *mgd* and *mgs* in Chen *et al.*, 2010b.

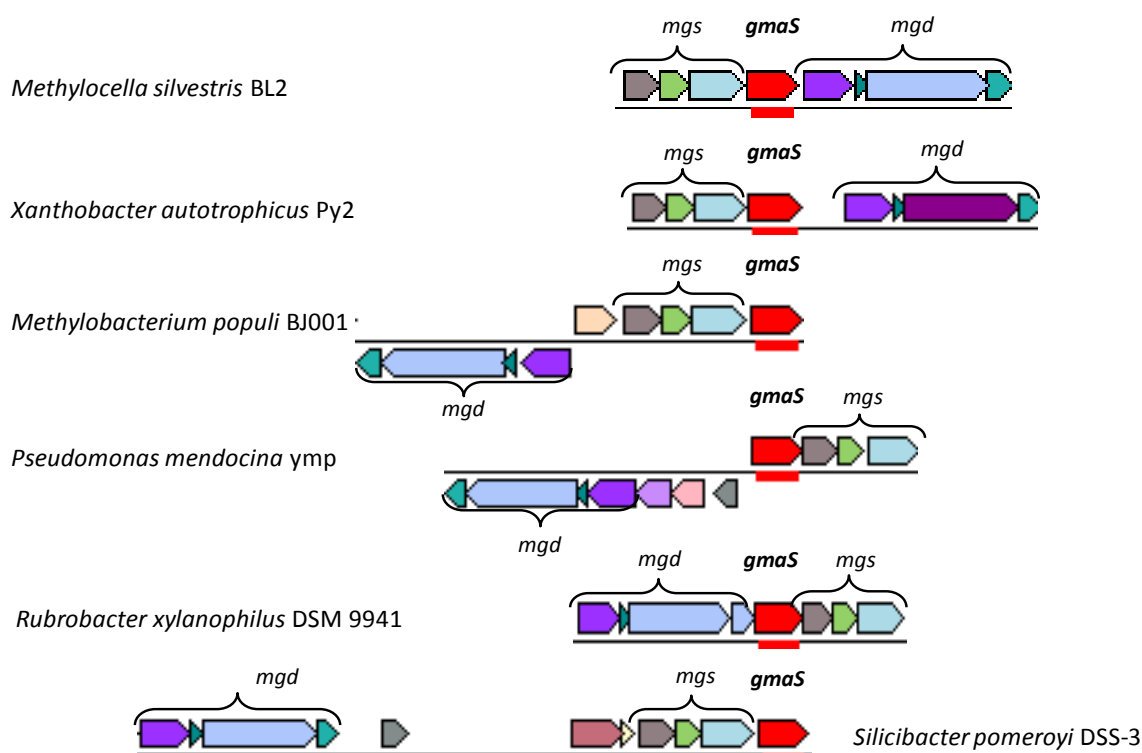


**Figure 5.2** Gene neighbourhoods of *gmaS* genes from representative organisms, indicating location of putative genes for NMG dehydrogenase (*mgd*) and NMG synthase (*mgs*). *GmaS* genes were retrieved from IMG / JGI by a blastx search against the *gmaS* sequence from *Methylocella silvestris*. The image was modified from gene neighbourhood illustrations generated on <https://img.jgi.doe.gov/cgi-bin/w/main.cgi>.

### 5.2.2 Design of PCR primers: Multiple alignments of *gmaS* sequences reveal distinct phylogenetic clusters

For the design of degenerate *gmaS* primers, multiple sequence alignments of verified *gmaS* sequences (see above) were established with the Clustal X program (Thompson *et al.*, 1997) and viewed using the GeneDoc software (Nicholas *et al.*, 1997). Because of their sequence similarity to *gmaS*, a number of *glnA* sequences were included in the alignment to enable identification of suitable primer-binding regions specific to *gmaS* and not found in *glnA* (a complete list of all *gmaS* and *glnA* sequences used for primer design is given in Table 2.3). Initially, *gmaS* sequences from marine bacteria were included in the alignment. Most of them were however too divergent from the remaining *gmaS* sequences to find shared primer-binding regions and were therefore removed from the alignment (see below).

Sequence alignment and establishment of nucleotide-based and amino acid-based phylogenetic trees clearly detached *glnA* from *gmaS* genes (Figure 5.3). Furthermore, two distinct *gmaS* clusters were revealed, separating (i) *Alphaproteobacteria* and (ii) *Beta-* and *Gammaproteobacteria*. The *alphaproteobacterial gmaS* cluster was further split into three subgroups, one group containing *gmaS* sequences belonging to Marine *Roseobacter* Clade (MRC) bacteria (order *Rhodobacterales*), and two groups containing sequences belonging to soil and freshwater *Alphaproteobacteria*, of which all except one belonged to the order *Rhizobiales* (Figure 5.3).

For primer design, the majority of *gmaS* sequences associated with the Marine *Roseobacter* Clade (MRC) had to be removed from the alignment as they were too divergent from the other sequences to be targeted by the same primers. For the forward primer, a common region shared by all remaining *gmaS* sequences could be identified at 557 bp, after removing a small number of organisms with too many mismatches (*Rubrobacter xylanophilus*, *Thiomicrospira crunogena*) (Figure 5.4a). The resulting primer *gmaS*<sub>557f</sub> (GARGAYGCSAACGGYCAGTT) hence targets *Alphaproteobacteria* (from non-marine environments) as well as *Beta-* / *Gammaproteobacteria*. Since no further region of sufficient similarity shared by both groups could be identified, separate reverse PCR primers were designed for *alphaproteobacterial gmaS* ( $\alpha$ <sub>*gmaS*</sub><sub>970r</sub>; TGGGTSCGRTRTTGCCSG, Figure 5.4b) and *beta-* / *gammaproteobacterial gmaS* ( $\beta$ <sub>*gmaS*</sub><sub>1332r</sub>; GTAMTCSAYCCAYTCCATG, Figure 5.4c). For simplicity, the primers are from here on referred to as 557f, 970r and 1332r. Specificity of the new PCR primer sets was established

by amplification and sequencing of *gmaS* from a range of genomic and non-genomic samples, as outlined in the sections below.

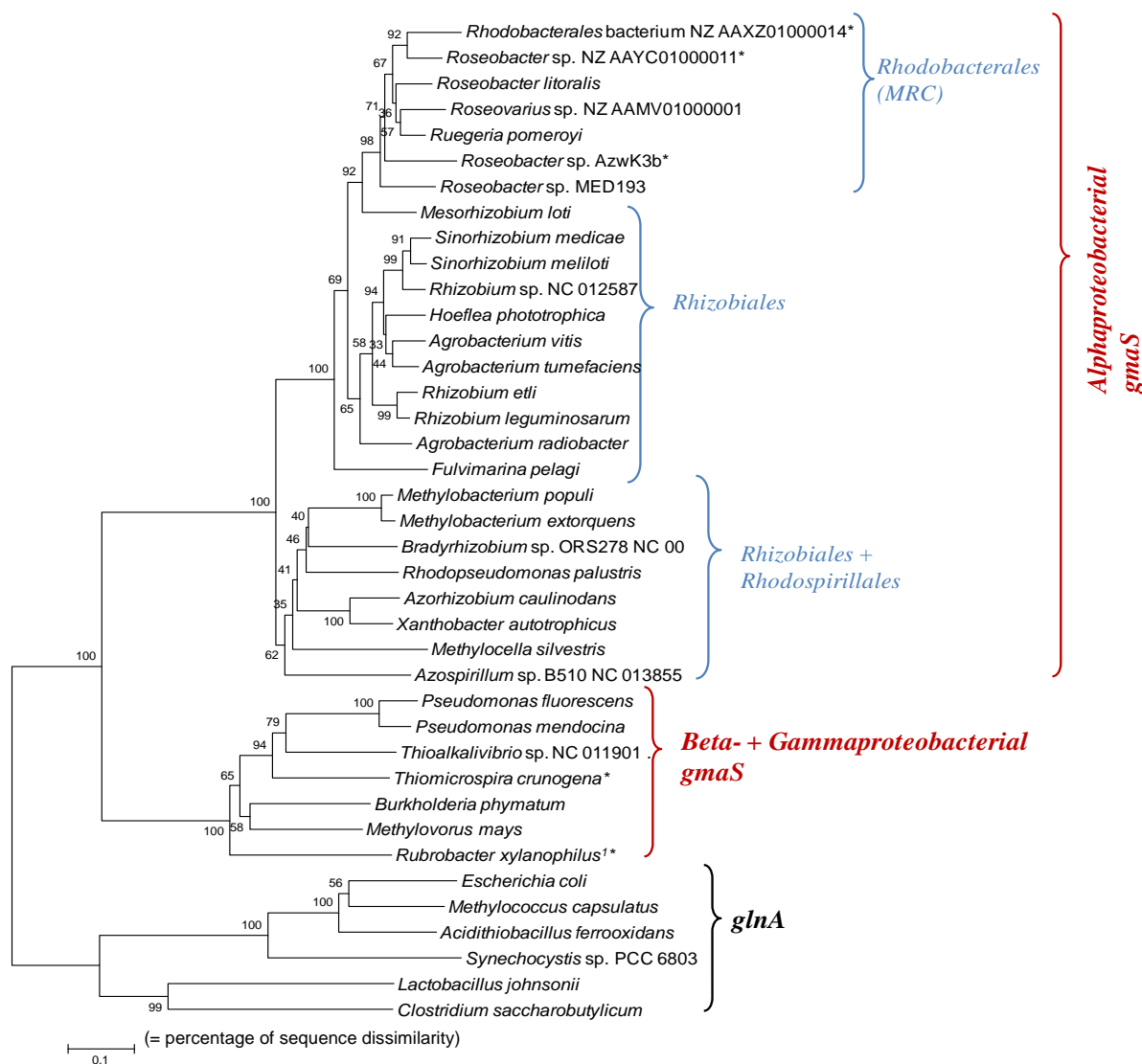
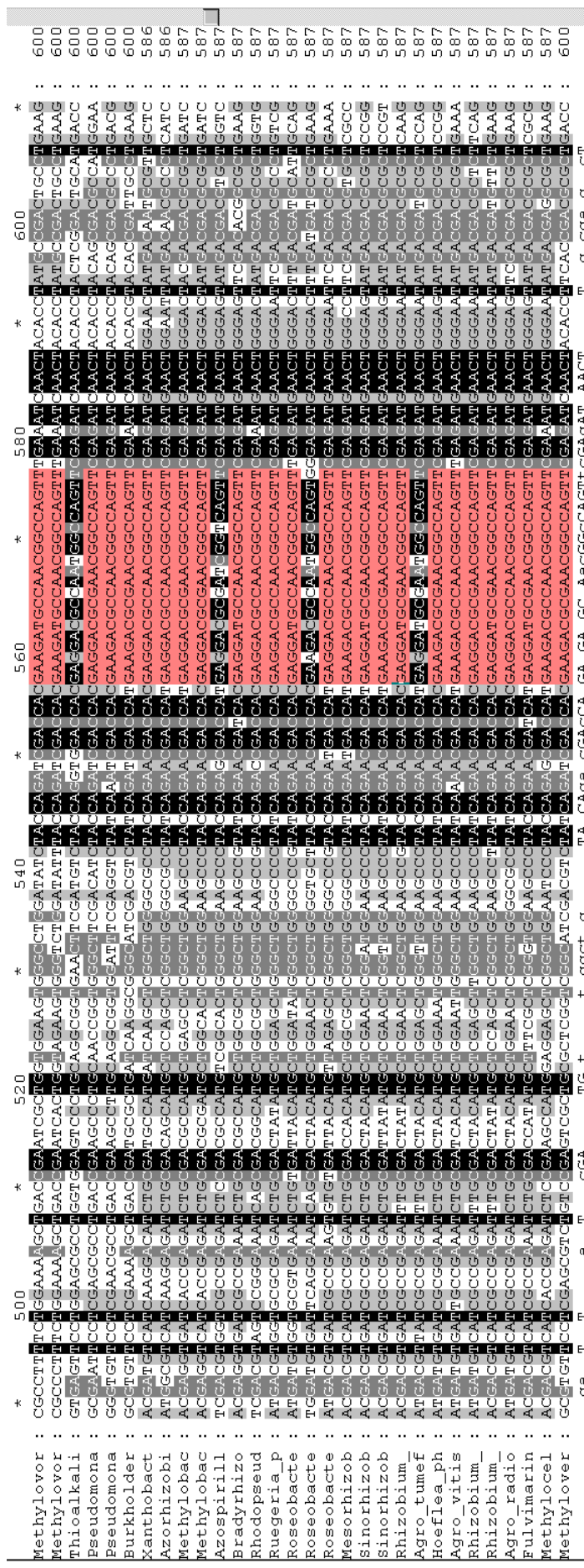


**Figure 5.3** Amino-acid based, phylogenetic tree of *gmaS* sequences from MMA-utilising isolates and published bacterial genomes. *GlnA* sequences present the outgroup. The tree was established using the neighbour-joining method (1,000 bootstrap replicates) and the Poisson correction method for computing evolutionary distances. Numbers at nodes indicate bootstrap values. All bacterial sequences refer to type strains (as listed on LPSN), unless strain names are indicated.

<sup>1</sup> *Rubrobacter xylanophilus* is a member of the *Actinobacteria* although its *gmaS* sequence affiliates with the *Beta-* and *Gammaproteobacterial* cluster.

<sup>2</sup> *gmaS* sequences containing a total of more than two mismatches across the forward / reverse primer set designed for the respective clusters in this study are marked with an asterisk.



**Figures 5.4a-c** Nucleotide sequence alignments for design of *gmaS* PCR primers *gmaS*\_557f, 970r and  $\beta$ \_*gmaS*\_1332r

**Figure 5.4a** Nucleotide sequence alignment for design of *gmaS* PCR primer *gmaS*\_557f (forward, targeting all non-marine *gmaS*). Note: the region between base pairs 557 and 579 was chosen for *gmaS* primer design because it was the most highly conserved region not present in *glnA* sequences. Adjacent, more highly conserved regions could not be used as they also featured in *glnA* sequences (not shown). It was crucial for *gmaS* primers to specifically amplify *gmaS*, but not *glnA*.



### 5.2.3 Validation of primers: PCR and sequencing of *gmaS* genes from control strains

For validation, the new PCR primer sets were tested on five non-marine bacteria with known *gmaS* sequences: *Sinorhizobium meliloti* 1021, *Mesorhizobium loti* MAFF303099, *Rhizobium leguminosarum* bv. *viciae* 3841, *Agrobacterium tumefaciens* C58 and *Pseudomonas fluorescens* SBW25 (Chen *et al.*, 2010b). *GmaS* sequences from these strains had been used in designing the new *gmaS* primers (see above). *GmaS* genes from *A. tumefaciens*, *S. meliloti*, *M. loti* and *R. leguminosarum* were amplified using primer set 557f / 970r, developed for *alphaproteobacterial gmaS*; *gmaS* from *P. fluorescens* was amplified using the *gamma-/betaproteobacterial-specific* primer set 557f / 1332r (Figure 5.5). PCR amplification was initially performed at an annealing temperature of 55°C using 30 cycles. To ensure the correct genes were amplified, the amplification products were submitted to sequence analysis.

PCR products of the expected sizes (~400 bp for 557f / 970r and ~750 bp for 557f / 1332r) were obtained for all five strains, as shown by agarose gel electrophoresis (Figure 5.5). However, the amount of PCR product was very low for one of the samples (*A. tumefaciens*, which has one bp mismatch with the forward primer), resulting in a very faint band on the agarose gel (Figure 5.5). The amount of DNA was however sufficient for sequencing, and sequence analysis confirmed that the correct gene had been amplified. In all cases, the amplified sequences were identical to the original *gmaS* sequences obtained from the bacterial genomes, affirming specificity of the primers. To improve amplification results, the PCR conditions were subsequently adjusted by testing a range of different conditions (see section 5.4).

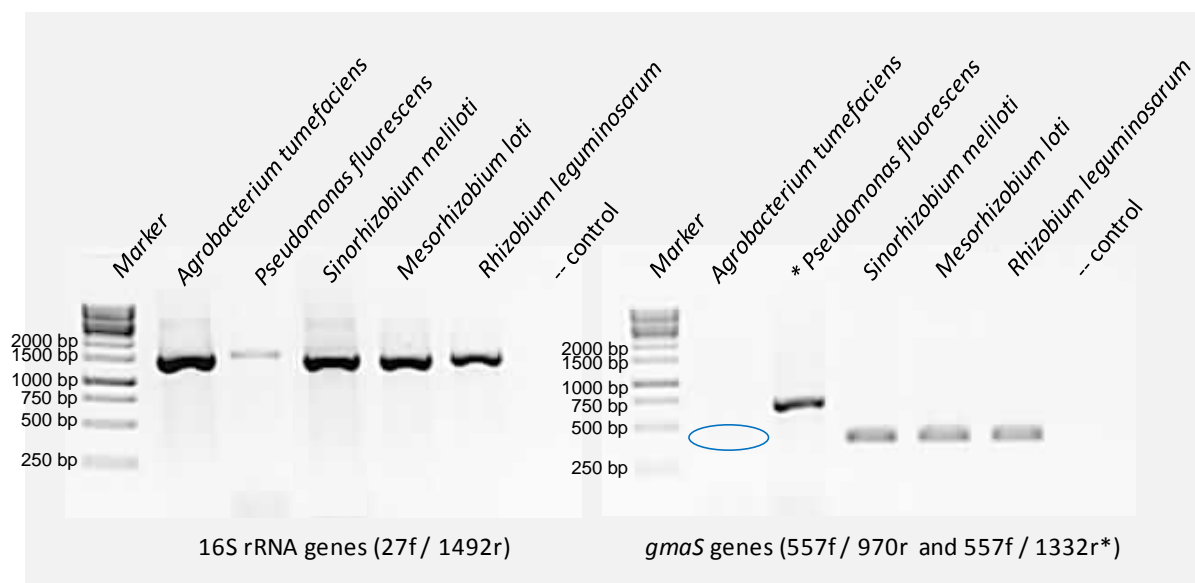


**Figure 5.5** Agarose gel images of 16S rRNA gene PCR products (left) and *gmaS* PCR products (right) of five MMA-utilising control strains using the new *gmaS* primer sets.

### 5.3 Testing *gmaS* PCR primers on genomic and non-genomic DNA from Movile Cave

#### 5.3.1 Genomic DNA: few isolates test positive

Once the *gmaS* primers had been verified using control strains, they were tested on methylotrophic and non-methylotrophic Movile Cave isolates obtained from enrichments with methylated amines (see Chapter 3). Using the same conditions as for the control strains (annealing temperature of 55°C and 30 cycles), *gmaS* amplification products were obtained for *Methylobacterium extorquens* 2W-7, *Xanthobacter tagetidis* LW-13, *Acinetobacter lwoffii* 2W-62 and *Pseudomonas* sp. 1W-57Y. Sequencing and phylogenetic analysis confirmed the amplified genes as *gmaS*. No PCR products were obtained for the isolates *Paracoccus yeei* 1W-61, *Catellibacterium* sp. LW-1, *Aminobacter niigataensis* 2W-12, *Zoogloea caeni* A2-14M, and *Acinetobacter johnsonii* 2W-62 under these conditions, or with added cycles. At this time it was unclear whether this was a result of these isolates not carrying *gmaS*, the primers not targeting them, or the PCR conditions being too stringent.

### *Non-genomic DNA: low levels of amplification and double bands*

The new *gmaS* primers were further tested on non-genomic DNA extracted from (i) floating mat samples from Movile Cave and (ii) MMA enrichment cultures with Movile Cave water (t=3 from SIP microcosms, refer to Chapter 4, section 4.3). The purpose of this was to first of all establish whether the new primers detected *gmaS* genes in environmental samples confirmed to contain MMA oxidisers. MMA enrichment samples were believed to provide relatively easy (enriched) templates for PCR as they should contain elevated levels of *gmaS*. However, using the same conditions as previously for genomic DNA, no PCR products were obtained for either of the two samples with primers 557f/1332r, targeting *beta*- and *gammaproteobacterial gmaS*. PCR with primers 557f/970r, targeting *alphaproteobacterial gmaS*, resulted in only a very faint band at the expected position (~400 bp) on the agarose gel for DNA from MMA-SIP enrichment, while no PCR product was visible for DNA from floating mat samples (Figure 5.6).

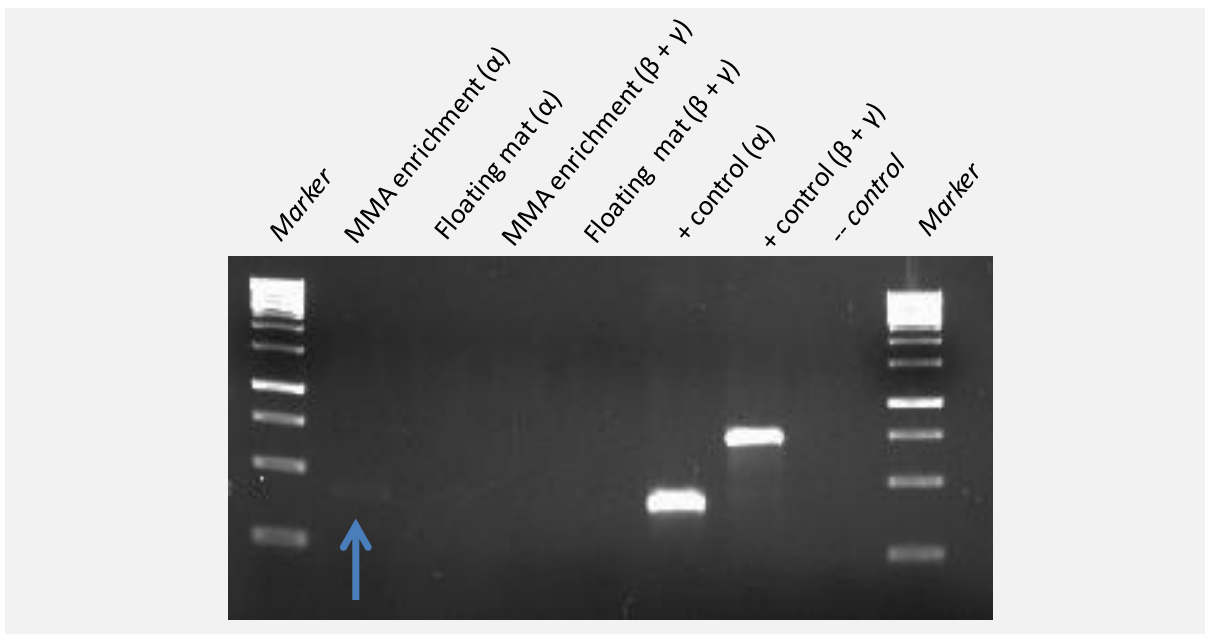


**Figure 5.6** Agarose gel electrophoresis image following *gmaS* PCR of non-genomic DNA extracted from (i) MMA-SIP enrichments with Movile Cave water and (ii) Movile Cave floating mat samples, using new primer sets 557f/970r (targeting *α*-proteobacterial *gmaS*) and 557f/1332r (targeting *β*- and *γ*-proteobacterial *gmaS*). PCR products were obtained only for MMA-enrichment DNA (*α*-proteobacterial *gmaS*; faint band in lane 1) and control DNA from isolates *M. extorquens* 2W-11 (*α*-proteobacterial *gmaS*) and *Pseudomonas* sp. 1W-57Y (*γ*-proteobacterial *gmaS*).

Increasing the number of PCR cycles did not improve the results. However, increasing the amount of template from 50 to 150 ng DNA yielded a PCR product for DNA from floating mat samples with primers 557f / 970r (Figure 5.7). Oddly though, an attempt to reproduce this PCR in order to obtain sufficient product for cloning and sequencing repeatedly resulted in an additional band on the gel, necessitating gel excision (Figure 5.8). However, cloning and sequencing from gel-excised products failed, and optimisation of the PCR protocol to avoid the second band was sought instead (see section 5.4)

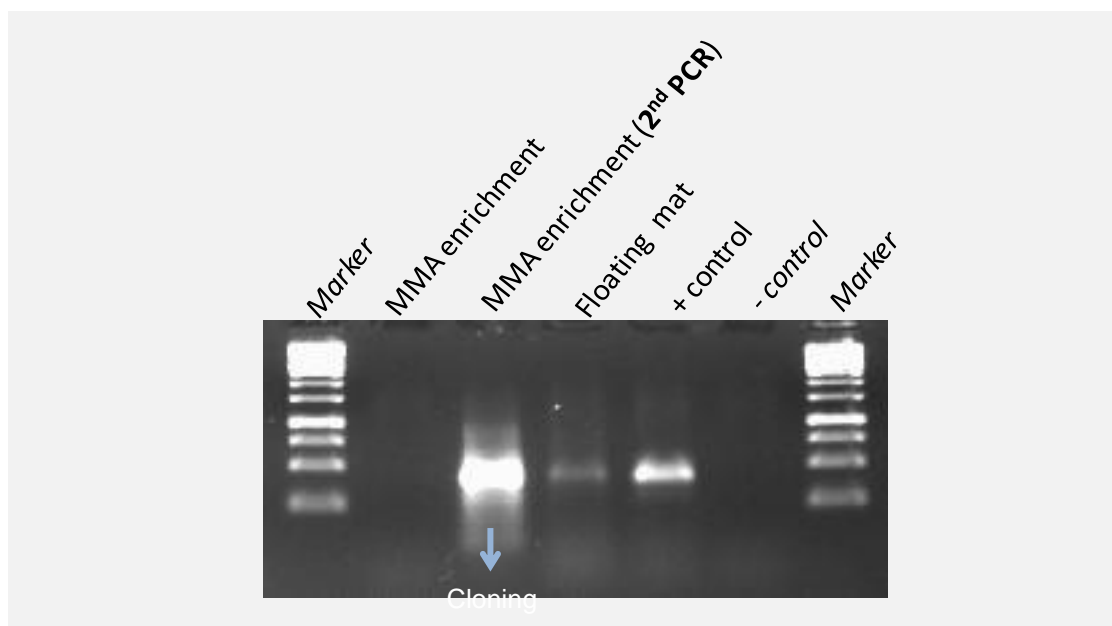


**Figure 5.7** Agarose gel electrophoresis image of PCR products obtained with primers 557f / 970r (targeting  *$\alpha$ -proteobacterial gmaS*). A single PCR using 150 ng of template resulted in a satisfactory amount of PCR product for DNA from floating mat samples. Two rounds of PCR (using 6 ng template in the first round, and 1  $\mu$ l of the resulting product for the second round) were necessary to generate sufficient product from MMA-enrichment DNA.

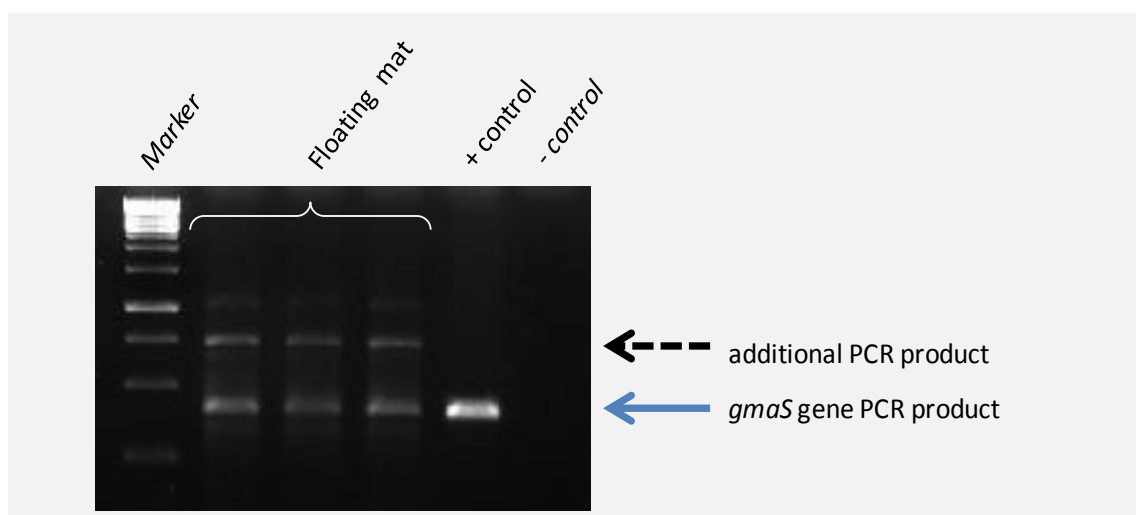


**Figure 5.8** Agarose gel electrophoresis image of *gmaS* PCR products obtained for DNA from floating mat samples. Despite using the same primers (557f / 970r, targeting  *$\alpha$ -proteobacterial gmaS*) and conditions as before (150 ng template, annealing temperature of 55°C, 30 cycles, see Figure 5.7), additional bands were obtained alongside *gmaS* products, necessitating gel excision.

Because of the low quantity of DNA obtained from MMA-SIP enrichments (see Chapter 4), the amount of template (6 ng) could not be increased for this sample, and a second round of PCR (using 1  $\mu$ l of the product resulting from the first reaction) was necessary in this case to generate sufficient amounts of *gmaS* PCR product for subsequent cloning and sequencing. While the double PCR was very specific and generated a large amount of PCR product (Figure 5.7), this approach increases PCR bias, which is why it was only used initially for the purpose of verifying that the amplified gene was indeed *gmaS*.

Increasing the amount of template did not improve results for *gmaS* PCR with primers 557f / 1332r. Therefore, a re-amplification approach (using 1  $\mu$ l of the product from the first round of PCR as template for the second round) was used for both the mat sample as well as the MMA enrichment sample. Even after two rounds of PCR however, the amount of PCR product obtained was still very low (Figure 5.9). Nevertheless, to establish that the correct gene had been amplified, PCR products from MMA enrichment samples (which had produced the better results of the two) were pooled for cloning and sequencing.

Sequence analysis of four *gmaS* clones from MMA enrichment confirmed that the correct gene had been amplified with both primer sets: Sequences obtained from PCR with the *alphaproteobacterial*-specific primer set were 100% identical to *gmaS* from the *M. extorquens* isolate (Figure 5.12; clones GAMC2, GAMC3). Sequences obtained from the *beta- / gammaproteobacterial*-specific primers were 100% identical to *gmaS* from *Pseudomonas mendocina* (JGI database) and *gmaS* from the *A. lwoffii* isolate, respectively

(Figure 5.12; clones GBMC4, GBMC5). To overcome the low levels of amplification and double bands, and avoid using a double PCR, which increases PCR bias, the *gmaS* PCR protocols were hereupon optimised (see below).

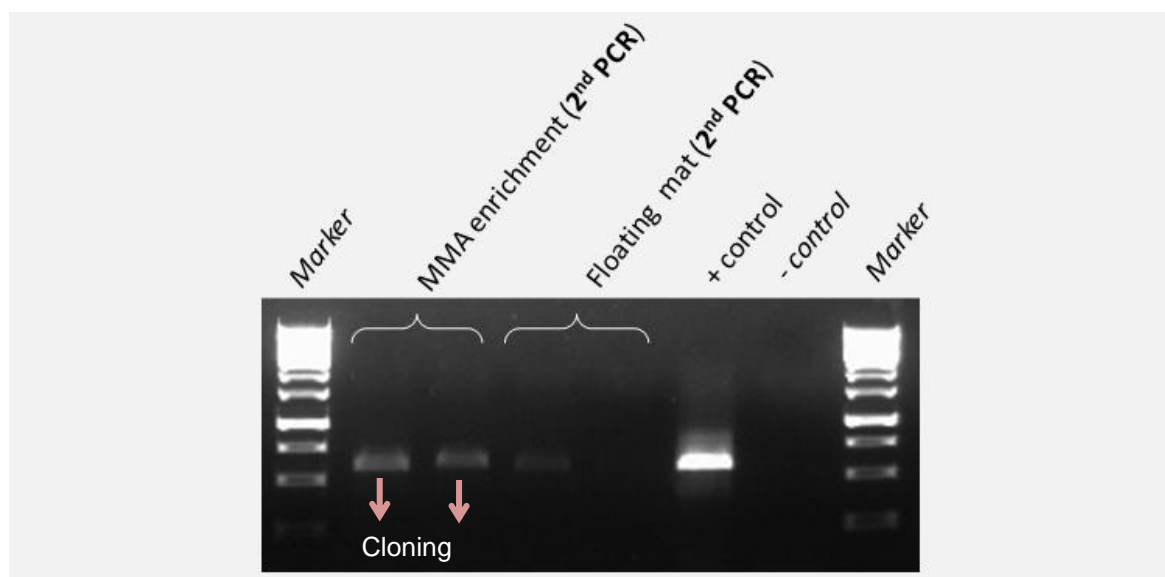


**Figure 5.9** Agarose gel electrophoresis image of PCR products obtained with primers 557f / 1332r (targeting  $\beta$ -proteobacterial and  $\gamma$ -proteobacterial *gmaS*) after two rounds of PCR (using 1  $\mu$ l of the product from the first round as template for the second round). Amounts of PCR product were still very low.

## 5.4 Optimisation of *gmaS* PCR protocols

### 5.4.1 Genomic DNA – improved detection of *gmaS* in isolates

To improve amplification results (i.e., overcome low levels of amplification as well as non-specific amplification) for genomic and non-genomic DNA, *gmaS* PCR protocols were adjusted by testing a range of conditions, annealing temperatures and cycle numbers. To begin with, optimisation was carried out with genomic DNA only; Movile Cave isolates for which *gmaS* genes had already been amplified successfully (*M. extorquens* 2W-7, *X. tagetidis* LW-13, *A. lwoffii* 2W-62, *Pseudomonas* sp. 1W-57Y) were used as controls. The best results were obtained using touchdown protocols, employing annealing temperatures ranging from 60 to 50°C (for amplification of *alphaproteobacterial gmaS*) and 55 to 45°C (for amplification of *beta*- and *gammaproteobacterial gmaS*), respectively (for the detailed PCR protocols, see Table 5.1). Using the new protocols, *gmaS* genes were amplified from a further five Movile Cave isolates (*Catellibacterium* sp. LW-1, *Rhodobacter* sp. 1W-5, *Aminobacter* sp. 2W-12, *Paracoccus yeei* 2W-61, *Shinella* sp. A2-41x).

**Table 5.1** Optimised PCR conditions (touch-down protocols) for *gmaS* PCR

Primer set 557f / 970r ( <i>α</i> -proteobacterial <i>gmaS</i> )			Primer set 557f / 1332r ( <i>β</i> - and <i>γ</i> -proteobacterial <i>gmaS</i> )		
Temp. (°C)	Time	Cycles (n)	Temp. (°C)	Time	Cycles (n)
94	5 min	1	94	5 min	1
94	45 sec		94	45 sec	
<b>60 → 50*</b>	45 sec	<b>10</b>	<b>55 → 45*</b>	45 sec	<b>10</b>
72	1 min		72	1 min	
94	45 sec		94	45 sec	
<b>56</b>	45 sec	<b>30</b>	<b>52</b>	45 sec	<b>35</b>
72	1 min		72	1 min	
72	8 min	1	72	8 min	1
4	∞		4	∞	

\*decreasing by 1°C each cycle

Nevertheless, even with the adjusted protocol, the level of PCR amplification remained rather low. Results were improved considerably when switching PCR enzymes from the Taq polymerase by Fermentas to the MyTaq™ DNA Polymerase by Bioline, (using the same touchdown protocols). In addition to increasing the level of amplification for the above organisms, *gmaS* genes were also amplified from Movile Cave isolates that had tested negative with the Fermentas Taq. The optimised *gmaS* PCR (using touch-down protocols in combination with a more efficient Taq polymerase) worked extremely well for genomic DNA and was hence used to screen Movile Cave isolates for the presence of the *gmaS* gene (see later, section 5.5.).

#### 5.4.2 Non-genomic DNA – Movile Cave samples prove difficult

While the optimised PCR protocols worked extremely well for genomic DNA, there were still some problems with *gmaS* amplification from non-genomic DNA derived from Movile Cave. After an additional sampling trip to the cave at a time where copious amounts of floating mats (i.e. microbial biomass) were present on the water surface, more sample material was available for setting up enrichments, as well as for extraction of DNA directly from floating mat material. First, *gmaS* PCR was carried out on DNA extracted from MMA enrichments. This was done because enrichment samples, containing elevated amounts of *gmaS*, had previously given the better results.

PCR amplification of *alphaproteobacterial gmaS* (using primers 557f / 970r) worked well with the new enrichment samples, producing single products of the expected size

(~410 bp). A small clone library was established and all sequences analysed were identified as *gmaS* (for details see section 5.6. on preliminary *gmaS* surveys and Figure 5.12, sequences E1a; E2a; E3a; E4a). PCR amplification of *beta-* / *gammaproteobacterial gmaS* (using primers 557f / 1332r) resulted in an additional, slightly larger PCR product alongside the *gmaS* gene fragment (Figure 5.10). This additional gene fragment shared high sequence identity with a viral coat protein (as revealed by sequence analysis using blastx) and could not be eliminated by using more stringent PCR conditions due to extremely high similarity with the target gene in the primer binding regions. For the purpose of cloning and sequencing, the secondary PCR product was avoided by gel excision of the *gmaS* band (~775 bp). All sequences obtained from clones carrying inserts of the correct size (Figure 5.11) were identified as *gmaS* (for details see section 5.6. on preliminary *gmaS* surveys and Figure 5.12, sequences E2g; E11g).

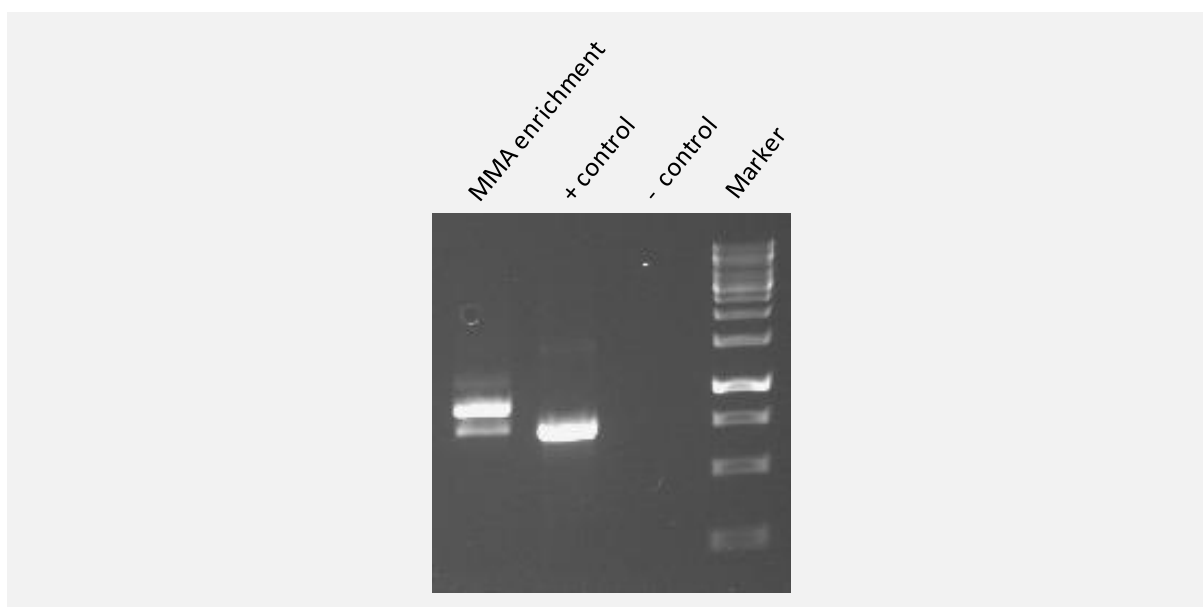


**Figure 5.10** Agarose gel electrophoresis image of PCR products obtained with primers 557f / 1332r (targeting *β*-proteobacterial and *γ*-proteobacterial *gmaS*). DNA from MMA enrichments generated an additional, slightly larger PCR product along with the *gmaS* PCR product.

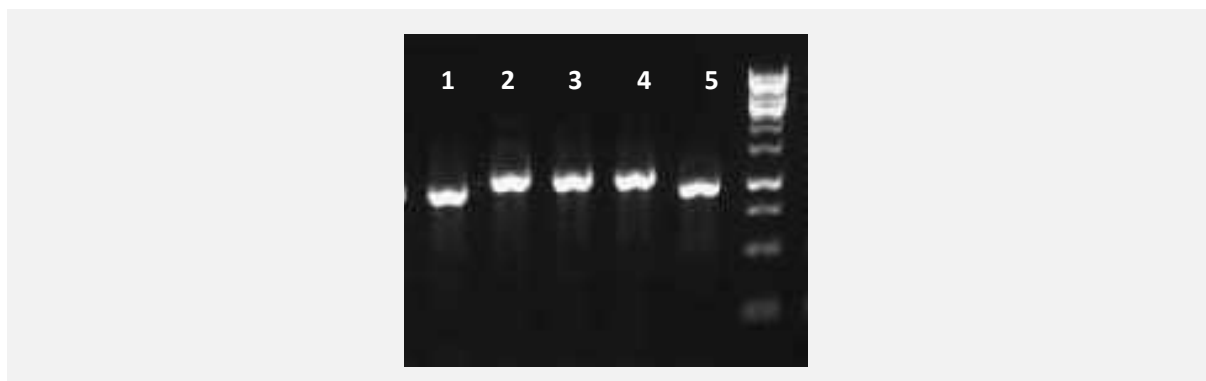


**Figure 5.11** Agarose gel electrophoresis image following reamplification (using primers M13f / M13r) of clones generated from the PCR product obtained with primers 557f / 1332r from MMA enrichment DNA (shown in Figure 5.10). As expected, the shorter, correct-sized inserts were identified as *gmaS* (lanes 1 and 5), while the larger gene fragments were unrelated to *gmaS* and appeared to be of viral origin (lanes 2-4).

Interestingly, the additional PCR product only occurred when amplifying *beta- / gammaproteobacterial gmaS* from Movile Cave enrichment samples. It was not observed when amplifying *gmaS* genes from DNA extracted directly from floating mat material (Figure 5.13), suggesting that it is not a general issue with the PCR primers or protocol.

## 5.5 Distribution of *gmaS* and *mauA* genes in Movile Cave isolates

### 5.5.1 *gmaS* is present in all MMA-utilising isolates

To assess the presence of *gmaS* and *mauA* in Movile Cave bacteria, and thereby obtain an indication of the relative distribution of the direct and indirect MMA oxidation pathways, MMA-utilising isolates (Chapter 3) were screened for the presence of both genes by PCR. Primer sets 557f / 970r and 557f / 1332r developed in this study were used to screen isolates for *gmaS* (indicative of the indirect MMA oxidation pathway, Figure 5.1b). PCR and sequence analysis of six methylotrophs and eight non-methylotrophs revealed the presence of *gmaS* in all fourteen of these isolates (Table 5.2).

Phylogenetic analysis placed the *gmaS* sequences retrieved from Movile Cave isolates within the *alphaproteobacterial* and the *beta- / gammaproteobacterial* clusters observed previously (Figure 5.12). Additional *gmaS* sequences were retrieved by BLAST (blastx) searches, using the *gmaS* sequences from Movile Cave isolates as queries, and added to the phylogenetic tree. With the added sequences (i.e., higher resolution), the division into the two main *gmaS* clusters (*alphaproteobacterial gmaS* and *beta- / gammaproteobacterial gmaS*)

remained, while there were now two, rather than three, major subgroups within the *alphaproteobacterial* cluster, each of which again contained several smaller sub-clusters (Figure 5.12). The first of the two *alphaproteobacterial* subgroups (referred to as Group 1 from here on) contained the Marine *Roseobacter* Clade (MRC) -associated *gmaS* sequences (in a separate sub-cluster), as well as several sub-clusters of *gmaS* sequences belonging to soil and freshwater bacteria from the orders *Rhodobacterales* and *Rhizobiales*. Eight *gmaS* sequences from Movile Cave isolates fell into Group 1. Interestingly, the majority of these formed a distinct sub-cluster within the group (Figure 5.12). The second of the two *alphaproteobacterial* subgroups (referred to as Group 2 from here on) contained only *gmaS* sequences from non-marine bacteria of the orders *Rhodospirillales*, *Rhizobiales* and *Sphingomonadales*. Four *gmaS* sequences from Movile Cave isolates fell into Group 2. The remaining four *gmaS* sequences from Movile Cave isolates fell into the *Beta*- and *Gammaproteobacterial* cluster.

Generally, organisms that were closely related based on their 16SrRNA genes did not necessarily cluster closely together in the *gmaS* tree (e.g. *Mesorhizobium loti* and Movile Cave isolate *Mesorhizobium* sp. 1M-11). Similarly, some *gmaS* sequences that shared a high level of identity belonged to organisms not closely related based on 16S rRNA genes (e.g. *Catellibacterium* sp. LW-1, *Mesorhizobium* sp. 1M-11 and *Rhodobacter* sp. 1W-5 isolates).

**Figure 5.12** Phylogenetic relationship of *gmaS* sequences derived from published bacterial genomes, methylotrophic (solid rectangles; coloured orange) and non-methylotrophic (hollow rectangles; coloured blue) bacterial isolates and clone library sequences (triangles; bold print) from Movile Cave. *glnA* sequences represent the outgroup. The tree was established using the neighbour-joining method (1,000 bootstrap replicates) and the Poisson correction method for computing evolutionary distances. Translated *gmaS* sequences had a length of ~135 amino acids (*alphaproteobacterial* isolates) and ~250 amino acids for (*beta-* and *gammaproteobacterial* isolates), tree is based on alignment of 135 amino acids (total deletion of gaps). Numbers at nodes indicate bootstrap values. All bacterial sequences refer to type strains (as listed on LPSN), unless strain names are indicated.

<sup>1</sup> *Rubrobacter xylanophilus* is a member of the *Actinobacteria* although its *gmaS* sequence affiliates with the *beta-* and *gammaproteobacterial* cluster.

<sup>2</sup> *gmaS* sequences containing a total of more than two mismatches across the forward / reverse primer set designed for the respective clusters in this study are marked with an asterisk.



### 5.5.2 *mauA* is only found in some methylotrophic MMA-utilising isolates

Movile Cave isolates were also screened for the presence of *mauA*, encoding methylamine dehydrogenase (biomarker for the direct MMA oxidation pathway, present in methylotrophs only, Figure 5.1a) using PCR primer set mauAf1 / mauAr1 (Neufeld *et al.* 2007a). *mauA* was detected in four out of seven methylotrophic isolates. Genome analysis later also revealed presence of *mauA* in the methylotroph *Catellibacterium* sp. LW-1 (Wischer & Kumaresan *et al.*, in prep) which was not detected with PCR-screening.

It is worth noting that PCR conditions detailed in Neufeld *et al.* (2007a) only generated products for *Xanthobacter tagetidis* LW-13 and *Methylobacterium extorquens* 2W-7. The stringency of the protocol had to be reduced in order to obtain products for the remaining organisms. A number of alternative *mauA* primer sets developed by Wei-Lian Hung (Hung *et al.*, 2012) were tested but resulted in unspecific amplification and were not used further. Markedly, all of the isolates that tested positive for *mauA* also contained *gmaS* (Table 5.2). Based on these results, the genes for the indirect MMA oxidation pathway appear to be prevalent amongst both methylotrophs and non-methylotrophs in Movile Cave. The absence of *mauA* in all of the non-methylotrophic isolates seems to confirm that the direct MMA oxidation pathway is restricted to methylotrophs. Moreover, the tight phylogenetic clustering of *gmaS* genes from those methylotrophic isolates that did not contain *mauA* (Figure 5.12), may suggest that these organisms belong to a distinct group of MMA-utilising methylotrophs that do not possess the direct MMA-oxidation pathway.

**Table 5.2** Movile Cave isolates – methylated amine metabolism and functional gene markers

Isolate	Phylogeny	Methylated amines used as		Functional genes	
		N-source	C-source	<i>gmaS</i>	<i>mauA</i>
<i>Alphaproteobacteria</i>					
1	<i>Methylobacterium extorquens</i> 2W-7	+	+	+	+
2	<i>Xanthobacter tagetidis</i> LW-13	+	+	+	+
3	<i>Paracoccus yeei</i> 1W-61	+	+	+	+
4	<i>Aminobacter niigataensis</i> 2W-12	+	+	+	-
5	<i>Catellibacterium</i> sp. LW-1	+	+	+	- <sup>(1)</sup>
6	<i>Mesorhizobium</i> sp. 1M-11	+	+	+	-
7	<i>Shinella</i> sp. A2-41x	+	-	+	-
8	<i>Rhodobacter</i> sp. 1W-5	+	-	+	-
9	<i>Oleomonas</i> sp. O1	+	-	+	-
10	<i>Oleomonas</i> sp. O3	+	-	+	-
<i>Gammaproteobacteria</i>					
11	<i>Acinetobacter johnsonii</i> 1W-6	+	-	+	-
12	<i>Acinetobacter lwoffii</i> 2W-62	+	-	+	-
13	<i>Pseudomonas</i> sp. 1W-57Y	+	-	+	-
<i>Betaproteobacteria</i>					
14	<i>Zoogloea caeni</i> A2-14M	+	-	+	-

Overview of bacterial isolates from Movile Cave, their capability of using methylated amines as a carbon (C) and / or nitrogen (N) source, and presence of functional genes indicating the direct (*mauA*) or indirect (*gmaS*) methylamine oxidation pathway.

<sup>(1)</sup>Results from genome analysis later indicated presence of *mauA*.

## 5.6 Preliminary *gmaS* surveys of Movile Cave floating mat samples

### 5.6.1 *gmaS* genes in MMA enrichments from floating mat correspond with MMA utilisers identified by isolation studies and DNA-SIP

Cloning and sequencing of *gmaS* genes from Movile Cave samples performed in this PhD project primarily served to validate the newly developed primers, rather than to assess the diversity of *gmaS* in Movile Cave (extensive diversity studies could not be conducted due to

time limitations). Nevertheless, the obtained sequences give a preliminary indication of the range of *gmaS*-containing bacteria in Movile Cave. Cloned *gmaS* sequences from MMA enrichments of floating mat samples corresponded to *gmaS* from methylotrophic and non-methylotrophic isolates (Table 5.2) and MMA-utilising bacteria identified in SIP enrichments (by 16S rRNA gene sequencing, Chapter 4), namely *Catellibacterium*, *Methylobacterium*, *Pseudomonas* and *Acinetobacter* (99-100% identity; sequences E2a; E3a; E4a; E2g; E11g; GMAC2; GMAC3; GBMC5 in Figure 5.12). A further sequence loosely affiliated with *Methylotenera*, *Methylophaga* and *Methylovorus* (89-90% identity with all three genera). A final *gmaS* sequence affiliated with *gmaS* from the methylotroph *Hyphomicrobium* (99% identity; sequence E1a in Figure 5.12) which was not detected by DNA-SIP or isolated in this study but is known to be present in Movile Cave (Hutchens *et al.*, 2004). Due to time limitations, *gmaS* genes amplified from DNA extracted directly from floating mat material (Figure 5.13) could not be cloned and sequenced. In future studies, extensive clone libraries of both floating mat and water samples from Movile Cave should be established in order to identify potential MMA-utilising bacteria that may not be detected in enrichment cultures. Indeed, preliminary data from metagenome analysis indicated some additional *gmaS* sequences to those related to organisms mentioned above (for details, see below).

### 5.6.2 Metagenome analysis of Movile Cave floating mat reveals additional *gmaS* sequences

As part of the larger Movile Cave food web study, the metagenome of DNA extracted from floating mat samples was sequenced by high-throughput sequencing (for details see Chapter 2, section 2.15.2). (DNA extraction and sample processing was conducted by Jason Stephenson). Metagenome sequences were subsequently screened for *mauA* and *gmaS* genes. Interestingly, no *mauA* genes were detected, while *gmaS* genes were identified. The major difficulty with mining for *gmaS* sequences is the lack of annotation: *gmaS* genes are largely annotated as *glnA*, but unless they are available on the JGI IMG database, it cannot easily be determined whether they are *glnA* or *gmaS*. Only one *gmaS* sequence was obtained based on GenBank annotation, it affiliated with *gmaS* from *Methylophaga thiooxydans* (91% similarity). Local BLAST databases were therefore established from the data and screened for *gmaS* sequences using *gmaS* from *Methylobacterium extorquens*, *Methylotenera mobilis* and *Pseudomonas fluorescens* as queries. Verified *gmaS* sequences obtained based on IMG annotation or local BLAST (blastx) search affiliated with *gmaS* from: *Thiobacillus thioparus* (99% similarity), *Dechloromonas aromatica* (92% similarity), *Sideroxydans lithotrophicus*

(92% similarity), *Methylobacillus flagellatus* (90% similarity), *Cupriavidus necator* (87% similarity), *Rhodoferax saidenbrachensis* (86% similarity), *Rhodopseudomonas palustris* (82% similarity) and *Azospirillum lipoferum* (81% similarity), revealing a number of new *gmaS* sequences not detected in enrichments. These *gmaS* sequences were not included in the phylogenetic tree in Figure 5.12 due to their short size (< 200 bp).

### 5.7 Preliminary *gmaS* surveys of soil and freshwater reveal new *gmaS* groups

In the next step, the new *gmaS* primer sets were tested on non-genomic DNA extracted from soil, freshwater, and freshwater sediment unrelated to Movile Cave. The soil and freshwater samples used were derived from generic locations not specifically associated with MMA metabolism (University of East Anglia campus and lake, for details of sampling locations see Chapter 2, section 2.11.3). The purpose was to assess whether the new primers could detect *gmaS* genes in different environmental samples. It was expected that amplification levels of *gmaS* from environmental samples not associated with MMA-utilising bacteria might be low. Surprisingly however, these samples proved to be much easier templates than those from Movile Cave: *gmaS* amplification from soil and sediment samples resulted in single PCR products of the correct size and a good levels of amplification (Figure 5.13), suggesting that the additional PCR product obtained previously was not an issue with the PCR primers or protocol, but a problem confined to Movile Cave enrichment samples.

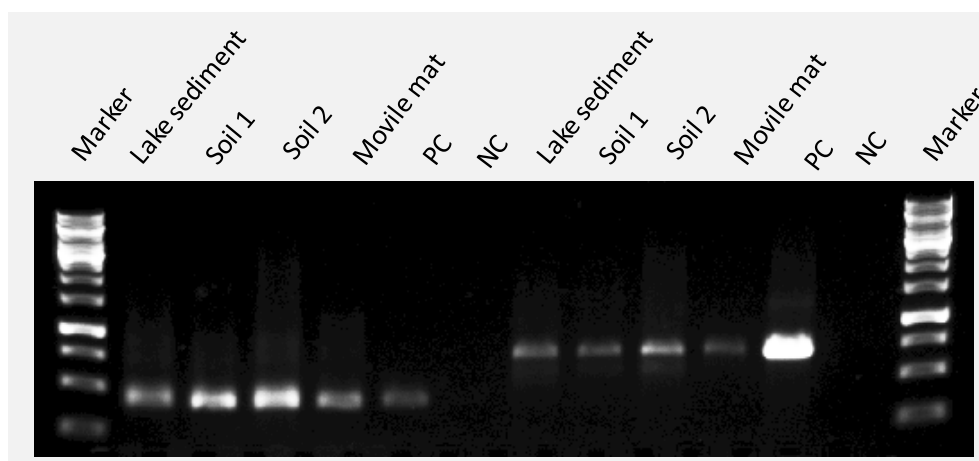


**Figure 5.13** Agarose gel electrophoresis image of *gmaS* PCR products obtained from non-genomic DNA samples with primer sets 557f/970r (targeting  $\alpha$ -proteobacterial *gmaS*, left-hand side) and 557f/1332r (targeting  $\beta$ -proteobacterial and  $\gamma$ -proteobacterial *gmaS*; right-hand side) using optimised PCR conditions (touchdown protocols as described in 5.4). PC = positive control; NC = negative control.

*GmaS*-based clone libraries were constructed and a total of 16 clones were randomly selected for sequencing. Identity of the amplified genes was confirmed by cloning and sequencing. Interestingly, many of the obtained *gmaS* sequences were not closely related to *gmaS* sequences from Movile Cave or published genomes, and formed several distinct clusters in the phylogenetic tree (Figure 5.14, “unknown *gmaS*”). These results suggest that there is a wide diversity of *gmaS* sequences, and hence, potential MMA-oxidising bacteria which have not yet been identified.

**Figure 5.14 (right)** *gmaS* phylogenetic tree incorporating *gmaS* sequences cloned from soil and lake sediment samples not associated with Movile Cave (coloured dark-red, marked with circles); showing phylogenetic relationships with *gmaS* sequences retrieved from published bacterial genomes, methylotrophic (orange, solid squares) and non-methylotrophic (blue, hollow squares) Movile Cave isolates and MMA-SIP clone library sequences (bold print, triangles). Gene sequences of the functionally unrelated glutamine synthetase (*glnA*) represent the outgroup. The tree was established using the neighbour-joining method (1,000 bootstrap replicates) and the Poisson correction method for computing evolutionary distances. Translated *gmaS* sequences had a length of ~135 amino acids (*alphaproteobacterial* isolates) and ~250 amino acids for (*beta*- and *gammaproteobacterial* isolates). Numbers at nodes indicate bootstrap values. All bacterial sequences refer to type strains (as listed on LPSN), unless strain names are indicated.

<sup>1</sup> *Rubrobacter xylanophilus* is a member of the *Actinobacteria* although its *gmaS* sequence affiliates with the *beta*- and *gammaproteobacterial* cluster.

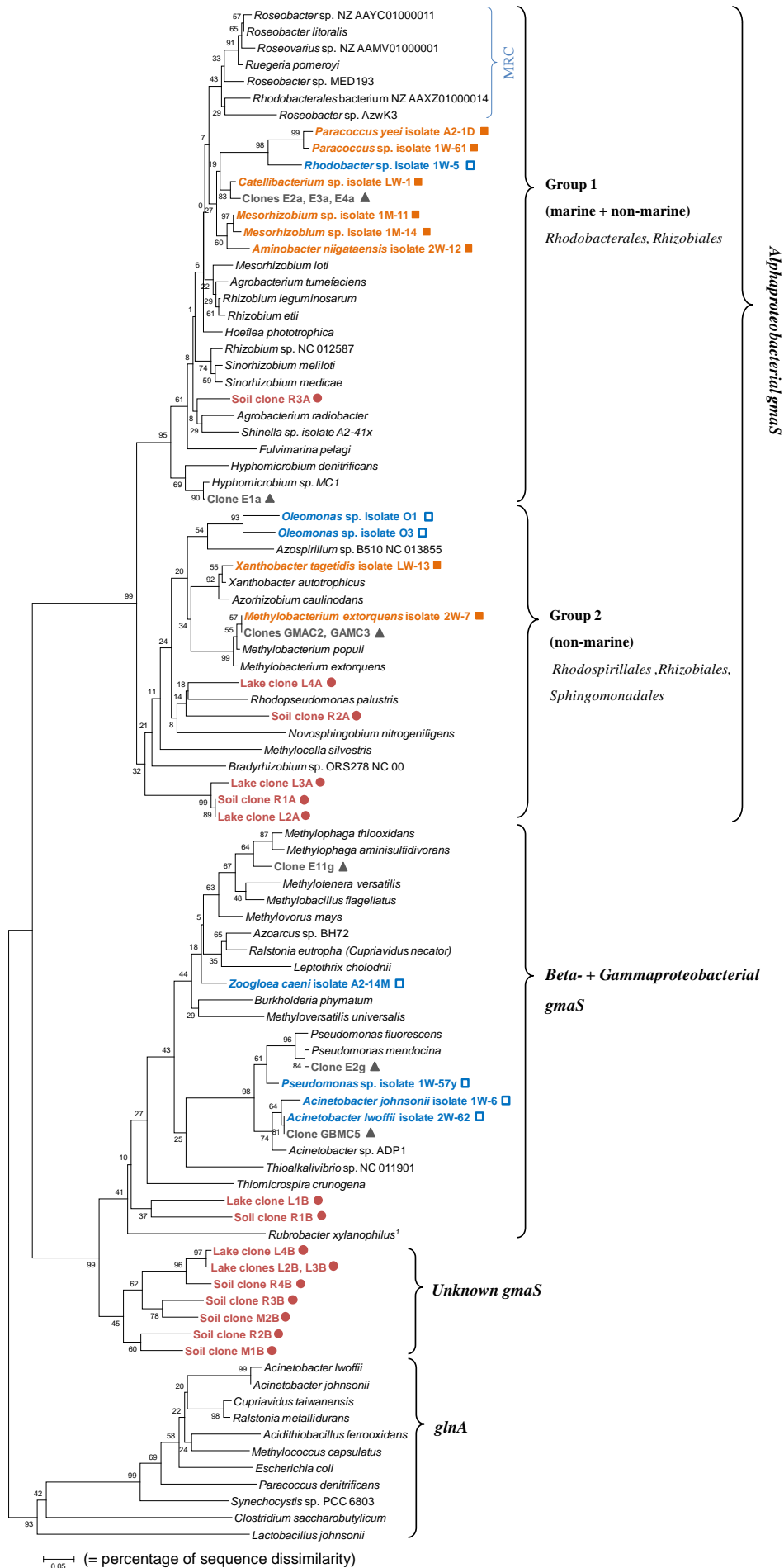


Figure 5.14

## 5.8 Distribution of *mauA* in Movile Cave

The *mauA* gene encodes methylamine dehydrogenase, the key enzyme in the direct MMA oxidation pathway found in some gram-negative methylotrophic bacteria (see section 5.1; Figure 5.1a). In addition to screening for *gmaS* genes, DNA extracted from water and floating mat samples from Movile Cave was also amplified with PCR primer sets targeting *mauA*. No amplicons were obtained for any of the samples using PCR primer set *mauAF1* / *mauAR1* (Neufeld *et al.*, 2007), even though the primers successfully amplified *mauA* from control DNA of the positive control *Paracoccus versutus*, as well as from DNA of some of the methylotrophic isolates obtained from Movile Cave in this study (see section 5.5.2). The negative results may be due to the PCR primers being too specific to detect *mauA* from a wide range of microorganisms that carry the gene. The results might however also suggest that the *mauA*-dependent MMA oxidation pathway is not as widespread amongst Movile Cave bacteria as the *gmaS*-mediated pathway. This hypothesis is supported by *gmaS* screening of MMA-utilising isolates from Movile Cave (Table 5.2.)

Alternative *mauA* primer sets by Hung *et al.*, 2012 did not give satisfactory results when tested on control organisms (*Paracoccus versutus*) and Movile Cave isolates (*M. extorquens* and *X. tagetidis*) and were not further used. The development of *mauA* primer sets targeting a wider range of organisms would be useful for future studies. In addition to looking at the presence and diversity of *mauA* and *gmaS* genes, it would also be useful to carry out expression-based studies of the two genes. This could give an indication on whether the indirect pathway is actually (i) more wide-spread and is also (ii) more widely used.

## 5.9 Putative *gmaS* in Cyanobacteria and Actinobacteria

### 5.9.1 Putative *gmaS* genes from soil and freshwater may be cyanobacterial

The “unknown *gmaS*” sequences obtained from soil and freshwater samples were analysed by doing a BLAST (blastx) search against sequences published on GenBank and IMG. The closest related *gmaS* sequences to soil and freshwater genes retrieved with primer set 557f / 1332r were from *betaproteobacterial* MMA utilisers *Methylophilus*, *Methylovorus*, *Methylophaga* and *Cupriavidus* at only ~80% similarity. Soil and freshwater genes obtained with primers 557f / 907r were ~88% similar to *alphaproteobacterial* *gmaS* sequences (*Rhizobiales* and *Rhodospirillales*). Interestingly, they shared the same level of similarity with

*glnA* sequences from various *Cyanobacteria* (orders *Oscillatoriales*, *Chroococcales*, *Stigonematales*). Alignment and phylogenetic analysis of the *cyanobacterial* sequences with known *gmaS* clearly placed them with *gmaS* rather than *glnA*. These *cyanobacterial* “*glnA*” sequences might therefore be mis-annotated *gmaS* sequences. For a higher resolution, additional *cyanobacterial* sequences affiliating with the soil and lake -derived *gmaS* sequences were retrieved from published genomes. In the resulting phylogenetic tree, *cyanobacterial* sequences formed several distinct subgroups within the *alphaproteobacterial gmaS* cluster (Supplementary Figures S2a-c). It thus seems logical that all soil and lake sequences affiliating with *cyanobacterial* genes were retrieved with the *alphaproteobacterial*-specific *gmaS* primers. It would also explain why the sequences from soil and freshwater were unrelated to *gmaS* from Movile Cave, as *Cyanobacteria* are not expected to be present in an ecosystem devoid of light. However, when analysing the immediate gene neighbourhoods of the *cyanobacterial* genes, none of the genes expected adjacent to *gmaS* (*mgs* and *mgd*) could be identified. Growth tests of the relevant organisms with MMA are therefore needed to assess whether or not the identified *cyanobacterial* genes may be genuine *gmaS*.

### 5.9.2 *gmaS* surveys uncover putative actinobacterial *gmaS* sequences

Intriguingly, BLAST (blastx) searches of published bacterial genomes on IMG also revealed a large number of potential *gmaS* genes from gram-positive *Actinobacteria* bacteria annotated as *glnA*. Unlike the *cyanobacterial* sequences, all *actinobacterial* sequences appeared to contain the complete genes for NMG synthase (*mgs*) immediately adjacent to the *gmaS* homologue. While the gene for NMG dehydrogenase (*mgd*) was not detected in any of the gene neighbourhoods analysed, alignment and phylogenetic analysis clearly placed the sequences (all of which belonged to the *Actinomycetales*) with *gmaS* rather than *glnA* (Supplementary Figures S2a-c). The *actinobacterial* sequences formed a distinct cluster outside of the *alphaproteobacterial* and *beta- gammaproteobacterial gmaS* clusters (Supplementary Figure S2a-c). The high level of divergence of the *actinobacterial* sequences could explain why the *gmaS* primers did not detect any sequences from this group during this study.

So far, the genes for the GMA / NMG mediated pathway have been identified only in gram-negative MMA-utilising bacteria. Whether the *actinobacterial* genes are genuine *gmaS* remains to be seen, but the absence of the complete *mgd* gene does not necessarily rule this out, as some proteobacterial *gmaS* sequences (e.g. that of *Cupriavidus*) also do not appear to

have *mgs* genes in the immediate gene neighbourhood of *gmaS*. Several members of the *Actinobacteria* are known MMA utilisers (e.g. Levering *et al.*, 1981; Nešvera *et al.*, 1991; Boden *et al.*, 2008; Hung *et al.*, 2011), so the presence of *gmaS* genes in this phylum would not be all too surprising. Several of the putative *gmaS* sequences from gram-positive bacteria (as well as *Cyanobacteria*) were in fact observed at the time of *gmaS* primer design; however, they were not further investigated because of their divergence from the proteobacterial *gmaS* sequences. Only one *gmaS* sequence of a gram-positive bacterium was used for *gmaS* primer design in this PhD project: *Rubrobacter xylanophilus*, which clusters with *beta*- and *gammaproteobacterial gmaS* (see Figures 5.12 and 5.14).

The identification of putative new *gmaS* genes is supported by data from a recent study by Gruffaz *et al.* (2014). When studying gene transcription of the GMA / NMG mediated MMA oxidation pathway in *Methylobacterium extorquens* strain DM4, they found a second *gmaS* homologue in addition to the canonical *gmaS* gene (which was functional for utilisation of MMA as a nitrogen but not carbon source). Interestingly, the authors also detected the same *gmaS* homologue in members of the *Cyanobacteria*, *Verrucomicrobia* and *Actinobacteria* (even though these results were not further discussed). An obvious way to determine whether the presence of *gmaS* homologues in *Actinobacteria*, *Verrucomicrobia* and *Cyanobacteria* signifies MMA utilising metabolism in these phyla would be to test representative organisms for growth with MMA as a nitrogen (perhaps even carbon source).

**Chapter 6. The microbial nitrogen cycle in Movile Cave, a first overview**

As part of a larger study of the microbial food web in Movile Cave, the overall objective of this PhD thesis was to gain insight into processes of the nitrogen cycle in this unusual ecosystem. Previous studies on the microbiology of Movile Cave have focused mostly on sulfur and carbon cycling, leaving the nitrogen cycle largely unexplored. (An overview of the overall microbial foodweb in Movile Cave is given in the Introduction to this thesis (Chapter 1.2; Figure 1.6). Due to the broad nature of the topic, not all aspects of the nitrogen cycle could be covered in equal measure in the course of this PhD project. In the end, the work predominantly focussed on the utilisation of methylated amines by Movile Cave bacteria, as this topic produced the most conclusive results. Other aspects of the nitrogen cycle were touched upon; PCR-based screening indicated the presence of marker genes for nitrification,  $N_2$ -fixation and denitrification, and process-based analyses suggested activity of nitrifiers, denitrifiers and anammox bacteria. These processes do however require further studies.  $N_2$ -fixation was not investigated further since no nitrogenase activity could be detected in cave samples throughout this project.

## 6.1 Proposed nitrogen cycle in Movile Cave

Figure 6.1 gives a schematic overview of the proposed nitrogen cycle in Movile Cave: Ammonia ( $NH_3 / NH_4^+$ ) enters the cave in hydrothermal waters from below.  $NH_4^+$  is the major nitrogen source for microorganisms in the cave and is assimilated into organic nitrogen by bacteria and fungi that form extensive mats on the water surface. When the microbial mats sink to the bottom of the water and die, methylated amines are released as a result of putrefaction, serving as a carbon, energy and / or nitrogen source for methylated amine-utilising bacteria, which in turn release  $NH_4^+$ . In addition to being a nitrogen source,  $NH_4^+$  also serves as an energy source for aerobic ammonia-oxidising bacteria and archaea, which grow autotrophically and release nitrite ( $NO_2^-$ ) which, in the second step of nitrification, gets converted to nitrate ( $NO_3^-$ ) by nitrite-oxidising bacteria. Both  $NO_3^-$  and  $NO_2^-$  serve as terminal electron acceptors for denitrifying bacteria, growing anaerobically in the anoxic regions of the water and sediment.  $NO_2^-$  is also the terminal electron acceptor for a second group of anaerobes, the “anammox” bacteria which gain energy from the anaerobic oxidation of  $NH_4^+$  to  $N_2$  (e.g. Kartal *et al.*, 2013).  $N_2$  from the cave atmosphere, along with  $N_2$  released by thermal emissions (Şerban Sârbu, personal communication) denitrifiers and anammox bacteria gets converted back to  $NH_4^+$  by  $N_2$ -fixing microorganisms, which may thrive in  $NH_4^+$ -starved regions of the thick floating mats.

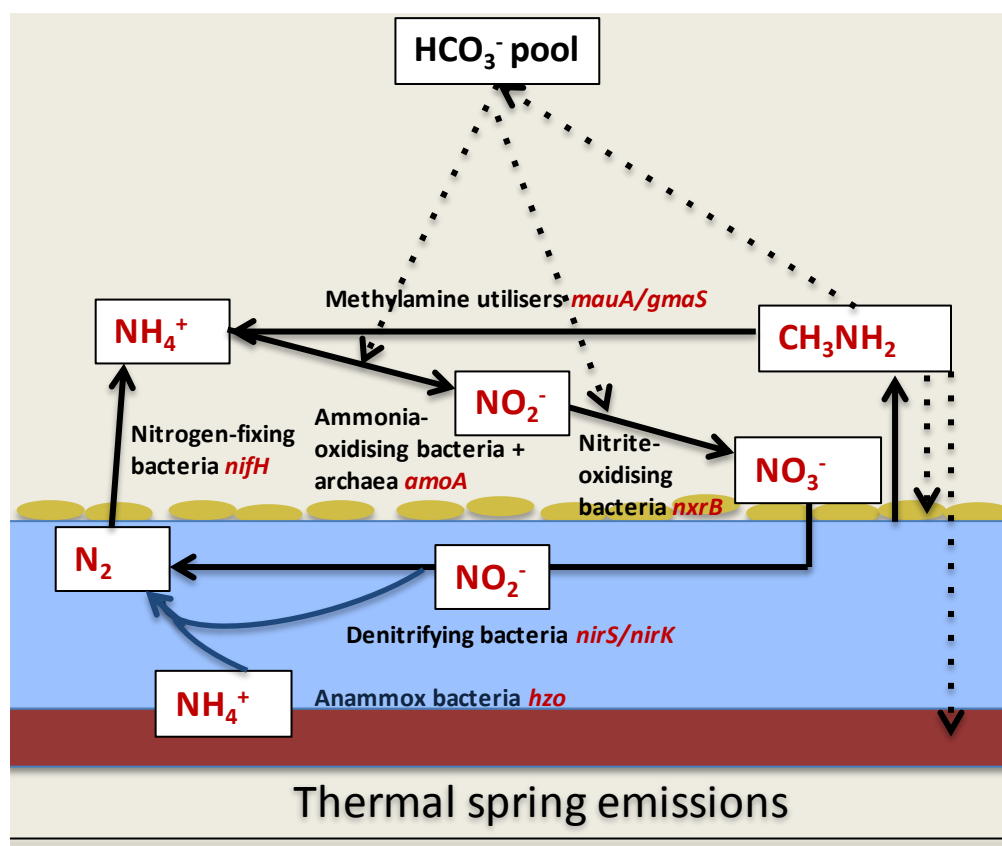


**Figure 6.1** Schematic overview of the proposed nitrogen cycle in Movile Cave (Image modified from Kumaresan *et al.*, 2014).

## 6.2 Aims and approach

The main focus of this PhD was to assess the role of methylated amines as carbon and nitrogen sources for Movile Cave bacteria (which was done using a combination of SIP experiments and cultivation, see Chapters 3 and 4). A further objective of this PhD was to gain insight into the contribution of nitrifying bacteria and archaea to primary production in this chemoautotrophy-sustained ecosystem. While previous studies have highlighted the roles of sulfur and methane oxidisers in carbon fixation in the cave, the involvement of ammonium and nitrite oxidisers remained uncertain. Furthermore, the potential role of microbial  $N_2$ -fixation was investigated.

To determine the possible contribution of the above processes to nitrogen cycling in the cave, process-based studies were carried out alongside PCR-based surveys of DNA extracts from cave water, floating mat material, wall biofilm and sediment samples (anammox only). PCR primers targeting key genes for nitrification, nitrogen fixation, denitrification, anammox and MMA oxidation, as well as  $CO_2$  fixation were used as biomarkers. The obtained sequences were analysed using BLAST (blastx). Table 6.1 lists all the genes and

group-specific PCR-primers used for the detection of the different functional groups involved in nitrogen cycling and carbon fixation (for details on primers, PCR conditions and references refer to Table 2.2 in Chapter 2). Amplification products of the expected lengths were obtained for nine of the thirteen genes screened for. With the exception of *hzo* (for which the DNA concentration of the amplicons was very low), all PCR products were confirmed as the correct genes by cloning and sequencing (for details refer to individual sections below). No amplification products were obtained for *cbbM*, *mauA*, *nrxB* and  $\gamma$ -proteobacterial *amoA* in this study. This might suggest that those genes are not very abundant in Movile Cave, or simply that the PCR primers failed to detect them.

### 6.3 Nitrification in Movile Cave

Past studies of primary producers in Movile Cave have focused mainly on bacteria that oxidise reduced sulfur compounds (e.g. Sârbu *et al.*, 1994; Vlăsceanu *et al.*, 1997; Rohwerder *et al.*, 2003) or more recently methane (Hutchens *et al.*, 2004). The contribution of ammonia- and nitrite-oxidising microorganisms to carbon fixation has not been investigated. The relatively high standing concentrations of  $\text{NH}_4^+$  in the cave water (0.2 - 0.3 mM, Sârbu 2000) and floating mats (0.5 - 0.8 mM, as measured in uptake enrichments in this PhD, see below) make it a likely energy source for chemolithoautotrophic microorganisms. Furthermore, active nitrifiers were detected in first SIP experiments with  $^{13}\text{C}$ -labelled bicarbonate (Chen *et al.*, 2009). Chen *et al.* detected 16S rRNA sequences belonging to both ammonia-oxidising bacteria (*Nitrosomonas*) and nitrite-oxidising bacteria (*Nitrospira* and *Candidatus* 'Nitrotoga') in  $^{13}\text{C}$ -labelled DNA fractions from incubations with  $\text{H}^{13}\text{CO}_3^-$ . In addition, the authors found bacterial *amoA* gene sequences (coding for ammonia monooxygenase, a key enzyme in ammonium oxidation) related to *Nitrosomonas* in the  $^{13}\text{C}$ -DNA fractions. Finally, recent metagenome data have suggested that *Nitrospira* make up a significant proportion of the overall microbial community (Kumaresan *et al.*, 2014).

For a more in-depth analysis of the contribution of nitrifying bacteria and archaea to primary production in Movile Cave, time-course SIP experiments were set up with  $^{13}\text{C}$ -labelled bicarbonate ( $\text{H}^{13}\text{CO}_3^-$ , for simplicity from here on referred to as  $^{13}\text{CO}_2$ ) with and without added energy sources in the form of  $\text{NH}_4^+$  or reduced sulfur compounds. In addition, enrichment cultures with  $\text{NH}_4^+$  were set up for the determination of potential nitrification rates, and PCR-based studies targeting bacterial and archaeal *amoA* were carried out.

**Table 6.1** Group-specific PCR primers used in this study for the detection of functional groups present in Mobile Cave

Gene	Enzyme	Process (Group)	PCR Primer set <sup>(1)</sup>	Gene detected in Mobile Cave
<i>cbbLG</i>	Form I RuBisCO, green-like type	CO <sub>2</sub> fixation, Calvin-Benson-Cycle	cbbLG1f / cbbLG1r	YES
<i>cbbLR</i>	Form I RuBisCO, red-like type	CO <sub>2</sub> fixation, Calvin-Benson-Cycle	cbbLR1f / cbbLR1r	YES
<i>cbbM</i>	Form II RuBisCO	CO <sub>2</sub> fixation, Calvin-Benson-Cycle	cbbMf / cbbMr	NO
<i>mauA</i>	Methylamine dehydrogenase	MMA oxidation, direct pathway (methylotrophs only)	mauAf1 / mauAf2	NO
<i>gmaS</i>	Gamma-glutamylmethylamide synthetase	MMA oxidation, indirect pathway (methylotrophs + non-methylotrophs)	gmaS_557f / $\alpha$ _gmaS_970r ( <i><math>\alpha</math>-proteobacterial gmaS</i> ) gmaS_557f / $\beta$ _gmaS_1332r ( <i><math>\beta</math>- / <math>\gamma</math>-proteobacterial gmaS</i> )	YES YES
<i>Bacterial amoA</i>	Ammonia monooxygenase	Nitrification, Step 1 (AOB)	amoA-1f / amoA-2r ( <i><math>\beta</math>-proteobacterial amoA</i> ) 189f / 682r ( <i><math>\gamma</math>-proteobacterial amoA + pmoA</i> )	YES NO
<i>Archaeal amoA</i>	Ammonia monooxygenase	Nitrification, Step 1 (AOA)	Arch-amoAf / Arch-amoAr	YES
<i>nxrB</i>	Nitrite oxidoreductase	Nitrification, Step 2 (NOB)	nxB169f / nxB638r ( <i>Nitrospira / Nitrospina</i> )	NO
<i>nifH</i>	Nitrogenase iron protein	N <sub>2</sub> -fixation	<i>nifHf / nifHr</i>	YES
<i>nirS</i>	Cu-containing dissimilatory nitrite reductase	Denitrification	nirS1f / nirS6r	YES
<i>nirK</i>	Heme-containing dissimilatory nitrite reductase	Denitrification	nirK1f / nirK5r	YES
<i>hzo</i>	Hydroxylamine / hydrazine oxidoreductase	Anaerobic ammonium oxidation (Anammox)	hzoC11f / hzoC11r2	YES <sup>(2)</sup>
16S rRNA gene		<i>Brocadia / Kuenenia</i>	Amx368f / Amx820r	YES

<sup>(1)</sup> For primer sequences and references please refer to Chapter 2. <sup>(2)</sup> Not verified by sequence analysis due to low product concentration.

Abbreviations: AOB = ammonia-oxidising bacteria; AOA = ammonia-oxidising archaea; NOB = nitrite-oxidising bacteria

### 6.3.1 Nitrification: a brief introduction

Nitrification is an essential part of the global nitrogen cycle and involves the microbial conversion of ammonia / ammonium ( $\text{NH}_3 / \text{NH}_4^+$ ) to nitrate ( $\text{NO}_3^-$ ) via nitrite ( $\text{NO}_2^-$ ). It is a major route for the production of  $\text{NO}_3^-$ , an important nutrient for many organisms (see Chapter 1, section 1.3 and Figures 1.6 and 6.1). Nitrification is a two-step process; each step is carried out by a separate group of aerobic, chemolithoautotrophic microorganisms that gain energy from these reactions (Fuchs & Schlegel, 2007):

**(1) Ammonia-oxidising bacteria (AOB) and ammonia-oxidising archaea (AOA)**



**(2) Nitrite-oxidising bacteria (NOB)**



(Note:  $\Delta G^{0'}$  calculated from  $\Delta G_f^{0'}$  of aqueous compounds as listed in Supplementary Table S1)

First discovered by Winogradsky in 1890, the two processes involved in nitrification were traditionally thought to be dominated by autotrophs belonging to a few specialist groups within the Proteobacteria, with small contributions in some soils from heterotrophic bacteria and fungi (De Boer *et al.*, 2001). Known nitrifying bacteria fall into two physiologically distinct groups; the ammonia-oxidising bacteria (AOB) and the nitrite-oxidising bacteria (NOB) (Kowalchuk & Stephen, 2001). To date, none have been shown to carry out the complete oxidation of  $\text{NH}_4^+$  to  $\text{NO}_3^-$ . In recent years, a novel phylum of *Archaea* has been revealed to contribute significantly to ammonium oxidation in addition to AOB (see below).

*(i) Ammonia-oxidising bacteria (AOB)*

Of the two groups of nitrifying bacteria, AOB are the most extensively studied, possibly owing to the difficulty in cultivating NOB and the phylogenetic divergence within this group. With the exception of the marine AOB *Nitrosococcus*, which belongs to the *Gammaproteobacteria*, all known genera of AOB belong to a single family (the *Nitrosomonadaceae*) within the *Betaproteobacteria* (Lücker, 2010). *Betaproteobacterial* AOB have been detected in many different environments, from aquatic habitats to soils and building stones (Coci *et al.*, 2008). The distribution patterns of individual species of AOB are determined by physiological differences between distinctive representatives and by environmental parameters such as substrate concentration, pH, temperature, oxygen

availability and salinity (Coci *et al.*, 2008). The close phylogenetic affiliation of the AOB has greatly facilitated the use of genetic markers for their detection: The gene for ammonia monooxygenase (*amoA*), the enzyme that catalyses the first step in nitrification (the oxidation of ammonium to hydroxylamine), is well preserved and present in all known AOB (Rotthau *et al.*, 1997; Purkhold *et al.*, 2000), providing a valuable functional biomarker for their identification. Archaeal ammonia oxidisers (AOA) also have a homologue of the *amoA* gene (reviewed by Pester *et al.*, 2012). Since their discovery, the *amoA* gene has been widely used to study the relative abundances of AOA and AOB in nitrifying communities.

(ii) *Ammonia-oxidising archaea (AOA)*

While AOB were discovered over 100 years ago (Winogradsky, 1890), ammonium oxidation within the domain *Archaea* was discovered less than 10 years ago using a combination of metagenomic data (Venter *et al.* 2004, Treusch *et al.*, 2005) and laboratory isolation (Könneke *et al.*, 2005). For many years, members of the domain *Archaea* were generally thought to occur only in extreme environments, usually under strict anaerobiosis, with metabolic pathways adapted to life under conditions too harsh for *Bacteria* and *Eukarya*. However, *in situ* measurements of nitrification in marine and terrestrial environments showed that ammonium oxidation often proceeds at substrate concentrations significantly below the growth threshold of cultivated AOB (Prosser, 1989, cited after Pester *et al.*, 2011) thus indicating the presence of unknown nitrifiers.

The presence of huge numbers of mesophilic “*Crenarchaeota*” in marine, terrestrial and freshwater habitats of moderate pH and temperature was first detected by cultivation-independent studies in the 1990s (e.g. Fuhrman *et al.*, 1992; DeLong *et al.*, 1992; Buckley *et al.*, 1998; Jürgens *et al.*, 1997; Schleper *et al.*, 1997; Karner *et al.*, 2001). These findings raised the question of what their physiological attributes and ecological roles might be. The uptake of inorganic carbon by mesophilic “*Crenarchaeota*” was demonstrated in a number of studies (e.g. Herndl *et al.*, 2005). However, these findings did not indicate a specific energy source. The discovery of autotrophic ammonia-oxidising *Archaea* confirmed that many mesophilic “*Crenarchaeota*” are chemolithoautotrophs. The mesophilic “*Crenarchaeota*” have since been re-assigned to a new phylum within the *Archaea*, the *Thaumarchaeota* (Brochier-Armanet *et al.*, 2008; Spang *et al.*, 2010). To date, only a few cultivated representatives exist, all of which are chemolithotrophic ammonia oxidisers (Könneke *et al.*, 2005; Lehtovirta-Morley *et al.*, 2011; Tourna *et al.*, 2011; Jung *et al.*, 2014). Despite the lack of cultivated species, ammonia-oxidising archaea (AOA) have been shown to be both highly

abundant and active in many marine, terrestrial and freshwater environments (e.g. Treusch *et al.*, 2005; Leininger *et al.*, 2006; Chen *et al.*, 2008; Di *et al.*, 2010; Verhamme *et al.*, 2011).

The relative contributions of bacterial and archaeal ammonia oxidisers to overall nitrification seems to be largely dependent on growth conditions such as substrate concentration, temperature and pH (e.g. review by Prosser & Nicol, 2012; Daebeler *et al.*, 2012; French *et al.*, 2012). Some AOA are adapted to extremely low pH and, in recent studies have been shown to be responsible for the majority of nitrification in acidic soils, solving a long-standing paradox (e.g. Gubry-Rangin *et al.*, 2010; Lehtovirta-Morley *et al.*, 2011). Several comprehensive reviews on archaeal ammonium-oxidisers have been published in recent years (e.g. Schleper & Nicol, 2010; Martens-Habbena & Stahl, 2011; Pester *et al.*, 2011; Hatzenpichler, 2012).

(iii) *Nitrite-oxidising bacteria (NOB)*

All known nitrite-oxidising bacteria (NOB) fall into a few specialised bacterial genera that are phylogenetically unrelated to each other: The genera *Nitrococcus* and *Candidatus Nitrotoga*, belonging to the *Gamma*- and *Betaproteobacteria*, respectively, each harbour only one species, isolated from marine samples (Watson and Waterbury, 1971) and arctic permafrost soil (Alawi *et al.*, 2007), respectively. NOB of the genus *Nitrospira* form a distinct phylum, the *Nitrospirae*, and occupy a great variety of habitats (Maixner 2010; Lucker, 2010). Similarly, the marine genus *Nitrospina*, originally classified within the *Deltaproteobacteria* (Teske *et al.*, 2004) appears to form an independent line of descent within the domain *Bacteria* (e.g. Maixner, 2010). Communities consisting of *Nitrospina* and AOA have been suggested to be key organisms performing nitrification in the ocean (Santoro *et al.*, 2010). Members of the genus *Nitrobacter*, belonging to the *Alphaproteobacteria*, are found in a wide variety of habitats, such as marine and freshwater, neutral and acidic soils, soda lakes and rock (reviewed by Lucker, 2010). They appear to be the least resistant to cultivation among the fastidious and slow-growing NOB and therefore present the best studied group (Lucker, 2010). Recently, a novel, thermophilic, NOB from the phylum *Chloroflexi* was isolated from a nitrifying bioreactor (Sorokin *et al.*, 2012). In contrast to AOB, knowledge of NOB ecology is very limited, partly because of lack of specific molecular tools (Pester *et al.*, 2014). Even though all known NOB oxidise nitrite using the enzyme nitrite oxidoreductase (Nxr), the phylogenetic divergence within this functional group of bacteria has made the design of functional PCR primers targeting all NOB problematic. PCR primer sets individually

targeting *nxr* genes from *Nitrobacter* (Vanparys *et al.*, 2007) or *Nitrospira* (Maixner, 2010; Pester *et al.*, 2014) are however available. *Nitrospira*-specific *nxB* primers were used in this PhD project, since 16S rRNA gene sequences associated with this organism were detected both in this study and in previous studies by Chen *et al.* (2009).

### 6.3.2 Potential nitrification rates in Movile Cave

Potential nitrification rates were examined by measuring depletion of  $\text{NH}_4^+$  coupled to production of  $\text{NO}_2^-$  in enrichments set up with cave water and floating mat samples following the addition of 1mM  $\text{NH}_4^+$ . Native  $\text{NH}_4^+$  concentrations prior to addition of substrate ranged between and 0.1–0.5 mM for water samples and 0.5–0.8 mM for mat samples. To determine whether *Archaea* play a role in nitrification, enrichments were also set up with 100  $\mu\text{M}$  added allylthiourea (ATU), a metal-chelating agent commonly used to inhibit bacterial ammonium oxidation, while having only minor effects on AOA (e.g. Santoro *et al.*, 2011). All cultures showed depletion of  $\text{NH}_4^+$  (Figures 6.2a and b), along with production of  $\text{NO}_2^-$  (Figures 6.2c and d; see also Figure 6.3). However, towards the beginning of incubation,  $\text{NH}_4^+$  concentrations temporarily increased (Figures 6.2a and b), and  $\text{NO}_2^-$  production did not match  $\text{NH}_4^+$  depletion in terms of measured concentrations (see below). No nitrification rates could therefore be calculated from the data.

The most notable differences between the different incubations were in the level and rate of  $\text{NO}_2^-$  production: In incubations from floating mat samples without added inhibitor, a significant increase in  $\text{NO}_2^-$  was observed after 3 days of incubation (Figures 6.2c and 6.3a), while with added inhibitor,  $\text{NO}_2^-$  concentrations started to rise only after 7 days (Figure 6.3b). This would suggest that oxidation of  $\text{NH}_4^+$  to  $\text{NO}_2^-$  in incubations with added ATU was carried out by slower-growing archaea (AOA). In water enrichments (with and without added ATU), an increase in  $\text{NO}_2^-$  was not observed until 10 days of incubation (Figures 6.3a and b). In all cases, the  $\text{NO}_2^-$  concentrations reached significantly higher concentrations in enrichments without added ATU. In both enrichments with added ATU, the steep increase in  $\text{NO}_2^-$  concentrations was followed by a drop in concentrations (Figure 6.3b). These results suggest that NOB may have become active following the release of  $\text{NO}_2^-$  by AOA, converting  $\text{NO}_2^-$  further to  $\text{NO}_3^-$  and thereby completing nitrification. Oddly, no decrease in  $\text{NO}_2^-$  concentrations was observed in incubations without inhibitor during the time of incubation (Figure 6.3a). A possible explanation for  $\text{NO}_2^-$  accumulation in these enrichments could be oxygen depletion.

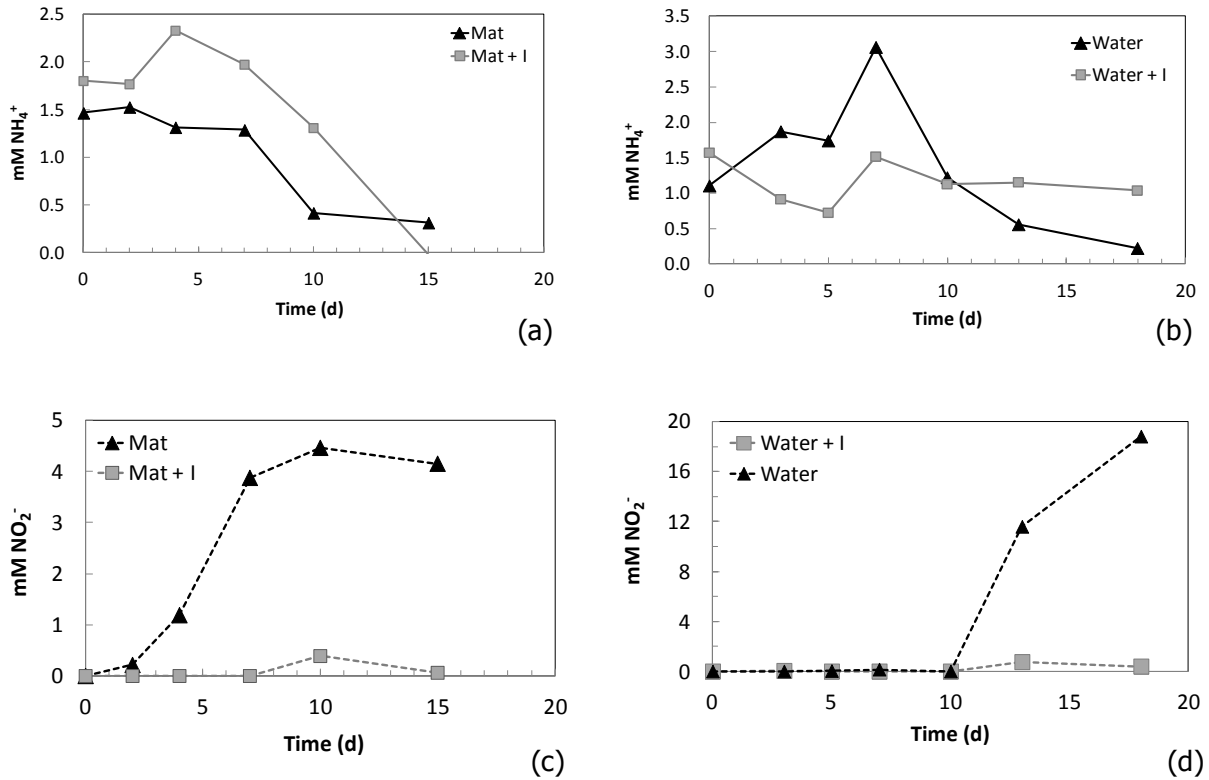


**Figure 6.2** Ammonium depletion (a and b) and nitrite production (c and d) in microcosms set up from water and floating mat samples from Movile Cave, respectively, for the selective enrichment of nitrifiers. 1 mM of  $\text{NH}_4^+$  was added at  $t=0$ . Enrichments were set up with and without added allylthiourea, an inhibitor of bacterial, but not archaeal ammonium-oxidation. Abbreviations: I = added inhibitor (allylthiourea).

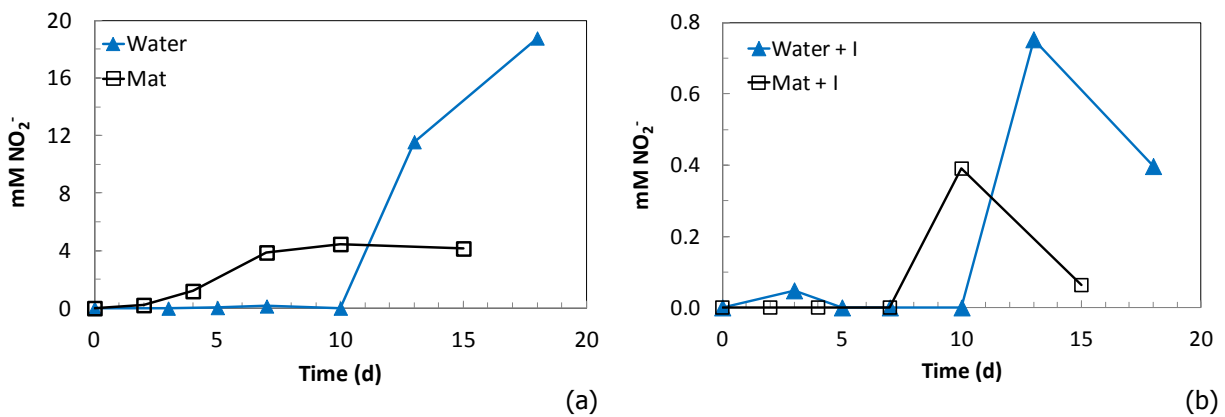


**Figure 6.3** Nitrite production (and depletion) in ammonium enrichment cultures from Movile Cave (1 mM  $\text{NH}_4^+$  was added at  $t=0$ ) with and without added allylthiourea. Abbreviations: I = added inhibitor (allylthiourea).

While  $\text{NO}_2^-$  concentrations in enrichments with added ATU stayed well below the highest measured  $\text{NH}_4^+$  concentrations (1.5 mM  $\text{NH}_4^+$  in water and 3 mM  $\text{NH}_4^+$  in mat, see Figures 6.4a and 6.4b),  $\text{NO}_2^-$  concentrations in enrichments without inhibitor rose to much higher concentrations than were measured for  $\text{NH}_4^+$  (Figures 6.4c and 6.4d): In water enrichments,  $\text{NO}_2^-$  concentrations reached 4.5 mM, while in mat enrichments,  $\text{NO}_2^-$  concentrations as high as 18 mM were measured.

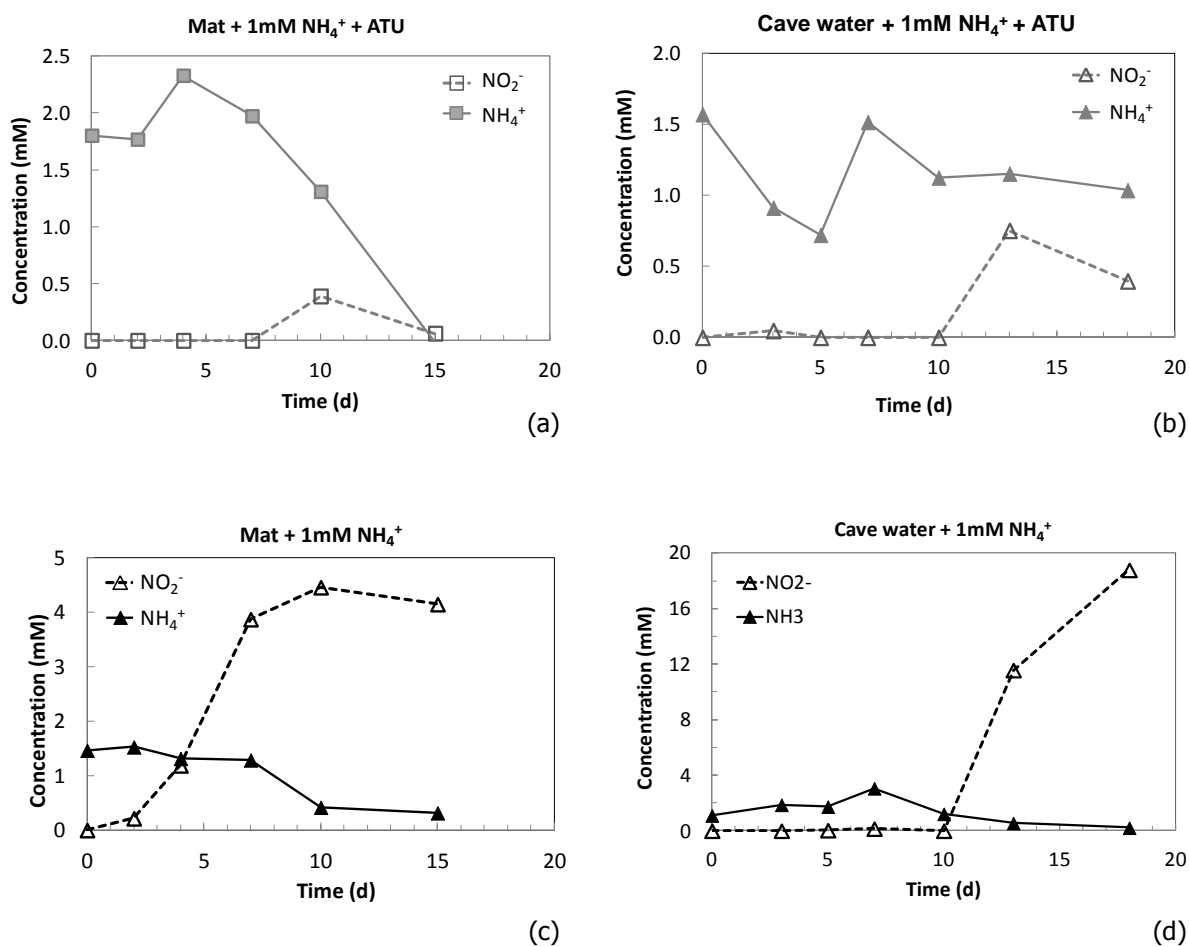


**Figure 6.4** Nitrite production, plotted alongside ammonium depletion in Movile Cave enrichment cultures with added  $\text{NH}_4^+$  (1 mM  $\text{NH}_4^+$  was added at  $t = 0$ ). While nitrite concentrations in microcosms with added allylthiourea (c and d) stayed well below measured  $\text{NH}_4^+$  concentrations, in cultures without inhibitor (c and d), measured nitrite concentrations far exceeded those of  $\text{NH}_4^+$ , suggesting a different source for nitrite, possibly the anaerobic reduction of  $\text{NO}_3^-$ . Additionally, nitrite concentrations dropped following the initial increase in enrichment cultures with ATU, possibly due to activity of nitrite-oxidising bacteria. Abbreviations: ATU = allylthiourea

One possible explanation for these observations could be that enrichments became anoxic and denitrification of  $\text{NO}_3^-$  to  $\text{NO}_2^-$  occurred.  $\text{NO}_3^-$  concentrations would have given important clues about the origin of the high  $\text{NO}_2^-$  concentrations, as well as confirm that the decrease in  $\text{NO}_2^-$  was due to nitrification. Unfortunately however, concentrations of  $\text{NO}_3^-$  could not be measured, as the  $\text{NO}_3^-$  assay (using zinc dust for reduction of  $\text{NO}_3^-$  to  $\text{NO}_2^-$ , followed by analysis with Griess' reagent) failed even for standard solutions. An alternative assay could not be during this PhD due to time limitations and lack of further fresh Movile Cave samples.

### 6.3.3 *amoA* surveys confirm the presence of AOB and AOA in Movile Cave

In addition to culture-based experiments, PCR-based studies with primer sets targeting archaeal and bacterial *amoA* were performed to screen Movile Cave samples for ammonia-oxidising bacteria (AOB) and archaea (AOA). The obtained PCR products were then cloned and sequenced to confirm they were indeed *amoA*. The *amoA* gene encodes the alpha subunit of ammonia monooxygenase, the enzyme that catalyses the first step in nitrification: the conversion of  $\text{NH}_4^+$  to hydroxylamine. This gene is present in all AOB and AOA, providing a valuable biomarker for their detection.

*amoA* surveys were carried out on crude DNA extracted from Movile Cave samples (water, floating mat and wall biofilm) for a first indication of key nitrifying organisms. Bacterial as well as archaeal *amoA* genes were amplified (Table 6.2): Water samples from all three locations (lake room, Airbells 1 and 2) tested positive for both betaproteobacterial and archaeal *amoA*. Floating mat samples from Airbells 1 and 2 did not generate any *amoA* amplification products, while only archaeal *amoA* genes were amplified from floating mat samples from the lake room (Table 6.2). PCR products of the right length were also obtained with primers targeting gammaproteobacterial *amoA*; however, sequence analysis identified all amplified genes as *pmoA* (particulate methane monooxygenase).

It should be noted that *amoA* PCR surveys were of a preliminary nature. Even though different annealing temperatures were tested to improve the level of amplification, the lack of PCR products in some samples does not offer a conclusive result for the absence of *amoA* in these parts of Movile Cave. Interestingly, *amoA* screening results from SIP enrichments later suggested that AOA, rather than AOB are the dominant ammonia oxidisers in Movile Cave water, while AOB appeared to dominate at higher ammonium concentrations, i.e. in floating

mats (see later, 6.3.4.(vi)). This pattern was not apparent from results obtained from PCR surveys of crude DNA (see above and Table 6.2).

**Table 6.2** Group-specific genes detected in different parts of Movile Cave by PCR amplification

		<i>nirS</i>	<i>nirK</i>	<i>cbbLR</i>	<i>cbbLG</i>	<i>nifH</i>	Arch. <i>amoA</i>	Bact. <i>amoA</i>	Amx <sup>(1)</sup>
Lake room	Water	-	-	+	+	+	+	+	
	Floating mat	+	+	+	+	+	+	-	
	Sediment								+
Airbell 1	Water	-	-	+	+	+	+	+	
	Floating mat	+	+	+	+	+	-	-	
Airbell 2	Water	-	-	+	+	+	+	+	
	Floating mat	+	-	+	+	+	-	-	
	Wall biofilm	+	-	+	+	+	+	+	
	Sediment								+

Pluses indicate sequences detected by PCR; minus signs indicate sequences were not detected. Empty fields: not analysed. Red pluses indicate PCR products used for cloning and sequence analysis. No *cbbM*, *mauA* or *nxB* sequences were detected in this study. *Hzo* amplicons were obtained from sediment but could not be verified by sequence analysis due to the low amount of PCR product.

<sup>(1)</sup> Amx = anammox-related 16S rRNA genes. For details on PCR primers please refer to Table 6.1 and Table 2.2.

(i) Sequence analysis identifies *amoA* genes related to *Nitrosomonas* and *Nitrosopumilus*

The main purpose of sequencing *amoA* clones derived from Movile Cave water and biofilm samples (Table 6.2) was to confirm that the correct gene had been amplified, so only two clones of each, bacterial and archaeal *amoA*, were sequenced. The two bacterial *amoA* sequences were 97% identical (98% similar) to each other. In both cases, the closest related sequence from a cultivated organism was *amoA* from *Nitrosomonas nitrosa* (Table 6.3). The two archaeal *amoA* sequences were 96% identical to each other (96% similar). The closest cultivated relative was *Nitrosopumilus maritimus* (Table 6.4). Extensive surveys of the *amoA* diversity in Movile Cave, which would involve sequencing a larger number of clones or using high-throughput amplicon sequencing, were not carried out due to time limitations.

**Table 6.3** Phylogenetic affiliations of translated bacterial *amoA* sequences from Movile Cave

(Airbell 2, water)

Clones	Closest GenBank relatives (accession code)	<sup>(1)</sup> Identity (%) / <sup>(1)</sup> Similarity (%)	Phylogenetic affiliations of GenBank relatives
MB_1	AMO [uncultured bacterium]; pond sediment (ACU27507.1)	99 / 99	
	AMO [ <i>Nitrosomonas nitrosa</i> ] (CAC82258.1)	96 / 97	<i>Betaproteobacteria</i> ; <i>Nitrosomonadales</i> ; <i>Nitrosomonadaceae</i> ; <i>Nitrosomonas</i>
	AMO [ <i>Nitrosomonas europaea</i> ] (CAC82254.1)	93 / 95	
	AMO [ <i>Nitrosomonas eutropha</i> ] (AAO60371.1)	92 / 95	
MB_2	AMO [uncultured bacterium]; wetland sediment (AGW02566.1)	100 / 100	
	AMO [ <i>Nitrosomonas nitrosa</i> ] (CAC82258.1)	94 / 97	<i>Betaproteobacteria</i> ; <i>Nitrosomonadales</i> ; <i>Nitrosomonadaceae</i> ; <i>Nitrosomonas</i>
	AMO [ <i>Nitrosomonas halophila</i> ] (CAC82248.1)	92 / 95	
	AMO [ <i>Nitrosomonas europaea</i> ] (CAC82254.1)	91 / 95	

Abbreviations: AMO = ammonia monooxygenase, alpha subunit.

<sup>(1)</sup> Sequence analysis was carried out using the blastx algorithm (alignment of translated nucleotide sequences against protein database), hence, identity and similarity values refer to amino acid sequences.

(ii) No detection of NOB in Movile Cave with *nrxB* PCR

PCR primers targeting nitrite oxidoreductase (*nrxB*) from *Nitrospira* (Maixner, 2009) were used in an attempt to detect nitrite-oxidising bacteria (NOB) in Movile Cave. However, no amplification products were obtained from water or floating mat samples, even under conditions of low stringency. This may suggest that NOB are not abundant enough to be detected by PCR. Since the *nrxB* gene is not as well conserved as *amoA*, it is also possible that a different set of *nrxB* primers is needed. At the time this PhD study was conducted, *nrxB* primer sets were only available for *Nitrospira* or *Nitrobacter*. *Nitrospira*-specific *nrxB* primers were chosen because this organism was detected by Chen *et al.* (2009), however, it may not be the most abundant NOB in Movile Cave.

**Table 6.4** Phylogenetic affiliations of translated archaeal *amoA* sequences from Movile Cave (Airbell 2, wall biofilm)

Clones	Closest GenBank relatives (accession code)	<sup>(1)</sup> Identity (%) / <sup>(1)</sup> Similarity (%)	Phylogenetic affiliations of GenBank relatives
MA8b-1 MA8b-3 MA8b-4	AMO [uncultured archaeon]; Icelandic grassland soil (AFA54037.1)	100 / 100	Not specified
	AMO [ <i>Nitrosopumilus maritimus</i> ] (ADJ95198.1)	94 / 97	<i>Thaumarchaeota</i> ; <i>Nitrosopumilales</i> ; <i>Nitrosopumilaceae</i> ; <i>Nitrosopumilus</i>
	AMO [ <i>Nitrosotalea devanaterrea</i> ] (AEN04471.1)	82 / 92	<i>Thaumarchaeota</i> ; unclassified <i>Thaumarchaeota</i> ; <i>Cand. Nitrosotalea</i>
	AMO [ <i>Nitrosphaera viennensis</i> ] (CBY93673.1)	78 / 87	<i>Thaumarchaeota</i> ; <i>Nitrososphaerales</i> ; <i>Nitrososphaeraceae</i> ; <i>Nitrososphaera</i>
MA8b-2	AMO [uncultured archaeon]; Dongjiang River sediment (AER50807.1)	98 / 98	Not specified
	AMO [ <i>Nitrosopumilus maritimus</i> ] (ADJ95198.1)	95 / 97	<i>Thaumarchaeota</i> ; <i>Nitrosopumilales</i> ; <i>Nitrosopumilaceae</i> ; <i>Nitrosopumilus</i>
	AMO [ <i>Nitrosotalea devanaterrea</i> ] (AEN04471.1)	83 / 90	<i>Thaumarchaeota</i> ; unclassified <i>Thaumarchaeota</i> ; <i>Cand. Nitrosotalea</i>
	AMO [ <i>Nitrosphaera viennensis</i> ] (CBY93673.1)	80 / 88	<i>Thaumarchaeota</i> ; <i>Nitrososphaerales</i> ; <i>Nitrososphaeraceae</i> ; <i>Nitrososphaera</i>

Abbreviations: AMO = ammonia monooxygenase, alpha subunit; *Cand.* = *Candidatus*

<sup>(1)</sup> Sequence analysis was carried out using the blastx algorithm (alignment of translated nucleotide sequences against protein database); hence, identity and similarity values refer to amino acid sequences.

#### 6.3.4 SIP experiments suggest that sulfur oxidisers are the dominant primary producers in Movile Cave and indicate niche separation of AOA and AOB

##### (i) <sup>13</sup>CO<sub>2</sub>-SIP experiments 2010: low levels of biomass and lack of enrichment

To assess the relative contributions of nitrifiers and sulfur oxidisers to primary production in Movile Cave, DNA-SIP experiments were set up using <sup>13</sup>C-labelled bicarbonate (for simplicity referred to as <sup>13</sup>CO<sub>2</sub> from here on) with and without addition of ammonium or reduced sulfur compounds as an additional energy source (for details on SIP setup see Chapter 2, section 2.4). In 2010, SIP enrichments with <sup>13</sup>CO<sub>2</sub> and NH<sub>4</sub><sup>+</sup> were set up with Movile Cave water only (as no floating mat material was available at time of sampling) over a time course of 5 weeks. The incubations were set up by adding 2.5 mM <sup>13</sup>CO<sub>2</sub> and 1 mM NH<sub>4</sub><sup>+</sup> to 20 ml cave water in

120 ml serum vials and incubating at 21°C in the dark (native  $\text{NH}_4^+$  concentrations prior to addition of substrate ranged between and 0.1–0.5 mM for water samples). Control incubations with unlabelled substrate ( $^{12}\text{CO}_2$ ) were set up alongside.

Similar to MMA- and DMA-SIP experiments, the total amount of DNA extracted from the incubations was rather low (as little as 650 ng DNA per 20 ml sample). The low level of enrichment was attributed to the low amount of biomass present in the cave water samples. When analysed by DGGE, the bacterial community profiles based on 16S rRNA genes amplified from DNA extracted at 48 hours, 96 hours and 5 weeks (using PCR primers 341f-GC / 907r) showed little change over time. Only at t=3 (5 weeks incubation) some additional DGGE bands were visible, however, they were not conserved between  $^{12}\text{CO}_2$  and  $^{13}\text{CO}_2$  enrichments (Figure 6.5).

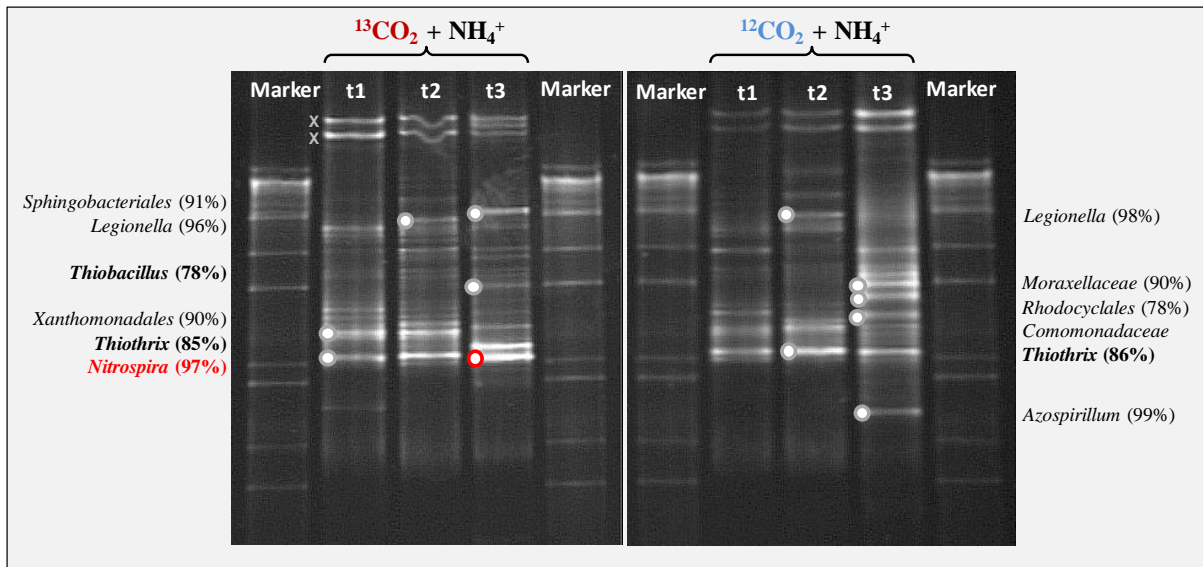


**Figure 6.5** DGGE profiles of the bacterial community in  $^{13}\text{CO}_2 / \text{NH}_4^+$  SIP enrichments set up with Movile Cave water (2010). DGGE analysis of bacterial 16S rRNA gene PCR products (341f GC / 907r) amplified from unfractionated DNA of different time points show little change in the microbial community over time with only a few additional bands appearing at t3 (t1 = 4 h; t2 = 96 h; t3 = 5 weeks). The variation between the two t<sub>3</sub> communities is most likely a result of the “bottle effect”, which is more pronounced at longer incubation times. 16S rRNA gene sequences obtained from dominant DGGE bands are indicated (numbers in brackets refer to nucleotide sequence identity with GenBank relatives). Apart from the nitrite-oxidising bacterium *Nitrospira*, no nitrifiers were identified.

Community variation between replicate enrichments at later time points was seen previously in MMA-SIP enrichments (refer to Figure 4.2) and is a commonly observed phenomenon in batchwise incubations, termed the “bottle effect”, whereby enrichment of microorganisms in a

confined environment unspecifically affects the community composition (Hammes *et al.*, 2010). A few dominant DGGE bands were nonetheless excised from the gel and sequenced (Figure 6.5); out of these, only one could be identified as a nitrifying bacterium, sharing 97% sequence identity to the 16S rRNA gene of the NOB *Nitrospira*. Sequencing did however reveal a number of sulfur-oxidising bacteria (*Thiobacillus* and *Thiotrix*). This may mean that nitrifiers are not the major primary producers in Movile Cave, or that they do not dominate under the growth conditions used in the laboratory. Archaeal 16S rRNA genes could not be amplified from DNA taken from any of the time points.

(ii) *<sup>13</sup>CO<sub>2</sub>-SIP experiments 2011: Change in the bacterial community over time*

Following a new sampling trip to Movile Cave in 2011, <sup>13</sup>CO<sub>2</sub> / NH<sub>4</sub><sup>+</sup> -SIP enrichments were repeated using both water and floating mat samples (separate experiments). For water samples, the volume was doubled to 40 ml compared to the previous time. Additionally, with more sample material available, enrichments were set up in duplicates. Between 900 - 1,800 ng DNA per sample was obtained from SIP enrichments with water, and as much as 6,000 - 30,000 ng DNA per sample from SIP enrichments with floating mat material. Bacterial 16S rRNA gene fragments were amplified using the same primer set as used previously (341-GCf / 907r PCR). DGGE analysis of the amplification products revealed a clear change in the bacterial community composition over time (in both water and mat SIP enrichments), which was similar between replicate bottles (Figures 6.6a and b). These results were promising, suggesting enrichment of autotrophic bacteria from water and mat samples. However, analysis of fractionated DNA (see section (iv) below) would reveal that the enriched organisms had not incorporated <sup>13</sup>CO<sub>2</sub>.

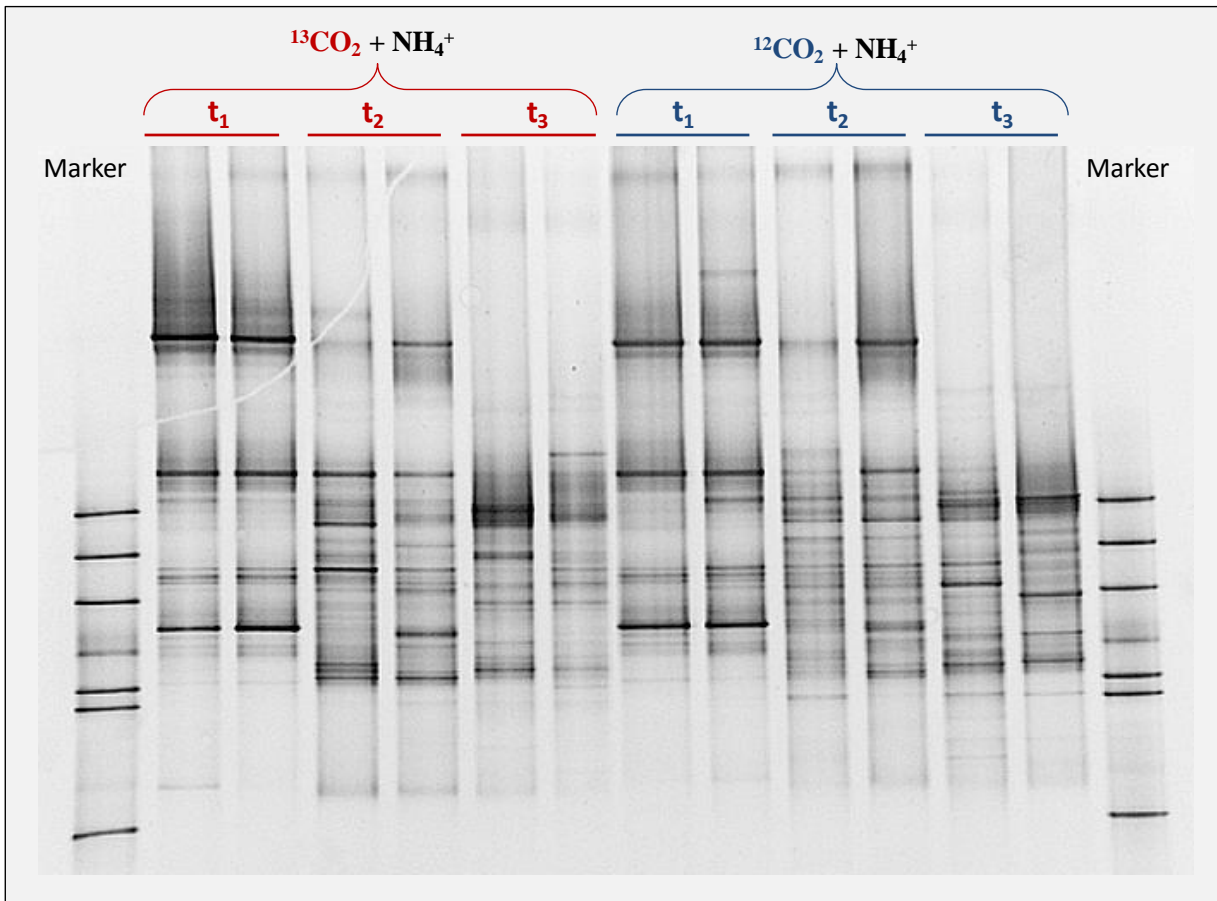


**Figure 6.6a** DGGE profiles of the bacterial community in  $^{13}\text{CO}_2 / \text{NH}_4^+$  SIP enrichments set up with Movile Cave water (2011). Each lane on the gel represents a separate enrichment, i.e. duplicates originate from separate serum vials. DGGE analysis of bacterial 16S rRNA genes amplified from unfractionated DNA of different time points shows a change in the bacterial community over time.  $t_1 = 48$  hours;  $t_2 = 1$  week;  $t_3 = 2$  weeks.

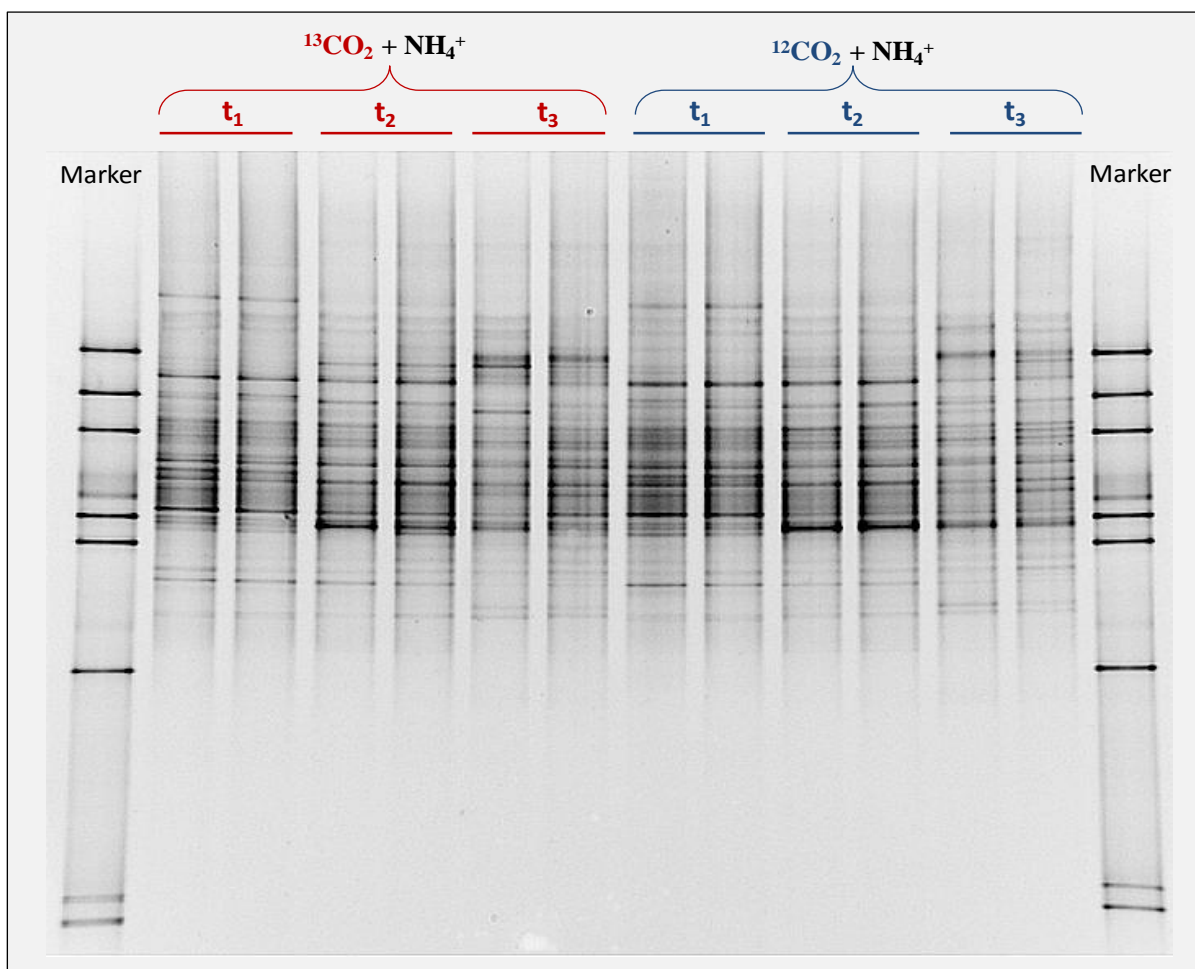


**Figure 6.6b** DGGE profiles of the bacterial community in  $^{13}\text{CO}_2 / \text{NH}_4^+$  SIP enrichments set up with samples from a floating mat in Movile Cave (2011). Each lane on the gel represents a separate enrichment, i.e. duplicates originate from separate serum vials. DGGE analysis of bacterial 16S rRNA genes amplified from unfractionated DNA of different time points shows a change in the bacterial community over time.  $t_1 = 48$  hours;  $t_2 = 1$  week;  $t_3 = 2$  weeks.

(iii)  $^{13}\text{CO}_2$  SIP experiments 2011: Archaeal community analysis

PCR was also carried out using a wide selection of *Archaea*-specific 16S rRNA primer sets (for details of primers see Table 2.2) but failed to generate any amplification products. Eventually, PCR primers targeting specifically *thaumarchaeal* 16S rRNA genes (A190f / 1492r, nested with Thaum\_771f / Thaum\_957-GCr), indicative of AOA, yielded PCR amplification products from both mat and water SIP enrichments. DGGE profiling of these PCR products did however not indicate any clear pattern when comparing community profiles between replicates and different time points (Figure 6.7). Based on the number of bands visible on the DGGE gel, the *thaumarchaeal* diversity appears to be higher in water compared to floating mats, where a small number of dominant bands were observed (Figure

6.7). All visible bands were excised from the DGGE gel, but unfortunately, due to time limitations, these could not be analysed by DNA sequencing. Therefore, 16S rRNA-gene based results from this study do not offer conclusive evidence for the presence of *thaumarchaeal* ammonia oxidisers in Movile Cave.

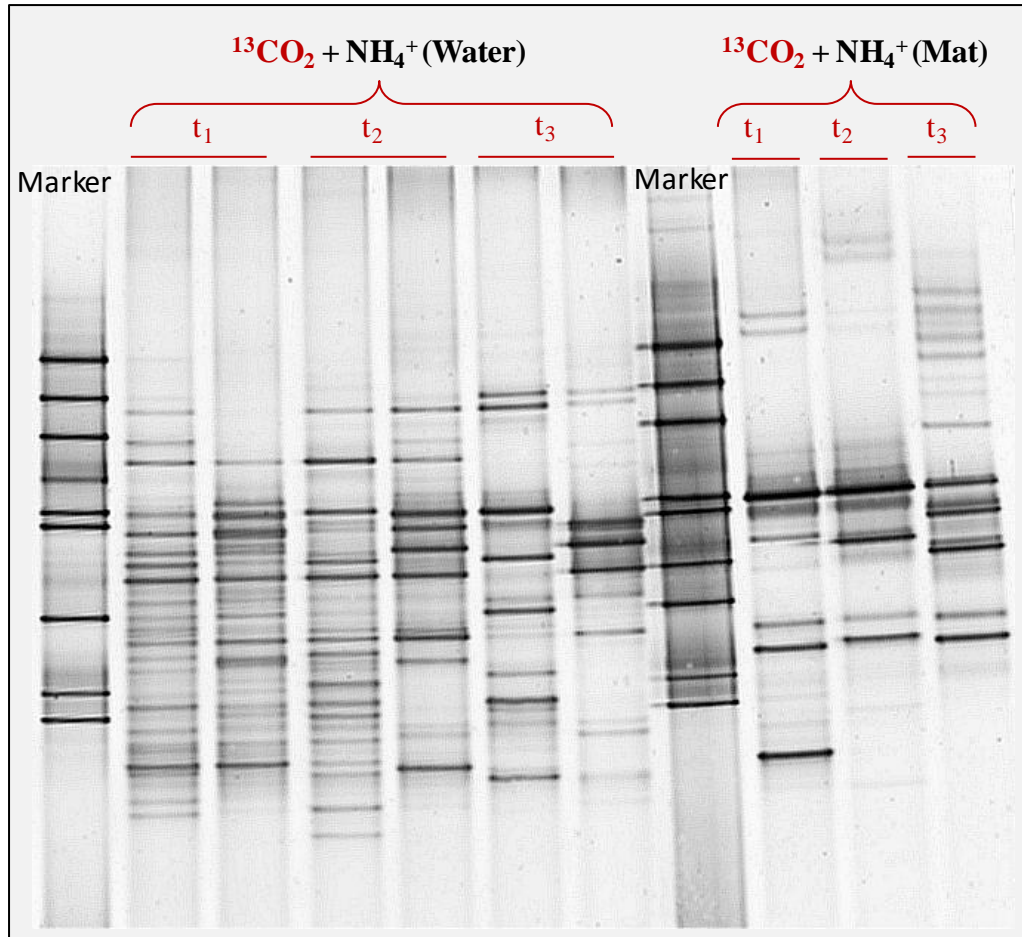


**Figure 6.7** DGGE profiles of putative *thaumarchaeal* 16S rRNA genes (indicative of AOA) amplified from  $^{13}\text{CO}_2 / \text{NH}_4^+$  SIP enrichments set up with water and floating mat samples from Movile Cave (2011). DGGE analysis suggests a high level of *thaumarchaeal* diversity in cave water, and a few dominant *thaumarchaeal* representatives in floating mats. t1 = 48 hours; t2 = 1 week; t3 = 2 weeks.

(iv)  $^{13}\text{C}$ -bicarbonate incorporation: insufficient labelling of DNA

Following analysis of native DNA from SIP incubations with  $^{13}\text{CO}_2$  and  $\text{NH}_4^+$ , heavy DNA was separated from light DNA by ultracentrifugation and fractionation in order to identify organisms that had incorporated  $^{13}\text{C}$ -label (i.e. active  $\text{CO}_2$  fixers). Fourteen fractions were obtained and correct formation of the gradient was confirmed by measuring the density of each fraction. Based on density measurements, heavy DNA was expected to be concentrated around fractions 8 and 9 (F8 and F9 in Figure 6.8); light DNA was expected in fractions 12 -

14 (F12 - F14 in Figure 6.8). However, analysis of the individual fractions by agarose gel electrophoresis of amplified 16S rRNA genes revealed only a weak DNA signal in heavy fractions (Figure 6.8), indicating insufficient incorporation of  $^{13}\text{C}$ -label. Since traces of DNA were also visible in those fractions where no DNA was expected (F1 – F7), it is possible that the presence of small amounts of DNA across fractions F1 – F9 was due to incomplete removal of the light DNA, rather than the presence of heavy DNA.

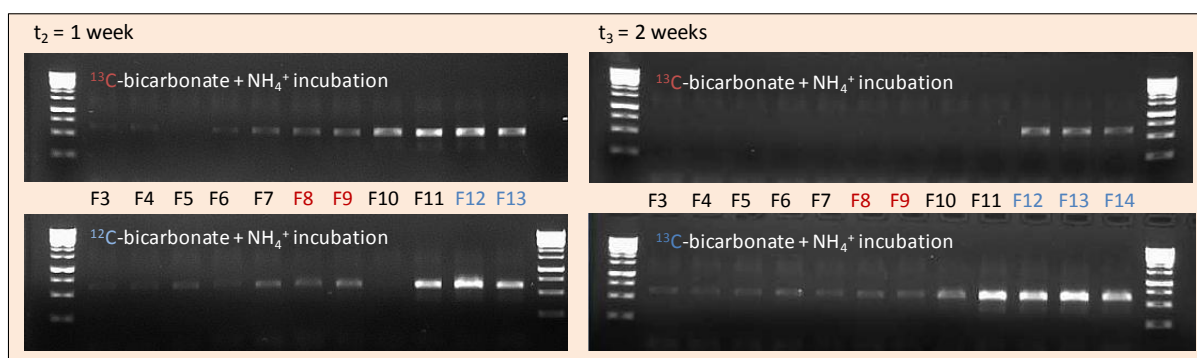


**Figure 6.8** Agarose gel electrophoresis of bacterial 16S rRNA gene fragments amplified from fractionated DNA of  $^{13}\text{CO}_2 / \text{NH}_4^+$  SIP enrichments with floating mat material at 1 week ( $t_2$ ) and 2 weeks ( $t_3$ ), showing no significant DNA signal in heavy fractions (F8 and F9).

All fractions were nonetheless analysed by DGGE in order to identify any potential difference in the community profile between light and heavy DNA. However, DGGE analysis revealed no difference in the community composition between light and heavy fractions (Figure 6.9). These results suggest that either the enriched bacteria were not autotrophs, or that excessive amounts of unlabelled  $\text{CO}_2$  led to insufficient labelling of active autotrophs. Excess amounts of unlabelled  $\text{CO}_2$  could be explained by higher amounts of biomass present in the samples compared to previous SIP incubations, leading to increased  $\text{CO}_2$  production from respiration by heterotrophic microorganisms. However, enrichments from water samples (which contained much less biomass than samples from floating mat) also showed no successful incorporation of  $^{13}\text{C}$ -label. It may also be possible that the excess bicarbonate was derived from the limestone itself. Knowledge of the dissolved organic carbon concentrations in the enrichments would give important information for future SIP experiments.

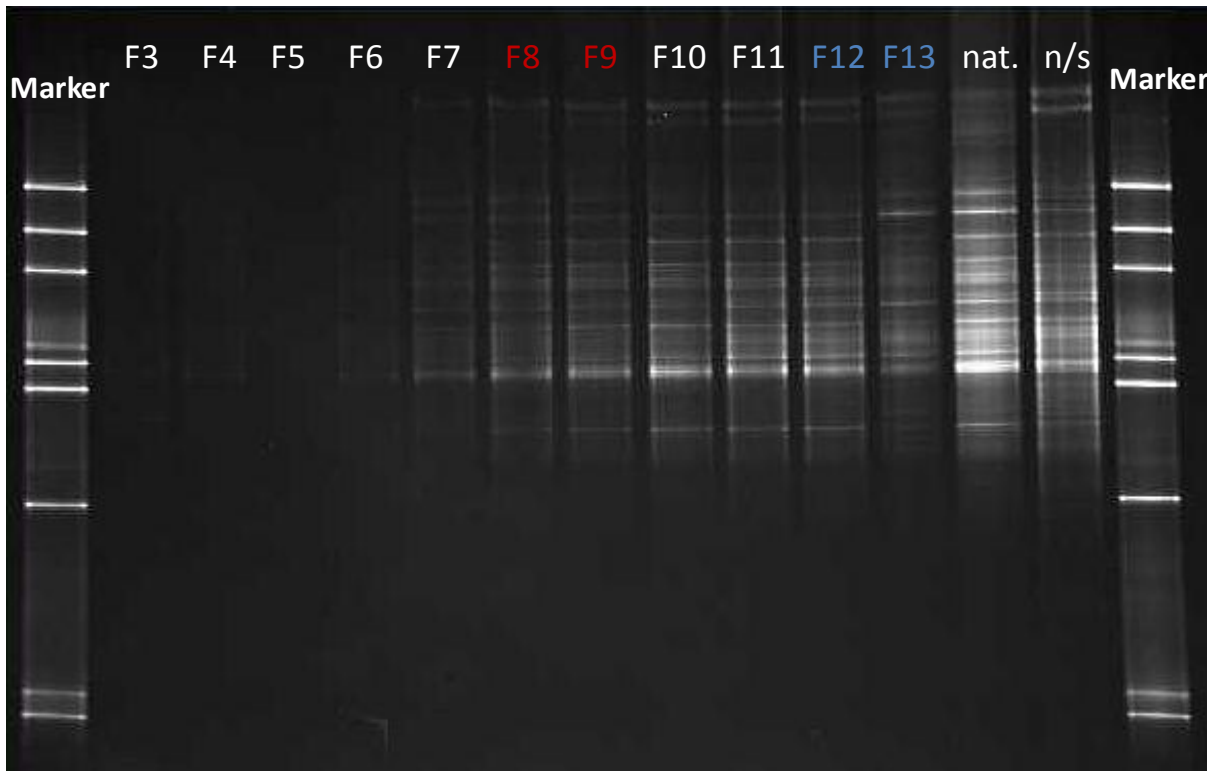


**Figure 6.9** DGGE analysis of 16S rRNA bacterial PCR products from fractionated DNA of  $^{13}\text{CO}_2 / \text{NH}_4^+$  SIP enrichments with Movable Cave mat ( $t_2 = 1$  week), revealing no noticeable difference in the community profile of heavy and light fractions. Abbreviations: F2 - F13 = fractions 2 - 13; nat. = native (unfractionated) DNA; n/s = “no substrate” control.

(v) No detection of nitrifiers in  $^{13}\text{CO}_2 / \text{NH}_4^+$  SIP incubations

Despite the lack of DNA in heavy fractions, dominant DGGE bands were excised for sequence analysis in order to identify any potential autotrophs present. Due to time limitations, only time point  $t=2$  (1 week) of enrichments set up with floating mat material was analysed (DGGE gel shown in Figure 6.9). This sample was chosen as enrichments from floating mat had shown higher levels of activity compared to enrichments with water ( $\text{NO}_2^-$  production after 3 days as opposed to 7 days, see section 6.3.2). However, no nitrifiers were detected. The majority of sequences affiliated with sulfur-oxidising bacteria (*Thiomonas*, *Thiobacillus*, *Leptothrix*, *Sulfuritalea*) and aerobic heterotrophs (*Thermomonas*, *Xanthomonas*, *Luteibacter*, *Sphingopyxis*), while sulfate-reducing bacteria (*Desulforhopalus*) were also present. These results support findings from previous SIP enrichments with  $^{13}\text{CO}_2$  as the only added carbon source (see Figure 6.5 and Chen *et al.*, 2009), suggesting that sulfur oxidisers, and not nitrifiers, are likely to be the dominant autotrophs in Movable Cave.

(vi) *amoA* gene surveys of SIP enrichments reveal the presence of AOA and AOB and suggest niche separation of the two groups

To complement 16S rRNA gene-based analysis of  $^{13}\text{CO}_2$  /  $\text{NH}_4^+$  SIP incubations, samples derived from different time points were also screened for the presence of bacterial and archaeal *amoA* genes. While 16S rRNA gene-based DGGE indicated that sulfur oxidisers are the dominant autotrophs in Movile Cave (section (iv) above), supporting results from past SIP experiments (SIP experiments 2010, see section 6.5), analysis of *amoA* genes would give clues as to whether any nitrifiers were present. Primers specific for (i) *archaeal amoA* genes and (ii) *betaproteobacterial amoA* genes were used with native DNA from  $^{13}\text{CO}_2$  /  $\text{NH}_4^+$  SIP enrichments as well as control enrichments with unlabelled  $\text{CO}_2$  (time points t1; t2; t3). The PCR reaction was optimised for each primer set using one sample that worked well, and subsequently repeated for all replicates and time points.

While no nitrifiers could be detected by 16S rRNA gene-based studies (see above), bacterial as well as archaeal *amoA* genes were amplified from the SIP enrichments (Figure 6.10). Interestingly, results from *amoA*-screening also suggested a niche separation of the two groups in Movile Cave, indicating that AOA are the main nitrifiers in water while AOB dominate at higher  $\text{NH}_4^+$  concentrations: Bacterial *amoA* genes were detected in both water and mat samples, but only after two weeks of incubation (Figure 6.10), suggesting that AOB were enriched over time following the addition of 1 mM  $\text{NH}_4^+$ . In contrast, archaeal *amoA* sequences were amplified only from water enrichments, and seemed to decrease following incubation with  $\text{NH}_4^+$  (Figure 6.10), suggesting that the incubation conditions favoured the growth of AOB over AOA. Standing concentrations of  $\text{NH}_4^+$  in Movile Cave are considerably higher in the floating mats (0.5 - 0.8 mM, see 6.3.2.) than in water (0.2 - 0.3 mM, Sârbu 2000). While PCR results do not offer quantitative data, the fact that archaeal *amoA* genes were not detected in incubations set up with floating mat samples or at later time points following the addition of  $\text{NH}_4^+$  may suggest that AOA in Movile Cave are outcompeted by AOB at higher  $\text{NH}_4^+$  concentrations. The hypothesis that AOB dominate at higher  $\text{NH}_4^+$  concentrations is supported by studies of nitrifying communities in soil (e.g. Verhamme *et al.*, 2011) and kinetic studies of pure cultures (Martens-Habbena *et al.*, 2009), both of which have shown that AOA are more competitive at low  $\text{NH}_4^+$  concentrations. However,  $\text{NH}_4^+$  concentrations in Movile Cave water are still very high at 0.3 mM compared to those of seawater (which are in the  $\mu\text{M}$  range).

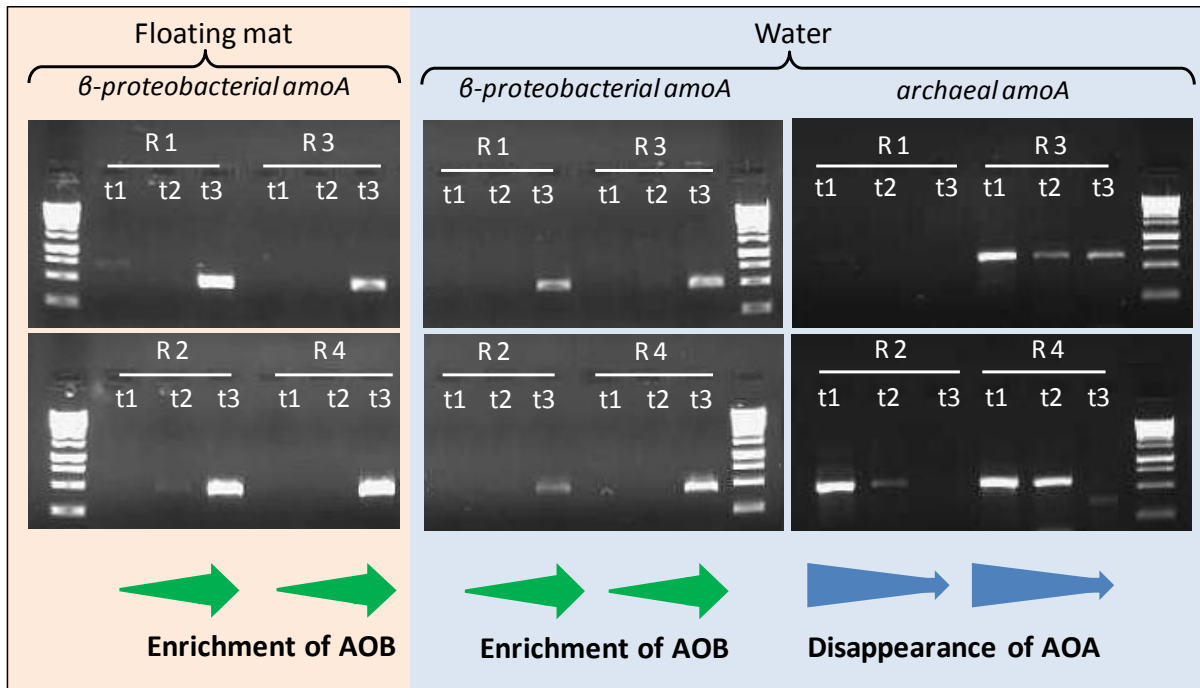


**Figure 6.10** Agarose gels of bacterial and archaeal *amoA* genes amplified from  $^{13}\text{CO}_2 / \text{NH}_4^+$  SIP enrichments (2011) with Movile Cave water and floating mat material, respectively. Results show an enrichment of bacterial *amoA*, and a depletion of archaeal *amoA*, indicating that the growth conditions used in the laboratory favoured ammonia-oxidising bacteria. No archaeal *amoA* genes were amplified from mat samples at any given time point. Abbreviations: AOB = ammonia-oxidising bacteria; AOA = ammonia-oxidising archaea; R = replicate; t1 = 48 hours; t2 = 1 week; t3 = 2 weeks. R1 and R2 are derived from  $^{13}\text{CO}_2 / \text{NH}_4^+$  enrichments, R3 and R4 from enrichments with unlabelled  $\text{CO}_2 / \text{NH}_4^+$ .

### 6.3.5 Enrichment of ammonia-oxidising bacteria and archaea

In an attempt to isolate nitrifying bacteria and archaea, long-term enrichments were set up with cave water, using 181 medium (according to the recipe described for *Nitrosomonas*, see Chapter 2, section 2.5), with  $\text{NH}_4^+$  as the only added energy source and no added carbon source to select for autotrophic ammonia oxidisers. Enrichment cultures for the selection of archaea were set up with cave water that had been filtered through 0.2  $\mu\text{m}$  Sterivex filters and additionally supplemented with the antibiotic streptomycin (50  $\mu\text{g} / \text{ml}$ ) to avoid bacterial growth. All enrichments were furthermore supplemented with phenol-red solution as pH indicator (a decrease in pH as a result of  $\text{NO}_2^-$  production changes the colour of the medium from pink to colourless, see Chapter 2, section 2.5). Enrichments were incubated at 20°C in the dark for nine months, at which point nitrifying enrichments without antibiotics had turned colourless, i.e. the pH had decreased, suggesting production of  $\text{NO}_2^-$  and activity of AOB. Microscopic analysis revealed mainly non-motile, rod-shaped bacteria (Figure 6.11) along

with a few motile spirilla. Enrichments with added antibiotics had also changed colour, albeit still slightly pink, suggesting a lower rate of nitrifying activity (this was expected due to slower growth of AOA). Microscopy indeed revealed tiny non-motile cells believed to be archaea based on their small size (Figure 6.11). Meanwhile, cells of the size of bacteria as seen in unfiltered enrichments without streptomycin, were completely absent in archaeal enrichments (Figure 6.11).

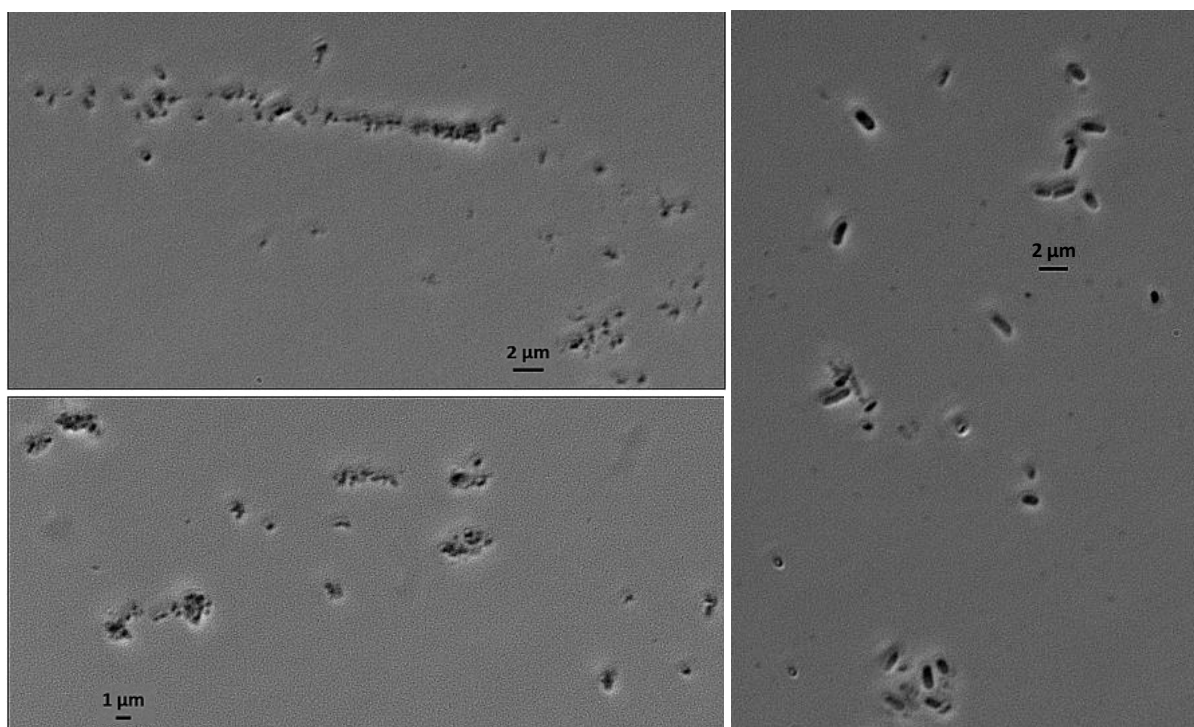


**Figure 6.11** Phase-contrast microscopy of nitrifying enrichments set up with Movile Cave water. Small cells ( $< 1 \mu\text{m}$  in length), believed to be archaeal ammonia oxidisers, were visible in enrichments that had been treated with antibiotics (left). Cells of bacterial dimension ( $1 - 2 \mu\text{m}$  long) were only visible in untreated enrichments (right).

At this point, the enrichments were subcultured into fresh 181 medium (at  $10^{-1}$  dilutions) with and without antibiotics as before. After a further 3 months of incubation at  $20^{\circ}\text{C}$  in the dark, dilutions of the transfers were added to pouring plates (at  $10^{-2}$  dilutions) as described for the isolation of AOB by Bollman *et al.* (2011). It was not expected to detect any growth for 3 to 6 months (Bollman *et al.*, 2011). However, after only one week of incubation, plates without antibiotics in the medium had turned from pink to colourless and showed an abundance of colonies inside the agar. The rapid growth was highly suspicious and suggested that the colonies were heterotrophs rather than nitrifiers. Colonies were picked out of the agar with a sterile Pasteur pipette for colony PCR and sequencing of 16S rRNA genes. Sequence analysis of colonies did not reveal any autotrophs, but instead identified species of

*Nocardioides*, *Variovorax*, *Sinorhizobium* and *Pseudomonas*. It is possible that these organisms grew with trace amounts of carbon present in the agar, or even used the phenol-red solution added for pH indication, as all of these genera contain species which have been described to degrade aromatic compounds. The decrease in pH might be due to CO<sub>2</sub> production. Phenol-red solution should hence be avoided for autotrophic enrichments in the future. Plates with added antibiotics showed no sign of growth, even after one year, and were discarded. While the attempt to isolate nitrifiers failed, results suggest that ammonia oxidisers were at least enriched. 16S rRNA gene-based clone libraries of the enrichments which might have confirmed this could not be established due to time limitations.

### 6.3.6 Summary

In summary, SIP incubations with <sup>13</sup>CO<sub>2</sub> and added NH<sub>4</sub><sup>+</sup> failed to identify active CO<sub>2</sub>-fixers due to insufficient <sup>13</sup>C-labelling, however, the overall results suggest that nitrifiers are both present and active in Movile Cave, based on functional gene-based PCR of enrichments (bacterial and archaeal *amoA*) as well as consumption of NH<sub>4</sub><sup>+</sup> and production of NO<sub>2</sub><sup>-</sup> in enrichments (see section 6.3.2). The results obtained in this PhD project however also indicate that sulfur oxidisers, and not nitrifiers, are likely to be the dominant primary producers in Movile Cave.

## 6.4 Dinitrogen fixation in Movile Cave

Only a relatively small number of prokaryotes are able to use elemental nitrogen (N<sub>2</sub>) as a cellular nitrogen source by N<sub>2</sub> fixation (the reduction of N<sub>2</sub> to NH<sub>4</sub><sup>+</sup>) (Madigan *et al.*, 2009):



However, the ability to fix N<sub>2</sub> is widespread amongst phylogenetically and physiologically diverse groups of microorganisms, including sulfate-reducing bacteria and methanogenic archaea (Mehta *et al.*, 2003). Several bacteria identified in Movile Cave are known to be capable of diazotrophic growth, e.g. *Thiobacillus denitrificans*, *Beggiatoa* and *Methylocystis*, (Sârbu *et al.*, 1994; Vlăsceanu *et al.* 1997; Hutchens *et al.*, 2004). However, N<sub>2</sub>-fixation is a highly energy-demanding process for microorganisms (requiring 16 ATP for reduction for one molecule of N<sub>2</sub>) and therefore carried out only under nitrogen limitation. Standing concentrations of NH<sub>4</sub><sup>+</sup> in Movile Cave are relatively high: Sârbu (2000) reported

concentrations of 0.2 - 0.3 mM in water, while  $\text{NH}_4^+$  measurements carried out in this PhD project ranged between 0.1 - 0.5 mM for water samples, and 0.5 - 0.8 mM for floating mat material. It is however possible that  $\text{NH}_4^+$ -depleted areas exist within the floating mats where microbial  $\text{N}_2$  fixation could be an important process. Indeed, nitrogen fixation by *Beggiatoa*-dominated microbial mats has been shown to be a major process in Frasassi Cave, a sulfidic cave system that has similar  $\text{NH}_4^+$  concentrations to Movile Cave (Sârbu *et al.*, 2002; Desai *et al.*, 2013). The role of  $\text{N}_2$ -fixation in Movile Cave has however not been investigated. In order to screen mat samples from Movile Cave for  $\text{N}_2$ -fixing activity, reduction of acetylene ( $\text{C}_2\text{H}_2$ ) to ethylene ( $\text{C}_2\text{H}_4$ ) was assayed by gas chromatography. In addition, PCR primers targeting *nifH*, key gene in nitrogen fixation were used to screen Movile Cave samples for potential  $\text{N}_2$ -fixing bacteria and archaea.

#### 6.4.1 PCR-based studies suggest a wide phylogenetic diversity of *nifH* in Movile Cave

The *nifH* gene encodes the dinitrogenase reductase (iron protein) of nitrogenase, the enzyme complex that catalyses  $\text{N}_2$  fixation. *nifH* is one of the most ancient and conserved structural genes (Mehta *et al.*, 2003) and is therefore widely used for the detection and taxonomy of nitrogen-fixing microorganisms. Degenerate *nifH*-specific PCR primers were used in order to target a wide range of  $\text{N}_2$ -fixers. Gene fragments of the correct length were amplified from all cave water, floating mat and wall biofilm samples tested (Table 6.2). While only four *nifH* clones were sequenced, there appears to be considerable diversity of  $\text{N}_2$ -fixing bacteria in Movile Cave (Table 6.5). All four clones were distinct from each other: One clone showed a high level of identity (99%) to dinitrogenase reductase from the metal-reducing bacterium *Geobacter lovleyi*. A further clone shared 94% identity with dinitrogenase reductase from the purple sulfur bacterium *Thiocapsa*. The remaining two *nifH* sequences shared only 86% and 72% identity to the nearest related proteins (91% and 83% similarity), respectively.

**Table 6.5** Phylogenetic affiliations of translated *nifH* sequences from Movile Cave (Airbell 2, floating mat)

Clones	Closest GenBank relatives (accession code)	<sup>(1)</sup> Identity (%) / <sup>(1)</sup> Similarity (%)	Phylogenetic affiliation of GenBank relative
NH7-5	Nitrogenase iron protein [ <i>Geobacter lovleyi</i> ] (NC_010814.1)	99 / 99	<i>Deltaproteobacteria</i> ; <i>Desulfuromonadales</i> ; <i>Geobacteraceae</i> ; <i>Geobacter</i>
	Nitrogenase iron protein [ <i>Bradyrhizobium japonicum</i> ] (GQ289574.1)	95 / 98	<i>Alphaproteobacteria</i> ; <i>Rhizobiales</i> ; <i>Bradyrhizobiaceae</i> ; <i>Bradyrhizobium</i>
NH7-1	Nitrogenase iron protein [ <i>Wolinella succinogenes</i> ] (NC_005090.1)	86 / 91	<i>Epsilonproteobacteria</i> ; <i>Campylobacterales</i> ; <i>Helicobacteraceae</i> ; <i>Wolinella</i>
	Nitrogenase iron protein [ <i>Sulfurospirillum multivorans</i> ] (DQ337206.1)	80 / 89	<i>Epsilonproteobacteria</i> ; <i>Campylobacterales</i> ; <i>Campylobacteraceae</i> ; <i>Sulfurospirillum</i>
NH7-4	Nitrogenase iron protein [ <i>Thiocapsa roseopersicina</i> ] (EU622784.1)	94 / 96	<i>Gammaproteobacteria</i> ; <i>Chromatiales</i> ; <i>Chromatiaceae</i> ; <i>Thiocapsa</i>
	Nitrogenase iron protein [ <i>Methylomonas rubra</i> ] (AF484673.1)	93 / 96	<i>Gammaproteobacteria</i> ; <i>Methylococcales</i> ; <i>Methylococcaceae</i> ; <i>Methylomonas</i>
NH7-6	Nitrogenase iron protein [ <i>Desulfovibrio magneticus</i> ] (NC_012796.1)	89 / 93	<i>Deltaproteobacteria</i> ; <i>Desulfiovibrionales</i> ; <i>Desulfiovibrionaceae</i> ; <i>Desulfiovibrio</i>
	Nitrogenase iron protein [ <i>Chloroherpeton thalassium</i> ] (NC_011026.1)	87 / 91	<i>Chlorobi</i> ; <i>Chlorobia</i> ; <i>Chlorobiales</i> ; <i>Chlorobiaceae</i> ; <i>Chloroherpeton</i>

<sup>(1)</sup> Sequence analysis was carried out using the blastx algorithm (alignment of translated nucleotide sequences against protein database); hence, identity and similarity values refer to amino acid sequences.

#### 6.4.2 No detection of N<sub>2</sub>-fixing activity in Movile Cave samples

No significant ethylene production could be detected in microbial mat samples following addition of acetylene over a time course of several hours (for details of assay and positive controls refer to Chapter 2, section 2.16). Only the floating mat sample taken from Airbell 1 produced a very small ethylene peak after 20 min following addition of acetylene (corresponding to a production of 6.5 nmol C<sub>2</sub>H<sub>4</sub> in 2g mat), but showed no further increase. There is therefore no indication for N<sub>2</sub> fixing activity in the microbial mat in Movile Cave at this point. However, it may be useful to back up these data with gene expression studies of *nifH*. Even though the samples were processed within 48 hours of sampling, the biomass may

have lost its activity so quickly that it could not be detected. Since Movile Cave is a protected ecosystem (the cave is only opened to scientists once or twice per year), *in situ* assays are unfortunately not an option. While *nifH* expression itself would not guarantee detection of N<sub>2</sub>-fixing activity in Movile Cave, it would be a good first indicator, and a lack of *nifH* expression would substantiate the hypothesis that microbial N<sub>2</sub> fixation does not contribute to the cycling of nitrogen in this system.

## 6.5 Anaerobic nitrogen respiration in Movile Cave: Denitrification and Anammox

### 6.5.1 Introduction to denitrification

Denitrification is an anaerobic respiration process that results in the stepwise reduction of nitrate (NO<sub>3</sub><sup>-</sup>) to molecular nitrogen (N<sub>2</sub>) via the intermediates nitrite (NO<sub>2</sub><sup>-</sup>), nitric oxide (NO) and nitrous oxide (N<sub>2</sub>O). It is the major mechanism by which fixed nitrogen is removed from soil and water, and returned to the atmosphere (Philippot, 2002). Denitrification is carried out in the absence of O<sub>2</sub> as a terminal electron acceptor by a phylogenetically wide range of microorganisms. While proteobacterial denitrifiers are the most intensively studied and isolated, denitrifiers are also found among gram-positive bacteria, archaea, fungi and benthic foraminifera (Kraft *et al.*, 2011). Nearly 130 species of bacteria and archaea belonging to more than 50 genera can denitrify (Zumft, 1992). Complete denitrification generally involves several microbial species. Nitrate reductase, the enzyme that catalyses the reduction of NO<sub>3</sub><sup>-</sup> to NO<sub>2</sub><sup>-</sup>, the first step in denitrification, can also be found in bacteria that are not denitrifiers (Kraft *et al.*, 2011). The second enzyme in the denitrification process, nitrite reductase, catalyses the conversion of NO<sub>2</sub><sup>-</sup> to N<sub>2</sub>O. This is the first step that distinguishes denitrifiers from NO<sub>3</sub><sup>-</sup>-respiring bacteria which do not reduce NO<sub>2</sub><sup>-</sup> to gas (Priemé *et al.*, 2002). In denitrifying bacteria, dissimilatory nitrite reductase exists in two structurally different forms: a copper-containing form (*nirK*), and a heme-containing form (*nirS*). The two enzymes are evolutionary unrelated and no bacteria have been found to possess both (Priemé *et al.*, 2002). The *nirS* and *nirK* genes are the main molecular biomarkers for the detection of denitrifying bacteria.

### 6.5.2 Introduction to anammox

The discovery of anaerobic ammonium oxidation (anammox) bacteria in recent years was an important finding in the nitrogen cycle (Mulder *et al.*, 1995; van de Graaf *et al.* 1995; Strous *et al.*, 1999). Previously, denitrification was thought to be the only significant pathway for N<sub>2</sub> formation and removal of fixed nitrogen from ecosystems (Trimmer *et al.*, 2003), even though the existence of anammox was already proposed many years ago based on theoretical calculations and anomalies in nitrogen balances (reviewed by van Niftrik, 2013). Anammox bacteria are able to grow autotrophically by oxidising NH<sub>4</sub><sup>+</sup> to N<sub>2</sub> under anoxic conditions, using NO<sub>2</sub><sup>-</sup> as the electron acceptor (with nitric oxide and hydrazine as intermediates), thereby bypassing the classic coupling of aerobic nitrification to denitrification (Trimmer *et al.*, 2003):



(Note:  $\Delta G^{0'}$  calculated from  $\Delta G_f^{0'}$  of aqueous compounds as listed in Supplementary Table S1)

The process is carried out by a specialised group of planctomycete-like bacteria that were first discovered in man-made ecosystems (Hu *et al.*, 2011). Since their discovery, numerous studies have investigated the role of anammox in natural ecosystems. It has been suggested that they are present in virtually any anoxic place where fixed nitrogen (NH<sub>4</sub><sup>+</sup>, NO<sub>3</sub><sup>-</sup>, NO<sub>2</sub><sup>-</sup>) is found, and they are believed to account for an estimated 50% of all nitrogen gas released into the atmosphere from oceans (Kartal *et al.*, 2012) and up to 40% in non-marine habitats (Hu *et al.*, 2011). Anammox has also emerged as a cost-effective and environment-friendly technology to remove NH<sub>4</sub><sup>+</sup> and NO<sub>2</sub><sup>-</sup> from both industrial and domestic waste (van Niftrik, 2013). Two different anammox species rarely live in a single habitat, suggesting that each species has a defined niche (Kartal *et al.*, 2007). It has been hypothesised that anammox bacteria are able to use a broad range of organic and inorganic electron donors besides NH<sub>4</sub><sup>+</sup>, and may be capable of alternative chemolithotrophic lifestyles (Kartal *et al.*, 2012). To date, all studies of anammox rely on molecular studies and enrichment cultures, as currently there are no anammox species in pure culture (anammox bacteria are difficult to cultivate and have very slow growth rates). Anammox bacteria form a distinct group within the phylum *Planctomycetes*, and a separate order, *Candidatus Brocadiales* (Jetten *et al.*, 2010) which consists exclusively of anammox bacteria and contains all five genera (10 species) capable of anaerobic NH<sub>4</sub><sup>+</sup> oxidation known to date (van Niftrik, 2013; Kartal *et al.* 2012): *Kuenenia*, *Brocadia*, *Anammoxoglobus*, *Jettenia*, *Scalindua* (Lücker, 2010). As no anammox species were obtained as classical pure cultures, all have the taxonomical status of ‘*Candidatus*’

(Kartal *et al.* 2012). Four of the five anammox genera were enriched from a single inoculum from wastewater sludge; the fifth (*Scalindua*) is of marine origin. It has been suggested that currently known species may only represent a minute fraction of anammox biodiversity (Kartal *et al.* 2012).

### 6.5.3 Denitrification and anammox in Movile Cave

With large parts of the water and sediment in Movile Cave being anoxic, many microbes will rely on anaerobic respiration processes. In addition to sulfate reduction (Rohwerder *et al.*, 2003; Engel, 2007), denitrification and anammox may be important processes in these areas. While no dedicated studies on the role of anaerobic nitrogen respiration in the Movile Cave food web have been carried out, microorganisms with the potential to denitrify, e.g. *Thiobacillus denitrificans* and *Denitratisoma*, have been identified by 16S rRNA gene-based surveys (Chen *et al.*, 2009 Porter *et al.*, 2009). Like *T. denitrificans*, many facultatively anaerobic sulfur oxidisers are able to use  $\text{NO}_3^-$  as an electron acceptor. High numbers of sulfur-oxidising bacteria were indeed detected in anoxic enrichments with  $\text{NO}_3^-$  by Rohwerder *et al.* (2003), indicating a potential link between sulfur oxidation and denitrification in Movile Cave. The fact that  $\text{NO}_3^-$  cannot be detected in the cave water, while standing concentrations of  $\text{NH}_4^+$  are relatively high (0.2-0.3 mM, Sârbu 2000) may suggest rapid turnover of  $\text{NO}_3^-$  by denitrifiers. To assess the role of denitrification and anammox in Movile Cave, isotope pairing studies were carried out along with PCR-based surveys in this PhD.

#### (i) Isotope pairing studies

In order to determine activity of denitrifying and anammox bacteria in Movile Cave, isotope pairing experiments were set up with anoxic water and sediment samples from Airbell 2 (for details on experimental set up refer to Chapter 2, section 2.19). The isotope pairing technique (IPT) is a well-established  $^{15}\text{N}$  method used in estimation of denitrification (Nielsen, 1992) and more recently to estimate the relative contribution of anammox to the overall total  $\text{N}_2$  production in environments where both processes coexist (e.g. Risgaard-Petersen *et al.*, 2003; Trimmer *et al.* 2003, Dalsgaard *et al.*, 2005; Ward *et al.*, 2009, cited after review by Li & Gu, 2011). Experimental samples are incubated in parallel with different inorganic  $^{15}\text{N}$ -labelled substrates: (1)  $^{15}\text{NH}_4^+$  alone, (2) a mixture of  $^{15}\text{NH}_4^+$  and  $^{14}\text{NO}_x^-$ , and (3)  $^{15}\text{NO}_x^-$  and  $^{14}\text{NH}_4^+$ . After incubation,  $\text{N}_2$  production from each treatment can be collected and measured on an isotope mass spectrometer for  $^{15}\text{N}$  concentrations ( $^{28}\text{N}_2$ ;  $^{29}\text{N}_2$ ;  $^{30}\text{N}_2$ ). The first incubation is used as a control to detect any oxidation of ammonium without the addition of nitrite, while

the second treatment is used to measure the anammox activity, where the production of  $^{29}\text{N}_2$  stoichiometrically is a confirmation of the oxidation of ammonium ( $^{15}\text{NH}_4^+$ ) with reduction of nitrite ( $^{14}\text{NO}_2^-$ ) or nitrate ( $^{14}\text{NO}_3^-$ ) through the anammox process:  $^{15}\text{NH}_4^+ + ^{14}\text{NO}_2^- \rightarrow ^{29}\text{N}_2 + 2 \text{H}_2\text{O}$  (it has been suggested that anammox bacteria can also reduce  $\text{NO}_3^-$  to  $\text{NO}_2^-$  and then further to  $\text{NH}_4^+$  under certain conditions, Kartal *et al.*, 2007). Production of  $^{28}\text{N}_2$  on the other hand would indicate denitrification ( $^{14}\text{NO}_x^- + ^{14}\text{NO}_x^- = ^{28}\text{N}_2$ ). The third incubation is to estimate the relative contribution of anammox and denitrification collectively, where the production of  $^{29}\text{N}_2$  and  $^{30}\text{N}_2$  indicate the activities of anammox and denitrification, respectively (Trimmer *et al.*, 2003; Li & Gu, 2011).

Movile Cave samples were incubated with  $^{15}\text{N}$ -labelled and unlabelled ( $^{14}\text{N}$ ) isotopes of  $\text{NH}_4^+$ ,  $\text{NO}_2^-$  and  $\text{NO}_3^-$  as described in Chapter 2, section 2.19, following the protocol of Trimmer *et al.* (2003) and subsequently analysed by mass spectrometry in Mark Trimmer's laboratory at QMU London as described by Trimmer *et al.* (2003). While the experiments did not produce conclusive results, data suggested that both denitrification and anammox were taking place, with denitrification being the dominant of the two processes (personal communication with Dr Kevin Purdy). More detailed studies are needed to confirm these results.

(ii) *PCR-based screening for denitrification*

To screen for Movile Cave bacteria with the genetic potential to denitrify, PCR primer sets targeting the two different forms of dissimilatory nitrite reductase, *nirS* and *nirK* (Braker *et al.*, 2000) were used on DNA extracted from water, mat and biofilm samples from the cave. PCR products of the expected lengths were obtained with both primer sets for samples taken from floating mats in the lake room and Airbell 1 (Table 6.2). *NirS* genes were additionally amplified from Airbell 2 floating mat and Airbell 2 wall biofilm samples. No amplification products were obtained with either primer set from any water samples. It should be noted that the negative PCR results may not be conclusive as no reduction of stringency of the PCR conditions was attempted. The PCR was performed strictly according to the protocol by Braker *et al.* (2000), which uses the same conditions as the original protocol (1998) by the same authors, except for higher annealing temperatures (for details, see Table 2.2). The more recent protocol with higher annealing temperatures was used in order to avoid unspecific amplification for the purpose of this study (i.e., a first indication of the presence of denitrifiers

in Movile Cave). A lower annealing temperature might be useful, however, to target all denitrifiers and increase the amount of PCR product.

All four sequenced *nirK* clones affiliated with *nirK* from *Rhizobium* (95 and 94% identity) as well as *nirK* from *Citromicrobium* (96 and 94% identity), with three of the clones being identical (Table 6.6). Out of the four sequenced *nirS* clones (Table 6.7), one was 96% identical (98% similar) to dissimilatory nitrite reductase of an uncultured bacterium from river sediment, while the closest related sequence of a cultured representative belonged to *nirS* of *Arenimonas donghaensis* (81% identity; 90% similarity), an organism not known to reduce nitrate or nitrite (Kwon et al., 2007). The other three *nirS* sequences were identical and did not result in any close matches, with the most closely related GenBank sequence belonging to dissimilatory nitrite reductase of an uncultured bacterium at only 83% identity (91% similarity), and the closest related sequence of a cultivated organism belonging to *Azoarcus tolulyticus* (81% identity; 89% similarity) (Table 6.7).

**Table 6.6** Phylogenetic affiliations of translated *nirK* sequences from Movile Cave (lake room, floating mat)

Clones	Closest GenBank relatives (accession code)	<sup>(1)</sup> Identity (%) / <sup>(1)</sup> Similarity (%)	Phylogentic affiliations of GenBank relatives
NK2-1	Dissimilatory nitrite reductase	95 / 95	<i>Alphaproteobacteria; Rhizobiales;</i>
NK2-3	[ <i>Rhizobium selenitireducens</i> ]		<i>Rhizobiaceae; Rhizobium</i>
NK2-4	(WP_028737952.1)		
	Dissimilatory nitrite reductase	96 / 97	<i>Alphaproteobacteria; Sphingomonadales;</i>
	[ <i>Citromicrobium bathyomarinum</i> ]		<i>Sphingomonadaceae; Citromicrobium</i>
	(WP_010240326.1)		
NK2-2	Dissimilatory nitrite reductase	94 / 94	<i>Alphaproteobacteria; Rhizobiales;</i>
	[ <i>Rhizobium selenitireducens</i> ]		<i>Rhizobiaceae; Rhizobium</i>
	(WP_028737952.1)		
	Dissimilatory nitrite reductase	94 / 97	<i>Alphaproteobacteria; Sphingomonadales;</i>
	[ <i>Citromicrobium bathyomarinum</i> ]		<i>Sphingomonadaceae; Citromicrobium</i>
	(WP_010240326.1)		

<sup>(1)</sup> Sequence analysis was carried out using the blastx algorithm (alignment of translated nucleotide sequences against protein database); hence, identity and similarity values refer to amino acid sequences.

**Table 6.7** Phylogenetic affiliations of translated *nirS* sequences from Movile Cave (Airbell 2, floating mat)

Clones	Closest GenBank Relatives (accession code)	<sup>(1)</sup> Identity (%) / <sup>(1)</sup> Similarity (%)	Phylogenetic affiliations of GenBank relatives
NS7-2	Dissimilatory nitrite reductase [uncultured bacterium]; River sediment (AEL12536.1)	96 / 98	Not specified
	Dissimilatory nitrite reductase [ <i>Arenimonas donghaensis</i> ] (WP_034222770.1)	81 / 90	<i>Gammaproteobacteria</i> ; <i>Xanthomonadales</i> ; <i>Xanthomonadaceae</i> ; <i>Arenimonas</i>
NS7-1	Dissimilatory nitrite reductase [uncultured bacterium];	83 / 91	Not specified
NS7-3	Landfill		
NS7-4	(AEK31212.1)		
	Dissimilatory nitrite reductase [ <i>Azoarcus tolulyticus</i> ] (AAL86941.1)	81 / 89	<i>Betaproteobacteria</i> ; <i>Rhodocyclales</i> ; <i>Rhodocyclaceae</i> ; <i>Azoarcus</i>

<sup>(1)</sup> Sequence analysis was carried out using the blastx algorithm (alignment of translated nucleotide sequences against protein database); hence, identity and similarity values refer to amino acid sequences.

(iii) *PCR-based screening for anammox bacteria*

The key enzyme in anaerobic ammonium oxidation is hydrazine oxidoreductase (*hzo*), which converts the intermediate hydrazine to N<sub>2</sub>. Primers targeting *hzo* (Schmid *et al.*, 2008) were used to screen DNA extracted from lake room and Airbell 2 sediment for the presence of anammox bacteria. Amplification products of the expected length were obtained; however, the bands were very faint and appeared alongside unspecific amplification products. For this reason, it could not be confirmed by sequence analysis that the amplified products were indeed *hzo* genes. In addition to *hzo*-targeting primers, PCR with primers targeting 16S rRNA genes from anammox-associated *Planctomycetes* (Schmid *et al.*, 2003) generated amplification products of the expected size. Two out of four sequenced clones were 99% related to anammox bacteria from the Brocadiales (Table 6.8). The remaining two genes however were only distantly related (78-84%) to 16S rRNA genes from both *Planctomycetes* and the *Deltaproteobacteria*. While the presence of Brocadiales-related 16S rRNA gene sequences does not as such provide evidence that these bacteria have the genetic potential for anaerobic ammonium oxidation, there is a high probability they do.

**Table 6.8** Phylogenetic affiliations of 16S rRNA gene sequences obtained from DNA from Mobile Cave sediment with PCR primers targeting *Candidatus* Brocadiales (putative anammox bacteria)

Clones	Closest GenBank relatives (accession code)	Identities (%)	Phylogenetic affiliations of GenBank relatives
Amx0 Amx3	<i>Candidatus</i> Scalindua sp. clone S-LC-9 (JQ889466.1)	99	<i>Planctomycetia</i> ; <i>Candidatus</i> Brocadiales; <i>Candidatus</i> Brocadiaceae; <i>Candidatus</i> Scalindua
	<i>Candidatus</i> Scalindua marina clone 12C (EF602039.1)	96	
	<i>Candidatus</i> Scalindua brodae clone 20S (EU142948.1)	95	
Amx1	<i>Hippea</i> sp. Lau09-781r (FR754501.1)	84	<i>Deltaproteobacteria</i> ; <i>Desulfurellales</i> ; <i>Desulfurellaceae</i> ; <i>Hippea</i>
	<i>Desulfovibrio alaskensis</i> (Y11984.3)	82	<i>Deltaproteobacteria</i> ; <i>Desulfovibrionales</i> ; <i>Desulfovibrionaceae</i> ; <i>Desulfovibrio</i>
	<i>Methylacidiphilum infernorum</i> (NR_074583.1)	78	<i>Verrucomicrobia</i> ; <i>Methylacidiphilales</i> ; <i>Methylacidiphilaceae</i> ; <i>Methylacidiphilum</i>
	<i>Singulisphaera acidiphila</i> (CP003364.1)	78	<i>Planctomycetia</i> ; <i>Planctomycetales</i> ; <i>Planctomycetaceae</i> ; <i>Singulisphaera</i>
	<i>Candidatus</i> Brocadia sp. clone AmxW-WSK-31 (JX243634.1)	78	<i>Planctomycetia</i> ; <i>Candidatus</i> Brocadiales; <i>Candidatus</i> Brocadiaceae; <i>Candidatus</i> Brocadia
Amx2	<i>Desulfovibrio vietnamensis</i> (NR_026303.1)	81	<i>Deltaproteobacteria</i> ; <i>Desulfovibrionales</i> ; <i>Desulfovibrionaceae</i> ; <i>Desulfovibrio</i>
	<i>Hippea</i> sp. Lau09-781r (FR754501.1)	81	<i>Deltaproteobacteria</i> ; <i>Desulfurellales</i> ; <i>Desulfurellaceae</i> ; <i>Hippea</i>
	<i>Candidatus</i> Scalindua wagneri (AY254882.1)	80	<i>Planctomycetia</i> ; <i>Candidatus</i> Brocadiales; <i>Candidatus</i> Brocadiaceae; <i>Candidatus</i> Scalindua
	<i>Deferribacter autotropicus</i> (NR_044488.1)	80	<i>Deferribacteres</i> ; <i>Deferribacterales</i> ; <i>Deferribacteraceae</i> ; <i>Deferribacter</i>

## 6.6 Autotrophic microorganisms (*cbbLR* / *cbbLG* / *cbbM* genes)

RuBisCO (ribulose 1,5 bisphosphate carboxylase / oxygenase) is the enzyme responsible for CO<sub>2</sub> fixation in the most widespread CO<sub>2</sub> fixation pathway, the Calvin-Benson-Bassham cycle. There are at least three forms of RuBisCO (Badger & Bek, 2010). Form I RuBisCO is the most common and is found in plants as well as in photo- and chemoautotrophic microorganisms. The *cbbL* gene encodes the large subunit of the enzyme and is about 1,400 bp long. Form II RuBisCO (*cbbM*) is found exclusively in microorganisms (both photo- and chemoautotrophs) and is said to have a lower catalytic activity, being efficient only at low O<sub>2</sub> and elevated CO<sub>2</sub> concentrations (Badger & Bek, 2010). Many bacteria have both form I and form II RuBisCO (such as *Thiobacillus denitrificans*) allowing these organisms to adjust to fluctuations in oxygen. Form I RuBisCO is further divided into the green-like group, *cbbLG*, (containing further subdivisions IA and IB), and the red-like group, *cbbLR*, (subdivided into IC and ID). The green-like RuBisCO is found in *Cyanobacteria* and *Proteobacteria*, while the red-like form is found in *Proteobacteria* and *Archaea*. Form II is found in *Proteobacteria*, while form III has so far only been found in *Archaea* (Badger & Bek, 2010).

For an indication of the autotrophs present in Movile Cave, PCR primers targeting the different forms of RuBisCO were used to screen water, floating mat and wall biofilm samples. DNA extracted from <sup>13</sup>C<sub>2</sub> SIP enrichments was not analysed with these primers due to the lack of <sup>13</sup>C-incorporation into DNA (see section 6.3.4 (iv)). Both green-like (*cbbLG*) and red-like (*cbbLR*) RuBisCO sequences were amplified from all samples tested (Table 6.2). No amplification products were obtained for RuBisCO II (*cbbM*). However, this probably requires optimisation of the PCR protocol since previous studies (e.g. Chen *et al.*, 2009) detected RuBisCO II genes in Movile Cave. Both *cbbLR* sequences analysed were identical and related most closely to RuBisCO from *Rhizobiales* and *Burkholderiales* with 93% amino acid sequence identity (96% similarity; Table 6.9). The two *cbbLG* sequences were also identical and related most closely to RuBisCO from sulfur and metal-oxidising bacteria (*Thiobacillus*, *Cupridavidus*, *Sideroxydans*) within the *Betaproteobacteria* (93% identity; 96% similarity; Table 6.10).

**Table 6.9** Phylogenetic affiliations of translated *cbbLR* sequences from Movile Cave (Lake room, floating mat)

Clones	Closest GenBank Relatives (accession code)	<sup>(1)</sup> Identities (%) / <sup>(1)</sup> Similarity (%)	Phylogenetic affiliation of GenBank relative
R2_1b R2_1a	RuBisCO [uncultured bacterium]; tar oil-contaminated aquifer (ACH70435.1)	98 / 99	Not specified
	RuBisCO [ <i>Ochrobactrum anthropi</i> ] (AAU86945.1)	95 / 98	<i>Alphaproteobacteria; Rhizobiales;</i> <i>Brucellaceae; Ochrobactrum</i>
	RuBisCO [ <i>Alcaligenes</i> sp. DSM 30128] (AAU86939.1)	95 / 98	<i>Betaproteobacteria; Burkholderiales;</i> <i>Alcaligenaceae; Alcaligenes</i>
	RuBisCO [ <i>Sinorhizobium meliloti</i> ] (NP_436731.1)	95 / 97	<i>Alphaproteobacteria; Rhizobiales;</i> <i>Rhizobiaceae; Sinorhizobium</i>

<sup>(1)</sup> Sequence analysis was carried out using the blastx algorithm (alignment of translated nucleotide sequences against protein database); hence, identity and similarity values refer to amino acid sequences.

**Table 6.10** Phylogenetic affiliations of translated *cbbLG* sequences from Movile Cave (Lake room, floating mat)

Clones	Closest GenBank relatives (accession code)	<sup>(1)</sup> Identities (%) / <sup>(1)</sup> Similarity (%)	Phylogenetic affiliations of GenBank relatives
G2_1 G2_2	RuBisCO [ <i>Thiobacillus denitrificans</i> ] (YP_316382.1)	93 / 96	<i>Betaproteobacteria; Hydrogenophilales;</i> <i>Hydrogenophilaceae; Thiobacillus</i>
	RuBisCO [ <i>Cupriavidus metallidurans</i> ] (YP_583653.1)	93 / 96	<i>Betaproteobacteria; Burkholderiales;</i> <i>Burkholderiaceae; Cupriavidus</i>
	RuBisCO [ <i>Sideroxydans lithotrophicus</i> ] (YP_003523610.1)	93 / 96	<i>Betaproteobacteria; Gallionellales;</i> <i>Gallionellaceae; Sideroxydans</i>
	RuBisCO [ <i>Thiobacillus thiophilus</i> ] (ACF06645.1)	92 / 95	<i>Betaproteobacteria; Hydrogenophilales;</i> <i>Hydrogenophilaceae; Thiobacillus</i>
	RuBisCO [ <i>Acidithiobacillus ferrooxidans</i> ] (6878659 rbcL)	92 / 95	<i>Gammaproteobacteria;</i> <i>Acidithiobacillales; Acidithiobacillaceae;</i> <i>Acidithiobacillus</i>

<sup>(1)</sup> Sequence analysis was carried out using the blastx algorithm (alignment of translated nucleotide sequences against protein database); hence, identity and similarity values refer to amino acid sequences.

For a more in-depth survey of the diversity of autotrophs in Movile Cave, larger clone libraries or high-throughput pyrosequencing data will be required. It should also be considered that some microorganisms use other pathways for CO<sub>2</sub> fixation, such as the reductive TCA cycle in some anaerobic bacteria, the reductive acetyl-CoA pathway in methanogenic archaea and acetogenic bacteria, and the 3-hydroxypropionate/4-hydroxybutyrate cycle found in some (facultatively) autotrophic bacteria and archaea (Fuchs & Schlegel, 2007). The latter pathway has been found in *Crenarchaeota* (*Sulfolobales*, *Desulfurococcales*, and *Thermoproteales*), *Euryarchaeota* (*Archaeoglobales* and *Thermoplasmatales*) as well as *Thaumarchaeota* (reviewed by Nicol & Prosser, 2011). This is of special interest with respect to ammonia-oxidising archaea in Movile Cave. Primers are available for *hcd*, coding for 4-Hydroxybutyryl-CoA dehydratase (4HCD), a key enzyme in this pathway (Offre *et al.*, 2011). Real-time PCR of *cbbL* and *hcd* genes might be a useful tool to assess the activity of bacterial and archaeal autotrophs in Movile Cave and gain an indication of their relative contributions to primary production. RNA-SIP could also be a useful way to identify active CO<sub>2</sub>-fixing organisms, as this is more sensitive than DNA-SIP.

## **Chapter 7. Summary and Outlook**

## 7.1 Well-known and new methylotrophs are active in Movile Cave

Active MMA-utilising bacteria identified by DNA-SIP experiments with CO<sub>2</sub>-labelled MMA and DMA (Chapter 4) included both well-characterised and novel methylotrophs: *Methylotenera mobilis* was confirmed as one of the major MMA-utilising methylotrophs in Movile Cave. In addition, SIP results revealed that novel methylotrophs from the genus *Catellibacterium* (known for aromatic compound degradation) are among the most active MMA and DMA utilisers in Movile Cave. Cultivation-based studies consolidated these results with the isolation of *Catellibacterium* sp. LW-1, a new methylotrophic bacterium able to grow on MMA and TMA (but interestingly not DMA). Cultivation work furthermore resulted in the isolation of *Mesorhizobium* sp. 1M-11, able to grow on MMA, DMA and TMA, and thereby representing the first member of the genus *Mesorhizobium* known to grow methylotrophically.

Data from SIP enrichments also suggested that *Cupriavidus*, *Porphyrobacter* and *Altererythrobacter* might play a role in methylotrophic MMA utilisation in Movile Cave alongside known methylotrophs such as *Methylobacterium* and *Methylovorus*. While these organisms were not isolated from the cave and have hence not been tested for growth with methylated amines in this study, published genomes of some *Cupriavidus* / *Ralstonia* species were found to contain *gmaS* (refer to phylogenetic trees in Figures 5.12 and 5.14), and recent studies have reported methylotrophic growth for two different *Cupriavidus* strains on c1 compounds (Hung *et al.*, 2011; Habibi & Vahabzadeh, 2013). Similarly, methylotrophic growth was reported for a *Porphyrobacter* species (Fuerst *et al.*, 1993). In conclusion, organisms not generally associated with methylotrophy may be key players in degradation of methylated amines and carbon cycling in Movile Cave.

## 7.2 Methylated amines are a nitrogen source for many non-methylotrophs

Cultivation-based studies (Chapter 3) revealed that a large variety of bacteria in Movile Cave are able to use methylated amines as a nitrogen (but not carbon) source. These results are intriguing considering the relatively high standing concentrations of NH<sub>4</sub><sup>+</sup> present in Movile Cave water. It is possible that NH<sub>4</sub><sup>+</sup>-depleted areas exist within the microbial mats where utilisation of MMA is advantageous. The fact that nitrogen in the mat is isotopically light while NH<sub>4</sub><sup>+</sup> in the cave water is heavy (Sârbu *et al.*, 1996) could be the result of isotopic fractionation during NH<sub>4</sub><sup>+</sup> assimilation or nitrification. It may however also indicate that a

nitrogen source other than  $\text{NH}_4^+$  is used. When growing methylotrophically, some bacterial species have been shown to use the nitrogen of MMA, even when high  $\text{NH}_4^+$  concentrations are present (Bellion *et al.*, 1983). The high concentrations of  $\text{NH}_4^+$  may even be partly due to release of excess nitrogen by bacteria using MMA as both a carbon and nitrogen source.

### 7.3 Distribution of the *gmaS* gene and its use as a biomarker

#### 7.3.1 *gmaS* is widespread among methylotrophic and non-methylotrophic bacteria

Based on PCR screening of Movile Cave isolates, *gmaS*, key gene for the recently characterised indirect MMA oxidation pathway, appears to be widespread amongst methylotrophic and non-methylotrophic methylated amine-utilising bacteria: While all tested isolates carried *gmaS*, *mauA* was detected only in a number of methylotrophic MMA utilisers in addition to *gmaS*. The presence of *gmaS* in all non-methylotrophic MMA-utilisers isolated from Movile Cave agrees with previously published results by Chen *et al.* (2011). Taken together, these results suggest that the indirect pathway is the major mode of MMA utilisation in bacteria using MMA as a nitrogen, but not as a carbon, source. Based on our results, the *gmaS*-dependent pathway also appears to be present in the majority of methylotrophic MMA utilisers. In conclusion, the indirect pathway via GMA and / or NMG may in fact be the dominant mode of MMA oxidation in bacteria, while the direct, MMA dehydrogenase (*mauA*) dependent pathway seems to be restricted to certain groups of methylotrophic bacteria. It will be interesting to understand how the two pathways are regulated under different growth conditions in bacteria containing both pathways.

#### 7.3.2 New *gmaS* primers are an effective biomarker

The PCR-primers developed in this study (Chapter 5) are the first primers which target *gmaS* from non-marine bacteria. The new primer sets proved successful in the detection of *gmaS* from bacterial isolates as well as non-genomic DNA. They therefore present a powerful tool for the detection of MMA-oxidising bacteria in the environment which remain undetected by currently available primer sets. In addition to amplifying *gmaS* from Movile Cave samples, the new PCR primer sets also detected *gmaS* sequences in soil and freshwater samples unrelated to Movile Cave. Preliminary *gmaS* surveys of these samples revealed a considerable diversity of *gmaS* sequences, many of which were not closely related to *gmaS* sequences from

known MMA utilisers (Figure 5.14). The new primers may therefore provide a useful tool for the detection of currently unidentified MMA-oxidising bacteria.

### 7.3.3 *Preliminary gmaS surveys suggest a wide diversity of gmaS-containing bacteria in the environment*

The fact that many of the *gmaS* sequences retrieved from lake and soil samples were not closely related to *gmaS* sequences from published genomes or Movile Cave isolates is intriguing and suggests that methylated amine-utilising bacteria in the environment may be more diverse than currently recognised. Considering that only a small number of *gmaS* clones from these samples were sequenced, one can assume that there is even greater diversity of *gmaS*-containing bacteria than indicated by this preliminary survey. More extensive PCR-based surveys (using larger clone libraries or high-throughput sequencing) are necessary to assess the full diversity of *gmaS*-containing bacteria, both in Movile Cave and in other environments. Expression-based studies of *gmaS* (and *mauA*) could provide a better understanding of activity of MMA oxidisers.

Intriguingly, preliminary data from BLAST searches and alignment of the new *gmaS* sequences with sequences from published genomes even suggests the possible presence of *gmaS* genes in *actinobacterial* and *cyanobacterial* species. Testing representatives of the identified organisms for growth with MMA as a nitrogen (possibly even carbon) source would be an important first step in determining whether these putative *gmaS* genes do indeed signify the presence of MMA-oxidising pathways in bacterial phyla not currently associated with methylamine metabolism.

## 7.4 Key processes of the nitrogen cycle in Movile Cave

### 7.4.1 *Nitrifiers are active, but not dominant, primary producers in Movile Cave*

Results presented in Chapter 6 revealed that nitrifiers are active in Movile Cave but may not be the dominant primary producers. While  $^{13}\text{CO}_2 / \text{NH}_4^+$  SIP incubations failed to identify any active autotrophs due to insufficient  $^{13}\text{C}$ -labelling of DNA, the results obtained from nitrifying enrichments and *amoA* gene surveys confirmed both the presence and activity of ammonium oxidisers in Movile Cave (supporting results from  $^{13}\text{CO}_2 / \text{NH}_4^+$  SIP enrichments by Chen et al., 2009). Both bacterial and archaeal *amoA* genes were identified and preliminary PCR-

based results suggested that there is a niche separation between the two groups, with bacteria dominating in the floating mats, and archaea thriving in the water, where lower  $\text{NH}_4^+$  concentrations were measured. While no nitrite oxidisers were detected using *nxrB* primers, *Nitrospira* was detected by 16S rRNA gene based DGGE of  $^{13}\text{CO}_2 / \text{NH}_4^+$  SIP enrichments.

The relative contribution of nitrifiers to primary production in Movile Cave will require further studies; however, preliminary results from this PhD project suggest that sulfur oxidisers, and not nitrifiers, are the dominant autotrophs in Movile Cave: 16S rRNA gene sequencing of DGGE bands from  $^{13}\text{CO}_2 / \text{NH}_4^+$  SIPs revealed only one nitrifier-related sequence (*Nitrospira*) along with many sequences of sulfur oxidizers. For future experiments, high throughput sequencing analysis of enriched DNA might provide a higher resolution than DGGE and detect additional sequences. Even though nitrifiers appear to be less abundant than sulfur oxidisers, their contribution to the food web may still be important, both in their contribution to  $\text{CO}_2$  fixation, and in providing  $\text{NO}_3^-$  to the system, which may even be used an electron acceptor by anaerobic sulfur oxidisers. For future SIP experiments, it may be advisable to adjust the amount of  $^{13}\text{CO}_2$  added to the incubations based on the amount of biomass present. In addition, the coupling of expression-based studies to process-based experiments will be useful for a better understanding of the contribution of nitrifiers to primary production and nitrogen cycling in Movile Cave.

#### 7.4.2 $\text{N}_2$ fixation

While PCR surveys of *nifH* genes revealed a diversity of bacteria with the genetic potential to fix  $\text{N}_2$ , process-based studies performed in this PhD did not give any indication for nitrogenase activity in Movile Cave samples. This is in contrast to reported  $\text{N}_2$  fixing activity in floating mats from Frasassi (Desai *et al.*, 2013), a sulfur-driven cave ecosystem with standing  $\text{NH}_4^+$  concentration similar to those measured in Movile Cave (Sârbu *et al.*, 2002). It may be worth complementing the results obtained from acetylene reduction assays with gene expression studies.

#### 7.4.3 Anaerobic nitrogen respiration

Confirming results from past studies, PCR surveys of key genes for denitrification (*nirS* and *nirK*) revealed a diversity of organisms with the genetic potential to denitrify. Similarly, 16S rRNA genes related to anammox-associated planctomycetes were present in the anoxic sediment. Process-based studies hinted at activity of both processes (with denitrification being dominant) but were of a preliminary nature and need to be consolidated.

## 7.5 Future studies

### 7.5.1 Methodological considerations

The combination of SIP and cultivation proved very effective for the identification of methylotrophs. SIP enrichments allowed identification of methylotrophs not obtained by cultivation: While resisting all isolation attempts, *M. mobilis* was the first organism that responded to addition of MMA at 96 hours in SIP incubations. Additionally DNA-SIP uncovered potential new methylotrophs not previously associated with methylated amine metabolism: *Porphyrobacter*, *Altererythrobacter* and *Cupriavidus*. On the other hand, growth studies were essential in consolidating DNA-SIP results and confirming *Catellibacterium* as a novel methylotroph and active MMA-utilising bacterium in Movile Cave. The benefit of analysing SIP enrichments at different time points is highlighted by the shift observed in the methylotrophic community during incubation (while early time points were dominated by *M. mobilis*, this organism gave way to a diverse community of known and novel methylotrophs at later time points), avoiding the issue of only detecting the fastest-growing organisms.

DGGE, when compared to amplicon pyrosequencing is a relatively low resolution profiling technique. However, the DGGE technique enabled the accurate comparison of SIP enrichments across different CsCl gradient fractions (heavy to light) and also to compare  $^{13}\text{C}$ -incubations to  $^{12}\text{C}$ -incubated controls. DGGE fingerprinting thereby allowed the identification of key players in the microbial food web. Building on data obtained in this study, high resolution community profiling involving pyrosequencing of amplicons can be carried out in the future.

At the time of the SIP experiments, no robust method was available for accurately measuring concentrations of methylated amines. In future SIP experiments, the recently developed ion chromatography method for measuring methylated amines down to a detection limit of 1  $\mu\text{M}$  (Lidbury *et al.*, 2014) can be used to monitor substrate consumption and select SIP time points accordingly, which will enable a more accurate monitoring of the change in the microbial community in connection with potential cross-feeding of methylated amines down the food chain.

Unlike SIP enrichments with methylated amines, the DNA-SIP technique failed to identify active autotrophs in  $^{13}\text{CO}_2 / \text{NH}_4^+$  SIP incubations due to insufficient  $^{13}\text{C}$ -labelling of DNA. DNA-based SIP may not have been sensitive enough in this case due to high amounts of intrinsic  $\text{CO}_2$ . These experiments need to be revisited; a determination of the amounts of

biomass and intrinsic CO<sub>2</sub> present in the samples may be helpful in order to adjust the amount of <sup>13</sup>CO<sub>2</sub> added to the incubations, and RNA-SIP may be a better option. Pre-incubation of the samples may also be helpful (as indicated by successful <sup>13</sup>C-labelling in initial DNA-SIP experiments with <sup>13</sup>CO<sub>2</sub> by Chen et al., 2009). As a further point, future SIP experiments would benefit from more replication, provided that sufficient sample material is present at time of sampling.

Finally, more thorough chemical measurements of the water and floating mats inside Movile Cave along with process-based measurements could give a better understanding of the carbon and energy sources available and their turnover in the microbial foodweb in Movile Cave, allowing setting up experiments accordingly. While SIP experiments were valuable in identifying active methylotrophs present in Movile Cave, it is important to remember that these results are based on laboratory enrichments and may not necessarily reflect the microbial key players in the *in situ* communities. Given that most of the methylotrophs identified in in this PhD are facultative in their use of C<sub>1</sub> compounds, knowledge of the dissolved organic carbon concentrations in Movile Cave could provide important information on the role of methylated amines as carbon sources for future studies.

### 7.5.2 H<sub>2</sub> oxidation and anaerobic processes in Movile Cave

In addition to methane, sulfur and ammonium, H<sub>2</sub> may be an important electron donor in Movile Cave, both for aerobic and anaerobic processes. H<sub>2</sub> is produced in large amounts during anaerobic degradation of organic matter, and a physiologically wide range of bacteria and archaea, both aerobic and anaerobic, can use H<sub>2</sub> chemolithotrophically (Fuchs & Schlegel, 2007). Hydrogenotrophs are often facultative chemolithoautotrophs and may be potential primary producers in Movile Cave. Hydrogenotrophs include species of *Paracoccus*, *Ralstonia* and *Hydrogenophaga* (Fuchs & Schlegel, 2007). Several species of *Hydrogenophaga* were identified in enrichments from floating mat samples (including no-substrate controls) in this PhD.

As outlined in Chapter 1, processes in the anoxic regions of Movile Cave remain largely unexplored. PCR-based surveys of *nirS* and *nirK* genes suggested a diversity of organisms possessing dissimilatory nitrite reductase. However, to determine activity of potential denitrifiers, more in depth process-based measurements and gene expression studies are required. In addition to further exploring the anaerobic processes touched upon in this PhD thesis (denitrification and anammox), it may be of interest to look more closely into the

role of H<sub>2</sub> as an electron donor for anaerobic processes such as sulfate reduction, homoacetogenesis and methanogenesis.

Considering the high amounts of methane in Movile Cave, and the fact that large parts of the water and sediment are anoxic, a further process of potential relevance may be anaerobic methane oxidation (linked to sulfate reduction, denitrification or reduction of metals such as iron and manganese). The recent isolation of a methylated amine-utilising methanogenic archaeon from Movile Cave raises the interesting question whether methylated amines may also have a role as carbon and energy source for anaerobic microorganisms in the cave.

## References

- Abdul-Rashid MK, Riley JP, Fitzsimons MF, Wolff GA. (1991). Determination of volatile amines in sediment and water samples. *Anal Chim Acta* **252**: 223-226.
- Alawi M, Lipski A, Sanders T, Pfeiffer EM, Spieck E. (2007). Cultivation of a novel cold-adapted nitrite oxidizing betaproteobacterium from the Siberian Arctic. *ISME J* **1**: 256-264.
- Altschul SF, Gish W, Miller W, Myers EW, Lipman DJ. (1990). Basic local alignment search tool. *J Mol Biol* **215**: 403-410.
- Anil Kumar P, Srinivas TN, Sasikala Ch, Ramana ChV. (2007). *Rhodobacter changlensis* sp. nov., a psychrotolerant, phototrophic alphaproteobacterium from the Himalayas of India. *Int J Syst Evol Microbiol* **57**: 2568-2571.
- Anthony C. (1982). *The Biochemistry of Methyloproteobacteria*. Academic Press: London.
- Antony CP, Kumaresan D, Ferrando L, Boden R, Moussard H, Scavino AF, Shouche YS, Murrell JC. (2010). Active methyloproteobacteria in the sediments of Lonar Lake, a saline and alkaline ecosystem formed by meteor impact. *ISME J* **4**: 1470-80.
- Badger MR, Bek EJ. (2008). Multiple RuBisCO forms in proteobacteria: their functional significance in relation to CO<sub>2</sub> acquisition by the CBB cycle *J Exp Bot* **59**: 1525-1541.
- Baev MV, Kiriukhin MY, Tsygankov YD. (1997). Regulation of ammonia assimilation in an obligate methyloproteobacterium *Methylobacillus flagellatum* under steady-state and transient growth conditions. *A Van Leeuw* **71**: 353-61.
- Barrett EL, Kwan HS. (1985). Bacterial reduction of trimethylamine oxide. *Annu Rev Microbiol* **39**: 131-149.
- Beal EJ, House CH, Orphan VJ. (2009). Manganese- and iron-dependent marine methane oxidation. *Science* **325**: 184-187.
- Bellion E, Bolbot J. (1983). Nitrogen assimilation in facultative methyloproteobacterial bacteria. *Curr Microbiol* **9**: 37-44.
- Bellion E, Hersh LB. (1972). Methylamine metabolism in a *Pseudomonas* species. *Arch Biochem Biophys* **153**: 368-374.
- Bellion E, Kent ME, Aud JC, Alikhan MY, Bolbot JA. (1983.) Uptake of methylamine and methanol by *Pseudomonas* sp. strain AM1. *J Bacteriol* **154**: 1168-1173.
- Berman T, Bronk DA. (2003). Dissolved organic nitrogen: a dynamic participant in aquatic ecosystems. *Aquat Microb Ecol* **31**: 279-305.
- Bicknell B, Owens JD. (1980). Utilization of methyl amines as nitrogen sources by non-methyloproteobacteria. *J Gen Microbiol* **117**: 89-96.
- Boden, R., Murrell, J.C., and Schäfer, H. (2011) Dimethylsulfide is an energy source for the heterotrophic marine bacterium *Sagittula stellata*. *FEMS Microbiol Lett* **322**: 188-193.
- Boden R, Thomas E, Savani P, Kelly DP, Wood AP. (2008). Novel methyloproteobacterial bacteria isolated from the River Thames (London, UK). *Environ Microbiol* **10**: 3225-3236.

- Bollmann A, French E, Laanbroek HJ. (2011). Isolation, cultivation, and characterization of ammonia-oxidizing bacteria and archaea adapted to low ammonium concentrations. *Methods Enzymol* **486**: 55-88.
- Bottomley PJ. (1992). Ecology of *Bradyrhizobium* and *Rhizobium*, In: Stacey G, Burris RH, Evans HJ (eds). *Biological Nitrogen Fixation*, Chapman and Hall: New York, pp 292-347.
- Braker G, Fesefeldt A, Witzel KP. (1998). Development of PCR primer systems for amplification of nitrite reductase genes (*nirK* and *nirS*) to detect denitrifying bacteria in environmental samples. *Appl Environ Microbiol* **64**: 3769-75.
- Braker G, Zhou J, Wu L, Devol AH, Tiedje JM. (2000). Nitrite reductase genes (*nirK* and *nirS*) as functional markers to investigate diversity of denitrifying bacteria in Pacific northwest marine sediment communities. *Appl Environ Microbiol* **66**: 2096–2104.
- Brochier-Armanet C, Boussau B, Gribaldo S, Forterre P. (2008). Mesophilic Crenarchaeota: proposal for a third archaeal phylum, the Thaumarchaeota. *Nat Rev Microbiol* **6**: 245-52.
- Bronk DA. (2002). Dynamics of organic nitrogen. In: Hansell DA, Carlson CA (eds) *Biogeochemistry of Marine Dissolved Organic Matter*, Academic Press: San Diego, p 153–247.
- Brooke AG, Attwood MM. (1984). Methylamine uptake by the facultative methylotroph *Hyphomicrobium* X. *J Gen Microbiol* **130**: 459–463.
- Buckley D, Graber J, Schmidt T. (1998). Phylogenetic analysis of nonthermophilic members of the kingdom Crenarchaeota and their diversity and abundance in soils. *Appl Environ Microbiol* **64**: 4333-4339.
- Budd JA, Spencer CP. (1968). The utilisation of alkylated amines by marine bacteria. *Mar Biol* **2**: 92-101.
- Burg MB, Ferraris JD. (2008). Intracellular organic osmolytes: function and regulation. *J Biol Chem* **283**: 7309-13.
- Camacho C, Coulouris G, Avagyan V, Ma N, Papadopoulos J, Bealer K, Madden TL. (2009). BLAST+: architecture and applications. *BMC Bioinformatics* **10**: 421.
- Campbell KA. (2006). Hydrocarbon seep and hydrothermal vent paleoenvironments and paleontology: past developments and future research directions. *Palaeogeogr Palaeoclimatol* **232**: 362–407.
- Chen WM, Cho NT, Huang WC, Young CC, Sheu SY. (2013). Description of *Gemmobacter fontiphilus* sp. nov., isolated from a freshwater spring, reclassification of *Catellibacterium nectariphilum* as *Gemmobacter nectariphilus* comb. nov., *Catellibacterium changlense* as *Gemmobacter changlensis* comb. nov., *Catellibacterium aquatile* as *Gemmobacter aquaticus* nom. nov., *Catellibacterium caeni* as *Gemmobacter caeni* comb. nov., *Catellibacterium nanjingense* as *Gemmobacter nanjingensis* comb. nov., and emended description of the genus *Gemmobacter* and of *Gemmobacter aquatilis*. *Int J Syst Evol Microbiol* **63**: 470-878.
- Chen Y. (2012) Comparative genomics of methylated amine utilization by marine *Roseobacter* clade bacteria and development of functional gene markers (*tmm*, *gmaS*). *Environ Microbiol* **14**: 2308–2322.
- Chen Y, McAleer KL, Murrell JC. (2010b). Monomethylamine as a nitrogen source for a non-methylotrophic bacterium, *Agrobacterium tumefaciens*. *Appl Environ Microbiol* **76**: 4102-4104.

- Chen Y, Scanlan J, Song L, Crombie A, Rahman MT, Schäfer H *et al.* (2010a). Gamma-glutamylmethylamide is an essential intermediate for monomethylamine metabolism in *Methylocella silvestris*. *Appl Environ Microbiol* **76**: 4530-4537.
- Chen Y, Wu L, Boden R, Hillebrand A, Kumaresan D, Moussard H *et al.* (2009). Life without light: microbial diversity and evidence of sulfur- and  $\text{NH}_4^+$ -based chemolithotrophy in Movile Cave. *ISME J* **3**: 1093-1104.
- Chen XP, Zhu YG, Xia Y, Shen JP, He JZ. (2008). Ammonia-oxidizing archaea: important players in paddy rhizosphere soil? *Environ Microbiol* **10**: 1978-1987.
- Chistoserdova L. (2011). Modularity of methylotrophy, revisited. *Environ Microbiol* **13**: 2603-2622.
- Chistoserdova L, Kalyuzhnaya MG, Lidstrom ME. (2009). The expanding world of methylotrophic metabolism. *Annu Rev Microbiol* **63**: 477-499.
- Coci M, Bodelier PLE, Laanbroek HJ. (2008). Epiphyton as a niche for ammonia-oxidizing bacteria: detailed comparison with benthic and pelagic compartments in shallow freshwater lakes. *Appl Environ Microbiol* **74**: 1963-1971.
- Colby J, Zatman LJ. (1973). Trimethylamine metabolism in obligate and facultative methylotrophs. *Biochem J* **132**: 101-12.
- Crombie AT, Murrell JC. (2014). Trace-gas metabolic versatility of the facultative methanotroph *Methylocella silvestris*. *Nature* **510**: 148-151.
- Daebeler A, Abell GC, Bodelier PL, Bodrossy L, Frampton DM, Hefting MM, Laanbroek HJ. (2012). Archaeal dominated ammonia-oxidizing communities in Icelandic grassland soils are moderately affected by long-term N fertilization and geothermal heating. *Front Microbiol* **3**: 352.
- Dalsgaard T, Thamdrup B, Canfield DE. (2005). Anaerobic ammonium oxidation (anammox) in the marine environment. *Res Microbiol.* **156**: 457-464.
- Dawes IW, Sutherland IW. (1992). *Microbial Physiology*. 2nd edition. Blackwell Scientific Publications: Oxford, UK, 289 pages.
- DeLong EF. (1992). *Archaea* in coastal marine environments. *Proc Natl Acad Sci USA* **89**: 5685-5689.
- de Boer W, Kowalchuk GA. (2001). Nitrification in acid soils: Micro-organisms and mechanisms. *Soil Biol Biochem* **33**: 853-866.
- Di HJ, Cameron KC, Shen JP, Winefield CS, O'Callaghan M, Bowatte S, He JZ. (2010). Ammonia-oxidizing bacteria and archaea grow under contrasting soil nitrogen conditions. *FEMS Microbiol Ecol* **72**: 386-394.
- Diekert G, Wohlfarth G. (1994). Metabolism of homoacetogens. *A Van Leeuw* **66**: 209-221.
- Dijkhuizen L, Arfman N, Attwood MM, Brooke AG, Harder W, Watling EM. (1988). Isolation and initial characterization of thermotolerant methylotrophic *Bacillus* strains. *FEMS Microbiol Lett* **52**: 209-214.
- Dilworth MJ. (1966). Acetylene reduction by nitrogen fixing preparations from *Clostridium pasteurianum*. *Biochim Biophys Acta* **127**: 285-294.
- Engel AS. (2007). Observation on the biodiversity of sulfidic karst habitats. *J Cave Karst Stud* **69**: 187-206.

Ettwig KF, Butler MK, Le Paslier D, Pelletier E, Mangenot S, Kuypers MM, Schreiber F, Dutilh BE, Zedelius J, de Beer D, Gloerich J, Wessels HJ, van Alen T, Luesken F, Wu ML, van de Pas-Schoonen KT, Op den Camp HJ, Janssen-Megens EM, Francoijs KJ, Stunnenberg H, Weissenbach J, Jetten MS, Strous M. (2010). Nitrite-driven anaerobic methane oxidation by oxygenic bacteria. *Nature*. **464**: 543-548.

Felsenstein J. (1985). Confidence limits on phylogenies: An approach using the bootstrap. *Evolution* (N Y) **39**: 783-791.

Fitzsimons MF, Jemmett AW, Wolff GA. (1997). A preliminary study of the geochemistry of methylamines in a salt marsh. *Org Geochem* **27**: 15-24.

Fitzsimons MF, Kamhi-Danon B, Dawit M. (2001). Distributions and adsorption of the methylamines in the inter-tidal sediments of an East Anglian estuary. *Environ Exp Bot* **46**: 225-236.

Fitzsimons MF, Millward GE, Revitt DM, Dawit MD. (2006). Desorption kinetics of  $\text{NH}_4^+$  and methylamines from estuarine sediments: consequences for the cycling of nitrogen. *Mar Chem* **101**: 12-26.

Forti P, Galdenzi S, Sârbu ŞM. (2002). The hypogenic caves: a powerful tool for the study of seeps and their environmental effects. *Cont Shelf Res* **22**: 2373-2386.

Francis C, Roberts K, Beman J, Santoro A, Oakley B. (2005). Ubiquity and diversity of ammonia-oxidizing archaea in water columns and sediments of the ocean. *Proc Natl Acad Sci USA* **102**: 14683-14688.

French E, Kozłowski JA, Mukherjee M, Bullerjahn G, Bollmann A. (2012). Ecophysiological characterization of ammonia-oxidizing archaea and bacteria from freshwater. *Appl Environ Microbiol* **78**: 5773-80.

Fuchs G. (2009). Diversity of metabolic pathways: Assimilation of macroelements and microelements. In: Lengeler J, Drews G, Schlegel H (eds). *Biology of the Prokaryotes*, John Wiley & Sons: New York, USA, 984 pages.

Fuchs G (ed.), Schlegel HG. (2007). *Allgemeine Mikrobiologie, 8th edition*. Thieme Verlag: Stuttgart, Germany, 678 pages.

Fuerst JA, Hawkins JA, Holmes A, Sly LI, Moore CJ, Stackebrandt E. (1993). *Porphyrobacter neustonensis* gen. nov., sp. nov., an aerobic bacteriochlorophyll-synthesizing budding bacterium from fresh water. *Int J Syst Bacteriol*. **43**: 125-34.

Fuhrman J, McCallum K, Davis A. (1992). Novel major archaeobacterial group from marine plankton. *Nature* **356**: 148-149.

Gantner S, Andersson AF, Alonso-Sáez L, Bertilsson S. (2011). Novel primers for 16S rRNA-based archaeal community analyses in environmental samples. *J Microbiol Methods* **84**: 12-18.

Ganzert L, Schirmack J, Alawi M, Mangelsdorf K, Sand W, Hillebrand-Voiculescu A, Wagner D. (2014) *Methanosarcina spelaei* sp. nov., a methanogenic archaeon isolated from a floating biofilm of a subsurface sulphurous lake in the Movile Cave, Romania. *Int J Syst Evol Microbiol* **64**: 3478-3484.

Geisseler D, Horwath WR, Joergensen RG, Ludwig B. (2010). Pathways of nitrogen utilization by soil microorganisms - A review. *Soil Biol & Biochem* **42**: 2058 - 2067.

- Gibb SW, Mantoura RFC, Liss PS, Barlow RG. (1999). Distributions and biogeochemistries of methylamines and  $\text{NH}_4^+$  in the Arabian Sea. *Deep-Sea Res II* **46**: 593-615.
- Gibert, J. & L. Deharveng (2002): Subterranean ecosystems: a truncated functional biodiversity. *Bioscience* **52**: 473-481.
- Giri BJ, BAno N, Hollibaugh JT. (2004). Distribution of RuBisCO genotypes along a redox gradient in Mono Lake, California. *Appl Environ Microbiol* **70**: 3443-3448.
- Glenn AR, Dilworth MJ. (1984). Methylamine and  $\text{NH}_4^+$  transport system in *Rhizobium leguminosarum* MNF 3841. *J Gen Microbiol* **130**: 1961-1968.
- Großkopf R, Janssen PH, Liesack W. (1998). Diversity and structure of the methanogenic community in anoxic rice paddy soil microcosms as examined by cultivation and direct 16S rRNA gene sequence retrieval. *Appl. Environ. Microbiol* **64**: 960-969.
- Gruffaz C, Muller EE, Louhichi-Jelail Y, Nelli YR, Guichard G, Bringel F. (2014). Genes of the *N*-methylglutamate pathway are essential for growth of *Methylobacterium extorquens* DM4 with monomethylamine. *Appl Environ Microbiol* **80**: 3541-3550.
- Gubry-Rangin C, Nicol GW, Prosser JI. (2010). *Archaea* rather than bacteria control nitrification in two agricultural acidic soils. *FEMS Microbiol Ecol* **74**: 566-574.
- Habibi A1, Vahabzadeh F. (2013). Degradation of formaldehyde at high concentrations by phenol-adapted *Ralstonia eutropha* closely related to pink-pigmented facultative methylotrophs. *J Environ Sci Health A Tox Hazard Subst Environ Eng* **48**: 279-92.
- Hammes F, Vital M, Egli T. (2010). Critical evaluation of the volumetric “bottle effect” on microbial batch growth. *Appl Environ Microbiol* **76**: 1278-1281
- Haroon MF, Hu S, Shi Y, Imelfort M, Keller J, Hugenholtz P, Yuan Z, Tyson GW. (2013). Anaerobic oxidation of methane coupled to  $\text{NO}_3^-$  reduction in a novel archaeal lineage. *Nature* **500**: 567-570.
- Hatzenpichler R. (2012). Diversity, physiology, and niche differentiation of ammonia-oxidizing archaea. *Appl Environ Microbiol* **78**: 7501-7510.
- Hayat R, Ali S, Amara U, Khalid R, Ahmed I. (2010). Soil beneficial bacteria and their role in plant growth promotion: a review. *Ann Microbiol* **60**: 579-598.
- Herndl G, Reinthaler T, Teira E, van Aken A, Veth C, Pernthaler A, Pernthaler J. (2005). Contribution of *Archaea* to total prokaryotic production in the deep Atlantic Ocean. *Appl Environ Microbiol* **71**: 2303-2309.
- Holmes AJ, Costello AM, Lidstrom ME, Murrell JC. (1995). Evidence that particulate methane monooxygenase and ammonia monooxygenase may be evolutionarily related. *FEMS Microbiol Lett* **132**: 203-208.
- Hu S, Zeng RJ, Keller J, Lant PA, Yuan Z. (2011). Effect of  $\text{NO}_3^-$  and nitrite on the selection of microorganisms in the denitrifying anaerobic methane oxidation process. *Environmental Microbiol Rep* **3**: 315-319.
- Hung WL, Wade WG, Boden R, Kelly DP, Wood AP. (2011). Facultative methylotrophs from the human oral cavity and methylotrophy in strains of *Gordonia*, *Leifsonia*, and *Microbacterium*. *Arch Microbiol* **193**: 407-17.

- Hung WL, Wade WG, Chen Y, Kelly DP, Wood AP. (2012). Design and evaluation of novel primers for the detection of genes encoding diverse enzymes of methylophony and autotrophy. *Pol J Microbiol* **61**: 11-22.
- Hutchens E, Radajewski S, Dumont MG, McDonald IR, Murrell JC. (2004). Analysis of methanotrophic bacteria in Movile Cave by stable isotope probing. *Environ Microbiol* **6**: 111-120.
- Jetten MS, Niftrik LV, Strous M, Kartal B, Keltjens JT, Op den Camp HJ. (2009). Biochemistry and molecular biology of anammox bacteria. *Crit Rev Biochem Mol Biol* **44**: 65-84.
- Jürgens G, Lindstrom K, Saano A. (1997). Novel group within the kingdom Crenarchaeota from boreal forest soil. *Appl Environ Microbiol* **63**: 803-805.
- Jung MY, Park SJ, Min D, Kim JS, Rijpstra WI, Sinninghe Damsté JS, Kim GJ, Madsen EL, Rhee SK. (2011). Enrichment and characterization of an autotrophic ammonia-oxidizing archaeon of mesophilic crenarchaeal group I.1a from an agricultural soil. *Appl Environ Microbiol*. **77**: 8635-8647.
- Kalyuzhnaya MG, Bowerman S, Jimmie CL, Lidstrom ME, Chistoserdova L. (2006a). *Methylotenera mobilis* gen. nov., sp. nov., an obligately methylamine-utilizing bacterium within the family *Methylophilaceae*. *Int J Syst Evol Microbiol* **56**: 2819-2823.
- Kalyuzhnaya MG, De Marco P, Bowerman S, Pacheco CC, Lara JC, Lidstrom ME et al. (2006b). *Methyloversatilis universalis* gen. nov., sp. nov., a novel taxon within the *Betaproteobacteria* represented by three methylophylic isolates. *Int J Syst Evol Microbiol* **56**: 2517-2522.
- Kalyuzhnaya MG, Martens-Habbena W, Wang T, Hackett M, Stolyar SM, Stahl DA, Lidstrom ME, Chistoserdova L. (2009). Methylophilaceae link methanol oxidation to denitrification in freshwater lake sediment as suggested by stable isotope probing and pure culture analysis. *Environ Microbiol Rept* **1**: 385-392.
- Kaneko T, Nakamura Y, Sato S, Asamizu E, Kato T, Sasamoto S, Watanabe A, Idesawa K, Ishikawa A, Kawashima K, Kimura T, Kishida Y, Kiyokawa C, Kohara M, Matsumoto M, Matsuno A, Mochizuki Y, Nakayama S, Nakazaki N, Shimpo S, Sugimoto M, Takeuchi C, Yamada M, Tabata S. (2000). Complete genome structure of the nitrogen-fixing symbiotic bacterium *Mesorhizobium loti*. *DNA Res* **7**: 331-338.
- Karner M, DeLong E, Karl D. (2001). Archaeal dominance in the mesopelagic zone of the Pacific Ocean. *Nature* **409**: 507-510.
- Kartal B, de Almeida NM, Maalcke WJ, Op den Camp HJ, Jetten MS, Keltjens JT. (2013). How to make a living from anaerobic  $\text{NH}_4^+$  oxidation. *FEMS Microbiol Rev* **37**: 428-61.
- Kartal B, Kuypers MM, Lavik G, Schalk J, Op den Camp HJ, Jetten MS, Strous M. (2007). Anammox bacteria disguised as denitrifiers: nitrate reduction to dinitrogen gas via nitrite and ammonium. *Environ Microbiol* **9**: 635-642.
- Kartal B, Rattray J, van Niftrik LA, van de Vossenberg J, Schmid MC, Webb RI, Schouten S, Fuerst JA, Damsté JS, Jetten MS, Strous M. (2007). *Candidatus "Anammoxoglobus propionicus"* a new propionate oxidizing species of anaerobic  $\text{NH}_4^+$  oxidizing bacteria. *Syst Appl Microbiol* **30**: 39-49.
- Kartal B, van Niftrik L, Keltjens JT, Op den Camp HJ, Jetten MS. (2012). Anammox -- Growth Physiology, Cell Biology, and Metabolism. *Adv Microb Physiol* **60**: 211-262.

- Kelly DP, Wood AP. (1998). Microbes of the sulfur cycle. In: Burlage RS, Atlas R, Stahl D, Geesey G, Saylor C (eds). *Techniques in microbial ecology*. Oxford university press: New York, USA, pp. 31–57.
- King GM. (1988). Distribution and metabolism of quaternary amines in marine sediments. In: Blackburn TH, Sørensen J (eds). *Nitrogen Cycling in Coastal Marine Environments*, John Wiley & Sons: New York, USA, pp 143-173.
- King GM, Klug MJ, Lovley DR. (1983). Metabolism of acetate, methanol, and methylated amines in intertidal sediments of Lowes Cove, Maine. *Appl Environ Microbiol* **45**: 1848–1853.
- King GM, Weber CF (2007). Distribution, diversity and ecology of aerobic CO-oxidizing bacteria. *Nat Rev Microbiol* **5**: 107–118
- Knittel K, Boetius A. (2009). Anaerobic oxidation of methane: progress with an unknown process. *Ann Rev Microbiol* **63**: 311–334.
- Könneke M, Bernhard A, de la Torre J, Walker C, Waterbury J, Stahl D. (2005). Isolation of an autotrophic ammonia-oxidizing marine archaeon. *Nature* **437**: 543-546.
- Kowalchuk GA, Stephen JR. (2001). Ammonia-oxidizing bacteria: A model for molecular microbial ecology. *Ann Rev Microbiol* **55**: 485-529.
- Kraft B, Strous M, Tegetmeyer HE. (2011). Microbial NO<sub>3</sub><sup>-</sup> respiration -- genes, enzymes and environmental distribution. *J Biotechnol.* **155**: 104-17.
- Kumaresan D, Wischer D, Stephenson J, Hillebrand-Voiculescu A, Murrell JC. (2014). Microbiology of Movile Cave - A Chemolithoautotrophic Ecosystem. *Geomicrobiol J* **31**: 186-19.
- Kung HF, Wagner C (1969). Gamma-glutamylmethylamide. A new intermediate in the metabolism of methylamine. *J Biol Chem* **244**: 4136–40.
- Kwon KK, Woo JH, Yang SH, Kang JH, Kang SG, Kim SJ, Sato T, Kato C. *Altererythrobacter epoxidivorans* gen. nov., sp. nov., an epoxide hydrolase-active, mesophilic marine bacterium isolated from cold-seep sediment, and reclassification of *Erythrobacter luteolus* Yoon *et al.* 2005 as *Altererythrobacter luteolus* comb. nov. (2007). *Int J Syst Evol Microbiol.* **57**: 2207-2211.
- Kwon SW, Kim BY, Weon HY, Baek YK., Go SJ. (2007). *Arenimonas donghaensis* gen. nov., sp. nov., isolated from seashore sand. *Int J Syst Evol Microbiol* **57**: 954–958.
- Lane DJ. (1991). 16S/23S rRNA sequencing. In: Stackebrandt E, Goodfellow M (eds). *Nucleic Acid Techniques in Bacterial Systematics*. John Wiley & Sons Inc: Chichester, UK, pp 115–175.
- Lane DJ, Pace B, Olsen GJ, Stahl DA, Sogin ML, Pace NR. (1985). Rapid determination of 16S ribosomal RNA sequences for phylogenetic analyses. *Proc Natl Acad Sci USA* **82**: 6955–6959.
- Laranjo M, Alexandre A, Oliveira S. (2014). Legume growth-promoting rhizobia: An overview on the *Mesorhizobium* genus. *Microbiol Res* **169**: 2– 17.
- Latypova, E, Yang S, Wang YS, Wang T, Chavkin TA, Hackett M, Schäfer H, Kalyuzhnaya MG. (2010). Genetics of the glutamate-mediated methylamine utilization pathway in the facultative methylotrophic beta-proteobacterium *Methyloversatilis universalis* FAM5. *Mol Microbiol* **75**: 426-439.
- Lee C. (1988). Amino acid and amine biogeochemistry in marine particulate material and sediments. In: Blackburn TH, Sørensen J (eds). *Nitrogen Cycling in Coastal Marine Environments*, John Wiley & Sons: New York, USA, pp 125-141.

- Lehtovirta-Morley LE, Stoecker K, Vilcinskas A, Prosser JI, Nicol GW. (2011). Cultivation of an obligate acidophilic ammonia oxidiser from a nitrifying acid soil. *Proc Natl Acad Sci USA*. **108**: 15892-15897.
- Leininger S, Urlich T, Schloter M, Schwark L, Qi J, Nicol G, Prosser J, Schuster S, Schleper C. (2006). *Archaea* predominate among ammonia-oxidizing prokaryotes in soils. *Nature* **442**: 806-809.
- Levering PR, van Dijken JP, Veenhuis M, Harder W. (1981). *Arthrobacter* P1, a fast growing versatile methylotroph with amine oxidase as a key enzyme in the metabolism of methylated amines. *Arch Microbiol* **129**: 72–80.
- Li M, Ji-Dong Gu. (2011). Advances in methods for detection of anaerobic ammonium oxidizing (anammox) bacteria. *Appl Microbiol Biotechnol* **90**: 1241-1252.
- Lidbury I, Murrell JC, Chen Y. (2014). Trimethylamine *N*-oxide metabolism by abundant marine heterotrophic bacteria. *Proc Natl Acad Sci USA* **111**: 2710-2715.
- Lidstrom ME. (2006). Aerobic methylotrophic prokaryotes. In: Dworkin M, Falkow S, Rosenberg E, Schleifer K-H, Stackebrandt E (eds). *The Prokaryotes, Vol 2 (Ecophysiology and biochemistry)* Springer-Verlag: New York, USA, pp 618–634.
- Lin TY, Timasheff SN. (1994). Why do some organisms use a urea-methylamine mixture as osmolyte? Thermodynamic compensation of urea and trimethylamine *N*-oxide interactions with protein. *Biochemistry US* **33**: 12695–12701.
- Lindström K, Murwira M, Willems A, Altier N. (2010) The biodiversity of beneficial microbe-host mutualism: the case of rhizobia. *Res Microbiol* **161**: 453-463.
- Liu Y, Xu CJ, Jiang JT, Liu YH, Song XF, Li H *et al.* (2010). *Catellibacterium aquatile* sp. nov., isolated from fresh water, and emended description of the genus *Catellibacterium* Tanaka *et al.* 2004. *Int J Syst Evol Microbiol* **60**: 2027-2031.
- López-García P, Philippe H, Gail F, Moreira D. (2003). Autochthonous eukaryotic diversity in hydrothermal sediment and experimental microcolonizers at the mid-Atlantic Ridge. *PNAS* **100**: 697-702.
- Lücker S. (2010). Exploring the ecology and genomics of globally important nitrite-oxidizing bacteria. (PhD thesis).
- Lueders T, Wagner B, Claus P, Friedrich MW. (2004). Stable isotope probing of rRNA and DNA reveals a dynamic methylotroph community and trophic interactions with fungi and protozoa in oxic rice field soil. *Environ Microbiol* **6**: 60–72.
- Lutz RA, Kennish MJ. (1993). Ecology of deep-sea hydrothermal vent communities: A review. *Rev Geophys* **31**: 211–242.
- Madigan MT, Martinko JM, Dunlap PV, Clark DP. (2009). Brock Biology of Microorganisms, 12th edition, Pearson Benjamin-Cummings, San Francisco.
- Maixner F. (2010). The ecophysiology of nitrite-oxidizing bacteria in the genus *Nitrospira*: Novel aspects and unique features. (PhD thesis).
- Margulies M, Egholm M, Altman WE, Attiya S, Bader JS, Bemben LA, Berka J, Braverman MS, Chen YJ, Chen Z, Dewell SB, Du L, Fierro JM, Gomes XV, Godwin BC, He W, Helgesen S, Ho CH, Irzyk GP, Jando SC, Alenquer ML, Jarvie TP, Jirage KB, Kim JB, Knight JR, Lanza JR, Leamon JH, Lefkowitz SM, Lei M, Li J, Lohman KL, Lu H, Makhijani VB, McDade KE, McKenna MP, Myers EW, Nickerson E, Nobile JR, Plant R, Puc BP, Ronan MT, Roth GT, Sarkis GJ, Simons JF, Simpson

- JW, Srinivasan M, Tartaro KR, Tomasz A, Vogt KA, Volkmer GA, Wang SH, Wang Y, Weiner MP, Yu P, Begley RF, Rothberg JM. (2005). Genome sequencing in microfabricated high-density picolitre reactors. *Nature* **437**: 376–380.
- Markowitz VM, Chen IMA, Palaniappan K, Chu K, Szeto E, Grechkin Y *et al.* (2010). The integrated microbial genomes (IMG) system: an expanding comparative analysis resource. *Nucleic Acids Res* **38**: D382-D390.
- Martens-Habbena W, Berube PM, Urakawa H, de la Torre JR, Stahl DA. (2009). Ammonia oxidation kinetics determine niche separation of nitrifying *Archaea* and *Bacteria*. *Nature* **461**: 976–979.
- Martens-Habbena W, Stahl DA. (2011). Nitrogen metabolism and kinetics of ammonia-oxidizing archaea. *Methods Enzymol* **496**: 465-87.
- Martinez-Romero E. Dinitrogen-fixing prokaryotes. (2006). In: Truper HG, Dworkin M, Harder W, Schleifer KH (eds). *The Prokaryotes, Vol 2 (Ecophysiology and biochemistry)*, Springer-Verlag: New York, USA, pp. 793–817.
- McCarthy JJ. (1972). The uptake of urea by natural populations of marine phytoplankton. *Limnol Oceanogr* **17**: 738-748.
- Mehta MP, Butterfield DA, Baross JA. (2003). Phylogenetic diversity of nitrogenase (*nifH*) genes in deep-sea and hydrothermal vent environments of the Juan de Fuca Ridge. *Appl Environ Microbiol* **69**: 960-970.
- Meyer F, Paarmann D, D'Souza M, Olson R, Glass EM, Kubal M, Paczian T, Rodriguez A, Stevens R, Wilke A, Wilkening J, Edwards RA. (2008). The metagenomics RAST server – a public resource for the automatic phylogenetic and functional analysis of metagenomes. *BMC Bioinformatics* **9**: 386.
- Moussard H, Stralis-Pavese N, Bodrossy L, Neufeld JD, Murrell JC. (2009). Identification of active methylotrophic bacteria inhabiting surface sediment of a marine estuary. *Environ Microbiol Rep* **1**: 424-33.
- Mulder A, van de Graaf AA, Robertson LA, Kuenen JG. (1995). Anaerobic  $\text{NH}_4^+$  oxidation discovered in a denitrifying fluidized bed reactor. *FEMS Microbiol Ecol* **16**: 177–183.
- Murrell JC, Lidstrom ME. (1983). Nitrogen metabolism in *Xanthobacter* H<sub>4</sub>-14. *Arch Microbiol* **136**: 219-221.
- Murrell JC, Whiteley AS. (2011). *Stable Isotope Probing and Related Technologies*. American Society for Microbiology Press: Washington.
- Muschiol D, Traunspurger W. (2007). Life cycle and the calculation of the intrinsic rate of natural increase of two bacterivorous nematodes, *Panagrolaimus* sp. and *Poikilolaimus* sp. from chemoautotrophic Movile Cave, Romania. *Nematology*. **9**: 271-284.
- Muyzer G, De Waal EC, Uitterlinden AG. (1993). Profiling of complex microbial populations by denaturing gradient gel electrophoresis analysis of polymerase chain reaction-amplified genes coding for 16S rRNA. *Appl Environ Microbiol* **59**: 695-700.
- Neff JC, Chapin FS, Vitousek PM. (2003). Breaks in the cycle: dissolved organic nitrogen in terrestrial ecosystems. *Front Ecol Environ* **1**: 205-211.
- Nercessian O, Noyes E, Kalyuzhnaya MG, Lidstrom ME, Chistoserdova L. (2005). Bacterial populations active in metabolism of C<sub>1</sub> compounds in the sediment of Lake Washington, a freshwater lake. *Appl Environ Microbiol* **71**: 6885-6899.

Nešvera J, Pátek M, Hochmannová J, Chibisova E, Sererijski I, Tsyganov Y, Netrusov A. (1991) Transformation of a new gram-positive methylotroph, *Brevibacterium methylicum*, by plasmid DNA. *Appl Microbiol Biotechnol* **35**: 777–780.

Negruță O, Csutak O, Stoica I, Rusu E, Vassu T. (2009). Methylotrophic yeasts: diversity and methanol metabolism. *Rom Biotech Lett* **15**: 5369-5375.

Neufeld JD, Chen Y, Dumont MG, Murrell JC. (2008). Marine methylotrophs revealed by stable-isotope probing, multiple displacement amplification and metagenomics. *Environ Microbiol* **10**: 1526-35.

Neufeld JD, Schäfer H, Cox MJ, Boden R, McDonald IR, Murrell, JC (2007a). Stable-isotope probing implicates *Methylophaga* spp and novel *Gammaproteobacteria* in marine methanol and methylamine metabolism. *ISME J* **6**: 480-491.

Neufeld JD, Vohra J, Dumont MG, Lueders T, Manefield M, Friedrich MW *et al.* (2007b). DNA stable-isotope probing. *Nat Protoc* **2**: 860–866.

Nicholas KB, Nicholas HB Jr, Deerfield DW. (1997). GeneDoc: Analysis and Visualization of Genetic Variation. *EMBnet News* **4**:14.

Nicol GW, Glover LA, Prosser JI. (2003). Spatial analysis of archaeal community structure in grassland soil. *Appl Environ Microbiol* **69**: 7420-9.

Nicol GW, Leininger S, Schleper C, Prosser JI. (2008). The influence of soil pH on the diversity, abundance and transcriptional activity of ammonia oxidizing archaea and bacteria. *Environ Microbiol* **10**: 2966-2978.

Nicol GW, Prosser JI. (2011). Strategies to determine diversity, growth, and activity of ammonia-oxidizing archaea in soil. *Methods Enzymol* **496**: 3-34.

Nielsen LP. (1992). Denitrification in sediments determined from nitrogen isotope pairing. *FEMS Microbiol Ecol* **86**: 357–362.

North & Stephens. (1971). Uptake and assimilation of amino acids by *Platymonas*. 2. Increased uptake in nitrogen-deficient cells. *Biol Bull* **140**: 242-254.

Oakley BB, Morales CA, Line JE, Seal BS, Hiatt KL. (2012). Application of high-throughput sequencing to measure the performance of commonly used selective cultivation methods for the foodborne pathogen *Campylobacter*. *FEMS Microbiol Ecol* **79**: 327-36.

Ochsenreiter T, Selezi D, Quaiser A, Bonch-Osmolovskaya L, Schleper C. (2003). Diversity and abundance of Crenarchaeota in terrestrial habitats studied by 16S RNA surveys and real time PCR. *Environ Microbiol* **5**: 787-797.

Oelgeschläger E, Rother M. (2008). Carbon monoxide-dependent energy metabolism in anaerobic bacteria and archaea. *Arch Microbiol* **190**: 257–269.

Offre P, Nicol GW, Prosser JI. (2011). Community profiling and quantification of putative autotrophic thaumarchaeal communities in environmental samples. *Environ Microbiol Rep.* **3**: 245-53.

Oremland RS, Marsh LM, Polcin S. (1982). Methane production and simultaneous sulphate reduction in anoxic, salt marsh sediments. *Nature* **296**: 143–145.

- Øvreås L, Forney LJ, Daae FL, Torsvik VL. (1997). Distribution of bacterioplankton in meromictic Lake Saelenvannet, as determined by denaturing gradient gel electrophoresis of PCR-amplified gene fragments coding for 16S rRNA. *Appl Environ Microbiol* **63**: 3367–3373.
- Padden AN, Rainey FA, Kelly DP, Wood AP. (1997). *Xanthobacter tagetidis* sp. nov., an organism associated with Tagetes species and able to grow on substituted thiophenes. *Int J Syst Bacteriol* **47**: 394–401.
- Pester M, Maixner F, Berry D, Rattei T, Koch H, Lückner S, Nowka B, Richter A, Spieck E, Lebedeva E, Loy A, Wagner M, Daims H. (2014). *NxrB* encoding the beta subunit of nitrite oxidoreductase as functional and phylogenetic marker for nitrite-oxidizing *Nitrospira*. *Environ Microbiol* **16**: 3055–3071.
- Pester M, Rattei T, Flechl S, Gröngroft A, Richter A, Overmann J, Reinhold-Hurek B, Loy A, Wagner M. (2012). *amoA*-based consensus phylogeny of ammonia-oxidizing archaea and deep sequencing of *amoA* genes from soils of four different geographic regions. *Environ Microbiol*. **14**: 525–539.
- Pester M, Schleper C, Wagner M. (2011). The *Thaumarchaeota*: an emerging view of their phylogeny and ecophysiology. *Curr Opin Microbiol*. **14**: 300–306.
- Pérez-Pantoja D1, De la Iglesia R, Pieper DH, González B. (2008). Metabolic reconstruction of aromatic compounds degradation from the genome of the amazing pollutant-degrading bacterium *Cupriavidus necator* JMP134. *FEMS Microbiol Rev* **3**: 736–94.
- Philippot L, Piutti S, Martin-Laurent F, Hallet S, Germon JC. (2002). Molecular analysis of the NO<sub>3</sub><sup>-</sup>-reducing community from unplanted and maize-planted soils. *Appl Environ Microbiol* **68**: 6121–6128.
- Porter ML, Engel AS, Kane TC, Kinkle BK. (2009). Productivity-diversity relationships from chemolithoautotrophically based sulfidic karst systems. *Int J Speleol* **28**: 27–40.
- Prell J, Poole P. (2006). Metabolic changes of rhizobia in legume nodules. *Trends Microbiol* **14**: 161–168.
- Priemé A, Braker G, Tiedje JM. (2002). Diversity of nitrite reductase (*nirK* and *nirS*) gene fragments in forested upland and wetland soils. *Appl Environ Microbiol* **68**: 1893–90.
- Prosser JI. Autotrophic nitrification in bacteria. (1989). *Adv Microb Physiol* **30**: 125–181.
- Prosser JI, Nicol GW. (2012). *Archaeal* and bacterial ammonia-oxidisers in soil: the quest for niche specialisation and differentiation. *Trends Microbiol*. **20**: 523–531.
- Purkhold U, Pommering-Röser A, Juretschko S, Schmid MC, Koops HP, Wagner M. (2000). Phylogeny of all recognized species of ammonia oxidisers based on comparative 16S rRNA and *amoA* sequence analysis: implications for molecular diversity surveys. *Appl Environ Microbiol* **66**: 5368–5382.
- Radajewski S, Ineson P, Parekh N, Murrell JC. (2000). Stable-isotope probing as a tool in microbial ecology. *Nature* **403**: 646–649.
- Radajewski S, Webster G, Reay DS, Morris SA, Ineson P, Nedwell DB, Prosser JI, Murrell JC. (2002). Identification of active methylotroph populations in an acidic forest soil by stable-isotope probing. *Microbiol* **148**: 2331–2342.
- Risgaard-Petersen N, Meyer RL, Schmid M, Jetten MSM, Enrich-Prast A, Rysgaard S, Revsbech NP. (2003). Anaerobic ammonium oxidation in an estuarine sediment. *Aquat Microb Ecol* **36**: 293–304.

- Robertson BR, Button DK. (1979). Phosphate-limited continuous culture of *Rhodotorula rubra*: Kinetics of transport, leakage, and growth. *J Bacteriol* **138**: 884-895.
- Rohwerder T, Sand W, Lascu C. (2003). Preliminary evidence for a sulphur cycle in Movile Cave, Romania. *Acta Biotechnol* **23**: 101-107.
- Rotthauwe, JH, Witzel KP, Liesack W. (1997). The ammonia monooxygenase structural gene *amoA* as a functional marker: molecular fine-scale analysis of natural ammonia-oxidizing populations. *Appl Environ Microbiol* **63**: 4704-4712.
- Saitou N, Nei M. (1987). The neighbor-joining method: A new method for reconstructing phylogenetic trees. *Mol Biol Evol* **4**:406-425.
- Sambrook J, Russell DW. (2001). *Molecular cloning: A laboratory manual*. Cold Spring Harbor Laboratory Press: New York, USA.
- Santoro AE, Casciotti KL, Francis CA. (2010). Activity, abundance and diversity of nitrifying archaea and bacteria in the central California Current. *Environ Microbiol* **12**: 1989-2006.
- Santoro AE1, Casciotti KL. (2011). Enrichment and characterization of ammonia-oxidizing archaea from the open ocean: phylogeny, physiology and stable isotope fractionation. *ISME J* **5**: 1796-1808.
- Sârbu ŞM. (2000). Movile Cave: a chemoautotrophically based groundwater ecosystem. In: Wilkens H, Culver DC, Humphreys WF (eds). *Subterranean Ecosystems*. Elsevier Press: Amsterdam, The Netherlands, pp 319-343.
- Sârbu ŞM, Galdenzi S, Menichetti M, Gentile G. (2002). Geology and biology of Grotte di Frasassi (Frassasi Caves) in central Italy, an ecological multi-disciplinary study of a hypogenic underground karst system. In: Wilken H, Culver DC, Humphreys WF (eds). *Subterranean Ecosystems*. Elsevier Press: New York, USA, pp 369-378.
- Sârbu ŞM, Kane TC. (1995). A subterranean chemoautotrophically based ecosystem. *Natl Speleol Soc Bull* **57**: 91-98.
- Sârbu ŞM, Kane TC, Krinkle BK. (1996). A chemoautotrophically based cave ecosystem. *Science* **272**: 1953-1955.
- Sârbu ŞM, Lascu C. (1997). Condensation corrosion in Movile Cave, Romania. *J Cave Karst Stud* **59(3)**: 99-102.
- Sârbu ŞM, Kinkle BK, Vlăsceanu L, Kane TC. (1994). Microbial characterization of a sulfide-rich groundwater ecosystem. *Geomicrobiol J* **12**: 175-182.
- Sârbu ŞM, Popa R. (1992). A unique chemoautotrophically based cave ecosystem. In: Camacho AI (ed). *The Natural History of Biospeleology*, Monografias Museo Nacional de Ciencias Naturales: Madrid, pp. 638-666.
- Scheller S, Goenrich M, Boecher R, Thauer RK, Jaun B. (2010). The key nickel enzyme of methanogenesis catalyses the anaerobic oxidation of methane. *Nature* **465**: 606-608.
- Schleper C, Holben W, Klenk HP. (1997). Recovery of Crenarchaeotal ribosomal DNA sequences from freshwater-lake sediments. *Appl Environ Microbiol* **63**: 321-323.
- Schleper C, Nicol GW. (2010). Ammonia-oxidising archaea -- physiology, ecology and evolution. *Adv Microb Physiol* **57**: 1-41.

- Schmid MC, Hooper AB, Klotz MG, Woebken D, Lam P, Kuypers MM, Pommerening-Roeser A, Op den Camp HJ, Jetten MS. (2008). Environmental detection of octahaem cytochrome c hydroxylamine/hydrazine oxidoreductase genes of aerobic and anaerobic  $\text{NH}_4^+$ -oxidizing bacteria. *Environ Microbiol* **10**: 3140–3149.
- Schmid M, Walsh K, Webb R, Rijpstra WI, van de Pas-Schoonen K, Verbruggen MJ, Hill T, Moffett B, Fuerst J, Schouten S, Damsté JS, Harris J, Shaw P, Jetten M, Strous M. (2003). *Candidatus* "Scalindua brodae", sp. nov., *Candidatus* "Scalindua wagneri", sp. nov., two new species of anaerobic  $\text{NH}_4^+$  oxidizing bacteria. *Syst Appl Microbiol* **26**: 529-38.
- Seitzinger SP, Sanders RW. (1999). Atmospheric inputs of dissolved organic nitrogen stimulate estuarine bacteria and phytoplankton. *Limnol Oceanogr* **44**: 721-730.
- Selesi D, Schmid M, Hartmann A. (2005). Diversity of green-like and red-like ribulose-1,5-bisphosphate carboxylase/oxygenase large-subunit genes (*cbbL*) in differently managed agricultural soils. *Appl Environ Microbiol* **71**: 175–184.
- Solórzano L. (1969). Determination of ammonia in natural waters by the phenol hypochlorite method. *Limnol Oceanogr* **15**: 799-801.
- Sorokin DY, Lückner S, Vejmekova D, Kostrikina NA, Kleerebezem R, Rijpstra WI, Damsté JS, Le Paslier D, Muyzer G, Wagner M, van Loosdrecht MC, Daims H. (2012). Nitrification expanded: discovery, physiology, and genomics of a nitrite oxidizing bacterium from the phylum Chloroflexi. *ISME J* **6**: 2245–2256.
- Spang A, Hatzenpichler R, Brochier-Armanet C, Rattei T, Tischler P, Spieck E, Streit W, Stahl DA, Wagner M, Schleper C. (2010). Distinct gene set in two different lineages of ammonia-oxidizing archaea supports the phylum *Thaumarchaeota*. *Trends Microbiol* **18**: 331-340.
- Strandberg GW, Wilson PW. (1967). Molecular  $\text{H}_2$  and the  $\text{PN}_2$  function of *Azotobacter*. *Proc Natl Acad Sci USA*. **58**: 1404-9.
- Sullivan JT, Eardly BD, van Berkum P, Ronson CW. (1996). Four unnamed species of nonsymbiotic rhizobia isolated from the rhizosphere of *Lotus corniculatus*. *Appl Environ Microbiol* **62**: 2818–2825.
- Sullivan JT, Ronson CW. (1998). Evolution of rhizobia by acquisition of a 500-kb symbiosis island that integrates into a phe-tRNA gene. *Proc Natl Acad Sci USA* **95**: 5145–5149.
- Sun S, Chen J, Li W, Altintas I, Lin A, Peltier S *et al.* (2011). Community cyberinfrastructure for Advanced Microbial Ecology Research and Analysis: the CAMERA resource. *Nucleic Acids Res* **39**: D546–D551.
- Sun, J., Steindler, L., Thrash, J.C., Halsey, K.H., Smith, D.P., Carter, A.E., *et al.* (2011) One carbon metabolism in SAR11 pelagic marine bacteria. *PLoS ONE* **6**: e23973.
- Tamura K, Nei M, Kumar S. (2004). Prospects for inferring very large phylogenies by using the neighbor-joining method. *Proc Natl Acad Sci USA* **101**:11030-11035.
- Tamura K, Peterson D, Peterson N, Stecher G, Nei M, Kumar S. (2011). MEGA5: molecular evolutionary genetics analysis using maximum likelihood, evolutionary distance, and maximum parsimony methods. *Mol Biol Evol* **28**: 2731-2739
- Tanaka Y, Hanada S, Manome A, Tsuchida T, Kurane R, Nakamura K *et al.* (2004). *Catellibacterium nectariphilum* gen. nov., sp. nov., which requires a diffusible compound from a strain related to the genus *Sphingomonas* for vigorous growth. *Int J Syst Evol Microbiol* **54**: 955-959.

- Tatsukami Y, Nambu M, Morisaka H, Kuroda K, Ueda M. (2013). Disclosure of the differences of *Mesorhizobium loti* under the free-living and symbiotic conditions by comparative proteome analysis without bacteroid isolation. *BMC Microbiol* **13**: 180.
- Teramoto M, Suzuki M, Hatmanti A, Harayama S. (2010). The potential of *Cycloclasticus* and *Altererythrobacter* strains for use in bioremediation of petroleum-aromatic-contaminated tropical marine environments. *J Biosci Bioeng* **110**: 48–52.
- Teske A, Alm E, Regan JM, Toze S, Rittmann BE, Stahl DA. (1994). Evolutionary relationships among ammonia- and nitrite-oxidizing bacteria. *J Bacteriol* **176**: 6623–6630.
- Thompson JD, Gibson TJ, Plewniak F, Jeanmougin F, Higgins DG. (1997). The CLUSTAL\_X windows interface: flexible strategies for multiple sequence alignment aided by quality analysis tools. *Nucleic Acids Res* **25**: 4876–4882.
- Tourna M, Stieglmeier M, Spang A, Konneke M, Schintlmeister A, Urich T, Engel M, Schlöter M, Wagner M, Richter A, Schleper C. (2011). *Nitrososphaera viennensis*, an ammonia oxidizing archaeon from soil. *Proc Natl Acad Sci USA* **108**: 8420–8425.
- Treusch A, Leininger S, Kletzin A, Schuster S, Klenk H, Schleper C. (2005). Novel genes for nitrite reductase and Amo-related proteins indicate a role of uncultivated mesophilic crenarchaeota in nitrogen cycling. *Environ Microbiol* **7**: 1985–1995.
- Trimmer M, Nicholls JC, Deflandre B. (2003). Anaerobic  $\text{NH}_4^+$  oxidation measured in sediments along the Thames estuary, United Kingdom. *Appl Environ Microbiol*. **69**: 6447–54.
- Trotsenko YA, Murrell JC. (2008). Metabolic aspects of aerobic obligate methanotrophy. *Adv Appl Microbiol* **6**: 183–229.
- Uchiumi T, Ohwada T, Itakura M, Mitsui H, Nukui N, Dawadi P, Kaneko T, Tabata S, Yokoyama T, Tejima K, Saeki K, Omori H, Hayashi M, Maekawa T, Sriprang R, Murooka Y, Tajima S, Simomura K, Nomura M, Suzuki A, Shimoda Y, Sioya K, Abe M, Minamisawa K. (2004). Expression islands clustered on the symbiosis island of the *Mesorhizobium loti* genome. *J Bacteriol* **186**: 2439–2448.
- van Breemen N. (2002). Natural organic tendency. *Nature* **415**: 381–382.
- van de Graaf AA, Mulder A, de Bruijn P, Jetten MS, Robertson LA, Kuenen JG. (1995). Anaerobic oxidation of  $\text{NH}_4^+$  is a biologically mediated process. *Appl Environ Microbiol* **61**: 1246–51.
- van Dijken JP, Bos P. (1981). Utilization of amines by yeasts. *Arch Microbiol* **128**: 320–4.
- van Dover CL, German CR, Speer KG, Parson LM, Vrijenhoek RC. (2002). Evolution and biogeography of deep-sea venting and seep invertebrates. *Science* **295**: 1253–1257.
- van Niftrik L. (2013). Cell biology of unique anammox bacteria that contain an energy conserving prokaryotic organelle. *A Van Leeuw* **104**: 489–97.
- Vanparys B, Spieck E, Heylen K, Wittebolle L, Geets J, Boon N, de Vos P. (2007). The phylogeny of the genus *Nitrobacter* based on comparative rep-PCR, 16S rRNA and nitrite oxidoreductase gene sequence analysis. *Syst Appl Microbiol* **30**: 297–308.
- Venter JC, Remington K, Heidelberg JF, Halpern AL, Rusch D, Eisen JA, Wu D, Paulsen I, Nelson KE, Nelson W, Fouts DE, Levy S, Knap AH, Lomas MW, Nealson K, White O, Peterson J, Hoffman J, Parsons R, Baden-Tillson H, Pfannkoch C, Rogers YH, Smith HO. (2004). Environmental genome shotgun sequencing of the Sargasso Sea. *Science* **304**: 66–74.

- Vlăsceanu L, Popa R, Kinkle BK. (1997). Characterization of *Thiobacillus thioparus* LV43 and its distribution in a chemoautotrophically based groundwater ecosystem. *Appl Environ Microbiol* **63**: 3123-3127
- Vlăsceanu L, Sârbu ŞM, Engel AS, Kinkle BK. (2000). Acidic cave wall biofilms located in the Frasassi Gorge, Italy. *Geomicrobiol J* **17**: 125–139.
- Verhamme DT, Prosser JJ, Nicol GW. (2011). Ammonia concentration determines differential growth of ammonia-oxidising archaea and bacteria in soil microcosms. *ISME J* **5**: 1067-1071.
- Vincze T, Posfai J, Roberts RJ. (2003). NEBcutter: a program to cleave DNA with restriction enzymes. *Nucleic Acids Res* **31**: 3688–3691.
- Wang XC, Lee C. (1990). The distribution and adsorption behavior of aliphatic amines in marine and lacustrine sediments. *Geochim Cosmochim Acta* **54**: 2759-2174.
- Ward BB, Devol AH, Rich JJ, Chang BX, Bulow SE, Naik H, Pratihary A, Jayakumar A. (2009). Denitrification as the dominant nitrogen loss process in the Arabian Sea. *Nature* **461**:78–81.
- Wheeler PA, Kirchman DL. (1986). Utilization of inorganic and organic nitrogen by bacteria in marine systems. *Limnol Oceanogr* **31**: 998-1009.
- Wheeler PA, North B, Littler M, Stephens G. (1977). Uptake of glycine by natural phytoplankton communities. *Limnol Oceanogr* **22**: 900-910.
- Whittenbury R, Phillips KC, Wilkinson JF. (1970). Enrichment, isolation and some properties of methane-utilizing bacteria. *J Gen Microbiol* **61**: 205–218.
- Winogradsky S. (1890). 2nd memoire. Recherches sur les organismes de la nitrification. *Ann Inst Pasteur* **4**: 257–275.
- Worsfold PJ, Monbet P, Tappin AD, Fitzsimons MF, Stiles DA, McKelvie ID. (2008). Characterisation and quantification of organic phosphorus and organic nitrogen components in aquatic systems: a review. *Anal Chim Acta* **624**: 37–58.
- Xu JL, Wu J, Wang ZC, Wang K, Li MY, Jiang JD, He J, Li SP. (2009). Isolation and characterization of a methomyl-degrading *Paracoccus* sp. mdw-1. *Pedosphere* **19**: 238-243.
- Yu Z, Zhang Q, Kraus TEC, Dahlgren RA, Anastasio C, Zasoski RJ. (2002). Contribution of amino compounds to dissolved organic nitrogen in forest soils. *Biogeochem* **61**: 173–198.
- Yurimoto H, Oku M, Sakai Y. (2011). Yeast methylotrophy: metabolism, gene regulation and peroxisome homeostasis. *Int J Microbiol* **101298**: Art ID 101298, 8 pages. doi: 10.1155/2011/101298.
- Zhang J, Chen SA, Zheng JW, Cai S, Hang BJ, He J *et al.* (2012). *Catellibacterium nanjingense* sp. nov., a propanil-degrading bacterium isolated from activated sludge, and emended description of the genus *Catellibacterium*. *Int J Syst Evol Microbiol* **62**: 495-499.
- Zheng JW, Chen YG, Zhang J, Ni YY, Li WJ, He J *et al.* (2011). Description of *Catellibacterium caeni* sp. nov., reclassification of *Rhodobacter changlensis* Anil Kumar *et al.* 2007 as *Catellibacterium changlense* comb. nov. and emended description of the genus *Catellibacterium*. *Int J Syst Evol Microbiol* **61**:1921-1926.
- Zubkov MV, Fuchs BM, Tarran GA, Burkill PH, Amann R. (2003). High rate of uptake of organic nitrogen compounds by *Prochlorococcus Cyanobacteria* as a key to their dominance in oligotrophic oceanic waters. (2003). *Appl Environ Microbiol* **69**: 1299–1304.

Zuckerlandl E, Pauling L. (1965). Evolutionary divergence and convergence in proteins. In: Bryson V, Vogel HJ (eds). *Evolving Genes and Proteins*, Academic Press: New York, pp. 97-166.

Zumft WG. (1992). The denitrifying prokaryotes. In: Balows A, Trüper HG, Dworkin M, Harder W, Schleifer KH (eds), *The Prokaryotes A Handbook of the Biology of Bacteria: Ecophysiology, Isolation, Identification, Applications, Vol 1*, Springer-Verlag: New York, USA, pp 554–582.

## Appendix

**Supplementary Table S1** Gibbs free energies of formation ( $\Delta G_f$ ) used to calculate the changes in Gibbs free energy ( $\Delta G$ ) of the reactions in Table 1.2 and sections 6.3.1 and 6.5.2

Substance	$\Delta G_f^0$ (kJ mol <sup>-1</sup> ) (pH0)	$\Delta G_f^{0'}$ (kJ mol <sup>-1</sup> ) (pH7)	Reference
O <sub>2</sub> (gas / aqueous)	0 / +16.4	0 / +16.4	Noor <i>et al.</i> , 2013
H <sub>2</sub> O	-238.7	-157.6	Noor <i>et al.</i> , 2013
H <sup>+</sup>	0	-39.8	Madigan <i>et al.</i> , 2009
OH <sup>-</sup>	-237.6	-198.8	Madigan <i>et al.</i> , 2009
NH <sub>4</sub> <sup>+</sup>	-79.3	+79	Noor <i>et al.</i> , 2013
NO <sub>2</sub> <sup>-</sup>	-32.2	-32.8	Noor <i>et al.</i> , 2013
NO <sub>3</sub> <sup>-</sup>	-108.7	-109.3	Noor <i>et al.</i> , 2013
N <sub>2</sub> (gas / aqueous)	0 / +18.7	0 / +18.7	Noor <i>et al.</i> , 2013
CO <sub>2</sub> (gas / aqueous)	-394 / -386	-394 / -386	Noor <i>et al.</i> , 2013
CH <sub>4</sub>	-34.4	+127.8	Noor <i>et al.</i> , 2013
CH <sub>3</sub> OH	-175.3	-13.1	Noor <i>et al.</i> , 2013
CH <sub>3</sub> NH <sub>2</sub> (methylamine)	+17.7	+220.4	Noor <i>et al.</i> , 2013
(CH <sub>3</sub> ) <sub>2</sub> NH (dimethylamine)	+56.7	+340.5	Noor <i>et al.</i> , 2013
(CH <sub>3</sub> ) <sub>3</sub> N (trimethylamine)	+91.8	+456.7	Noor <i>et al.</i> , 2013
C <sub>2</sub> H <sub>3</sub> O <sub>2</sub> <sup>-</sup> (acetate)	-368	-246	Noor <i>et al.</i> , 2013
C <sub>2</sub> H <sub>4</sub> O <sub>2</sub> (acetic acid)	-394	-230	Noor <i>et al.</i> , 2013

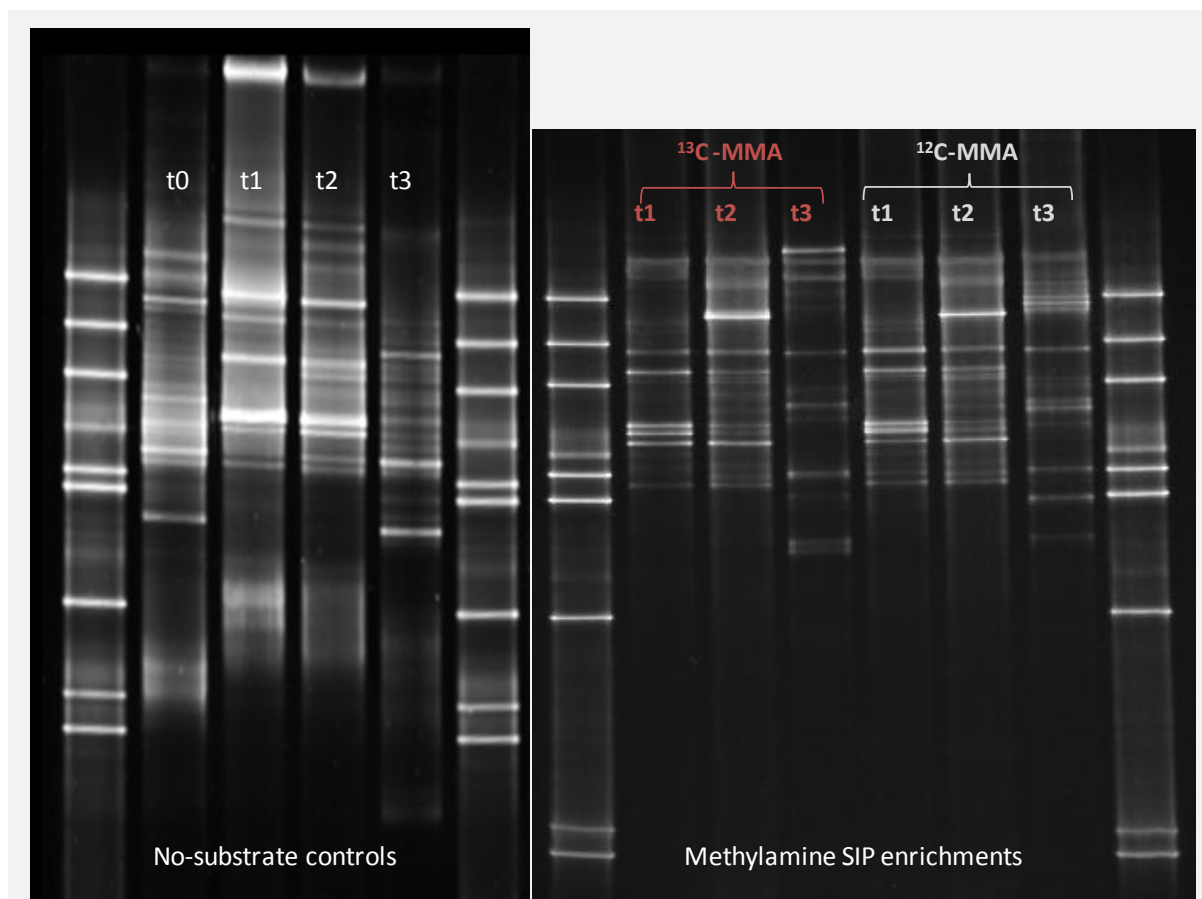
$$\Delta G = \sum \Delta G_{f[\text{products}]} - \sum \Delta G_{f[\text{reactants}]}$$

Note: Most textbooks and available tables for  $\Delta G_f$  values list only  $\Delta G_f^0$  and not  $\Delta G_f^{0'}$  for the majority of substances. However, since pH7 is more relevant than pH0 for the microbial reactions listed in Table 1.2,  $\Delta G^{0'}$  rather than  $\Delta G^0$  values were calculated, using  $\Delta G_f^{0'}$  values (for aqueous substances) estimated based on component contributions (Noor *et al.*, 2013), with the exception of values for H<sup>+</sup> and OH<sup>-</sup> which were not available from this source and were hence adopted from standard tables (Madigan *et al.*, 2009).

#### References:

Noor E, Haraldsdóttir HS, Milo R, Fleming RMT. (2013). Consistent Estimation of Gibbs Energy using Component Contributions. *PLoS Comput Biol* **9**: e1003098.  
[DOI: 10.1371/journal.pcbi.1003098].

Madigan MT, Martinko JM, Dunlap PV, Clark DP. (2009). Brock Biology of Microorganisms, 12th edition, Pearson Benjamin-Cummings, San Francisco.

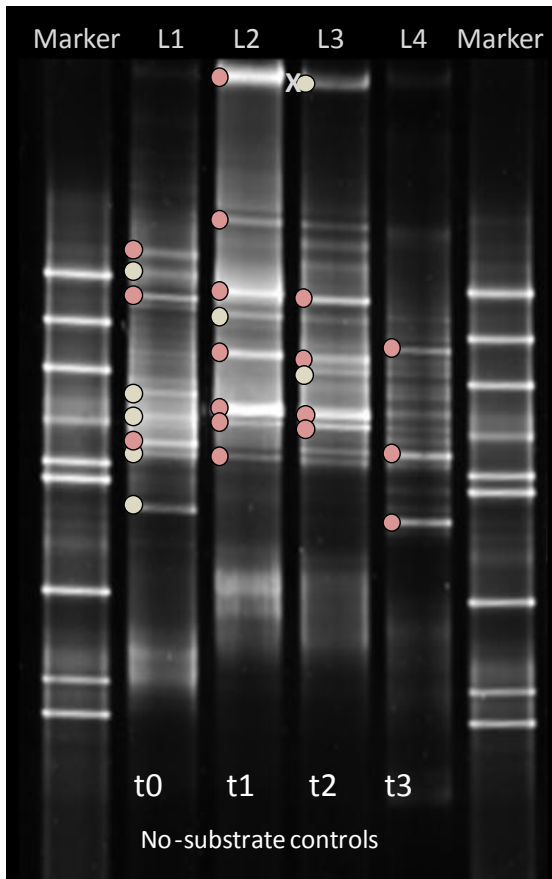


### Supplementary Figure S1a

Left: DGGE profiles of bacterial 16S rRNA gene fragments (341f-GC / 907r) from control incubations of Movile Cave water with no added substrate after 48 hours (t=1), 96 hours (t=2) and 5 weeks (t=3).

Right: DGGE profiles of bacterial 16S rRNA gene fragments (341f-GC / 907r) from incubations with  $^{13}\text{C}$ -labelled and unlabelled ( $^{12}\text{C}$ ) MMA are shown for reference.

Abbreviations: MMA, monomethylamine.



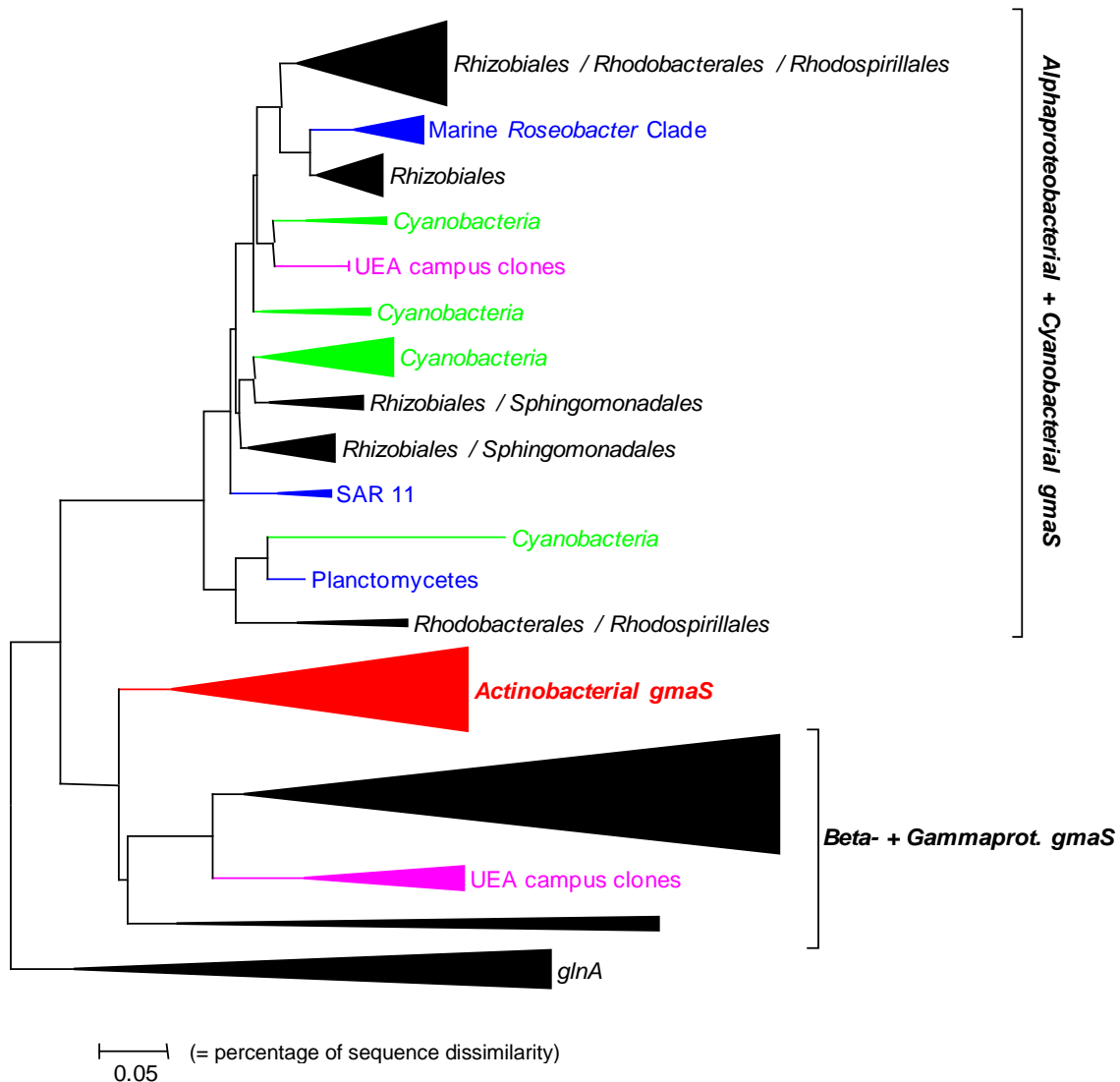
**Supplementary Figure S1b:** DGGE analysis of 16S rRNA gene fragments (341f-GC / 907r) of no-substrate-control incubations for SIP experiments, indicating bands that were excised from the DGGE gel and sequenced; red-coloured circles indicate good-quality sequences; gray circles indicate messy sequences (due to more than one phylotype present in the DNA sample), X indicates failed sequencing. For phylogenetic affiliations of the sequences refer to Supplementary Table S2 below (numbered from top to bottom for each of the lanes). t0 = 0 h; t1 = 48 h; t2= 96 h; t3 = 5 weeks.

**Supplementary Table S2** Phylogenetic affiliations of amplified 16S rRNA gene fragments (retrieved from excised DGGE bands indicated above) of no-substrate-control incubations

Band on gel (from top)	Closest GenBank relatives	Identity (%)	Accession code
<b>Lane 1 (t = 0)</b>			
L1-1	Endosymbiont of deep-sea polychaete <i>Osedax mucofloris</i>	97	FN773289.1
	<i>Sulfurovum lithotrophicum</i> strain ATCC BAA-797	96	CP011308.1
L1-2	<i>Sphingomonadales</i>	(messy)	
L1-3	Bacterium associated with marine nematode <i>Eubostrichus topiarius</i>	93	AJ319042.1
	<i>Desulforhopalus singaporensis</i> strain S'pore T1	93	NR_028742.1
L1-4	<i>Rhizobiales</i>	(messy)	
L1-5	<i>Rhodobacterales</i>	(messy)	
L1-6	<i>Rhodobacter blasticus</i> strain Ku-2	96	KC967307.1
	<i>Rhodobacter gluconicum</i>	96	AB077986.1
L1-7	<i>Xanthomonadales</i>	(messy)	
L1-8	<i>Clostridiales</i>	(messy)	

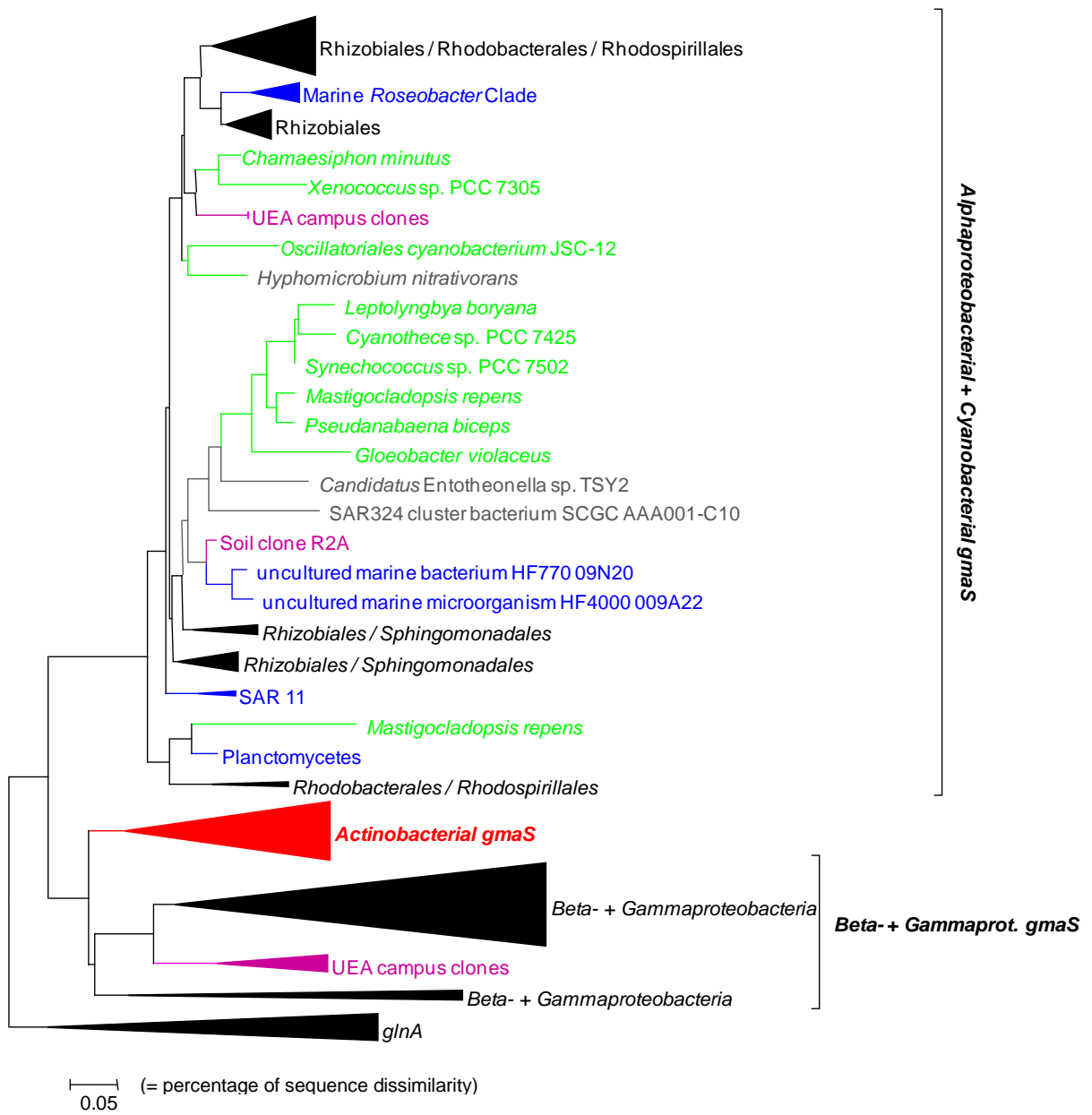
**Supplementary Table S2** (continued)

Band on gel (from top)	Closest GenBank relatives	Identity (%)	Accession code
<b>Lane 2 (t = 1)</b>			
L2-1	Endosymbiont of tubeworm <i>Ridgeia piscesae</i>	96	JX570598.1
	<i>Arcobacter cryaerophilus</i>	96	KJ364503.1
L2-2	Endosymbiont of deep-sea polychaete <i>Osedax mucofloris</i>	97	FN773289.1
	<i>Sulfurovum lithotrophicum</i> ATCC BAA-797	96	CP011308.1
L2-3	<i>Thiovirga sulfuroxydans</i> SO07	99	NR_040986.1
	<i>Luteibacter rhizovicinus</i> 1-O-2	88	AB272376.1
L2-4	<i>Neisseriales</i>	(messy)	
L2-5	<i>Hydrogenophaga caeni</i> EMB71	98	NR_043769.1
	<i>Hydrogenophaga atypica</i> DT34-12	97	KC920941.1
L2-6	<i>Vogesella perlucida</i> CGB1	99	KJ522788.1
	<i>Vogesella mureinivorans</i> 389	99	NR_104556.1
L2-7	<i>Hydrogenophaga taeniospiralis</i> isolate TOWS-122	99	LN650479.1
	<i>Hydrogenophaga carboriundus</i> KRH_YZ	99	EU095331.1
L2-8	<i>Rhodobacter blasticus</i> HWS0448	97	LN835431.1
	<i>Rhodobacter gluconicum</i>	95	AB077986.1
<b>Lane 3 (t = 2)</b>			
L3-1	(failed)		
L3-2	Uncultured proteobacterium deep sea brine clone ATIntfc1_RS44	90	KM018375.1
	<i>Nevskia terrae</i> KIS13-15	86	NR_104525.1
	<i>Kushneria indalinina</i> CG2.1	86	NR_115092.1
L3-3	<i>Vogesella mureinivorans</i> 389	94	NR_104556.1
	<i>Hydrogenophaga caeni</i> EMB71	94	NR_043769.1
L3-4	<i>Neisseriales</i>	(messy)	
L3-5	<i>Vogesella perlucida</i> CGB1	99	KJ522788.1
	<i>Vogesella mureinivorans</i> 389	99	NR_104556.1
L3-6	<i>Hydrogenophaga defluvii</i> hyd1	99	AM942546.1
	<i>Hydrogenophaga atypica</i> BSB 41.8	99	NR_029023.1
	<i>Hydrogenophaga taeniospiralis</i> Iso10-15	99	AB795550.1
<b>Lane 4 (t = 3)</b>			
L4-1	<i>Methylosarcina lacus</i> LW14	98	NR_042712.1
	<i>Methylomicrobium agile</i> ATCC	96	NR_116197.1
L4-2	<i>Oleomonas sagaranensis</i> HD-1		NR_115564.1
L4-3	<i>Niveispirillum fermenti</i> CC-LY736	99	NR_126263.1
	<i>Azospirillum irakense</i> L-6	98	JF508370.1
	<i>Rhodospirillum centenum</i> SW	98	CP000613.2

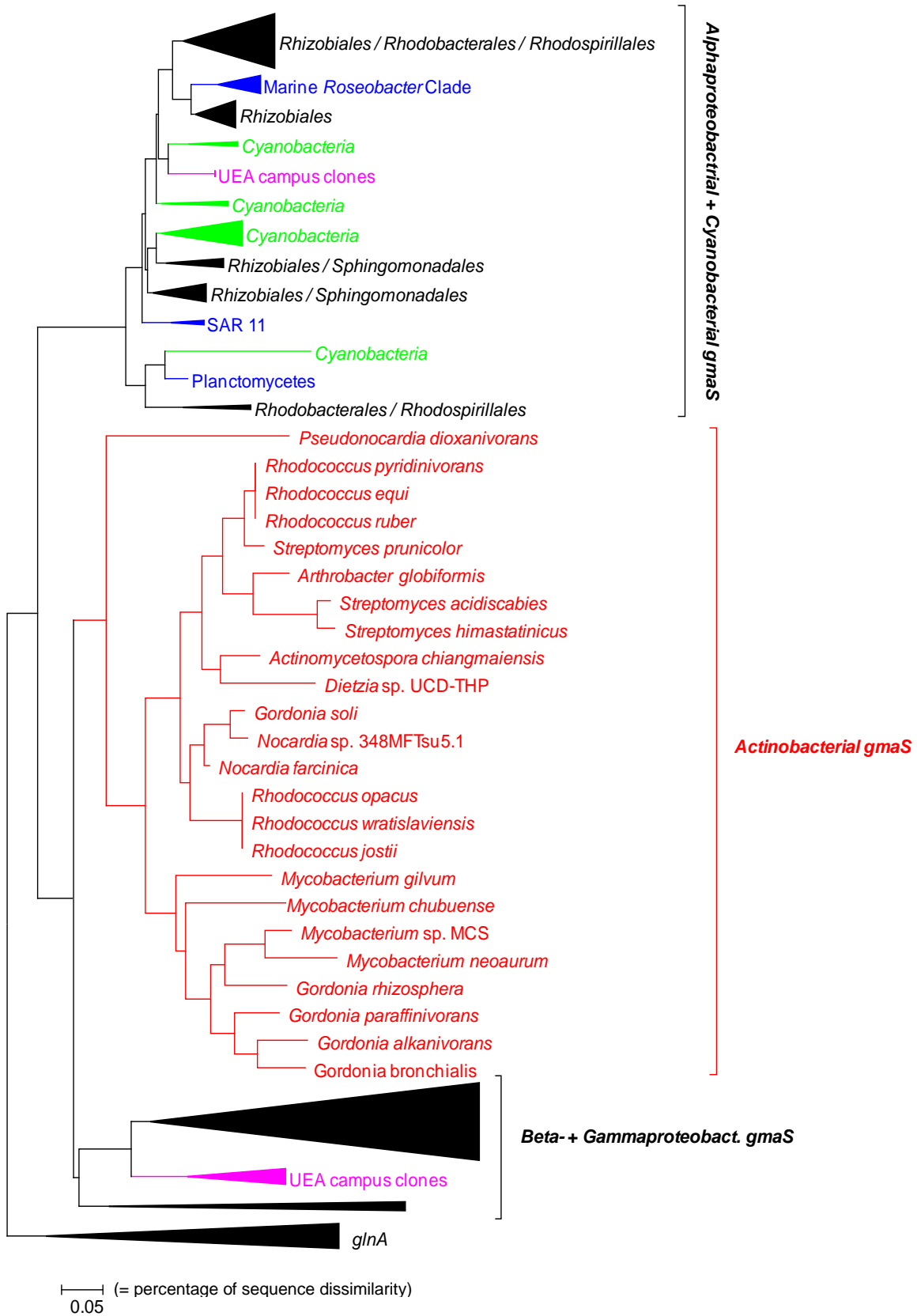


### Supplementary Figure S2a

**Supplementary Figures S2a-c** Phylogenetic affiliation of putative *gmaS* sequences from *Cyanobacteria* and *Actinobacteria* derived from published bacterial genomes with alpha-, beta- and gammaproteobacterial *gmaS* sequences. Proteobacterial sequences were derived from published genomes, Movile Cave isolates and clone library sequences from Movile Cave (water and floating mat samples) and UEA campus (soil and lake water); for a detailed view of proteobacterial sequences refer to Figures 5.3; 5.12; 5.14 in main text. *glnA* sequences represent the outgroup. The tree was established using the neighbour-joining method (1,000 bootstrap replicates) and the Poisson correction method for computing evolutionary distances. The tree is based on alignment of 135 amino acids (total deletion of gaps). All bacterial sequences refer to type strains (as listed on LPSN), unless strain names are indicated.



Supplementary Figure S2b (Detailed view of putative *cyanobacterial gmaS* sequences)



Supplementary Figure S2c (Detailed view of putative *actinobacterial gmaS* sequences)

## **Publications**



## ORIGINAL ARTICLE

# Bacterial metabolism of methylated amines and identification of novel methylotrophs in Movile Cave

Daniela Wischer<sup>1</sup>, Deepak Kumaresan<sup>1,4</sup>, Antonia Johnston<sup>1</sup>, Myriam El Khawand<sup>1</sup>, Jason Stephenson<sup>2</sup>, Alexandra M Hillebrand-Voiculescu<sup>3</sup>, Yin Chen<sup>2</sup> and J Colin Murrell<sup>1</sup>  
<sup>1</sup>*School of Environmental Sciences, University of East Anglia, Norwich, UK;* <sup>2</sup>*School of Life Sciences, University of Warwick, Coventry, UK and* <sup>3</sup>*Department of Biospeleology and Karst Edaphobiology, Emil Racoviță Institute of Speleology, Bucharest, Romania*

**Movile Cave, Romania, is an unusual underground ecosystem that has been sealed off from the outside world for several million years and is sustained by non-phototrophic carbon fixation. Methane and sulfur-oxidising bacteria are the main primary producers, supporting a complex food web that includes bacteria, fungi and cave-adapted invertebrates. A range of methylotrophic bacteria in Movile Cave grow on one-carbon compounds including methylated amines, which are produced via decomposition of organic-rich microbial mats. The role of methylated amines as a carbon and nitrogen source for bacteria in Movile Cave was investigated using a combination of cultivation studies and DNA stable isotope probing (DNA-SIP) using <sup>13</sup>C-monomethylamine (MMA). Two newly developed primer sets targeting the gene for gamma-glutamylmethylamide synthetase (*gmaS*), the first enzyme of the recently-discovered indirect MMA-oxidation pathway, were applied in functional gene probing. SIP experiments revealed that the obligate methylotroph *Methylotenera mobilis* is one of the dominant MMA utilisers in the cave. DNA-SIP experiments also showed that a new facultative methylotroph isolated in this study, *Catellibacterium* sp. LW-1 is probably one of the most active MMA utilisers in Movile Cave. Methylated amines were also used as a nitrogen source by a wide range of non-methylotrophic bacteria in Movile Cave. PCR-based screening of bacterial isolates suggested that the indirect MMA-oxidation pathway involving GMA and *N*-methylglutamate is widespread among both methylotrophic and non-methylotrophic MMA utilisers from the cave.**

*The ISME Journal* advance online publication, 22 July 2014; doi:10.1038/ismej.2014.102

## Introduction

Most ecosystems rely on phototrophic carbon fixation, or, in the absence of light, an external supply of phototrophically-fixed carbon into the ecosystem. Exceptions are deep sea hydrothermal vents, where carbon is derived from chemosynthesis using energy sources other than light (reviewed by Lutz and Kennish, 1993; Van Dover *et al.*, 2002; Campbell, 2006). Movile Cave, located near the coast of the Black Sea in Mangalia, Romania, is an underground cave system that has been completely sealed off from the outside world for several million years (Sarbu *et al.*, 1996). Unlike other cave systems, where dissolved and particulate organic carbon enters the cave with meteoric waters from above, the food web in Movile Cave is sustained exclusively by non-phototrophic carbon fixation. Since its discovery in 1986, Movile Cave has provided an

excellent natural ecosystem to study a highly unusual, light-independent, microbially-driven food web (Sarbu *et al.*, 1994; Sarbu and Kane, 1995; Sarbu *et al.*, 1996; Vlasceanu *et al.*, 1997; Rohwerder *et al.*, 2003; Hutchens *et al.*, 2004; Porter *et al.*, 2009; Chen *et al.*, 2009). Movile Cave harbours rich and diverse populations of cave-adapted invertebrates, all of which are sustained by chemolithoautotrophic microorganisms that thrive along the redox interface created between the oxygenated atmosphere and the high concentrations of reduced compounds such as hydrogen sulfide (H<sub>2</sub>S) and methane (CH<sub>4</sub>) present in the water (Sarbu and Kane, 1995). Microbial mats composed of bacteria, fungi and protists float on the water surface (kept afloat by CH<sub>4</sub> bubbles) and also grow on the limestone walls of the cave (Sarbu *et al.*, 1994).

Methylotrophs are organisms capable of using one-carbon (C1) compounds, that is, compounds lacking carbon-carbon bonds, as their sole source of carbon and energy (Anthony, 1982; Lidstrom, 2006; Chistoserdova *et al.*, 2009). In addition to CH<sub>4</sub>, C1 compounds such as methanol and methylated amines are important carbon and energy sources for a range of methylotrophic bacteria in Movile Cave (Hutchens *et al.*, 2004; Chen *et al.*, 2009). Methylated amines are typically associated with

Correspondence: JC Murrell, School of Environmental Sciences, University of East Anglia, Norwich Research Park, Norwich NR4 7TJ, UK.

E-mail: j.c.murrell@uea.ac.uk

<sup>4</sup>Current address: School of Earth and Environment, The University of Western Australia, Crawley, Perth, Australia.

Received 11 March 2014; revised 13 May 2014; accepted 22 May 2014

saline environments (Gibb *et al.*, 1999; Fitzsimons *et al.*, 2006) where they are formed by the degradation of glycine betaine and trimethylamine *N*-oxide, osmolytes commonly found in marine organisms (Barrett and Kwan, 1985; Lin and Timasheff, 1994). There are fewer studies on the distribution of methylated amines in terrestrial and freshwater environments, although the dissolved organic nitrogen fraction as a whole is increasingly being recognised as an important source of microbial nitrogen nutrition (Berman and Bronk, 2003; Worsfold *et al.*, 2008). Generally, environments with high concentrations of organic matter have a high potential for dissolved organic nitrogen generation (Neff *et al.*, 2003). We hypothesise that in Movile Cave, degradation of the extensive, organic-rich microbial mats produces large amounts of methylated amines, which are used as growth substrates by certain microorganisms that are the subject of this study.

Methylotrophs that use methylated amines as a carbon source are phylogenetically diverse, ubiquitous in the environment and often metabolically versatile (for example, Bellion and Hersh, 1972; Colby and Zatman, 1973; Levering *et al.*, 1981; Anthony, 1982; Bellion and Bolbot, 1983; Brooke and Attwood, 1984; Kalyuzhnaya *et al.*, 2006b; Boden *et al.*, 2008). New methylotrophs are still being identified from a wide range of environments, including genera not previously associated with methylotrophy, and novel metabolic pathways (see recent reviews by Chistoserdova *et al.*, 2009; Chistoserdova, 2011).

Methylated amines are also a nitrogen source for a wide range of non-methylotrophic bacteria. While utilisation of monomethylamine (MMA) as a bacterial nitrogen source was reported over 40 years ago (Budd and Spencer, 1968; Bicknell and Owens, 1980; Anthony, 1982; Murrell and Lidstrom, 1983; Glenn and Dilworth, 1984), details of the metabolic pathways involved have only recently been identified (Chen *et al.*, 2010b).

The key intermediates in methylotrophic metabolism are formaldehyde or formate, respectively, as they represent the branching point at which carbon is either oxidised further to CO<sub>2</sub>, or assimilated into cell carbon. Carbon is assimilated from formaldehyde via the ribulose monophosphate cycle, or from formate via the serine cycle (Anthony, 1982; Chistoserdova *et al.*, 2009; Chistoserdova, 2011). In the metabolism of methylated amines, there are two possible pathways for the oxidation of MMA (Supplementary Figures S1a and b): In the well-characterised, direct MMA-oxidation pathway, a single enzyme oxidises MMA to formaldehyde, releasing ammonium. In methylotrophic Gram-positive bacteria the enzyme responsible is MMA oxidase, while in Gram-negative methylotrophs it is MMA dehydrogenase (Anthony, 1982). PCR primers are available for *mauA* (Neufeld *et al.*, 2007a), the gene coding for the small subunit of MMA dehydrogenase. However, these primers do

not detect all MMA-utilising bacteria. An alternative, indirect pathway oxidises MMA not to formaldehyde but to 5,10-methylenetetrahydrofolate (CH<sub>2</sub>=THF) in a stepwise conversion via the methylated amino acids gamma-glutamylmethylamide (GMA) and/or *N*-methylglutamate (NMG) (Latypova *et al.*, 2010; Chistoserdova, 2011). Although this pathway has been known since the 1960s (Kung and Wagner, 1969), the enzymes and genes involved have only recently been characterised (Latypova *et al.*, 2010; Chen *et al.*, 2010a): MMA is converted to GMA by GMA synthetase (*gmaS*), GMA is then converted to NMG by NMG synthase (*mgsABC*), and finally to CH<sub>2</sub>=THF by NMG dehydrogenase (*mgdABCD*). A variation of this pathway is found in *Methyloversatilis universalis* FAM5, where *gmaS* is not essential for oxidation of MMA to CH<sub>2</sub>=THF via NMG (Latypova *et al.*, 2010). Importantly, the GMA-/NMG-mediated pathway is also found in bacteria that use MMA only as a nitrogen (but not carbon) source (Chen *et al.*, 2010b; Chen 2012). In a recent study (Chen, 2012), PCR primers targeting *gmaS* from marine *Roseobacter* clade (MRC) bacteria were developed for the detection of MMA utilisers in marine environments, highlighting the potential of the *gmaS* gene as a biomarker for MMA utilisation.

The objectives of this study were to determine the role of methylated amines as carbon and nitrogen sources for microorganisms in Movile Cave, and to identify active MMA utilisers in this unique ecosystem using DNA stable isotope probing (DNA-SIP) (Radajewski *et al.*, 2000; Murrell and Whiteley, 2011). DNA-SIP has been successfully applied in the study of methanotrophic and autotrophic communities in Movile Cave (Hutchens *et al.*, 2004; Chen *et al.*, 2009). Time-course SIP experiments with <sup>13</sup>C-labelled MMA were set up in order to monitor changes in the methylotrophic community. Cultivation-based studies were also used to isolate and characterise methylated amine-utilising bacteria from the cave. The distribution of genes for the GMA-dependent MMA-oxidation pathway in Movile Cave microbes was examined using new PCR primer sets developed to target *gmaS* from non-marine bacteria.

## Material and methods

### *Study site and sampling*

Movile Cave near Mangalia on the coast of the Black Sea is located in an area rich in hydrothermal activity with numerous sulfurous springs and lakes, as well as creeks bubbling with methane. The cave consists of a network of passages, including a dry, upper level and a lower level, which is partly flooded by thermal sulfidic waters (for a detailed cross-section of the cave see Supplementary Figure S2). A small lake room (ca 3 m in diameter) is located between the dry and the flooded sections of the cave, and two

air bells are located in the submerged region. The temperature in the cave is a constant 21 °C (Sarbu and Kane, 1995). The atmosphere in the air bells shows O<sub>2</sub> depletion (7–10% v/v) and is rich in CO<sub>2</sub> (2.5% v/v) and CH<sub>4</sub> (1–2% v/v) (Sarbu and Kane, 1995). The water contains H<sub>2</sub>S (0.2–0.3 mM), NH<sub>4</sub><sup>+</sup> (0.2–0.3 mM) and CH<sub>4</sub> (0.02 mM) and is buffered by high amounts of bicarbonate from the limestone walls at ~pH 7.4 (Sarbu, 2000). Dissolved O<sub>2</sub> decreases to less than 1 μM after the first few centimetres from the water surface, with the deeper water being essentially anoxic (Sarbu, 2000). Methylamine concentrations in the cave water were measured by our recently developed ion chromatography method with a detection limit of ~1 μM for MMA (Lidbury *et al.*, 2014). Preliminary measurements carried out using this assay suggested that the *in situ* concentration of MMA in Movile Cave water is below the detection limit of 1 μM, which could indicate rapid turnover of MMA by bacteria in the cave.

Water and floating mat samples for enrichment and isolation experiments were collected from the lake room and the two air bells in October 2009, stored at 4 °C in the nearby field station and processed within 48 h. Biofilm covering the limestone walls of both air bells was scraped off into sterile tubes. Similar samples for further isolation experiments, SIP enrichments and nucleic acid extractions were obtained from Movile Cave in April 2010. Material for DNA work was concentrated by centrifugation within 1 h of sampling and frozen at –20 °C for storage until processing.

#### DNA-SIP with <sup>13</sup>C-MMA

SIP incubations were set up at the field station in Mangalia, within 1 h of sampling, using water from Airbell 2. For each incubation, a 20 ml aliquot of cave water was added to a pre-sterilised 120 ml serum vial containing 50 μmol of labelled (<sup>13</sup>C) or unlabelled MMA-HCl (dissolved in 0.2 ml sterilised distilled water). Control incubations with no added MMA (referred to as ‘no-substrate controls’ from here on) were also set up. All serum vials were immediately sealed with a butyl rubber cap and an aluminium crimping lid and incubated at 21 °C in the dark. Samples for *t*<sub>0</sub> (*t* = 0 days) were prepared by centrifugation of 20 ml of cave water, discarding the supernatant and freezing the pellet at –20 °C. SIP incubations and no-substrate controls were harvested in the same way at time intervals of 48 h (*t*<sub>1</sub>), 96 h (*t*<sub>2</sub>) and 4 weeks (*t*<sub>3</sub>). In future SIP experiments, the recently developed ion chromatography method for measuring MMA (see above, Lidbury *et al.*, 2014) could be used to monitor consumption of substrate over time. From each sample, up to 1 μg of total extracted DNA was added to caesium chloride (CsCl) solutions for isopycnic ultracentrifugation and

gradient fractionation following published protocols (Neufeld *et al.*, 2007b).

#### Enrichment and isolation of methylated amine-utilising bacteria from Movile Cave

Methylotrophic bacteria capable of using methylated amines as a carbon and nitrogen source were selectively enriched using MMA, dimethylamine (DMA) and trimethylamine (TMA). Separate enrichments were set up for each of the three substrates by adding a final concentration of 1 mM substrate to 20 ml cave water in sterile 120 ml serum vials. For mats and biofilms, 2 g sample material was placed into 27 ml serum vials and made up to a final volume of 4 ml with nitrogen-free dilute basal salts (DBS) medium. DBS medium (modified after Kelly and Wood, 1998) contained (per litre): 0.1 g MgSO<sub>4</sub> · 7H<sub>2</sub>O, 0.05 g CaCl<sub>2</sub> · 2H<sub>2</sub>O, 0.11 g K<sub>2</sub>HPO<sub>4</sub>, 0.085 g KH<sub>2</sub>PO<sub>4</sub>, adjusted to pH 7. The medium was supplemented with a vitamins solution as described by Kanagawa *et al.* (1982) and 1 ml of a trace element solution (modified after Kelly and Wood, 1998) containing (per 1 L): 50 g EDTA, 11 g NaOH, 5 g ZnSO<sub>4</sub> · 7H<sub>2</sub>O, 7.34 g CaCl<sub>2</sub> · 2H<sub>2</sub>O, 2.5 g MnCl<sub>2</sub> · 6H<sub>2</sub>O, 0.5 g CoCl<sub>2</sub> · 6H<sub>2</sub>O, 0.5 g (NH<sub>4</sub>)<sub>6</sub>Mo<sub>7</sub>O<sub>24</sub> · 4H<sub>2</sub>O, 5 g FeSO<sub>4</sub> · 7H<sub>2</sub>O, 0.2 g CuSO<sub>4</sub> · 5H<sub>2</sub>O, adjusted to pH 6.0. After flushing the headspace of each vial with N<sub>2</sub>, the headspace was made up to a final concentration of 7% (v/v) O<sub>2</sub> and 3.5% (v/v) CO<sub>2</sub> to resemble the cave atmosphere. Enrichments were incubated at 21 °C in the dark. After 4 weeks, 10 ml (for water samples) or 4 ml (for mat samples) of fresh DBS medium were added and cultures were spiked with 20 mM MMA, 10 mM DMA or 10 mM TMA. After amending the headspace as previously, enrichment cultures were incubated at 21 °C in the dark. When enrichments became turbid (after a further 2 weeks), dilutions were spread onto agar plates (DBS medium, 1.5% agar) containing 5 mM MMA, DMA, or TMA as the only added carbon and nitrogen source. Plates were incubated at 21 °C in the dark until colonies became visible (2–10 days). In order to achieve isolation of a variety of methylotrophs, individual colonies were examined by microscopy and a selection of morphotypes was transferred onto fresh plates containing the same substrates as before. Cells were observed at ×1000 magnification in phase-contrast under a Zeiss Axioskop 50 microscope (Carl Zeiss Ltd, Cambridge, UK). Isolates were submitted to a series of transfers on plates and microscopy was used routinely to check purity before transferring individual isolates into liquid media (containing 5 mM MMA, DMA or TMA). Once grown in liquid (2–7 days), isolates were transferred back onto methylated amine plates.

In a separate enrichment approach, non-methylotrophic bacteria capable of using methylated amines as a nitrogen (but not carbon) source were isolated. These enrichments were set up in the same manner and using the same sample material as described

above for the methylotrophs. In addition to 1 mM of MMA, DMA or TMA, a mixture of alternative carbon compounds (comprising glucose, fructose, succinate, glycerol, pyruvate and acetate) was added to a final concentration of 5 mM. Isolates obtained in this way were additionally tested for growth in liquid medium containing no alternative carbon source to detect any co-enriched methylotrophs, as well as in liquid medium containing carbon sources but no methylated amines to eliminate the possibility that they might be fixing N<sub>2</sub> rather than using methylated amines as nitrogen source.

#### *DNA extraction and PCR amplification of bacterial 16S rRNA genes*

DNA from cave samples, SIP enrichments and bacterial isolates was extracted as previously described (Neufeld *et al.*, 2007a). DNA from soil and lake sediment samples retrieved from the University of East Anglia campus (used for *gmaS* primer validation, see later) was extracted using the FastDNA SPIN Kit for soil by MP Biomedicals LLC (Santa Ana, CA, USA). Bacterial 16S ribosomal RNA (rRNA) genes from SIP enrichments were amplified using primer set 341f-GC/907r (Muyzer *et al.*, 1993; Lane, 1991) for analysis by denaturing gradient gel electrophoresis (DGGE). For cloning and sequencing, bacterial 16S rRNA genes from isolates were amplified with primer set 27f/1492r (DeLong, 1992; Lane *et al.*, 1985).

#### *Denaturing gradient gel electrophoresis (DGGE)*

DGGE analysis of bacterial 16S rRNA gene fragments was carried out as described by Neufeld *et al.* (2007a) using the DCode Universal Mutation Detection System (Bio-Rad, Hercules, CA, USA). After electrophoresis for 16 h at 60 °C and 80 V, gels were stained using SYBR Gold Nucleic Acid Gel Stain (Invitrogen, Paisley, UK) and viewed under the Bio-Rad Gel Doc XR gel documentation system using Amber Filter 5206 (Bio-Rad). For gene sequence analysis, well-defined DNA bands were physically excised from the gel for re-amplification using the same PCR conditions and primers described above, followed by sequencing analysis using primer 341f (Muyzer *et al.*, 1993).

DGGE, when compared with amplicon pyrosequencing, is a relatively low resolution technique. However, the DGGE technique enabled us to accurately compare SIP enrichments across different CsCl gradient fractions (heavy to light) and also to compare <sup>13</sup>C-incubations to <sup>12</sup>C-incubated controls. This first study on MMA degraders in Movile Cave thereby allowed us to identify key players in the microbial food web. Building on data obtained in this study, more detailed studies involving pyrosequencing of amplicons can be carried out in the future.

*Functional gene PCR and development of gmaS primers*  
*mauA* genes were amplified using PCR primer set *mauAf1/mauAr1* (Neufeld *et al.*, 2007a). Currently

there is one *gmaS* PCR primer set available (Chen, 2012) which targets specifically the MRC. This PCR primer set therefore may not detect *gmaS* from non-marine bacteria. Three new *gmaS* PCR primers were designed in this study, based on multiple alignment of 34 *gmaS* sequences derived from (i) methylotrophic isolates confirmed to use the NMG-/GMA-mediated pathway and (ii) bacterial genomes published on the Integrated Microbial Genomes (IMG) platform (Markowitz *et al.*, 2010) of the Joint Genome Institute (JGI) Genome Portal (<http://genome.jgi.doe.gov>). Genomes were screened for *gmaS*-related sequences using *gmaS* from *Methylocella silvestris* as a query sequence (Chen *et al.*, 2010a). Corresponding full length sequences included both *gmaS* and glutamine synthetase type III (*glnA*) sequences, due to the high level of sequence similarity between the two genes. In order to identify genuine *gmaS* sequences, the gene neighbourhood of all obtained sequences was manually inspected for predicted neighbouring open reading frames typically found adjacent to *gmaS* (genes encoding NMG dehydrogenase and NMG synthase). Confirmed *gmaS* sequences included many sequences apparently mis-annotated as *glnA*. For primer design, multiple sequence alignments of chosen sequences were established with the Clustal X program (Thompson *et al.*, 1997) and viewed using the GeneDoc software (Nicholas *et al.*, 1997). Because of their sequence similarity to *gmaS*, a number of *glnA* sequences were included in the alignment in order to identify suitable primer-binding regions specific only to *gmaS* (for a complete list of all *gmaS* and *glnA* sequences used for primer design, see Supplementary Table S1). The resulting forward primer *gmaS*\_557f (5'-GARGAYG CSAACGGYCAGTT-3') was used in all cases, with the reverse primers  $\alpha$ \_*gmaS*\_970r (3'-TGGGTSCGRT TRTTGCCSG-5') and  $\beta$ \_ $\gamma$ \_*gmaS*\_1332r (3'-GTAMTC SAYCCAYTCCATG-5') being used to target the *gmaS* gene of non-marine *Alphaproteobacteria* and that of *Beta*- and *Gammaproteobacteria*, respectively. Touchdown PCR protocols for *gmaS* amplification were used as follows: for *gmaS*\_557f/ $\alpha$ \_*gmaS*\_970r, an initial step at 94 °C for 5 min was followed by 10 cycles of denaturation at 94 °C for 45 s, annealing at variable temperatures for 45 s and extension at 72 °C for 1 min. In the first cycle, the annealing temperature was set to 60 °C, and for each of the nine subsequent cycles the annealing temperature was decreased by 1 °C. This was followed by 30 cycles of 45 s at 94 °C, 45 s at 56 °C and 1 min at 72 °C, and a final extension time of 8 min at 72 °C. For *gmaS*\_557f/ $\beta$ \_ $\gamma$ \_*gmaS*\_1332r, a modification of the first touchdown protocol was used; the annealing temperature was set to 55 °C in the first cycle and decreased by 1 °C for each of the nine subsequent cycles. The first 10 cycles were followed by 35 cycles with an annealing temperature of 52 °C.

The primer sets were tested for their specificity by (i) amplification and sequencing of *gmaS* sequences

from genomic DNA of the following bacterial strains known to use the indirect MMA-oxidation pathway: *Sinorhizobium meliloti* 1021, *Mesorhizobium loti* MAFF303099, *Rhizobium leguminosarum* bv. viciae 3841, *Agrobacterium tumefaciens* C58 and *Pseudomonas fluorescens* SBW25 (Chen *et al.*, 2010b). For further validation of the primers, *gmaS* was amplified from DNA extracted from (ii) MMA enrichments from Movile Cave, (iii) fresh Movile Cave mat and (iv) soil and freshwater sediment from a small lake (the 'Broad') on the University of East Anglia campus. *gmaS*-based clone libraries were constructed for (ii)–(iv) and a total of 30 clones were randomly selected for sequencing.

#### DNA sequencing and phylogenetic analysis

DNA sequencing employed the Sanger method on a 3730A automated sequencing system (PE Applied Biosystems, Warrington, UK). To determine approximate phylogenetic affiliations, partial 16S rRNA gene sequences were analysed with the Basic Local Alignment Search Tool (BLAST) on the NCBI GenBank database (Altschul *et al.*, 1990). Amino acid and nucleotide-based phylogenetic trees were established using the MEGA5 program (Tamura *et al.*, 2011). The evolutionary history was inferred by neighbour-joining (Saitou and Nei, 1987). For nucleotide-based trees (Supplementary Figures 1a and b), the evolutionary distances were computed using the maximum composite likelihood method (Tamura *et al.*, 2004). For amino-acid-based trees, the evolutionary distances were computed using the Poisson correction method (Zuckerkanndl and Pauling, 1965). All positions containing gaps and missing data were eliminated. Bootstrap analysis (1000 replicates) was performed to provide confidence estimates for phylogenetic tree topologies (Felsenstein, 1985). Phylogenetic analysis of *gmaS* genes was carried out at the amino-acid level (135–250 amino-acyl residues).

#### Nucleotide sequence accession numbers

Nucleotide gene sequences obtained from this study were deposited in the GenBank nucleotide sequence database under the accession numbers KM083620–KM083705.

## Results

#### Active methylotrophic bacteria identified by DNA-SIP with $^{13}\text{C}$ -MMA

DNA-SIP enrichments with  $^{13}\text{C}$ -labelled MMA were set up from Movile Cave water in order to identify active, methylotrophic bacteria capable of using MMA as a carbon source. DNA was extracted from microcosms enriched with  $^{13}\text{C}$ -labelled and unlabelled MMA after 48 h ( $t_1$ ), 96 h ( $t_2$ ) and 4 weeks ( $t_3$ ). The bacterial communities in the microcosms were investigated by DGGE analysis of bacterial 16S rRNA

gene fragments. Comparison of DGGE profiles from unfractionated DNA from the different time points revealed a significant shift in the bacterial community over time, which was similar between  $^{12}\text{C}$ -MMA and  $^{13}\text{C}$ -MMA incubations (Figure 1).

For identification of active methylotrophs, DNA extracted from all time points was subjected to density gradient centrifugation and fractionation, allowing separation of  $^{13}\text{C}$ -labelled DNA (contained in heavy fractions) from unlabelled  $^{12}\text{C}$ -DNA (contained in light fractions). Bacterial 16S rRNA gene fragments were amplified from all DNA fractions and analysed by DGGE and sequencing. Time point  $t_1$  (48 h) did not show any significant enrichment in  $^{13}\text{C}$ -DNA and was therefore not further analysed. DGGE analysis of heavy and light DNA fractions from time points  $t_2$  and  $t_3$  ( $^{13}\text{C}$ -MMA incubation) revealed major differences in the community profiles of the heavy fractions (Figures 2a and c): A single band dominated the heavy fractions at  $t_2$  (96 h, Figure 2a) but was absent at  $t_3$  (4 weeks, Figure 2c). Sequence analysis of the excised band revealed that the sequence affiliated with *Methylotenera mobilis* (99% identity), an obligate methylotroph (Kalyuzhnaya *et al.*, 2006a) known to be abundant in Movile Cave from previous studies (Chen *et al.*, 2009). At  $t_3$ , several different phylogenotypes appeared in the heavy fractions of the  $^{13}\text{C}$ -MMA incubation (Figure 2c), that is, a more diverse bacterial community had incorporated the label following extended incubation with MMA.

Bacterial 16S rRNA gene sequences from these DGGE bands affiliated with well-characterised methylotrophs such as *Methylobacterium extorquens* (100% identity) and *Methylovorus* (97% identity to

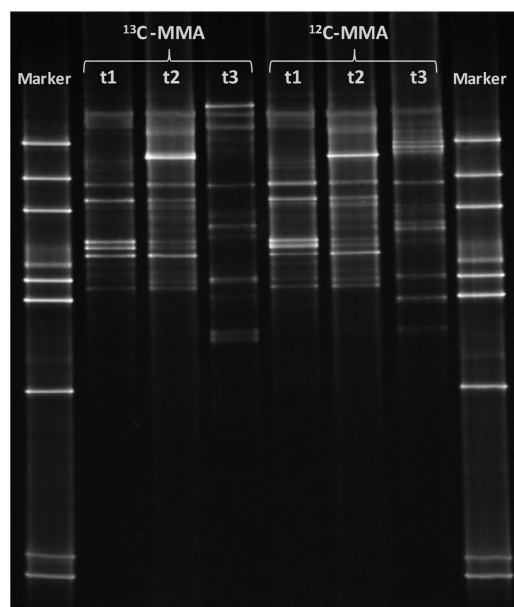


**Figure 1** Denaturing gradient gel electrophoresis analysis of bacterial 16S rRNA gene fragments in native (unfractionated) DNA from incubations of Movile Cave water with  $^{13}\text{C}$ -MMA (left) and unlabelled MMA (right), after 48 h ( $t_1$ ), 96 h ( $t_2$ ) and 4 weeks ( $t_3$ ).

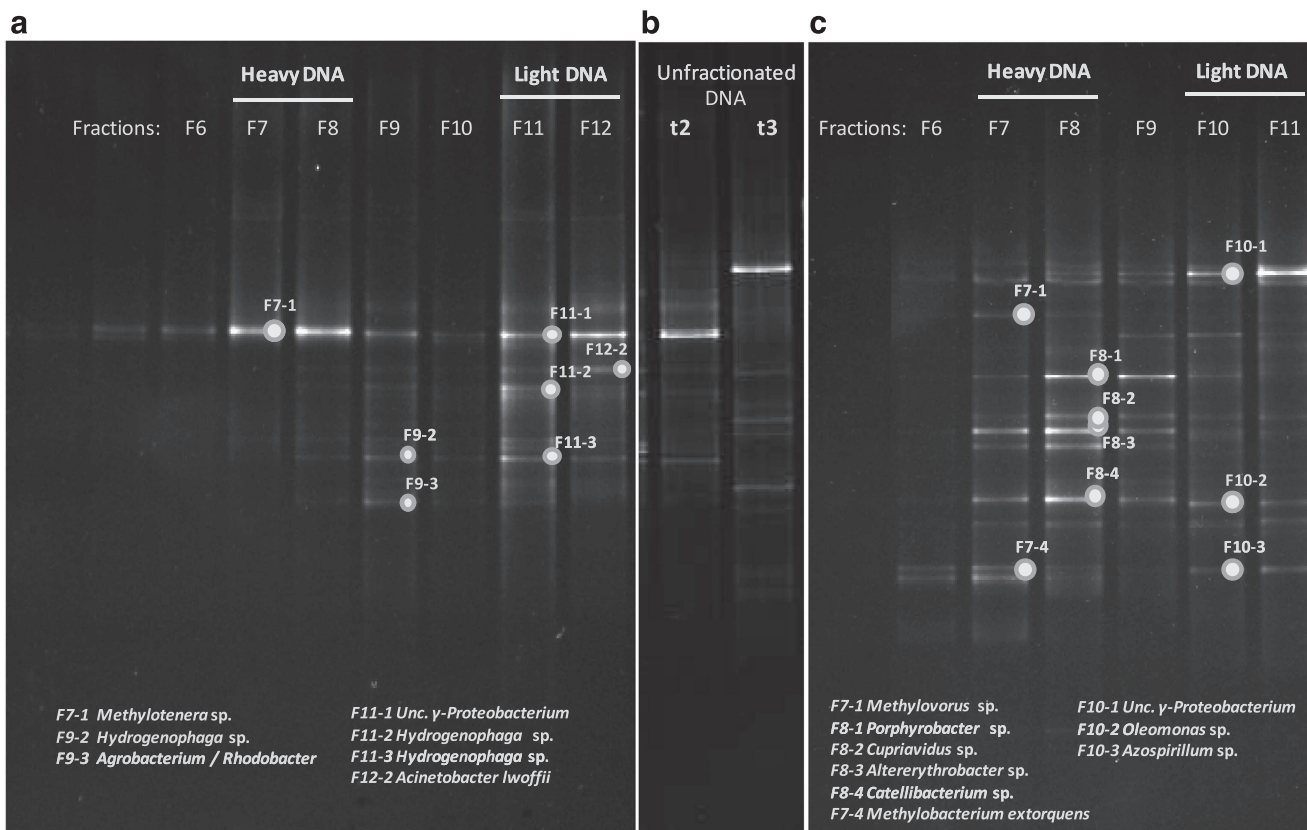


**Figure 2** Denaturing gradient gel electrophoresis analysis of bacterial 16S rRNA gene fragments in light and heavy DNA fractions from  $^{13}\text{C}$ -MMA incubations of Movile Cave water after 96 h (a) and 4 weeks (c) DGGE profiles of unfractionated DNA of both time points (b) are shown for reference.

*Methylovorus menthalis*), but also included *Catellibacterium* (98% identity to *Catellibacterium caeni*), *Cupriavidus* (99% identity to *Cupriavidus necator*), *Porphyrobacter* (99% identity to *Porphyrobacter neustonensis*) and *Altererythrobacter* (99% identity to *Altererythrobacter epoxidivorans*), none of which have previously been reported to grow methylotrophically. The *Catellibacterium* sequence identified from DGGE shared 98–100% sequence identity with a novel organism subsequently isolated from Movile Cave during this study (see below) and cloned 16S rRNA gene sequences from  $^{13}\text{C}$ -labelled DNA from t<sub>3</sub> (data not shown, refer to Supplementary Figure S3a).

The non-methylotrophic bacterial community co-enriched in  $^{13}\text{C}$ -MMA incubations was investigated by PCR-DGGE of 16S rRNA bacterial genes present in the light fractions ( $^{12}\text{C}$ -DNA). Light fractions harboured a diversity of mostly heterotrophic bacterial sequences (Figure 2a and b), namely *Rhodobacter*, *Acinetobacter*, *Azospirillum*, *Oleomonas* and *Hydrogenophaga* and a number of sequences not closely related to cultivated representatives (as little as 84–87% identity).

All bacterial sequences obtained from DGGE bands in lanes loaded with heavy DNA (that is,  $^{13}\text{C}$ -labelled organisms) were exclusive to MMA enrichments, and not seen in no-substrate controls (data not shown). Two sequences detected in the light fractions from MMA incubations

(*Acinetobacter* and *Azospirillum*) also appeared to be absent in the no-substrate controls, suggesting that these bacteria may have been selectively enriched due to their capability of using MMA as a nitrogen source (but not as a carbon source, and so their DNA was not labelled). One of these sequences (*Acinetobacter lwoffii*) did indeed correspond to a bacterium isolated from Movile Cave in this study with MMA as the only nitrogen source (see below).

#### *Methylotrophic and non-methylotrophic isolates from Movile Cave*

To complement data from  $^{13}\text{C}$ -MMA-SIP experiments, methylated amine-utilising bacteria were isolated from different locations (lake room, Airbell 1 and Airbell 2) in Movile Cave. Methylotrophs were isolated with DBS medium containing MMA, DMA or TMA as sole added source of carbon, energy and nitrogen. A selection of isolates differing in colony and cell morphology was transferred into liquid DBS medium containing the respective methylated amine (to distinguish true methylotrophs from organisms growing on agar). Seven methylotrophic strains were isolated, identified based on 16S rRNA gene sequencing analysis (Table 1, Supplementary Figure S3a). The highest diversity of methylotrophs was obtained on MMA enrichments (based on morphology and 16S rRNA gene sequencing data),

**Table 1** Growth of bacterial isolates from Movile Cave on methylated amines with and without added carbon

Isolates	Phylogeny	Identity (%)	Growth on methylated amines					
			MMA + C	DMA + C	TMA + C	MMA	DMA	TMA
<i>Alphaproteobacteria</i>								
2W-7	<i>Methylobacterium extorquens</i>	100	+	+	+	+	+	+
LW-13	<i>Xanthobacter tagetidis</i>	100	+	+	+	+	+	+
A2-1D	<i>Paracoccus yeei</i>	100	+	+	+	+	+	+
2W-61	<i>Paracoccus yeei</i>	98	+	+	+	+	+	+
2W-12	<i>Aminobacter niigataensis</i>	100	+	+	+	+	+	+
LW-1	<i>Catellibacterium caeni</i>	99	+	–	+	+	+	+
1M-11	<i>Mesorhizobium loti</i>	99	+	+	+	+	+	+
A2-41x	<i>Shinella yambaruensis</i>	98	+	–	–	–	NA	NA
1W-5	<i>Rhodobacter blasticus</i>	96	+	+	+	–	–	–
O1	<i>Oleomonas sagaranensis</i>	98	+	+	–	–	–	–
O3	<i>Oleomonas sagaranensis</i>	99	+	–	–	–	–	–
<i>Gammaproteobacteria</i>								
1W-58	<i>Acinetobacter johnsonii</i>	100	+	+	+	–	–	–
2W-62	<i>Acinetobacter lwoffii</i>	100	+	+	–	–	–	–
1W-57Y	<i>Pseudomonas oleovorans</i>	99	+	–	–	–	–	–
<i>Betaproteobacteria</i>								
A2-14M	<i>Zoogloea caeni</i>	100	+	+	+	–	–	–

Abbreviations: C, carbon mixture; DMA, dimethylamine; MMA, monomethylamine; NA, not analysed; TMA, trimethylamine. Carbon mixture consists of sucrose, glucose, fructose, glycerol, pyruvate and acetate. Carbon sources were supplied at 5 mM, nitrogen sources at 1 mM.

while DMA and TMA enrichments were dominated by *Xanthobacter tagetidis* (Padden *et al.*, 1997). Notably, no *Methylotenera* isolates were obtained (even after using a variety of different cultivation media which are commonly used for methylotrophic bacteria, changing incubation conditions such as temperature, pH, ionic strength of media and dilution-to-extinction experiments), despite the active role of this methylotroph in MMA metabolism as determined by DNA-SIP results (see above), and its apparent abundance in Movile Cave (Chen *et al.*, 2009). In addition to well-characterised methylotrophs such as *M. extorquens*, two novel methylotrophs were also isolated. A member of the relatively new genus *Catellibacterium* (Tanaka *et al.*, 2004; Liu *et al.*, 2010; Zheng *et al.*, 2011; Zhang *et al.*, 2012), provisionally named *Catellibacterium* sp. LW-1 was isolated from lake water enrichments with MMA. 16S rRNA gene sequences relating to this organism were also detected in heavy DNA fractions from <sup>13</sup>C-MMA enrichments (see above, Figure 2c, Supplementary Figure S1b), indicating that *Catellibacterium* may have a significant role in the cycling of methylated amines in Movile Cave. In addition, a new member of the genus *Mesorhizobium* (a genus not currently known to contain any methylotrophic species), was isolated from an MMA enrichment set up with floating mat from Airbell 1. All methylotrophic isolates were facultative, that is, also able to use sugars or carboxylic acids for growth. Notably, all methylotrophs could use all three methylated amines as sole growth substrates, with the exception of *Catellibacterium* sp. LW-1 which did not grow on DMA (Table 1).

In a separate experiment, heterotrophic bacteria capable of using methylated amines as a nitrogen but not carbon source were enriched and isolated using the same sample material as above. MMA, DMA or TMA were the only added nitrogen sources in these enrichments and a mixture of sugars and carboxylic acids were added as carbon and energy source. A diversity of non-methylotrophic methylated amine-utilising bacteria was obtained—in total eight bacterial species, as determined by 16S rRNA gene sequencing analysis (Table 1, Supplementary Figures S3a and b). All of these isolates used MMA as a nitrogen source, while only some could use DMA and TMA (Table 1), suggesting that many lack the enzymes for de-methylation of secondary and tertiary methylated amines to MMA. None of the isolates grew methylotrophically with MMA, DMA or TMA. While all methylotrophic isolates obtained in this study belonged to the *Alphaproteobacteria*, non-methylotrophic MMA utilisers also included *Beta*- and *Gammaproteobacteria* (Table 1). *A. lwoffii*, isolated from Airbell 2 water with MMA as a nitrogen source, was also detected in <sup>12</sup>C-DNA fractions from MMA-SIP incubations (see above), while not seen in control incubations without added MMA. These results suggest that *Acinetobacter* (and other non-methylotrophs) may have an active role in the cycling of methylated amines in Movile Cave.

#### *Development and validation of functional gene primer sets targeting gmaS*

The gene *gmaS* codes for GMA synthetase, the enzyme catalysing the first step in the conversion of MMA to

CH<sub>2</sub>=THF in the recently characterised indirect MMA-oxidation pathway (Latypova *et al.*, 2010; Chen *et al.*, 2010a, 2010b). We selected *gmaS* as a functional biomarker to assess the distribution of this pathway among MMA-utilising bacteria. Since currently available *gmaS* primers are specific to the MRC (Chen, 2012), we designed two new primer sets covering *gmaS* of non-marine bacteria. Suitable primer regions were identified by alignment of *gmaS* sequences obtained from (i) isolates confirmed to use the GMAS-/NMG-mediated pathway and (ii) published bacterial genomes. Due to sequence similarity between the two genes, a number of *glnA* gene sequences were included in the alignment to enable identification of suitable *gmaS* primer-binding regions not found in *glnA*.

Sequence alignment and establishment of nucleotide-based and amino-acid-based phylogenetic trees clearly separated *glnA* from *gmaS* genes and revealed two distinct *gmaS* clusters dividing (i) *Alphaproteobacteria* and (ii) *Beta-* and *Gammaproteobacteria* (Figure 3). The alphaproteobacterial *gmaS* cluster was further split into two major subgroups: 'Group 1' contained MRC-associated sequences (in a separate sub-cluster), as well as sequences belonging to soil and freshwater bacteria from the orders *Rhodobacterales* and *Rhizobiales*, while 'Group 2' contained only *gmaS* sequences from non-marine bacteria of the orders *Rhodospirillales*, *Rhizobiales* and *Sphingomonadales* (Figure 3). For primer design, sequences associated with the MRC were removed from the alignment as they were too divergent from the other sequences to be targeted by the same primers. A common region shared by all remaining *gmaS* sequences was used to design the forward primer (*gmaS*\_557f). Two different reverse primers were designed for *Alphaproteobacteria* ( $\alpha$ \_gmaS\_970r) and *Beta-* and *Gammaproteobacteria* ( $\beta$ \_gmaS\_1332r) because no further region of sufficient similarity shared by both groups could be identified (alignments in Supplementary Figures S4a–c).

Specificity of these PCR primer sets was confirmed by amplification and sequencing of *gmaS* from (i) five bacteria known to use the *gmaS*-dependent pathway (as specified in Material and methods) (ii) MMA enrichments from Movile Cave (iii) Movile Cave biofilm and (iv) soil and lake sediment from a different environment (UEA campus; as described in Material and methods). All PCR products obtained were of the expected size, that is, ~410 bp (alphaproteobacterial *gmaS*) and ~770 bp (beta- and gammaproteobacterial *gmaS*). With DNA from MMA enrichments, a slightly larger, second band was obtained in addition to the *gmaS* product when using 557f/1332r. This gene fragment shared high sequence identity with a viral coat protein and could not be eliminated by using more stringent PCR conditions due to extremely high similarity with the target gene in the primer-binding regions. This alternative amplification product was restricted to Movile Cave

enrichment DNA and was avoided by gel excision of the *gmaS* band. All sequences obtained from genomic DNA (i) and clone libraries (a total of 30 randomly selected clones from (ii), (iii) and (iv)) were identified as *gmaS* (Figure 3, Supplementary Figure S5), confirming specificity of the primers.

The *gmaS* sequences obtained from Movile Cave DNA affiliated with *gmaS* from both methylotrophic and non-methylotrophic bacteria—namely *Methylobacterium*, *Catellibacterium*, *Pseudomonas* and *Acinetobacter* (99–100% similarity, Figure 3)—identified by DNA-SIP and isolation work in this study. A further sequence loosely affiliated with *Methylothera*, *Methylovorus* and *Methylophaga* (89–90% similarity with all three genera). A final *gmaS* sequence was related to *gmaS* from the methylotroph *Hyphomicrobium* (99% similarity) which had not been detected by DNA-SIP or isolation.

#### *Distribution of gmaS and mauA genes in Movile Cave isolates*

To assess the distribution of the direct and indirect MMA-oxidation pathways in Movile Cave, bacterial isolates were screened for the presence of *mauA* and *gmaS* genes. While the *mauA*-dependent, direct MMA-oxidation pathway is so far only known to exist in bacteria using MMA as a carbon source (that is, methylotrophs), the *gmaS*-dependent, indirect pathway has recently been shown to also exist in bacteria using MMA for nitrogen nutrition only (that is, non-methylotrophs) (Chen *et al.*, 2010b). Using the *gmaS* primer sets developed in this study, PCR and sequence analysis of DNA from isolates revealed the presence of *gmaS* in all eight non-methylotrophic MMA-utilising bacteria and in all seven methylotrophic MMA utilisers (Table 2). Phylogenetic analysis placed the retrieved *gmaS* sequences within the alphaproteobacterial and the beta-/gammaproteobacterial clusters as expected. Interestingly however, *gmaS* from *Aminobacter*, *Paracoccus*, *Catellibacterium*, *Mesorhizobium* and *Rhodobacter* formed a distinct subgroup within the *Alphaproteobacteria*, separate from the other freshwater and soil group, and separate from the marine group (Figure 3). *mauA* was detected in addition to *gmaS* in four of the seven methylotrophic isolates. These data indicate that the *gmaS* gene is widespread among MMA-utilising bacteria in Movile Cave.

## Discussion

### *Methylated amine-utilising methylotrophs in Movile Cave*

The combination of SIP and cultivation proved very effective for the identification of methylotrophs. DNA-SIP results revealed *M. mobilis* as one of the major MMA-utilising methylotrophs in Movile Cave, which is in agreement with previous studies which showed high abundance of this organism (Chen *et al.*, 2009). While resisting all isolation

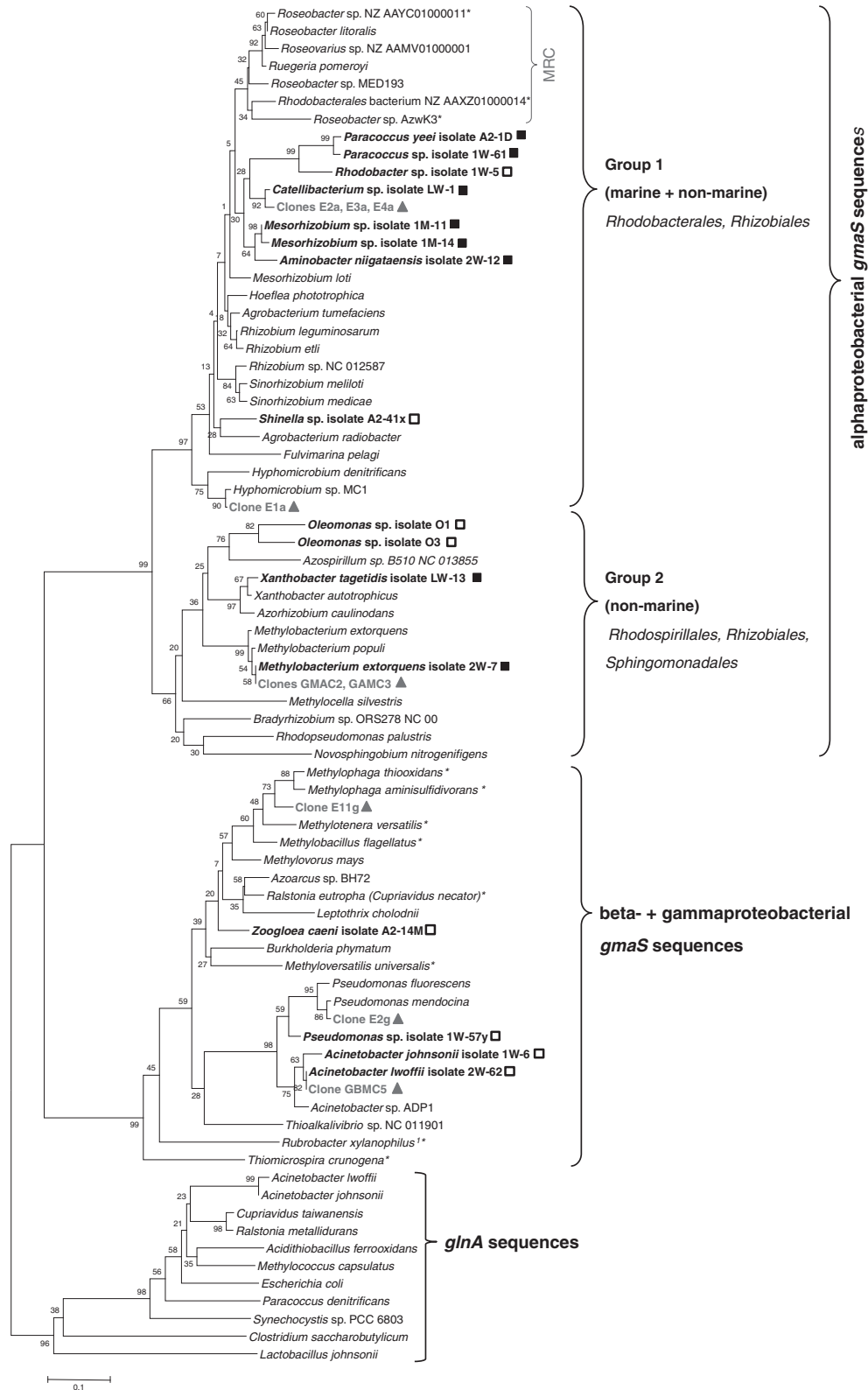


**Figure 3** Phylogenetic relationship of *gmaS* sequences (135–250 amino acids) derived from published bacterial genomes, methylophilic (solid rectangles/orange font) and non-methylophilic (hollow rectangles/blue font) bacterial isolates and clone library sequences (triangles/bold print) from Movile Cave. *glnA* sequences present the outgroup. The tree was established using the neighbour-joining method (1000 bootstrap replicates) and the Poisson correction method for computing evolutionary distances. <sup>1</sup>*Rubrobacter xylanophilus* is a member of the *Actinobacteria* although its *gmaS* sequence affiliates with the beta- and gammaproteobacterial cluster. \**gmaS* sequences containing a total of more than two mismatches across the forward/reverse primer set designed for the respective *gmaS* clusters are marked with an asterisk. MRC, marine Roseobacter clade.

**Table 2** Methylated amine metabolism and the presence of functional gene markers in Movile Cave isolates

Isolate	Methylated amines used as		Functional genes		
	N-source	C-source	<i>gmaS</i>	<i>mauA</i>	
<b>Alphaproteobacteria</b>					
1	<i>Methylobacterium extorquens</i> 2W-7	+	+	+	+
2	<i>Xanthobacter tagetidis</i> LW-13	+	+	+	+
3	<i>Paracoccus yeei</i> A2-1D	+	+	+	+
4	<i>Paracoccus</i> sp. 1W-61	+	+	-	+
5	<i>Aminobacter niigataensis</i> 2W-12	+	+	+	-
6	<i>Catellibacterium</i> sp. LW-1	+	+	+	-
7	<i>Mesorhizobium</i> sp. 1M-11	+	+	+	-
8	<i>Shinella</i> sp. A2-41x	+	-	+	-
9	<i>Rhodobacter</i> sp. 1W-5	+	-	+	-
10	<i>Oleomonas</i> sp. O1	+	-	+	-
11	<i>Oleomonas</i> sp. O3	+	-	+	-
<b>Gammaproteobacteria</b>					
12	<i>Acinetobacter johnsonii</i> 1W-6	+	-	+	-
13	<i>Acinetobacter lwoffii</i> 2W-62	+	-	+	-
14	<i>Pseudomonas</i> sp. 1W-57Y	+	-	+	-
<b>Betaproteobacteria</b>					
15	<i>Zoogloea caeni</i> A2-14M	+	-	+	-

Overview of bacterial isolates from Movile Cave, their capability of using methylated amines as a carbon (C) and/or nitrogen (N) source, and presence of functional genes indicating the direct (*mauA*) or indirect (*gmaS*) methylamine oxidation pathway.

attempts, at 96 h in SIP incubations *M. mobilis* was the first organism that responded to addition of MMA.

The combination of cultivation-based studies and SIP furthermore revealed that a new methylotroph, *Catellibacterium* sp. LW-1, is an active MMA utiliser in Movile Cave. Growth studies were essential in consolidating DNA-SIP results and confirming *Catellibacterium* as a novel methylotroph and active MMA-utilising bacterium in Movile Cave. These results also highlight the benefit of analysing SIP enrichments at different time points.

Data from SIP enrichments also suggested that *Cupriavidus*, *Porphyrobacter* and *Altererythrobacter* might have a major role in methylotrophic MMA utilisation alongside known methylotrophs such as *Methylobacterium* and *Methylovorus*. While these organisms were not isolated from the cave and have hence not been tested for growth with methylated amines, published genomes of some *Cupriavidus*/*Ralstonia* species contain *gmaS* (refer to trees in Figure 3, Supplementary Figure S5).

#### Use of methylated amines by non-methylotrophic bacteria in Movile Cave

The large variety of bacterial isolates in Movile Cave using methylated amines as nitrogen sources but not as carbon sources is intriguing, considering the relatively high standing concentrations of ammonium present in Movile Cave water. It is possible that ammonium-depleted areas exist within the microbial mats where utilisation of MMA is advantageous. The fact that nitrogen in the mat is isotopically light while ammonium in the cave water is heavy (Sarbu *et al.*, 1996) could be explained by isotopic

fractionation during ammonium assimilation and nitrification. However, it may also indicate that a nitrogen source other than ammonium is used. When growing methylotrophically, some bacterial species have been shown to use the nitrogen of MMA, even when high ammonium concentrations are present (Bellion *et al.*, 1983). The high concentrations of ammonium may even be partly due to the release of excess nitrogen by bacteria using MMA as both a carbon and nitrogen source.

#### Distribution of the *gmaS* gene and its use as a biomarker

The newly developed PCR primers targeting *gmaS* were successful in the detection of MMA-utilising bacteria not covered by currently available primers which target *mauA*-containing methylotrophs. Results from functional gene screening of non-methylotrophic Movile Cave isolates support previous findings (Chen *et al.*, 2010a) which showed that the *gmaS*-dependent pathway is used by the non-methylotroph *Agrobacterium tumefaciens*. Taken together, these results suggest that the *gmaS* pathway may be the major mode of MMA utilisation in bacteria using MMA as a nitrogen, but not as a carbon, source. Based on our results, the *gmaS*-dependent pathway also appears to be present in the majority of methylotrophic MMA-utilising bacteria. The direct MMA dehydrogenase (*mauA*)-dependent pathway, which was detected in a number of methylotrophic isolates in addition to *gmaS*, seems to be restricted to certain groups of methylotrophic bacteria. It will be interesting to understand how the two pathways are regulated under different growth conditions in organisms containing both.

## Conclusions

Combining DNA-SIP and isolation studies, key methylotrophs in Movile Cave were identified and it was shown that methylated amines are important intermediates in Movile Cave, serving as a source of carbon, energy and/or nitrogen for a wide range of bacteria. The GMAS-/NMG-mediated pathway appears to be widespread among both methylotrophic and non-methylotrophic MMA utilisers and newly developed primer sets targeting *gmaS* have great potential as biomarkers for identification of MMA-utilising bacteria.

## Conflict of Interest

The authors declare no conflict of interest.

## Acknowledgements

We thank Vlad Voiculescu and Mihai Baciu, Rich Boden and Sharmishta Dattagupta for help in sampling Movile Cave, Rich Boden for help and advice in experimental design and discussions, Serban Sarbu for his advice and encouragement and Andy Johnston and Andrew Crombie for their insightful comments on the work.

We acknowledge funding from the Natural Environment Research Council to JCM (NE/G017956) and YC (NE/H016236) and the University of Warwick and the University of East Anglia Earth and the Life Systems Alliance postgraduate research scholarships to DW. We are also grateful to the custodian of Movile Cave, the Group for Underwater and Speleological Exploration (GESS), for letting us use its field station in Mangalia and for providing the logistic support for sampling trips.

## References

- Altschul SF, Gish W, Miller W, Myers EW, Lipman DJ. (1990). Basic local alignment search tool. *J Mol Biol* **215**: 403–410.
- Anthony C. (1982). *The Biochemistry of Methylotrophs*. Academic Press: London.
- Barrett EL, Kwan HS. (1985). Bacterial reduction of trimethylamine oxide. *Annu Rev Microbiol* **39**: 131–149.
- Bellion E, Bolbot J. (1983). Nitrogen assimilation in facultative methylotrophic bacteria. *Curr Microbiol* **9**: 37–44.
- Bellion E, Hersh LB. (1972). Methylamine metabolism in a *Pseudomonas* species. *Arch Biochem Biophys* **153**: 368–374.
- Bellion E, Kent ME, Aud JC, Alikhan MY, Bolbot JA. (1983). Uptake of methylamine and methanol by *Pseudomonas* sp. strain AM1. *J Bacteriol* **154**: 1168–1173.
- Berman T, Bronk DA. (2003). Dissolved organic nitrogen: a dynamic participant in aquatic ecosystems. *Aquat Microb Ecol* **31**: 279–305.
- Bicknell B, Owens JD. (1980). Utilization of methyl amines as nitrogen sources by non-methylotrophs. *J Gen Microbiol* **117**: 89–96.
- Boden R, Thomas E, Savani P, Kelly DP, Wood AP. (2008). Novel methylotrophic bacteria isolated from the River Thames (London, UK). *Environ Microbiol* **10**: 3225–3236.
- Brooke AG, Attwood MM. (1984). Methylamine uptake by the facultative methylotroph *Hyphomicrobium* X. *J Gen Microbiol* **130**: 459–463.
- Budd JA, Spencer CP. (1968). The utilisation of alkylated amines by marine bacteria. *Mar Biol* **2**: 92–101.
- Campbell KA. (2006). Hydrocarbon seep and hydrothermal vent paleoenvironments and paleontology: past developments and future research directions. *Palaeogeogr Palaeoclimatol* **232**: 362–407.
- Chen Y. (2012). Comparative genomics of methylated amine utilization by marine *Roseobacter* clade bacteria and development of functional gene markers (tmm, gmaS). *Environ Microbiol* **14**: 2308–2322.
- Chen Y, McAleer KL, Murrell JC. (2010b). Monomethylamine as a nitrogen source for a non-methylotrophic bacterium, *Agrobacterium tumefaciens*. *Appl Environ Microbiol* **76**: 4102–4104.
- Chen Y, Scanlan J, Song L, Crombie A, Rahman MT, Schäfer H et al. (2010a). Gamma-glutamylmethylamide is an essential intermediate for monomethylamine metabolism in *Methylocella silvestris*. *Appl Environ Microbiol* **76**: 4530–4537.
- Chen Y, Wu L, Boden R, Hillebrand A, Kumaresan D, Moussard H et al. (2009). Life without light: microbial diversity and evidence of sulfur- and ammonium-based chemolithotrophy in Movile Cave. *ISME J* **3**: 1093–1104.
- Chistoserdova L. (2011). Modularity of methylotrophy, revisited. *Environ Microbiol* **13**: 2603–2622.
- Chistoserdova L, Kalyuzhnaya MG, Lidstrom ME. (2009). The expanding world of methylotrophic metabolism. *Annu Rev Microbiol* **63**: 477–499.
- Colby J, Zatman LJ. (1973). Trimethylamine metabolism in obligate and facultative methylotrophs. *Biochem J* **132**: 101–112.
- DeLong EF. (1992). Archaea in coastal marine environments. *Proc Natl Acad Sci USA* **89**: 5685–5689.
- Felsenstein J. (1985). Confidence limits on phylogenies: an approach using the bootstrap. *Evolution* **39**: 783–791.
- Fitzsimons MF, Millward GE, Revitt DM, Dawit MD. (2006). Desorption kinetics of ammonium and methylamines from estuarine sediments: consequences for the cycling of nitrogen. *Mar Chem* **101**: 12–26.
- Gibb SW, Mantoura RFC, Liss PS, Barlow RG. (1999). Distributions and biogeochemistries of methylamines and ammonium in the Arabian Sea. *Deep-Sea Res II* **46**: 593–615.
- Glenn AR, Dilworth MJ. (1984). Methylamine and ammonium transport system in *Rhizobium leguminosarum* MNF 3841. *J Gen Microbiol* **130**: 1961–1968.
- Hutchens E, Radajewski S, Dumont MG, McDonald IR, Murrell JC. (2004). Analysis of methanotrophic bacteria in Movile Cave by stable isotope probing. *Environ Microbiol* **6**: 111–120.
- Kanagawa T, Dazai M, Fukuoka S. (1982). Degradation of organo-phosphorus wastes. 2. Degradation of O,O-dimethyl phosphorodithioate by *Thiobacillus thioparus* TK-1 and *Pseudomonas* AK-2. *Agric Biol Chem* **46**: 2571–2578.
- Kalyuzhnaya MG, Bowerman S, Jimmie CL, Lidstrom ME, Chistoserdova L. (2006a). *Methylotenera mobilis* gen. nov., sp. nov., an obligately methylamine-utilizing bacterium within the family *Methylophilaceae*. *Int J Syst Evol Microbiol* **56**: 2819–2823.
- Kalyuzhnaya MG, De Marco P, Bowerman S, Pacheco CC, Lara JC, Lidstrom ME et al. (2006b). *Methyloversatilis universalis* gen. nov., sp. nov., a novel taxon within the *Betaproteobacteria* represented by three methylotrophic isolates. *Int J Syst Evol Microbiol* **56**: 2517–2522.
- Kelly DP, Wood AP. (1998). Microbes of the sulfur cycle. In: Burlage RS, Atlas R, Stahl D, Geesey G, Sayler C (eds) *Techniques in Microbial Ecology*. Oxford university press: New York, NY, USA, pp 31–57.
- Kung HF, Wagner C. (1969). Gamma-glutamylmethylamide. A new intermediate in the metabolism of methylamine. *J Biol Chem* **244**: 4136–4140.
- Lane DJ. (1991). 16S/23S rRNA sequencing. In: Stackebrandt E, Goodfellow M (eds) *Nucleic Acid Techniques in Bacterial Systematics*. John Wiley & Sons Inc: Chichester, UK, pp 115–175.
- Lane DJ, Pace B, Olsen GJ, Stahl DA, Sogin ML, Pace NR. (1985). Rapid determination of 16S ribosomal RNA sequences for phylogenetic analyses. *Proc Natl Acad Sci USA* **82**: 6955–6959.
- Latypova E, Yang S, Wang YS, Wang T, Chavkin TA, Hackett M et al. (2010). Genetics of the glutamate-mediated methylamine utilization pathway in the facultative methylotrophic beta-proteobacterium *Methyloversatilis universalis* FAM5. *Mol Microbiol* **75**: 426–439.
- Levering PR, van Dijken JP, Veenhuis M, Harder W. (1981). *Arthrobacter* P1, a fast growing versatile methylotroph with amine oxidase as a key enzyme in the metabolism of methylated amines. *Arch Microbiol* **129**: 72–80.

- Lidbury I, Murrell JC, Chen Y. (2014). Trimethylamine N-oxide metabolism by abundant marine heterotrophic bacteria. *Proc Natl Acad Sci USA* **111**: 2710–2715.
- Lidstrom ME. (2006). Aerobic methylotrophic prokaryotes. In: Dworkin M, Falkow S, Rosenberg E, Schleifer K-H, Stackebrandt E (eds), *The Prokaryotes, vol. 2: ecophysiology and biochemistry*. Springer-Verlag: New York, USA, pp 618–634.
- Lin TY, Timasheff SN. (1994). Why do some organisms use a urea-methylamine mixture as osmolyte? Thermodynamic compensation of urea and trimethylamine N-oxide interactions with protein. *Biochemistry* **33**: 12695–12701.
- Liu Y, Xu CJ, Jiang JT, Liu YH, Song XF, Li H *et al.* (2010). *Catellibacterium aquatile* sp. nov., isolated from fresh water, and emended description of the genus *Catellibacterium* Tanaka *et al.* 2004. *Int J Syst Evol Microbiol* **60**: 2027–2031.
- Lutz RA, Kennish MJ. (1993). Ecology of deep-sea hydrothermal vent communities: a review. *Rev Geophys* **31**: 211–242.
- Markowitz VM, Chen IMA, Palaniappan K, Chu K, Szeto E, Grechkin Y *et al.* (2010). The integrated microbial genomes (IMG) system: an expanding comparative analysis resource. *Nucleic Acids Res* **38**: D382–D390.
- Murrell JC, Lidstrom ME. (1983). Nitrogen metabolism in *Xanthobacter* H4-14. *Arch Microbiol* **136**: 219–221.
- Murrell JC, Whiteley AS. (2011). *Stable Isotope Probing and Related Technologies*. American Society for Microbiology Press: Washington, DC, USA.
- Muyzer G, De Waal EC, Uitterlinden AG. (1993). Profiling of complex microbial populations by denaturing gradient gel electrophoresis analysis of polymerase chain reaction-amplified genes coding for 16S rRNA. *Appl Environ Microbiol* **59**: 695–700.
- Neff JC, Chapin FS, Vitousek PM. (2003). Breaks in the cycle: dissolved organic nitrogen in terrestrial ecosystems. *Front Ecol Environ* **1**: 205–211.
- Neufeld JD, Schäfer H, Cox MJ, Boden R, McDonald IR, Murrell JC. (2007a). Stable-isotope probing implicates *Methylophaga* spp and novel *Gammaproteobacteria* in marine methanol and methylamine metabolism. *ISME J* **6**: 480–491.
- Neufeld JD, Vohra J, Dumont MG, Lueders T, Manefield M, Friedrich MW *et al.* (2007b). DNA stable-isotope probing. *Nat Protoc* **2**: 860–866.
- Nicholas KB, Nicholas HB Jr, Deerfield DW. (1997). GeneDoc: Analysis and visualization of genetic variation. *EMBNEW NEWS* **4**: 14.
- Padden AN, Rainey FA, Kelly DP, Wood AP. (1997). *Xanthobacter tagetididis* sp. nov., an organism associated with Tagetes species and able to grow on substituted thiophenes. *Int J Syst Bacteriol* **47**: 394–401.
- Porter ML, Engel AS, Kane TC, Kinkle BK. (2009). Productivity-diversity relationships from chemolithoautotrophically based sulfidic karst systems. *Int J Speleol* **28**: 27–40.
- Radajewski S, Ineson P, Parekh N, Murrell JC. (2000). Stable-isotope probing as a tool in microbial ecology. *Nature* **403**: 646–649.
- Rohwerder T, Sand W, Lascu C. (2003). Preliminary evidence for a sulphur cycle in Movile Cave, Romania. *Acta Biotechnol* **23**: 101–107.
- Saitou N, Nei M. (1987). The neighbor-joining method: a new method for reconstructing phylogenetic trees. *Mol Biol Evol* **4**: 406–425.
- Sarbu SM. (2000). Movile cave: a chemoautotrophically based groundwater ecosystem. In: Wilkens H, Culver DC, Humphreys WF (eds), *Subterranean Ecosystems*. Elsevier Press: Amsterdam, The Netherlands, pp 319–343.
- Sarbu SM, Kane TC. (1995). A subterranean chemoautotrophically based ecosystem. *Natl Speleol Soc Bull* **57**: 91–98.
- Sarbu SM, Kane TC, Kinkle BK. (1996). A chemoautotrophically based cave ecosystem. *Science* **272**: 1953–1955.
- Sarbu SM, Kinkle BK, Vlasceanu L, Kane TC. (1994). Microbial characterization of a sulfide-rich groundwater ecosystem. *Geomicrobiol J* **12**: 175–182.
- Tamura K, Nei M, Kumar S. (2004). Prospects for inferring very large phylogenies by using the neighbor-joining method. *Proc Natl Acad Sci USA* **101**: 11030–11035.
- Tamura K, Peterson D, Peterson N, Stecher G, Nei M, Kumar S. (2011). MEGA5: molecular evolutionary genetics analysis using maximum likelihood, evolutionary distance, and maximum parsimony methods. *Mol Biol Evol* **28**: 2731–2739.
- Tanaka Y, Hanada S, Manome A, Tsuchida T, Kurane R, Nakamura K *et al.* (2004). *Catellibacterium nectariophilum* gen. nov., sp. nov., which requires a diffusible compound from a strain related to the genus *Sphingomonas* for vigorous growth. *Int J Syst Evol Microbiol* **54**: 955–959.
- Thompson JD, Gibson TJ, Plewniak F, Jeanmougin F, Higgins DG. (1997). The CLUSTAL\_X windows interface: flexible strategies for multiple sequence alignment aided by quality analysis tools. *Nucleic Acids Res* **25**: 4876–4882.
- Van Dover CL, German CR, Speer KG, Parson LM, Vrijenhoek RC. (2002). Evolution and biogeography of deep-sea venting and seep invertebrates. *Science* **295**: 1253–1257.
- Vlasceanu L, Popa R, Kinkle BK. (1997). Characterization of *Thiobacillus thioparus* LV43 and its distribution in a chemoautotrophically based groundwater ecosystem. *Appl Environ Microbiol* **63**: 3123–3127.
- Worsfold PJ, Monbet P, Tappin AD, Fitzsimons MF, Stiles DA, McKelvie ID. (2008). Characterisation and quantification of organic phosphorus and organic nitrogen components in aquatic systems: a review. *Anal Chim Acta* **624**: 37–58.
- Zhang J, Chen SA, Zheng JW, Cai S, Hang BJ, He J *et al.* (2012). *Catellibacterium nanjingense* sp. nov., a propanil-degrading bacterium isolated from activated sludge, and emended description of the genus *Catellibacterium*. *Int J Syst Evol Microbiol* **62**: 495–499.
- Zheng JW, Chen YG, Zhang J, Ni YY, Li WJ, He J *et al.* (2011). Description of *Catellibacterium caeni* sp. nov., reclassification of *Rhodobacter changlensis* Anil Kumar *et al.* 2007 as *Catellibacterium changlense* comb. nov. and emended description of the genus *Catellibacterium*. *Int J Syst Evol Microbiol* **61**: 1921–1926.
- Zuckerkindl E, Pauling L. (1965). Evolutionary divergence and convergence in proteins. In: Bryson V, Vogel HJ (eds) *Evolving Genes and Proteins*. Academic Press: New York, NY, USA, pp 97–166.

Supplementary Information accompanies this paper on The ISME Journal website (<http://www.nature.com/ismej>)

# Microbiology of Movile Cave—A Chemolithoautotrophic Ecosystem

DEEPAK KUMARESAN<sup>1</sup>, DANIELA WISCHER<sup>1</sup>, JASON STEPHENSON<sup>2</sup>,  
ALEXANDRA HILLEBRAND-VOICULESCU<sup>3</sup>, and J. COLIN MURRELL<sup>1\*</sup>

<sup>1</sup>*School of Environmental Sciences, University of East Anglia, Norwich, United Kingdom*

<sup>2</sup>*School of Life Sciences, University of Warwick, Coventry, United Kingdom*

<sup>3</sup>*Institute of Speleology 'Emil Racoviță,' Bucharest, Romania*

Received February 2013, Accepted August 2013

Discovered in 1986, Movile Cave is an unusual cave ecosystem sustained by *in situ* chemoautotrophic primary production. The cave is completely isolated from the surface and the primary energy sources are hydrogen sulfide and methane released from hydrothermal fluids. Both condensation and acid corrosion processes contribute to the formation of Movile Cave. Invertebrates, many of which are endemic to Movile Cave, are isotopically lighter in both carbon and nitrogen than surface organisms, indicating that they derive nutrition from chemoautotrophic primary producers within the cave. Here we review work on the microbiology of the Movile Cave ecosystem, with particular emphasis on the functional diversity of microbes involved in sulfur, carbon and nitrogen cycling, and discuss their role in chemosynthetic primary production.

**Keywords:** chemoautotrophs, methanotrophs, Movile Cave, nitrifiers, sulfur oxidizers

## Introduction

Cave ecosystems are characterized by lack of light, nearly constant air and water temperatures and relative humidity at near saturation. They are considered to be challenging environments for microbes to colonize due to nutrient and energy limitations. Usually the formation of cave systems results from the seepage of meteoric surface waters into limestone structures and the energy required for the formation of these caves is entirely supplied by water, air, gravity and fauna from the surface (Palmer 1991). Similarly, the biological communities within these cave ecosystems are dependent on the flow of nutrients and energy from the surface (Engel 2007; Forti et al. 2002).

A small percentage of the world's caves are of hypogenic origin, formed by ascending fluids. In this case, the energy needed to dissolve the rock and support the biological communities inhabiting the caves is supplied by ascending water and gases (Forti et al. 2002). The geochemistry of hypogenic caves differs depending on the origin of the rising waters, the type of host rock and the temperature and composition of the released gases. From a microbiological perspective, the most interesting hypogenic caves are those with inputs of gases such as hydrogen sulfide (H<sub>2</sub>S) and/or methane (CH<sub>4</sub>), which could provide energy sources for microbial communities.

Life sustained by chemosynthesis has been extensively studied using deep-sea hydrothermal vents as model ecosystems (reviewed in Nakagawa and Takai 2008). Hydrothermal-vent animals depend on the activity of microorganisms that derive energy from the oxidation of inorganic compounds (H<sub>2</sub>S, H<sub>2</sub>) or methane for the conversion of inorganic carbon from CO<sub>2</sub> into organic matter. These chemoautotrophic bacteria and archaea form the base of the food web, with heterotrophic bacteria, protists and invertebrates completing the trophic structure of the ecosystem. Although deep-sea hydrothermal vent environments can represent unique ecosystems that depend on energy sources other than light, they are not completely independent from inputs of photosynthetically derived nutrients produced higher in the water column.

Movile Cave, unlike other cave ecosystems, does not receive significant inputs of meteoric water from the surface, mainly due to layers of impermeable clays and loess that cover the limestone in which the cave is developed (Forti et al. 2002). In this review, we focus on the microbiology of the Movile Cave ecosystem, particularly on sulfur, carbon and nitrogen cycling and the role of microbes that act as the primary producers in this unique ecosystem. It should be noted that microbiological studies in Movile Cave ecosystem have primarily focussed on microbial mat floating on the water in the cave.

## Movile Cave

Movile Cave ([www.gesslab.org](http://www.gesslab.org)) is located near the town of Mangalia in Romania, a few kilometers from the Black Sea (43.825487N; 28.560677E). Geologist Christian Lascu

\*Address correspondence to Prof. J. Colin Murrell, School of Environmental Sciences, University of East Anglia, Norwich NR4 7TJ, United Kingdom; Email: [j.c.murrell@uea.ac.uk](mailto:j.c.murrell@uea.ac.uk)

Color versions of one or more of the figures in the article can be found online at [www.tandfonline.com/ugmb](http://www.tandfonline.com/ugmb).

discovered the cave in 1986 when an artificial shaft, dug for geological investigation created access to the narrow cave passages. Despite the lack of photosynthetically fixed carbon, the cave hosts a remarkable diversity of invertebrates, such as worms, insects, spiders and crustaceans (Sarbu 2000). Life within the Movile Cave ecosystem is maintained entirely by chemoautotrophy (Sarbu et al. 1996) an analogous system to some deep-sea hydrothermal vents where chemoautotrophic and methylotrophic bacteria make a substantial contribution to primary production, which in turn support a variety of macrofauna (reviewed in Campbell 2006; Dubilier et al. 2008; Lutz and Kennish 1993).

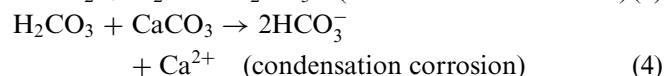
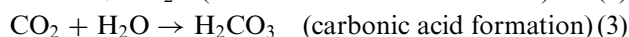
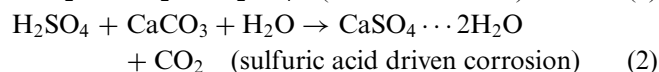
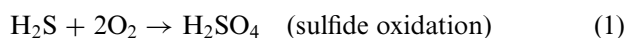
Paleogeographical evidence suggests that some animal species were trapped in Movile Cave as early as 5.5 million years ago (Falniowski et al. 2008; Sarbu and Kane 1995). Over time, these animals have become adapted to life in the dark and 33 out of 48 invertebrate species observed are endemic to Movile Cave (Sarbu et al. 1996). In comparison to deep-sea hydrothermal vents, the Movile Cave ecosystem offers easier access to an interesting model ecosystem to study food-web interactions, primarily driven by chemoautotrophic primary production and microbial biomass.

#### Movile Cave—Formation and Features

Movile Cave is formed from two major corrosion processes: condensation corrosion by carbon dioxide (CO<sub>2</sub>) and acid corrosion by sulfuric acid (H<sub>2</sub>SO<sub>4</sub>) (Sarbu and Lascu 1997). Sulfuric acid corrosion that is active in the lower partially submerged cave passages is a result of the oxidation of H<sub>2</sub>S to H<sub>2</sub>SO<sub>4</sub> in the presence of oxygen from the cave atmosphere (Equation 1). Sulfuric acid then reacts with the limestone walls of the cave, causing accelerated dissolution and leading to formation of gypsum (calcium sulfate dihydrate) deposits on the cave walls along with release of CO<sub>2</sub> (Equation 2). This type of corrosion is highly efficient and also promotes condensation corrosion due to the release of large quantities of CO<sub>2</sub> (Forti et al. 2002).

Condensation corrosion, a slower process compared to sulfuric acid corrosion, affects the walls in the upper dry passages of the cave and occurs when warm water vapour from the ther-

mal waters ascends and condenses on the colder walls and ceilings in the upper cave passages. Carbon dioxide from the cave atmosphere dissolves in the condensate to form carbonic acid (Equation 3), which dissolves the carbonate bedrock forming bicarbonate (Equation 4) (Sarbu and Lascu 1997). Carbon dioxide in the cave is released from limestone dissolution, the biological oxidation of methane and heterotrophic respiration processes. Due to the absence of H<sub>2</sub>S in the upper level of the cave, no effects of sulfuric acid corrosion are encountered here.



Although the upper passages of the cave (approximately 200 m long) are completely dry (as a consequence of the lack of water infiltration from the surface), the lower level (approximately 40 m long) is partly flooded by hydrothermal waters, which contain substantial concentrations of H<sub>2</sub>S (0.3 mM), CH<sub>4</sub> (0.2 mM) and ammonium (NH<sub>4</sub><sup>+</sup>) (0.3 mM) (Figure 2) (Sarbu and Lascu 1997). The air bells (air pockets, shown in Figure 1; Sarbu et al. 1996) present in the cave create an active redox interface on the surface of the water in the cave where bacteria in floating microbial mats oxidize the reduced sulfur compounds, methane and ammonium from the water using O<sub>2</sub> from the atmosphere. Consequently, macrofauna in Movile Cave appear only to live in proximity to the microbial mats within these air bells, while the upper dry nonsulfidic cave passages are devoid of macrofauna (Forti et al. 2002).

#### Physicochemical Conditions in Movile Cave

The water flooding the lower level of the cave is of hydrothermal origin and high in H<sub>2</sub>S (0.2–0.3 mM), CH<sub>4</sub> (0.02 mM) and NH<sub>4</sub><sup>+</sup> (0.2–0.3 mM), whereas oxidized compounds were not detected (Sarbu 2000). The flow rate of the water is reported to

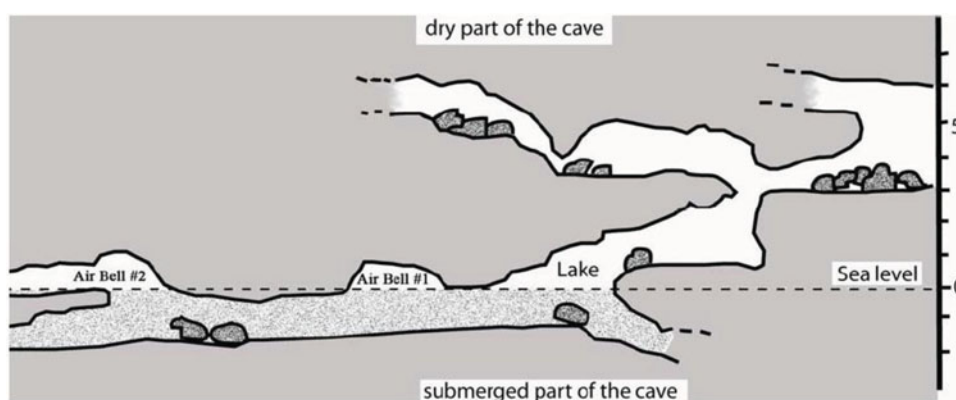


**Fig. 1.** Cross-section of Movile Cave (taken from the PhD thesis of Daniel Muschiol). © Dr. Walter Traunspurger, University of Bielefeld, Germany. Reproduced by permission of Dr. Walter Traunspurger, University of Bielefeld, Germany. Permission to reuse must be obtained from the rightsholder.

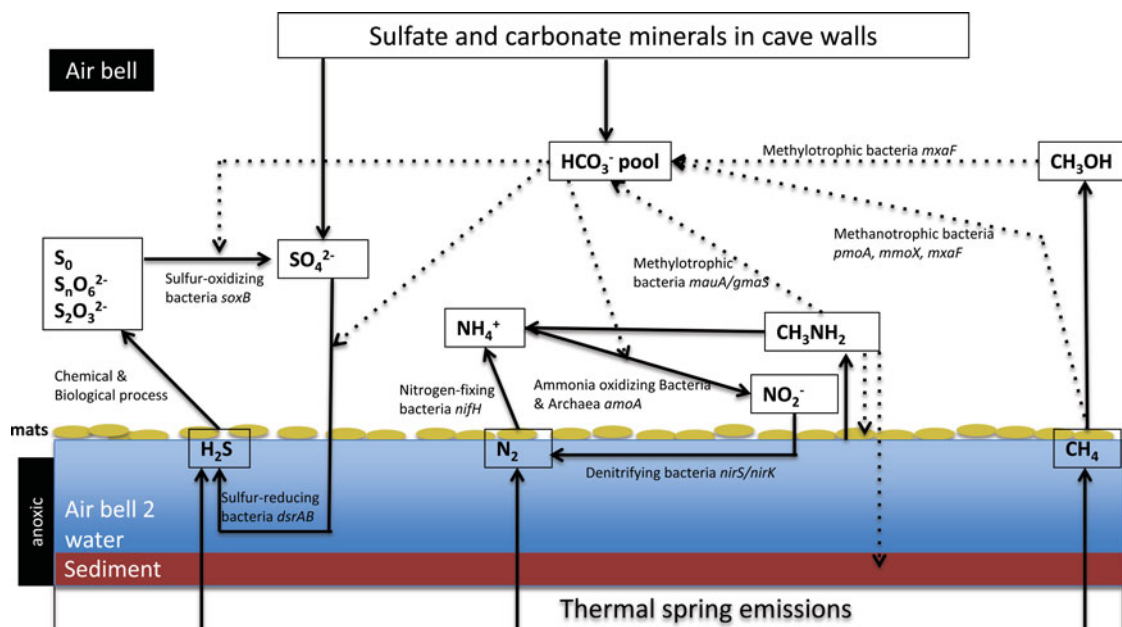


**Fig. 2.** Schematic representation of microbial carbon, nitrogen and sulfur cycling in Movile Cave. *soxB* gene encodes the SoxB component of the periplasmic thiosulfate-oxidizing Sox enzyme complex; *dsrAB* gene encodes for the  $\alpha$  and  $\beta$  subunits of the dissimilatory sulfite reductase enzyme; *nifH* encodes for the nitrogenase reductase subunit; *amoA* encodes for the  $\alpha$  subunit of ammonia monooxygenase (both bacteria and archaea); *nirS* and *nirK* encodes for a copper and a cytochrome cd1-containing nitrite reductase enzyme, respectively. *pmoA* encodes the  $\alpha$  subunit of the particulate methane monooxygenase enzyme, *mmoX* encodes the  $\alpha$  subunit of the hydroxylase of the soluble methane monooxygenase enzyme and *mxoF* encodes the  $\alpha$  subunit of the methanol dehydrogenase enzyme. *mauA* encodes for the small subunit of the methylamine dehydrogenase enzyme. *gmaS* encodes for the gamma-glutamylmethylamide synthetase.

be 5 L per sec (Sarbu and Lascau 1997) and its physiochemical properties are not affected by seasonal climatic changes (S. Sarbu, personal communication, April 2011). The water is at a constant pH of 7.4 due to the buffering capacity of the carbonate bedrock. Dissolved oxygen ranges between 9–16  $\mu\text{M}$  at the water surface and decreases to less than 1  $\mu\text{M}$  after the first few centimeters, with anoxic conditions encountered in deeper water (Sarbu 2000).

The air temperature in the lower cave passage ranged from 20.7–20.9°C, and the temperature of the water is 20.9°C (Sarbu and Lascau 1997) and the relative humidity ranges between 98 and 100% (Sarbu 2000). The air in the upper dry level of the cave contains 20–21%  $\text{O}_2$  and 1–2%  $\text{CO}_2$ , yet the air bells in the lower level contain only 7–10%  $\text{O}_2$ , up to 2.5%  $\text{CO}_2$  and 1–2% (v/v) methane (Sarbu 2000). Hydrogen sulfide is found in proximity to the air-water interface but not in the upper level (Sarbu 2000). Extensive microbial mats composed of bacteria, fungi and protozoa float on the water surface (kept afloat by rising methane bubbles) and also grow on the limestone walls of the cave (Sarbu et al. 1994a).

Since the discovery of Movile Cave, studies have provided evidence that the ecosystem is isolated from the surface. Radioactive artificial nuclides  $^{90}\text{Sr}$  and  $^{137}\text{Cs}$ , which were released as a result of the 1986 Chernobyl nuclear accident, have been found in high concentrations in soil and in lakes surrounding Movile Cave, as well as in the Black Sea and in sediments of other caves but not within Movile Cave itself (Sarbu et al. 1996).

### A Chemolithoautotrophic Ecosystem

In order to study chemolithoautotrophy in Movile Cave, microbial mat samples were incubated with  $^{14}\text{C}$ -bicarbonate. This resulted in incorporation of radioactive carbon into microbial lipids, providing the first evidence for chemoautotrophic carbon fixation at the redox interface (Sarbu et al. 1994b; Sarbu et al. 1996). Furthermore, activity of ribulose-1,5-bisphosphate carboxylase/oxygenase (RuBisCO), a key enzyme of the Calvin cycle, was observed in homogenates of microbial mat samples, as well as in lysates of bacteria cells cultivated from cave water, supporting the hypothesis that chemosynthate is being produced *in situ* (Sarbu et al. 1994b). Stable isotope ratio analyses of carbon and nitrogen provided conclusive evidence that Movile Cave is a self-sustained ecosystem dependent on chemoautotrophically fixed carbon (for detailed discussion, refer to Sarbu et al. 1996).

### Sulfur Metabolism

Sulfur-oxidizing bacteria, first described by Winogradsky (1887), are a heterogeneous group of organisms sharing the ability to oxidize reduced inorganic sulfur compounds, and are distributed within the domains of *Bacteria* and *Archaea*. A comprehensive overview of the biochemistry and molecular biology of sulfur oxidation can be found in Ghosh and Dam (2009). The Movile Cave ecosystem contains a high

concentration of H<sub>2</sub>S and primary production is dominated by sulfur oxidizing bacteria (Sarbu et al. 1996).

Sulfur-oxidizing bacteria (SOB) were the main focus of early studies characterizing microbial diversity and activity in Movile Cave (Rohwerder et al. 2003; Sarbu et al. 1994a; Vlasceanu et al. 1997). Sarbu and colleagues (1994a), using microscopic observations, identified *Thiothrix* and *Beggiatoa*-like filamentous bacteria in the floating mat, and Vlasceanu et al., (1997) isolated a *Thiobacillus thioparus* strain from cave water samples and characterized this bacterium at both the physiological and molecular level. Using most probable number (MPN) enumeration, Rohwerder and colleagues (2003) showed that SOB that could use sulfur, tetrathionate and thio-sulfate as energy sources, existed at up to 10<sup>7</sup> colony forming units (CFU) per g mat and that sulfate reducers capable of reduction of sulfate to H<sub>2</sub>S were also present in the microbial mat.

Clone libraries targeting bacterial 16S rRNA gene sequences in microbial mat DNA revealed sequences related to the 16S rRNA genes of *Thiobacillus* (*Betaproteobacteria*), *Thiovirga*, *Thiothrix*, *Thioploca* (*Gammaproteobacteria*) and *Sulfuricurvum* (*Epsilonproteobacteria*) (Chen et al. 2009). Employing an identical approach, also using Movile Cave mat DNA, Porter et al. (2009) reported similar results on the diversity of SOB with retrieval of additional 16S rRNA gene sequences related to *Halothiobacillus* and *Thiomonas* (*Betaproteobacteria* and *Gammaproteobacteria*, respectively) and *Sulfurospirillum* (*Epsilonproteobacteria*). Clone libraries of *soxB* genes (encoding the SoxB component of the periplasmic thiosulfate-oxidizing enzyme complex) revealed the widespread distribution of *soxB* sequences from *Alpha*-, *Beta*- and *Gammaproteobacteria*. The retrieved sequences were closely related to the *soxB* genes of *Thiobacillus*, *Methylobium petroleiphilum* (both belonging to *Betaproteobacteria*), *Thiothrix* and *Halothiobacillus* (65% identity) belonging to *Gammaproteobacteria*.

By targeting RuBisCO, specifically the form I green type RuBisCO gene (*cbbL*) sequences, Chen et al. (2009) detected sequences closely related (80 – 85% identity) to RuBisCO gene sequences of *Thiobacillus denitrificans* and *T. thioparus*. DNA-stable isotope probing (SIP) (Dumont and Murrell 2005; Radajewski et al. 2000) experiments using <sup>13</sup>C-labelled bicarbonate showed that SOB from the *Beta*- and *Gammaproteobacteria* (*Thiobacillus*, *Thiovirga*, *Thiothrix*, *Thioploca*) were particularly active in assimilating CO<sub>2</sub> (Chen et al. 2009).

Rohwerder and colleagues (2003) detected an extremely acidophilic SOB, which is interesting considering the pH of the water in Movile Cave is neutral. Based on a study in Frasassi Caves (Galdenzi et al. 2008), Sarbu et al. (2002) reported pH values of 3.8–4.5 on the surface of the microbial mats covering the limestone walls in the remote air bells, suggesting that not all of the sulfuric acid produced by SOB is immediately buffered and indicating the possibility of ecological niches that can be occupied by acidophilic bacteria in Movile Cave.

Rohwerder et al. (2003) also reported activity of facultatively anaerobic SOB in Movile Cave, which were capable of using nitrate (NO<sub>3</sub><sup>-</sup>) rather than oxygen as an alternative electron acceptor, and which were present at the same levels as

obligately aerobic SOB (10<sup>7</sup> CFU per gram dry weight of mat), suggesting that both groups could contribute substantially to the biomass produced. Chen et al. (2009) detected 16S rRNA gene sequences related to *Sulfuricurvum* (*Epsilonproteobacteria*), which can oxidize sulfur anaerobically (Kodama and Watanabe 2004) in DNA extracted from Movile Cave microbial mat, supporting the evidence for anaerobic sulfur oxidation demonstrated by Rohwerder et al. (2003).

Endosymbiotic sulfur-oxidizing bacteria, living within invertebrates, have been reported in various habitats, such as deep sea hydrothermal vents and mangrove swamps (Distel 1998; Dubilier et al. 2008; Wood and Kelly 1989). Although SOB benefit from sulfide, oxygen and CO<sub>2</sub> from the host, the bacteria in turn supply organic compounds to the host (Dahl and Prange 2006). Recently, Bauermeister et al. (2012) reported the presence of *Thiothrix* ectosymbionts associated with *Niphargus* species in Frasassi caves. It would be interesting to look for the presence of symbiotic sulfur-oxidizing bacteria associated with higher organisms present in the Movile Cave ecosystem.

Although less abundant than SOB, sulfate-reducing bacteria (SRB) have been shown to be present in Movile Cave. They appear to belong to a higher trophic level, using the organic carbon released by SOB and other primary producers as the electron donor (Rohwerder et al. 2003). Sulfate reducers in sulfidic caves appear to fall mainly within the *Deltaproteobacteria* (Engel 2007). Sequences related to members of the family *Desulfobulbaceae* have been found in Movile Cave in two independent 16S rRNA gene based clone library analyses (Chen et al. 2009; Porter et al. 2009). Thus far, no *Archaea* capable of oxidizing reduced sulfur compounds have been reported in the Movile Cave ecosystem, or in fact from any other sulfidic caves, probably due to the fact that most characterized *Archaea* that oxidize reduced sulfur compounds grow at elevated temperatures (Chen et al. 2009; Engel 2007).

## One-Carbon Metabolism—Methanotrophy and Methylophony

### *Methanotrophs*

Aerobic methanotrophy, the ability to use methane as a sole carbon and energy source, is found in bacteria within the phyla *Proteobacteria* and *Verrucomicrobia*. The biochemistry and molecular biology of aerobic methane oxidation in *Bacteria* has been extensively reviewed (Trotsenko and Murrell 2008). Use of specific biomarkers targeting both 16S rRNA and key metabolic genes of methanotrophs to infer phylogeny has also been reviewed (McDonald et al. 2008). Air bells within the Movile Cave contain methane and oxygen and are therefore favourable environments for aerobic methane-oxidizing bacteria.

Hutchens et al. (2004) using DNA-SIP experiments with <sup>13</sup>CH<sub>4</sub>, identified active methanotrophs, belonging to both the *Alpha*- and *Gammaproteobacteria* in Movile Cave water and microbial mat. Based on analysis of 16S rRNA and functional genes (*pmoA* and *mmoX*, encoding the active-site subunit of particulate methane monooxygenase and soluble

methane monooxygenase, respectively) it was shown that strains of *Methylomonas*, *Methylococcus* and *Methylocystis/Methylosinus* had assimilated  $^{13}\text{C}$ . Sequences of non-methanotrophic bacteria and an alga (*Ochromonas danica*, based on 18S rRNA gene sequence analysis) were also retrieved from  $^{13}\text{C}$ -labelled DNA in heavy fractions, indicating the possibility of non-methanotrophs cross-feeding on  $^{13}\text{C}$ -labelled biomass or metabolites arising from the initial consumption of  $^{13}\text{C}$  by methanotrophs.

Both 16S rRNA and *mxoF* (encoding the active-site subunit of methanol dehydrogenase) clone libraries from the heavy DNA ( $^{13}\text{C}$ -labelled DNA) contained sequences similar to the extant methylotrophs *Methylophilus* and *Hyphomicrobium*, suggesting that these organisms had assimilated  $^{13}\text{C}$ -methanol excreted by methanotrophs metabolizing  $^{13}\text{C}$ . The extent of the contribution of methanotrophs to primary production within the Movile Cave ecosystem is not known and future research should focus on understanding their role as primary producers. The possibility of anaerobic methane oxidation (Knittel and Boetius 2009) occurring in Movile Cave also warrants investigation in the future.

### Other Methylotrophs

Methylotrophs utilize reduced carbon substrates that have no carbon – carbon bond (eg methanol and methylated amines), as their sole carbon and energy source (Chistoserdova et al. 2009). Enumeration studies by Rohwerder et al. (2003) revealed methylotrophs in the floating mat at up to  $10^6$  CFU per gram dry weight of mat. It is possible that these methylotrophs can feed on methanol released by methanotrophs during methane oxidation. Chen et al. (2009) retrieved *soxB* and *cbfL* sequences related to those of *M. petroleiphilum*, a facultative methylotroph. Recently, Kalyuzhnaya et al. (2009) reported that methylotrophs within the *Methylophilaceae*, particularly some species of *Methylotenera*, require nitrate for growth on methanol. Investigating the role of methylotrophy-linked to denitrification within the Movile Cave ecosystem will yield more insights into the interactions between the carbon cycle and the nitrogen cycle in this ecosystem.

Chen et al. (2009) reported that the obligate methylated amine-utilizing methylotroph *Methylotenera mobilis* was present in high numbers, while *Methylophilus* and *Methylovorus* were also detected. Similar studies by Porter et al. (2009) also detected 16S rRNA gene sequences related to the 16S rRNA genes of *Methylotenera* and *Methylophilus*. Methylated amines are also a nitrogen source for a wide range of nonmethylotrophic bacteria and the metabolic pathways involved have been examined recently (Chen et al. 2010a, 2010c; Latypova et al. 2010). DNA stable isotope probing experiments with  $^{13}\text{C}$ -mono methylamine ( $\text{CH}_3\text{NH}_2$ ) revealed *Methylotenera mobilis* as a dominant methylotroph utilizing  $\text{CH}_3\text{NH}_2$  in Movile Cave mat samples, and also indicated the presence of a novel facultative methylotroph which has now been isolated and characterized (Wischer et al. unpublished). As methylated amines can serve as both C and N source for microbial communities, a deeper understanding of the functional

diversity of methylated amines utilizers in this ecosystem will add vital information on nutrient cycling in Movile Cave.

### Nitrogen Cycling

Over the past two decades, studies targeting microbial nutrient cycling within the Movile Cave ecosystem have focused largely on sulfur and carbon, whereas microbial nitrogen cycling has received little attention. Although the nitrifiers were not the major focus, results from the DNA-SIP based study by Chen et al. (2009) implied that ammonia- and nitrite-oxidizing bacteria might be important primary producers in the Movile Cave ecosystem alongside sulfur- and methane-oxidizing bacteria. Although ammonium concentrations in the cave waters are relatively high (0.2–0.3 mM), nitrate has not been detected (Sarbu 2000). This could be due to a rapid turnover of nitrate by either assimilatory nitrate reduction or denitrification. Facultatively anaerobic sulfur oxidizers, such as *Thiobacillus denitrificans*, are known to use  $\text{NO}_3^-$  as an alternative electron acceptor for respiration in oxygen-depleted conditions (Claus and Kutzner 1985).

Therefore sulfur oxidation linked to denitrification could be an important process in Movile Cave. This hypothesis was also supported by Rohwerder et al. (2003), who detected high numbers of SOB in enrichments with thiosulfate and nitrate incubated under anoxic conditions. Chen et al. (2009) also reported retrieval of 16S rRNA gene sequences related to denitrifiers from the phylum *Denitratisoma* from DNA isolated from Movile Cave mat samples.

Microbial  $\text{N}_2$  fixation may be another significant process of the nitrogen cycle in the Movile Cave ecosystem. The ability to fix  $\text{N}_2$  is widespread among bacteria and archaea and many bacteria present in Movile Cave are known  $\text{N}_2$  fixers (such as *Beggiatoa* and *Methylocystis*) (Murrell and Dalton 1983; Nelson et al. 1982). However, reduction of  $\text{N}_2$  to  $\text{NH}_4^+$  is highly energy-consuming and generally carried out during nitrogen-limited conditions (Postgate 1972). Although there are relatively high standing concentrations of  $\text{NH}_4^+$  in the cave water, there may well be nitrogen-depleted niches within the microbial mats where  $\text{N}_2$  fixation could play a role. Process-based  $\text{N}_2$ -fixation measurements and assaying for *nifH* transcripts in cave mat samples could determine whether  $\text{N}_2$  fixation occurs in this ecosystem.

### Archaeal Microbial Communities

Archaeal microbial communities are suggested to play an important role in nutrient recycling within cave ecosystems (Chelius and Moore 2004; Gonzalez et al. 2006; Northup et al. 2003). Over the years, the focus of research on microbial systems in Movile Cave has been on *Bacteria* whereas no in-depth study has been performed on the contribution of *Archaea* to nutrient cycling.

Recent results from Chen et al. (2009) revealed that the archaeal community in the Movile Cave (based on 16S rRNA gene libraries) possessed some archaea that have been found in deep-sea hydrothermal vents (originally shown by Takai and

Horikoshi 1999) although no sequences related to ammonia-oxidizing archaea (major nitrifiers in deep-sea hydrothermal environments), methanogens, sulfur-oxidizing archaea or anaerobic methane oxidizing-archaea were found in their study. It is essential to target *Archaeal* communities in future experiments to determine if they play a significant role in C, N and S cycling.

Also, it should be noted that in the few studies investigating the microbiology of Movile Cave using cultivation-independent techniques (Chen et al. 2009; Hutchens et al. 2004; Porter et al. 2009) mat and water samples were used, while microbial communities in Movile Cave sediment remain largely unexplored. The likely lack of oxygen as an electron acceptor in sediments suggests that alternative electron acceptors such as nitrate, nitrite, sulfate, CO<sub>2</sub> and metals such as Fe<sup>2+</sup> and Mn<sup>2+</sup>, together with organic matter deposited from floating mats, could be important in sediment and anoxic zones of the cave water. In fact we have evidence for the presence of methanogens in Movile Cave sediments, based on amplification of the *mcrA* gene from DNA extracted from sediment samples.

### Whole Genome Sequencing of Microbial Isolates

Whole genome sequencing of microorganisms has provided important insights into their genetic capacity and the plethora of available microbial genome sequences enables us to perform comparative genomics between organisms that might occupy different ecological niches but perform the same function. Whereas molecular ecology studies using genes (16S rRNA gene and metabolic genes) as biomarkers reveal the phylogeny of microbes in a complex ecosystem, efforts should also be focussed on isolating new microorganisms.

Rapidly reducing sequencing costs will enable us to sequence the genomes of novel and interesting microbial isolates, which will not only provide access to their genetic and metabolic potential, but also the ability to design focussed biochemical and physiological experiments based on the information from the genome sequence. We have isolated a *Methylomonas* strain from Movile Cave mat samples and the genome is being sequenced. This will provide a comprehensive overview of its genetic potential and also allow us to compare it with the genomes of *Methylomonas* species from other environments.

### Outlook: Microbial Community Composition Analysis Using Next-Generation Sequencing Techniques

Next generation sequencing provides a new vista for molecular microbial ecology research, allowing us to carry out a detailed examination of microbial diversity in an ecosystem. Tremendous progress has been made in understanding microbial systems by using either targeted gene sequencing (PCR-based screen) or shotgun metagenomic sequencing that eliminates any bias due to primer design and PCR (Gilbert and Dupont 2011).

A preliminary small-scale metagenomic sequencing of DNA from Movile Cave mat samples yielded approximately 960,000 sequences, with a mean length of 360bp. Analysis of the metagenomic data using MG-RAST (Meyer et al. 2008) assigned the sequences to annotated proteins (36.8%), unknown proteins (33.7%) and ribosomal sequences (1.9%). Of the annotated sequences, 96.5% were of bacterial origin, 1.8% eukaryotic, 1.3% archaeal and 0.2% were viral sequences. Phylum-level phylogenetic classification revealed that ~60% of the total annotated sequences belong to *Proteobacteria*, alongside bacteroidetes (12.1%) and firmicutes (7.6%). Interestingly, nearly 3% of the total sequences retrieved were representative of cyanobacterial sequences, which would not be expected in a Movile Cave ecosystem devoid of light. In-depth analysis of metagenomic data will yield better insights into the functional diversity, genetic potential and role in nutrient cycling of microbial communities in the ecosystem.

Using a combination of techniques such as SIP and metagenomic sequencing of <sup>13</sup>C-labelled-DNA (Chen et al. 2008; Chen and Murrell 2010; Chen et al. 2010b) we can reduce the complexity of sequence information obtained and particular functional groups can be targeted. Using this approach, a composite genome of *Methylotenera mobilis* was extracted from the metagenomic sequences from Lake Washington sediment DNA (Kalyuzhnaya et al. 2008). Similar strategies can be used in Movile Cave to obtain genome information for microbes that are difficult to isolate and cultivate in the laboratory. Although metagenomic analysis provides us with information about the genetic potential of the microbial communities within an ecosystem, use of metatranscriptomics (Moran et al. 2013) and metaproteomics (Seifert et al. 2012) will allow access to the transcriptomes and proteomes, respectively, of the active microbial communities.

Although we do have a basic understanding of individual communities e.g., SOB, methanotrophs, further research is required to understand the trophic interactions between different microbial functional guilds in Movile Cave. Sediment and anoxic water microbial communities remain largely unexplored and questions, such as whether there is any biogenic methane production or anaerobic methane oxidation, remain unanswered. Next-generation sequencing, combined with a suite of molecular ecology techniques and a concerted effort to isolate novel organisms, will improve our understanding of the functional diversity of the microbial communities and allow us to study the contributions of different functional guilds in maintaining this self-sustaining chemoautotrophic ecosystem.

### Acknowledgments

We thank Serban Sarbu and Rich Boden for valuable discussions, Vlad Voiculescu and Mihai Baciu for sampling and Andrew Crombie for critical comments on the manuscript.

### Funding

We acknowledge the funding from the Natural Environment Research Council (NERC) to JCM (NE/G017956),

the NERC and Earth and Life Systems Alliance (ELSA) for funding DK, a Warwick Postgraduate Research Fellowship and University of East Anglia-ELSA funding for DW and a NERC-CASE studentship for JS.

## References

- Bauermeister J, Ramette A, Dattagupta S. 2012. Repeatedly evolved host-specific ectosymbioses between sulfur-oxidizing bacteria and amphipods living in a cave ecosystem. *Plos One* 7:e50254
- Campbell KA. 2006. Hydrocarbon seep and hydrothermal vent paleoenvironments and paleontology: Past developments and future research directions. *Palaeogeogr Palaeoclimatol Palaeoecol* 232:362–407.
- Chelius MK, Moore JC. 2004. Molecular phylogenetic analysis of archaea and bacteria in wind cave, South Dakota. *Geomicrobiol J* 21:123–134.
- Chen Y, Dumont MG, Neufeld JD, Bodrossy L, Stralis-Pavese N, McNamara NP, Ostle N, Briones MJ, Murrell JC. 2008. Revealing the uncultivated majority: combining DNA stable-isotope probing, multiple displacement amplification and metagenomic analyses of uncultivated *Methylocystis* in acidic peatlands. *Environ Microbiol* 10:2609–2622.
- Chen Y, Wu L, Boden R, Hillebrand A, Kumaresan D, Moussard H, Baciu M, Lu Y, Murrell JC. 2009. Life without light: microbial diversity and evidence of sulfur-and ammonium-based chemolithotrophy in Movile Cave. *ISME J* 3:1093–1104.
- Chen Y, Murrell JC. 2010. When metagenomics meets stable-isotope probing: progress and perspectives. *Trends Microbiol* 18:157–163.
- Chen Y, McAleer KL, Murrell JC. 2010a. Monomethylamine as a nitrogen source for a nonmethylophilic bacterium, *Agrobacterium tumefaciens*. *Appl Environ Microbiol* 76:4102–4104.
- Chen Y, Neufeld JD, Dumont MG, Friedrich MW, Murrell JC. 2010b. Metagenomic analysis of isotopically enriched DNA. *Meth Mol Biol* 668:67–75.
- Chen Y, Scanlan J, Song L, Crombie A, Rahman MT, Schafer H, Murrell JC. 2010c. gamma-Glutamylmethylamide is an essential intermediate in the metabolism of methylamine by *Methylocella silvestris*. *Appl Environ Microbiol* 76:4530–4537.
- Chistoserdova L, Kalyuzhnaya MG, Lidstrom ME. 2009. The expanding work of methylophilic metabolism. *Ann Rev Microbiol* 63:477–499.
- Claus G, Kutzner H. 1985. Physiology and kinetics of autotrophic denitrification by *Thiobacillus denitrificans*. *Appl Environ Microbiol* 22:283–288.
- Dahl C, Prange A. 2006. Bacterial sulfur globules: occurrence, structure and metabolism. In: Shively J, editor. *Inclusions in Prokaryotes*, Berlin, Heidelberg: Springer, p21–51.
- Distel DL. 1998. Evolution of chemoautotrophic endosymbioses in bivalves. *Bioscience* 48:277–286.
- Dubilier N, Bergin C, Lott C. 2008. Symbiotic diversity in marine animals: The art of harnessing chemosynthesis. *Nat Rev Micro* 6:725–740.
- Dumont MG, Murrell JC. 2005. Stable isotope probing – linking microbial identity to function. *Nat Rev Microbiol* 3:499–504.
- Engel AS. 2007. Observation on the biodiversity of sulfidic karst habitats. *J Cave Karst Stud* 69:187–206.
- Falniowski A, Szarowska M, Sirbu I, Hillebrand A, Baciu M. 2008. *Heleobio drbrogica* (Grossu & Negrea, 1989) and the estimated time of its isolation in a continental analogue of hydrothermal vents. *Mollusc Res* 28:165–170.
- Forti P, Galdenzi S, Sarbu SM. 2002. The hypogenic caves: a powerful tool for the study of seeps and their environmental effects. *Cont Shelf Res* 22:2373–2386.
- Galdenzi SA, Cocchioni MA, Morichetti LU, Amici VA. 2008. Sulfidic ground-water chemistry in the Frasassi Caves, Italy. *J Cave Karst Stud* 70: 94–107.
- Ghosh W, Dam B. 2009. Biochemistry and molecular biology of lithotrophic sulfur oxidation by taxonomically and ecologically diverse bacteria and archaea. *FEMS Microbiol Rev* 33:999–1043.
- Gilbert JA, Dupont CL. 2011. Microbial metagenomics: beyond the genome. *Ann Rev Mar Sci* 3:347–371.
- Gonzalez JM, Portillo MC, Saiz-Jimenez C. 2006. Metabolically active *Crenarchaeota* in Altamira Cave. *Naturwissenschaften* 93:42–45.
- Hutchens E, Radajewski S, Dumont MG, McDonald IR, Murrell JC. 2004. Analysis of methanotrophic bacteria in Movile Cave by stable isotope probing. *Environ Microbiol* 6:111–120.
- Kalyuzhnaya MG, Lapidus A, Ivanova N, Copeland AC, McHardy AC, Szeto E, Salamov A, Grigoriev IV, Suci D, Levine SR, Markowitz VM, Rigoutsos I, Tringe SG, Bruce DC, Richardson PM, Lidstrom ME, Chistoserdova L. 2008. High-resolution metagenomics targets specific functional types in complex microbial communities. *Nat Biotech* 26:1029–1034.
- Kalyuzhnaya MG, Martens-Habbena W, Wang T, Hackett M, Stolyar SM, Stahl DA, Lidstrom ME, Chistoserdova L. 2009. Methylophilaceae link methanol oxidation to denitrification in freshwater lake sediment as suggested by stable isotope probing and pure culture analysis. *Environ Microbiol Rept* 1:385–392.
- Knittel K, Boetius A. 2009. Anaerobic oxidation of methane: progress with an unknown process. *Ann Rev Microbiol* 63:311–334.
- Kodama Y, Watanabe K. 2004. *Sulfuricurvum kujiense* gen. nov., sp. nov., a facultatively anaerobic, chemolithoautotrophic, sulfur-oxidizing bacterium isolated from an underground crude-oil storage cavity. *Int J Syst Evol Microbiol* 54: 2297–2300.
- Latypova E, Yang S, Wang Y, Wang T, Chavkin TA, Hackett M, Schäfer H, Kalyuzhnaya MG. 2010. Genetics of the glutamate-mediated methylamine utilization pathway in the facultative methylophilic beta-proteobacterium *Methyloversatilis universalis* FAM5. *Mol Microbiol* 75:426–439.
- Lutz RA, Kennish MJ. 1993. Ecology of deep-sea hydrothermal vent communities: A review. *Rev Geophys* 31:211–242.
- McDonald IR, Bodrossy L, Chen Y, Murrell JC. 2008. Molecular ecology techniques for the study of aerobic methanotrophs. *Appl Environ Microbiol* 74:1305–1315.
- Meyer F, Paarmann D, D'Souza M, Olson R, Glass EM, Kubal M, Paczian T, Rodriguez A, Stevens R, Wilke A, Wilkening J, Edwards RA. 2008. The metagenomics RAST server – a public resource for the automatic phylogenetic and functional analysis of metagenomes. *BMC Bioinformatics* 9:386.
- Moran MA, Satinsky B, Gifford SM, Luo H, Rivers A, Chan LK, Meng J, Durham BP, Shen C, Varaljay VA, Smith CB, Yager PL, Hopkinson BM. 2013. Sizing up metatranscriptomics. *ISME J* 7:237–243.
- Murrell JC, Dalton H. 1983. Nitrogen fixation in obligate methanotrophs. *J Gen Microbiol* 129:3481–3486.
- Muschio D. 2009. Meiofauna in a chemosynthetic groundwater ecosystem: Movile Cave, Romania. PhD Thesis University of Bielefeld, Germany.
- Nakagawa S, Takai K. 2008. Deep-sea vent chemoautotrophs: diversity, biochemistry and ecological significance. *FEMS Microbiol Ecol* 65:1–14.
- Nelson D, Waterbury J, Jannasch H. 1982. Nitrogen fixation and nitrate utilization by marine and freshwater Beggiatoa. *Arch Microbiol* 133:172–177.
- Northup DE, Barns SM, Yu LE, Spilde MN, Schelble RT, Dano KE, Crossey LJ, Connolly CA, Boston PJ, Natvig DO, Dahm CN. 2003. Diverse microbial communities inhabiting ferromanganese deposits in Lechuguilla and Spider Caves. *Environ Microbiol* 5:1071–1086.
- Palmer AN. 1991. Origin and morphology of limestone caves. *Geol Soc Amer Bull* 103:1–21.

- Porter ML, Engel AS, Kane TC, Kinkle BK. 2009. Productivity-diversity relationships from chemolithoautotrophically based sulfidic karst systems. *Intl J Speleol* 38:27–40.
- Postgate JR. 1972. Biological nitrogen fixation. *Nature* 226:25–27.
- Radajewski S, Ineson P, Parekh NR, Murrell JC. 2000. Stable-isotope probing as a tool in microbial ecology. *Nature* 403:646–649.
- Rohwerder T, Sand W, Lascu C. 2003. Preliminary evidence for a sulfur cycle in Movile Cave, Romania. *Acta Biotechnol* 23: 101–107.
- Sarbu SM. 2000. Movile Cave: A chemoautotrophically based groundwater ecosystem. In Wilken H, Culver DC, Humphreys WF, editors. *Subterranean Ecosystems*. Amsterdam: Elsevier, p319–343.
- Sarbu SM, Galdenzi S, Menichetti M, Gentile G. 2002. Geology and biology of Grotte di Frasassi (Frassasi Caves) in central Italy, an ecological multi-disciplinary study of a hypogenic underground karst system. In: Wilken H, Culver DC, Humphreys WF, editors. *Subterranean Ecosystem*, New York: Elsevier. p369–378.
- Sarbu SM, Kane TC. 1995. A subterranean chemoautotrophically based ecosystem. *NSS Bull* 57:91–98.
- Sarbu SM, Kane TC, Kinkle BK. 1996. A chemoautotrophically based cave ecosystem. *Science* 272:1953–1955.
- Sarbu SM, Kinkle BK, Vlasceanu L, Kane TC, Popa R. 1994a. Microbiological characterization of a sulfide-rich groundwater ecosystem. *Geomicrobiol J* 12:175–182.
- Sarbu SM, Lascu C. 1997. Condensation corrosion in Movile cave, Romania. *J Cave Karst Stud* 59:99–102.
- Sarbu SM, Vlasceanu L, Popa R, Sheridan P, Kinkle BK, Kane TC. 1994b. Microbial mats in a thermomineral sulfurous cave. In: Stal LJ, Caumette P, editors. *Microbial Mats: Structure, Development and Environmental Significance*. Berlin: Springer-Verlag. p45–50.
- Seifert J, Taubert M, Jehmlich N, Schmidt F, Völker U, Vogt C, Richnow H, von Bergen M. 2012. Protein-based stable isotope probing (protein-SIP) in functional metaproteomics. *Mass Spec Rev* 31:683–697.
- Takai K, Horikoshi K. 1999. Genetic diversity of archaea in deep-sea hydrothermal vent environments. *Genetics* 152:1285–1297.
- Trotsenko YA, Murrell JC. 2008. Metabolic aspects of aerobic obligate methanotrophy. In: Allen I, Laskin SS, Geoffrey MG, editors. *Advances in Applied Microbiology*. New York: Academic Press. p183–229.
- Vlasceanu L, Popa R, Kinkle BK. 1997. Characterization of *Thiobacillus thioparus* LV43 and its distribution in a chemoautotrophically based groundwater ecosystem. *Appl Environ Microbiol* 63:3123–3127.
- Winogradsky S. 1887. Über Schwefelbakterien. *Botanische Zeitung* XLV:489–507.
- Wood AP, Kelly DP. 1989. Isolation and physiological characterisation of *Thiobacillus thyasiris* sp. nov., a novel marine facultative autotroph and the putative symbiont of *Thyasira flexuosa*. *Arch Microbiol* 152:160–166.